



Durham E-Theses

Systematic studies of hydrogen bonding

Mondal, Raju

How to cite:

Mondal, Raju (2004) *Systematic studies of hydrogen bonding*, Durham theses, Durham University.
Available at Durham E-Theses Online: <http://etheses.dur.ac.uk/2986/>

Use policy

The full-text may be used and/or reproduced, and given to third parties in any format or medium, without prior permission or charge, for personal research or study, educational, or not-for-profit purposes provided that:

- a full bibliographic reference is made to the original source
- a [link](#) is made to the metadata record in Durham E-Theses
- the full-text is not changed in any way

The full-text must not be sold in any format or medium without the formal permission of the copyright holders.

Please consult the [full Durham E-Theses policy](#) for further details.

Systematic Studies of Hydrogen Bonding

Raju Mondal

**Thesis submitted in part fulfilment of the requirement for the degree of
Doctor of Philosophy
at the
University of Durham**

**A copyright of this thesis rests
with the author. No quotation
from it should be published
without his prior written consent
and information derived from it
should be acknowledged.**



**Department of Chemistry
September 2004**

28 FEB 2005

Systematic Studies of Hydrogen Bonding

Submitted for the degree of Doctor of Philosophy, September 2004, by Raju Mondal,

University of Durham

ABSTRACT

This thesis deals with wider application and implications of the hydrogen bond in crystal engineering studies and beyond; in addition, it also highlights the Cambridge Structural Database (CSD) as the potential *knowledge-mine* for inorganic chemists.

The content of this thesis covers mainly three areas, viz, the role of hydrogen bonding in crystal engineering studies, the bridging between mainstream crystal engineering studies and solvates via hydrogen bond, and CSD studies on metal coordination spheres.

Chapter 2 deals with crystal structure prediction through understanding the driving forces for forming supramolecular synthons and some rare supramolecular networks (Carborundum III). With the help of a series of supraminols we attempt to identify the underlying reason for forming β -As networks. Chapter 3 covers the much debated topic of acceptor capabilities of organic halogens and consequently, how the so-called illusory hydrogen bond involving an organic halogen as an acceptor can explain a complex topic like synthon change-over, in a perfectly comprehensible manner.

The aim of the Chapters 4 to 6 is to bring two separate fields, "crystal engineering" and "solvates" closer via a common root, like hydrogen bonding. The serendipitous host molecules are part of our crystal engineering studies, yet they form solvates due to less than optimum hydrogen bonding in their respective crystal structures. Alongside some usual solvates, in an unconventional way, different amines with varying steric, strain and donor hydrogen atoms were used. Different geometrical as well as crystallographical aspects and their explicit role in synthon selection has also been discussed.

In Chapter 7, geometrical distortions of three-coordinate metal complexes in the crystal structures in the CSD have been analysed using symmetry modified Principal Component Analysis (PCA). Results shows that 90% of three coordinate species are accounted for by the five elements Cu, Ag, Hg, Au and Zn. Among the three major types of geometries, trigonal planar dominates the data sets, with smaller contribution for Y- and T-shaped structure. For Hg^{II} complexes, a possible reaction pathway for ligand addition reaction to two-coordinate linear complexes via T-shaped geometries leading to trigonal planar is discussed in detail.

The background information and an overview of the experiments are discussed in the Introductory Chapter.

DECLARATION

The work described in this thesis was carried out in the Department of Chemistry at the University of Durham between October 2001 and September 2004, under the supervision of Prof. Judith A. K. Howard. All the work is my own, unless otherwise stated, and has not been submitted previously for a degree at this, or any other university.

A handwritten signature in black ink, appearing to read 'Raju Mondal', with a stylized flourish at the end.

Raju Mondal

The copyright of this thesis rests with the author. No quotation from it should be published without his prior written consent and information derived from it should be acknowledged.

Acknowledgements

I take this opportunity to express my sincere gratitude to my supervisor Prof. Judith A. K. Howard, CBE, FRS and my co-supervisor Dr. Frank Allen for their constant support and guidance through the course of this study.

I would like to thank all my University friends at Javdavpur, especially, Ambarish, Arijit, Dola, Partha, Kakoli, Sangeeta and others, without their help, support and encouragement, I might not be writing this acknowledgement in the first place. It was not in the plan, but amazingly most of us now either 'Dr.' or will be soon

I would also like to thank two of my IIT Bombay classmate, Pradip and Sai Ganash for being such nice friends; also all my friends in IISc, Bangalore.

Support from ORS and CCDC is gratefully acknowledged.

I would like to thank Dr. Andrei Bastanov for teaching me whatever (if any) I know about crystallography; Dr. Olga Chetina for sharing her expertise on growing crystals.

Special thanks goes to Prof. Gautam R. Desiraju and Dr. Aswini Nangia and their research students for their involvement in the joint projects; specially Rahul for providing masses of crystal.

Also I would like to thank Prof T. N. Guru Row and Dr. V. R. Pedireddi for their help and encouragement.

Finally, I would like to thank all my lab mates and also all those who have been of some help or the other but whom I may have missed out.

Table of Contents:

Chapter 1: Introduction

1.1 Crystal Engineering.....	1
1.2 Methods of studying molecular interactions.....	4
1.3 Hydrogen Bond.....	5
1.4 Cambridge Structural Database.....	6
1.5 Single Crystal Diffraction.....	10
1.6 Experimental Set-up.....	13
1.6.1. Diffractometer.....	15
1.6.2. The Cooling System.....	17
1.7. Scope of This Thesis.....	17
1.8. References.....	20

Chapter 2. Molecular Recognition Among Alcohols and Amines. Novel

Carborundum Network in a Supramolecular Homologous Series.

2.1. Introduction.....	22
2.2. Amine-Alcohol recognition.....	22
2.3. Crystal structure prediction.....	26
2.4. Structural homology.....	33
2.5. Aminophenols show novel network structures.....	37
2.3 References.....	42

Chapter 3. Organic Chlorine as Hydrogen Bond Acceptor

3.1 Introduction.....	45
3.2. Result and Discussion.....	50
3.3. Hydrogen Bonding Patterns.....	53
3.4. Synthons Disruptions.....	59
3.5. Competition Between Organic Chlorine and a Strong Acceptor.....	66
3.6. Novel synthon creation.....	68
3.7. Reinforcement from NMR Data.....	69
3.8. References.....	73

Chapter 4. Correlation between the molecular symmetry and crystallographic symmetry in gem-alkynol family and their pseudopolymorphs

4.1. Introduction.....	76
4.2 Result and Discussion.....	79
4.3 Pseudopolymorphism.....	85
4.3 References.....	94

Chapter 5 Conformational Pseudopolymorphism : Unprecedented Observation of Both Gauche and Staggered Forms of Diethylamine in Solvates With the Same Host

5.1 Introduction.....	96
5.2 Result and Discussion.....	99

5.3. Cis isomer of DDDA.....	100
5.4. Solvates of cis-diol.....	103
5.5. <i>Trans</i> Diol Solvate.....	108
5.6. Nomenclature.....	111
5.7. References.....	113

Chapter 6. Correspondence between Molecular Functionality and Crystal Structures. Supramolecular Chemistry of Amine Solvates of a Gem-alkynol

6.1. Introduction.....	115
6.2 Crystallization.....	116
6.3. Result and Discussion.....	117
6.4 CSD Search.....	120
6.5. Primary amine solvates.....	120
6.5.1. (Cyclopentyl amine) ₂ . DDDA.....	121
6.5.2. (Cyclohexyl amine) ₂ . DDDA.....	123
6.5.3. (Cycloheptyl amine) ₂ . DDDA.....	124
6.5.4. (Cyclooctyl amine) ₂ . DDDA, (Cyclooctyl amine) DDDA,.....	125
6.5.5. (tert-Octylamine) ₂ . DDDA.....	127
6.5.6. (1,2-cyclohexyl diamine) ₂ . DDDA.....	129
6.6. General Discussion of primary amine solvates.....	130
6.7. Secondary Amines.....	133
6.7.1. (Et ₂ NH) ₂ . DDDA.....	133
6.7.2. (Pr ₂ NH) ₂ . DDDA.....	135
6.7.3. (Bu ₂ NH) ₂ . DDDA.....	136
6.7.4. (Dicyclohexyl amine) ₂ . DDDA.....	137

6.7.5. ($i\text{-Pr}_2\text{NH}$) ₂ . DDDA.....	138
6.8. General Discussion of secondary amine solvates.....	139
6.9. Tertiary amines.....	141
6.9.1. (EtMe_2N) ₂ . DDDA.....	142
6.9.2. (Et_3N) ₂ . DDDA.....	144
6.9.3. ($\text{Me}_2\text{CyclohexylN}$) ₂ . DDDA.....	144
6.9.4. (4-methyl-pyrrolidine) ₂ . DDDA.....	145
6.10. General Discussion of tertiary amine solvates.....	146
6.11. Conclusion.....	148
6.12. References.....	150

Chapter 7 A Systematic Study of the Coordination Geometry of Three-Coordinate Metal Complexes

7.1. Introduction.....	153
7.2. Geometry of three coordinated Species.....	156
7.3. Principal Component Analysis (PCA).....	158
7.3.1. Advantage of PCA: Dimension Reduction.....	160
7.3.2. Advantage of PCA: Better Visualisation of Result.....	160
7.3.3. Advantage of PCA: Correlation With Chemical Parameter.....	161
7.4. Symmetry Deformation Coordinates (SDC).....	161
7.5. Symmetry Consideration.....	163
7.6. Database search and retrieval mechanism.....	164
7.7. Result and Discussion.....	165
7.7.1. PCA results-All TrL_3 species.....	166

7.7.2. PCA results for individual TrL_3 species.....	169
7.8. Symmetry Deformation Coordinate (SDC) results for individual TrL_3	177
7.9. Out-of-Plane Displacement of The Metal Atom.....	180
7.10. Reaction pathway for ligand addition to two coordinate species.....	183
7.11. Conclusion.....	188
7.10. References.....	189

List of Figures

Chapter 1. Introduction

Figure 1.1.a,b. Growth of the CSD 1970-2000 and projected growth of the CSD 2001-2010.....	8
Figure 1.2. A Graphical representation of the CSD.....	9
Figure 1.3. A schematic representation of a diffraction experiment of crystal.....	10
Figure 1.4. A 2-D representation of lattice with molecule sitting on it	11
Figure 1.5. A schematic representation of Bragg's Law.....	12
Figure 1.6. Part of an X-ray diffraction pattern.....	13
Figure 1.7. A schematic view of a four circle diffractometer.....	14
Figure 1.8. A general flow chart of the diffractometer set-up.....	15
Figure 1.9. SMART-1000 and Apex Microsource diffractometer.....	16

Chapter 2. Molecular Recognition Among Alcohols and Amines. Novel

Carborundum Network in a Supramolecular Homologous Series.

Figure 2.1a,b. β -As Sheets in hexagonal and cyclohexane form.....	24
Figure 2. 2. Crystal structure of 2 and 5	28
Figure 2.3. Crystal structure of 6 and 8	30
Figure 2.4. Crystal packing of 9	32
Figure 2.5. Crystal packing of 10 and 12	33
Figure 2.6. Network depictions of zinc blende, wurzite and carborundum III	36
Figure 2.7. Crystal packing of 7 and 9 showing carborundum III type network.....	38

Chapter 3. Organic Chlorine as Hydrogen Bond Acceptor

Figure 3.1. Histograms of intermolecular and intramolecular O–H...Cl–C interactions.....	51
Figure 3.2. Packing diagram of 15DDA.....	53
Figure 3.3 Packing diagram of 14DDDA.....	54
Figure 3.4 Packing diagram of 18DDDA.....	55
Figure 3.5. Packing diagram of CDDA.....	61
Figure 3.6. Packing diagram of 15MKA.....	67
Figure 3.7 Packing diagram of TDDA.....	68
Figure 3.8. ¹ H NMR spectra of 14DDDA.....	70
Figure 3.9. Time resolved D ₂ O exchange NMR spectra of CDDA.....	72

Chapter 4. Correlation between the molecular symmetry and crystallographic symmetry in gem-alkynol family and their pseudopolymorphs

Figure 4.1. Dimer synthon formed by the DDDA.....	82
Figure 4.2. Packing diagram of (DDDA).(DMSO) ₂ and (DDDA).(DMSO).....	86
Figure 1.3. Packing diagram of (DDDA).(HMPA) ₂ and (DDDA).(NMP) ₂	89
Figure 1.4 Packing diagram of (DDDA)(DMF) ₂	90

Chapter 5 Conformational Pseudopolymorphism : Unprecedented Observation of Both Gauche and Staggered Forms of Diethylamine in Solvates With the Same Host

Figure 5.1. Schematic diagram of <i>cis</i> - and <i>trans</i> - 1,5-dichloro- <i>cis</i> -9,10-diethynyl-9,10-dihydroanthracene-9,10-diol.....	99
---	----

Figure 5.2. Crystal structure of <i>cis</i> -diol.....	101
Figure 5.3. Gauche and staggered conformations of Et ₂ NH found in the solvates and their corresponding schematic representations.....	104
Figure 5.4. Crystal structures of solvates of <i>cis</i> -diol with gauche staggered conformers of Et ₂ NH.....	105
Figure 5.5. Orientation of <i>cis</i> diol in two different solvates.....	107
Figure 5.6. Crystal structure of the <i>trans</i> -diol solvate.....	109

Chapter 6. Correspondence between Molecular Functionality and Crystal Structures. Supramolecular Chemistry of Amine Solvates of a Gem-alkynol

Figure 6.1. Crystal packing of 1 , showing synthon I	121
Figure 6.2. Hydrogen bridges in 2-aminophenol and 3-aminophenol.....	122
Figure 6.3. Crystal packing of 2 showing synthon I	123
Figure 6.4. Crystal packing of 3 showing synthon I	124
Figure 6.5. Two different conformations of cyclooctyl amines in 4 and in 5 and Crystal packing of 4 showing synthon I	126
Figure 6.6. Crystal packing of 5 showing synthon V	127
Figure 6.7. Crystal packing of 6 showing synthon III	128
Figure 6.8. Crystal packing of 7 showing square synthon II sandwiched between two interaction patterns similar to synthon I	129
Figure 6.9. Crystal packing of 8 showing square motifs.....	134
Figure 6.10. Crystal packing of 4,-(4aminobenzyl)phenol showing square motifs.....	134
Figure 6.11. Crystal packing of <i>cis</i> -DDDA with diethyl amine.....	135
Figure 6.12. Crystal structure of 9 showing synthon II	136

Figure 6.13. Crystal packing of 10 showing square synthon II	137
Figure 6.14. Crystal packing of 11 showing square motifs.....	138
Figure 6.15. Crystal packing of 12 showing synthon I like interaction pattern.....	139
Figure 6.16. Crystal packing of 13 showing synthon III	142
Figure 6.17. Crystal packing of 14 showing synthon III	143
Figure 6.18. Crystal packing of 15 showing synthon III	144
Figure 6.19. Crystal packing of 16 showing synthon III	145

Chapter 7 A Systematic Study of the Coordination Geometry of Three-Coordinate Metal Complexes

Figure 7.1. Three most common geometries of three coordinate species and corresponding lengths (d_n and θ_n) angles.....	157
Figure 7.2. The $3N=12$ Cartesian displacement vectors for the D_{3h} trigonal planar reference structure.....	162
Figure 7.3. One possible labelling scheme, together with the necessary permutations of these labels that are required to describe fully the configurational space	163
Figure 7.4. Scatterplots of PC1 vs. PC2 and PC1 vs. PC3 for all TrL_3 species.....	168
Figure 7.5. Schematic diagram indicating the deformation directions revealed in the PC1 vs. PC2 scatterplots.....	169
Figure 7.6. Scatterplots of PC1 vs. PC2 and PC1 vs PC3 for Cu.....	170
Figure 7.7. Scatterplot of PC1 vs. PC2 for Ag.....	172
Figure 7.8. Scatterplot of PC1 vs. PC2 for Au.....	173

Figure 7.9. Scatterplot of PC1 vs. PC2 for Hg.....	174
Figure 7.10. Scatterplot of PC1 vs. PC2 for Zn	175
Figure 7.11. A schematic impression of the substructure causing Y-shaped deformations of three coordinate Zn species.....	175
Figure 7.12. SDC1 vs. SDC2 plots for Copper and Silver, SDC vs. PCA plots with correlation coefficient of 1.0 for Hg and Ag.....	179
Figure 7.13. Histograms of out-of-plane displacements (Å) of mercury, gold, silver and copper from the plane of three ligand atoms.....	181
Figure 7.14. Schematic representation of the reaction mechanism for the conversion of two coordinated species to three coordinated D_{3h} geometry.....	182
Figure 7.15. Plots of d(norm) vs. a(opp) and d(norm) vs. a(adj) for Hg^{II}	184

List of Tables

Chapter 1. Introduction

Table 1.1. Entry statistics (April 2003) for the major crystallographic databases.....	8
--	---

Chapter 2. Molecular Recognition Among Alcohols and Amines. Novel

Carborundum Network in a Supramolecular Homologous Series.

Table 2.1. Crystallographic data and structure refinement parameters.....	31
Table 2.2. Crystallographic data and structure refinement parameters of molecular complexes	40

Chapter 3. Organic Chlorine as Hydrogen Bond Acceptor

Table 3.1 Hydrogen bond table for the 14DDDA.....	56
Table 3.2 Hydrogen bond table for the 18DDA.....	56
Table 3.3. Crystallographic data and structure refinement parameters.....	57
Table 3.3a. Crystallographic data and structure refinement parameters.....	58
Table 3.4 Hydrogen bond table for the CDDA.....	61
Table 3.5. Hydrogen bond table for the 15MKA.....	66
Table 3.6. ¹ H NMR Chemical shifts of hydroxyl H-atoms in <i>gem</i> -alkynols.....	71

Chapter 4. Correlation between the molecular symmetry and crystallographic symmetry in *gem*-alkynol family and their pseudopolymorphs

Table 4.1. Selected hydrogen bond table for the solvates.....	87
Table 4.2. A comparison of the five solvates with regard to selected solvent and crystal properties.....	88
Table 4.3. Crystallographic data and structure refinement parameters.....	91-92

**Chapter 5 Conformational Pseudopolymorphism : Unprecedented Observation
of Both Gauche and Staggered Forms of Diethylamine in Solvates With the Same
Host**

Table 5.1. Hydrogen bond parameters for the cis-diol.....	102
Table 5.2. Hydrogen bond parameter for the gauche conformer.....	108
Table 5.3. Hydrogen bond parameter for the staggered conformer.....	108
Table 5.4. Crystallographic data and structure refinement parameters.....	110

**Chapter 6. Correspondence between Molecular Functionality and Crystal
Structures. Supramolecular Chemistry of Amine Solvates of a Gem-alkynol**

Table 6.1. Crystallographic data and structure refinement parameters of 1° amine solvates.....	132
Table 6.2. Crystallographic data and structure refinement parameters of 2° amine solvates.....	140
Table 6.3. Crystallographic data and structure refinement parameters of 3° amine solvates.....	147

**Chapter 7 A Systematic Study of the Coordination Geometry of Three-
Coordination Metal Complexes**

Table 7.1. Statistics of TrL ₃ substructures in crystal structures recorded in the CSD.....	166
Table 7.2. Results of PC analysis for various datasets.....	167

List of Illustrations

Chapter 2. Molecular Recognition Among Alcohols and Amines. Novel Carborundum Network in a Supramolecular Homologous Series.

Scheme 2.1 Schematic representation of the supraminols and the 1:1 molecular complexes of interest for this study.....	27
Scheme 2.2. A vis-à-vis comparison of zinc blende and carborundum III network as observed in crystal structures 10 and 7 respectively.....	39

Chapter 3. Organic Chlorine as Hydrogen Bond Acceptor

Scheme 3.1. Compounds in this study with the metrics of the solid state O–H...Cl–C interactions marked.....	49
Scheme 3.2. Schematic representation of supramolecular synthon V and VI	59
Scheme 3.3. Schematic representation of the two different faces in CDDA.....	60
Scheme 3.4. Supramolecular distortion of synthon I by the chloro group via intramolecular hydrogen bonding for CDDA.....	62
Scheme 3.5. Supramolecular distortion of synthon V by two Cl-groups in 14DDDA.....	63
Scheme 3.6. Supramolecular distortion of synthon V by two Cl-groups in 18DDDA.....	64
Scheme 3.7. Supramolecular distortion of synthon V by two Cl-groups in 15DDDA.....	65
Scheme 3.8. Formation of synthon VII from the 1:1 linear combination of V and VI	69

Chapter 4. Correlation between the molecular symmetry and crystallographic symmetry in gem-alkynol family and their pseudopolymorphs

Scheme 4.1. Schematic diagram and single molecule of DDDA and DDA.....81

Chapter 6. Correspondence between Molecular Functionality and Crystal Structures. Supramolecular Chemistry of Amine Solvates of a Gem-alkynol

Scheme 6.I. Showing the DDDA molecules and synthons of interest for this study.....119

Chapter 7 A Systematic Study of the Coordination Geometry of Three-Coordination Metal Complexes

Scheme 7.I. Representative molecules from Cu, Ag and Au datasets highlighting the T- and T-shaped geometry.....171

Scheme 7.II. Characteristic molecules from Zn dataset showing trigonal planar geometry176

Scheme 7. III. Some characteristic molecules from Zn dataset showing the Y-shaped structures with four membered ring formation via N, Cl and O.....177

Scheme 7.IV. Representative molecules showing large out-of-plane displacement of the metal atom from ligand plane with pyramidallisation.....180

Scheme 7.V. Characteristic molecules from Hg^{II} datasets showing different structural variations like trigonal planar, T-shaped, Y-shaped and pyramidal.....186

Chapter 1

Introduction

1.1. Crystal Engineering:

One of the continuing scandals in the physical sciences is that it remains in general impossible to predict the structure of even the simplest crystalline solids from a knowledge of their chemical composition¹

Among the many other techniques and methods, single crystal X-ray diffraction analysis has become the quickest and most reliable method for structure determination. The crystal structure of a molecule is of enormous importance to chemistry, be it for optical, magnetic, electrical and other physical properties or for determination of the structure of an intermediate state of a reaction. According to Dunitz², a crystal of an organic molecule is “a supermolecule par excellence” which assembles together with an amazing precision.

However the bottom-up approach for ‘molecule to crystal’ started almost two decades ago when crystallography emerges from a method of choice to the most reliable and quickest routine analytical tool. Scientists from both structural chemistry and crystallography started seeking an analogy between supramolecular chemistry and classic organic chemistry³, which consequently led to the paradigm shift towards crystal engineering. Although crystal engineering was the study of organic chemistry, today it also deals with several fields of inorganic chemistry, such as nanostructures and coordination polymers⁴.

The term “crystal engineering” comes in effect from when Gerhard Schmidt⁵, in an attempt to make an interface between traditional organic chemistry and crystallography, wrote:

“...we shall, in the present context of synthetic and mechanistic photochemistry, be able to ‘engineer’ crystal structures having intermolecular contact geometries appropriate



for chemical reaction.....”. However the term, ‘crystal engineering’ was coined by R. Pepinsky of the Pennsylvania State University at the American Physical Society Meeting held in Mexico City in August 1955. With an abstract entitled “ Crystal Engineering: a new concept in Crystallography”⁶, he proposed an idea of

“Crystallization of organic ions with metal containing complex ions of suitable sizes, charges and solubilities, results in structures with cell and symmetries determined chiefly by the packing of complex ions. These cells and symmetries are to a good extent controllable; hence crystals with advantageous properties can be ‘engineered’....”

Although the scope of modern mainstream crystal engineering is much more diverse, nonetheless it is astonishing to find that *making crystals by design* first surfaced as early as half a century ago.

Crystal engineering methodologies attempt to identify common patterns in a series of crystal structures, to understand them in terms of mutual interplay between particular intermolecular interactions. Since interactions arise from molecular functionalities, one of the important aims of crystal engineering is in effect to establish correspondence between molecular and crystal structures. Based on this background, Desiraju⁷ further define the crystal engineering as

“ the understanding of intermolecular interactions in the context of crystal packing and in the utilization of such understanding in the design of new solids with desired physical and chemical properties”.

Unlike in molecular chemistry, crystal structures do not follow any explicit relationship with molecular functionality. The relationship is implicit and arises from the

complementary nature of molecular recognition, wherein the supramolecular behaviour not only depends on the functional group but also on the position and location of the other functionalities. Crystal structures can be perceived as a result of complex convolution of recognition effects⁸. Structural chemists, in order to simplify this complexity, attempt to identify the small structural unit made of robust and reproducible interaction patterns, better known as the 'supramolecular synthon'. Although the term 'synthon' was first introduced by Corey⁹ in 1967, Desiraju⁷ in 1995 further modified this and translated it to apply to the supramolecular synthon as:

“structural units within supermolecules which can be formed and/or assembled by known or conceivable synthetic operations involving intermolecular interactions”

Once identified, crystal packing can be described more accurately and efficiently utilizing the concept of supramolecular synthons, rather than tediously accumulating the knowledge of individual interaction patterns and consequently their roles towards the crystal packing. Essentially, the major aims of crystal engineering studies therefore involve the identification of these robust and reproducible supramolecular synthons.

There are several types of intermolecular interactions that can mediate molecular recognition, some of them are directional and some are not. These interactions can be broadly classified into, strong, O-H...O, N-H...O, O-H...N hydrogen bonds, and weak C-H...O, C-H...N, N-H... π (ethynyl, benzene) C-H... π (ethynyl, benzene), hetroatom interactions X...X, X...O (X=Cl, Br, I), π - π interactions and van der Waals forces. A proper understanding of directionality and strength of these hydrogen bonds and other interactions lies at the heart of controlling the target crystal structures.

As part of the ongoing Indo-UK cooperative project on crystal engineering studies between University of Durham and University of Hyderabad, I have been studying the influence of hydrogen bonds on crystal structures, as well as polymorphism and several other related topics. The complete description of the work, is beyond the scope of the thesis and we will concentrate mainly on the aminophenol series, and some of the structures of the gem-alkynol family. The rest of the work will be reported at some point later.

1.2. Methods of Studying Molecular Interactions:

As we have seen in the previous section, crystal engineering methodologies attempt to identify the common patterns in a series of crystal structures of related molecules, in order to understand these patterns in terms of mutual interplay between particular types of intermolecular interactions. A strategic study of crystal engineering would involve an analysis of a series of compounds with different substituents, or changing geometry and subsequently the understanding their effects upon identification of the supramolecular synthon. For instance, in Chapter 2, we have used several compounds with almost similar molecular structures, or some positional isomers. The major aim is to find out the structural change brought about by the molecular change, as well as to assess the robustness of the supramolecular synthon. Chapter 5, on the other hand, presents an ideal demonstration of how a single, apparently not-so-important intramolecular interaction, can consistently change the whole course of the crystal packing in a completely understandable and progressive manner. In chapter 6, we investigate the mutual properties of molecular and crystal structures by studying a series of molecules by changing a few aspects or parameters.

The study of intermolecular interaction is, therefore, of the utmost importance in crystal engineering studies. Usually four different techniques or methods, namely, X-ray and

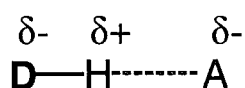
neutron crystallography, Database study, spectroscopy and computational methods are widely used for the study of intermolecular interactions.

Spectroscopic methods, especially NMR spectroscopy have become a useful tool for the study of structural properties. Although data from the spectroscopic methods are not as explicit and automated as X-ray crystallography, scientists in this field feel that a subject, what may be called “NMR Crystallography” is just a matter of time or rather an emerging subject¹⁰.

In this thesis, for structural studies, we have used mainly X-ray diffraction methods and the Cambridge Structural Database. A brief discussion of Database and X-ray diffraction study is given in section 1.4 and section 1.5 respectively.

1.3. Hydrogen Bond

A hydrogen bond can be defined as an interaction that occurs between an electropositive hydrogen atom (hydrogen atom attached to an electronegative atom) and an electronegative atom, such as oxygen, nitrogen and halogens. An oversimplified hydrogen bond can be represented as

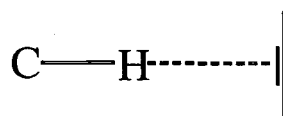
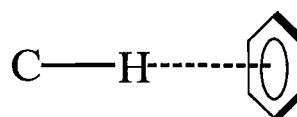
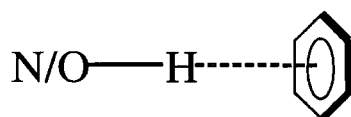
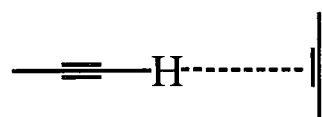
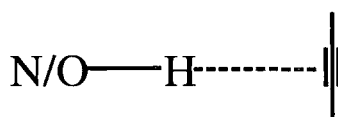


D (known as hydrogen bond donor) covalently bonded with hydrogen and A (known as hydrogen bond acceptor) is another electronegative atom or group which can provide some electron density. Initially, the studies of molecular recognition and crystal engineering in organic systems focused on the strong D-H...A hydrogen bonds, the structure defining role of which is now well understood. Other types of intermolecular interactions, such as quadrupole-quadrupole, π - π or weaker hydrogen bonds such as

C-H... π , C-H...Cl are now attracting attention. Although these interactions are individually weaker and (geometrically) less conspicuous, their combined effects can be equally important. For these types of weak interactions, often the term 'hydrogen bridge' is preferred over 'hydrogen bond', as in these interactions the hydrogen atom is attached to at least two atoms (more than two for bi-, tri-furcating hydrogen bonds), and in effect, acts like a bridge between donor and acceptor atoms¹¹.

There is, as such, no structural parameter that can be used to determine the strength of the hydrogen bonds, however two parameters, namely, bond length (donor to acceptor distance, D and acceptor to hydrogen atom distance, d) and bond angles (θ), can be used to give an indication of relative strength of the hydrogen bond. In principle, a stronger hydrogen bond should be shorter and closer to linearity and vice versa.

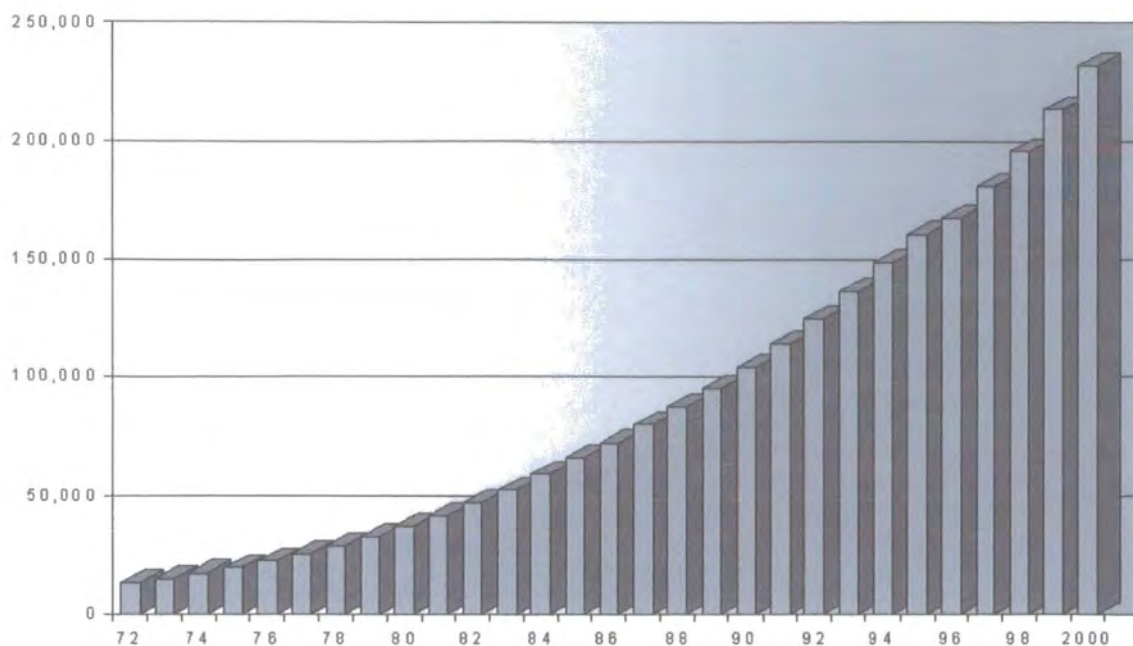
Hydrogen Bonds of Interest



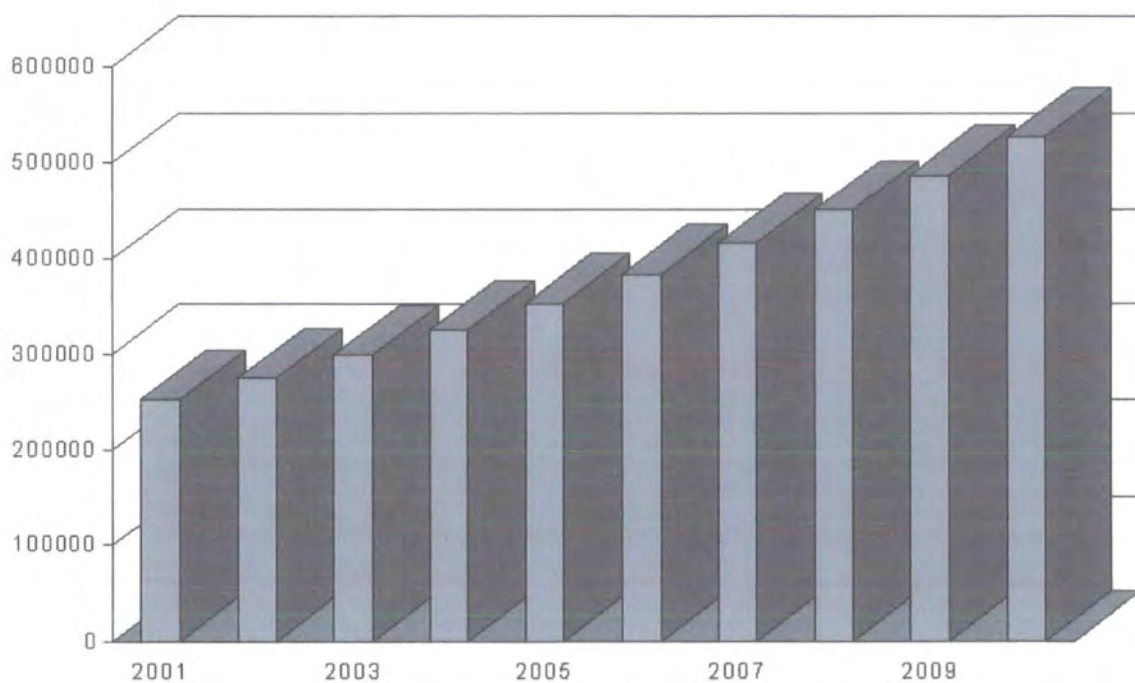
1.4. Cambridge Structural Database

In the early years of crystallography, the elucidation of a crystal structure was a time consuming process. Naturally, crystallography was used to establish, primarily, atomic position and stereochemistry, whilst crystal packing or molecular geometry were often ignored. Before the advent of computers, so-called 'Crystal Engineers' must have been nothing short of aliens. Usually bibliographic information, crystal data and atomic coordinates were recorded as a 'Structure Report' which were published by the International Union of Crystallography (IUCr). Crystal structure analysis was literally a last resort for structural characterisation. In the 1960's, improved diffractometer design and advanced automation made data collection less time consuming, consequently there was a steady increase in the number of crystal structure determinations. At the same time, hand in hand advancement of computing technology with the "Direct Method" for structure solution literally open the floodgate for crystal structure determination¹². Again development in computer technology shows the much easier and convenient option for the electronic storage of 'Structure Report'. An option, that scientists, with better foresight, like Olga Kennard, FRS were quick to realise, in particular the importance of structural knowledge for the future user community.

The Cambridge Structural Database (CSD)¹³ is the largest of the five major crystallographic databases (Table 1.1) and the database now holds over 320,000 crystal structures. However, the CSD activities are not confined to data storage only. Programs like Isostar, Gold, Superstar, Relibase+ provide fields as diverse as knowledge base research to protein-ligand interactions, while programs like DASH have become a major tool for structure determination from powder diffraction data.



(a)



(b)

Figure 1.1. (a) Growth of the CSD 1970-2000 and (b) projected growth of the CSD 2001-2010. (Figure 1.1 and Table 1.1 are reproduced from reference 12 with permission.)

The information stored in the CSD can be classified into three different sets, (i) 1D information, containing all the bibliographic information, such as author, journal, R-factors and so on. (ii) 2D information, i.e., the chemical connectivity and structural diagrams and finally (iii) in 3D level, atomic coordinates and symmetry information are stored.

As part of the long-standing collaboration between University of Durham and CSD, I was involved with two major collaborative works with CSD, namely, the study of coordination spheres of three and four coordinate species and a structural correlation study of crystal structure parameters in the CSD using theoretical calculations.

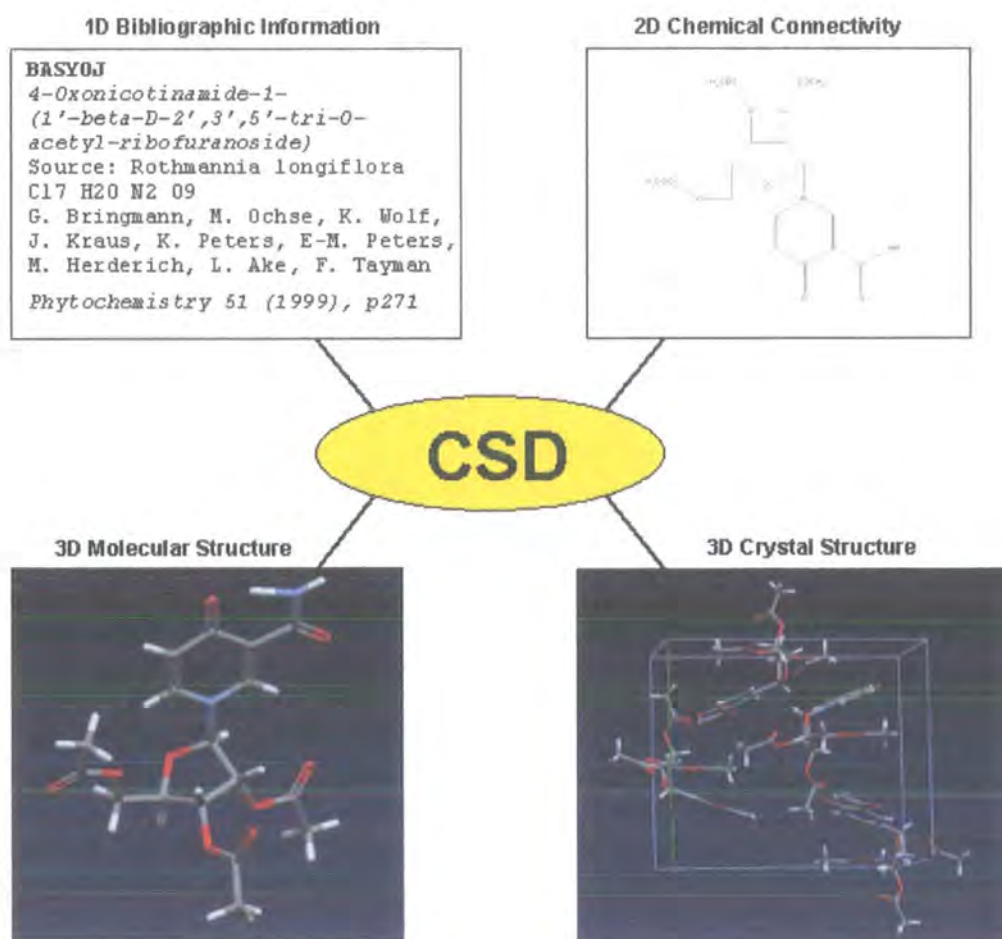


Figure 1.2. A Graphical representation of the Cambridge Structural Database (CSD).

Table 1.1. Entry statistics (April 2003) for the major crystallographic databases

Database	Chemical coverage	Structures	Annual increment
CRYSTMET® (TothCanada)	Metals, alloys and intermetallics	77242	2500
ICSD (FIZ, Germany)	Inorganic and minerals	64730	3000
CSD (CCDC, UK)	Organics and metal-organics	289164	24000
PDB (RCSB, USA)	Proteins	19673	3500
NDB (Rutgers Univ.,USA)	Nucleic acids	1636	A few

The current work concentrates on the description of the molecular coordination geometry of three-coordinate molecules, and processes involved in changing this geometry, using principal component analysis¹⁴. Detailed study of four-coordinate metal complexes and their transformation from three-coordinate species, which is the second and subsequent part of this ongoing project and theoretical calculations are beyond the scope of this thesis and will be reported at some point later.

1.5. Single Crystal X-ray Diffraction:

Molecular structure determination by X-ray was initiated, way back in *ca.*1912, from von Laue's hypothesis that X-rays are wave-like with the wavelength of *ca.*1Å, which was subsequently proved from X-ray diffraction experiments using copper sulphate single crystals by Friedrich and Knipping.

The result of this experiment started a new era of structure determination by X-ray diffraction methods. The very next year W. L. Bragg came up with the crystal structure of sodium chloride, the first crystal structure determined by X-ray methods¹⁵. Today, with all the advances structure solution theory and computer technology, allied with

invention of area detectors, crystal structure analysis has moved from being the method of last resort, to the method of choice.

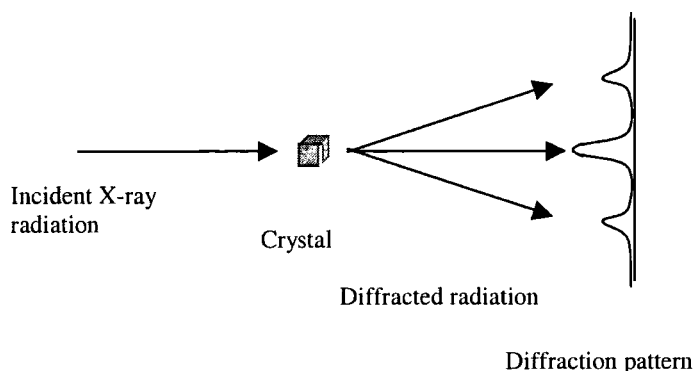


Figure 1.3. A schematic representation of a diffraction experiment of crystal.

Crystals may be regarded as being built-up by the continuing three-dimensional translational repetition of some basic structural pattern, which may comprise one or more atoms, a molecule or a complex assembly of molecules.

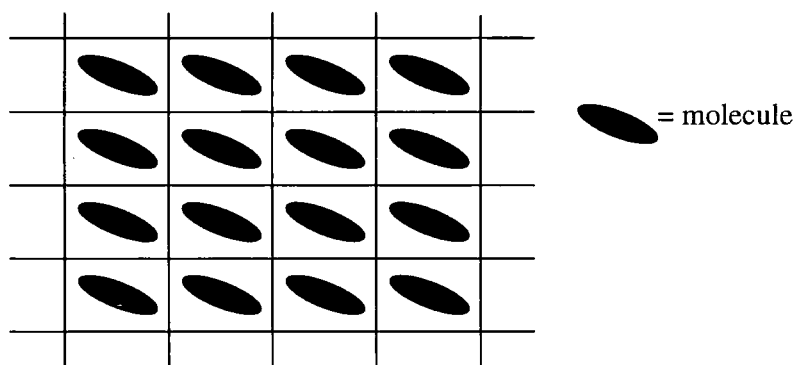


Figure 1.4. A 2-D representation of lattice with molecule sitting on it.

The smallest three-dimensional translational repeating “building block” in a crystal is called the unit cell. The replacement of each unit cell by a point leads to a crystal lattice. The difference between a crystal and lattice is that while the lattice is an array of points, the structure is an array of objects (atoms, molecules, ions).

Diffraction can be defined as the interaction of radiation with an object in space. From the basic theory of optics, we know that when light from point source passes through a narrow slit or pinhole, where the size of the hole is of the same order of magnitude as the wavelength, the beam splits. When two diffracted waves are 'in phase', i.e., with zero phase difference, there is total reinforcement, which leads to constructive interference. On the other hand, when phase difference is $\lambda/2$, the waves are 'out of phase', destructive interferences take place with no resultant wave (or a wave with zero amplitude, zero intensity).

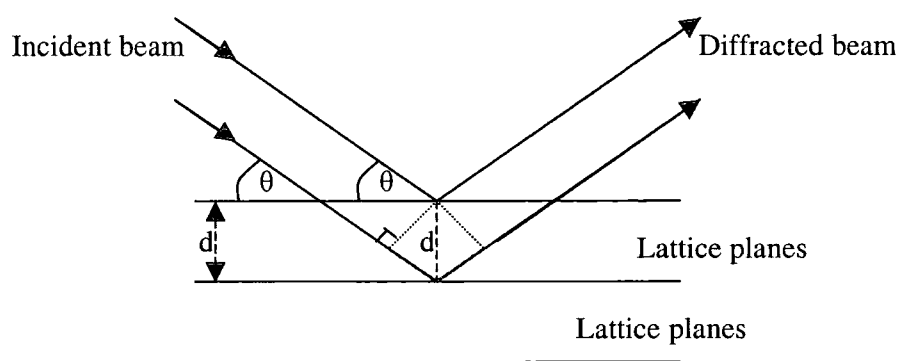


Figure 1.5. A schematic representation of Bragg's Law.

W. L. Bragg extended this principle of diffraction to crystals; he introduced the idea that the lattice planes within the crystal behave as mirrors and the diffracted beams are reflected off the lattice planes, where electrons are acting as scatterers for X-rays. The constructive interference will be observed when the path difference is equal to an integral multiple of wave length (λ), which he summarised into the famous Bragg equation,

$$n \lambda = 2d \sin\theta$$

where d is the perpendicular spacing between the lattice planes in the crystal which can be used to determine the size and the shape of the unit cell, θ is the angle of incidence of X-ray beam and n is an integer.

Figure 1.4 shows a part of computer-generated reproduction of an X-ray diffraction pattern¹⁶. The full diffraction pattern obviously is three-dimensional. The pattern shows a definite geometry, degree of symmetry in the positions as well as the intensities of the individual spots.

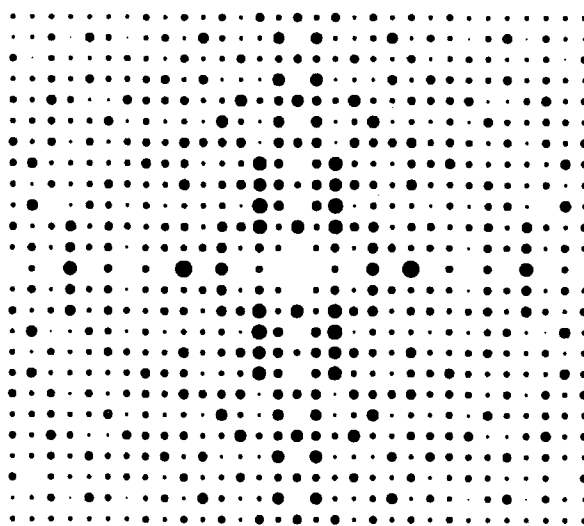


Figure 1.6. Part of an X-ray diffraction pattern

Measurement of diffraction pattern can provide us with the information about the regular arrangement of molecules in the crystal structure. While the symmetry of the diffraction pattern is related to the symmetry of individual atoms or molecules in the solid state or crystal, the intensities, which barring symmetry, do not hold any explicit relationship among themselves. However they hold information about the actual shape and orientation of the molecules, i.e., the positions of atoms in the crystal structures.

1.6. Experimental Setup:

A standard X-ray diffractometer consists of (a) an X-ray generator with a beam collimator and monochromator, for this work we used a graphite monochromator. (b) A goniometer head, upon which the crystal is mounted. It's a device for orienting the crystal by means of translational motions, and in some models, movable arcs. (c) 2 to 4 circles (for our studies 3-circles), which allow the crystal to be rotated in different orientations. (d) a beam stop (e) Detector to measure diffraction peaks.

There are two major types of detector, point detector and area detector. A point detector mainly used for four-circle diffractometers, which is designed to measure each reflection individually, naturally takes much longer time for a complete data collection. Area detectors on the other hand, can measure number of reflections simultaneously, irrespective of Bragg reflection.

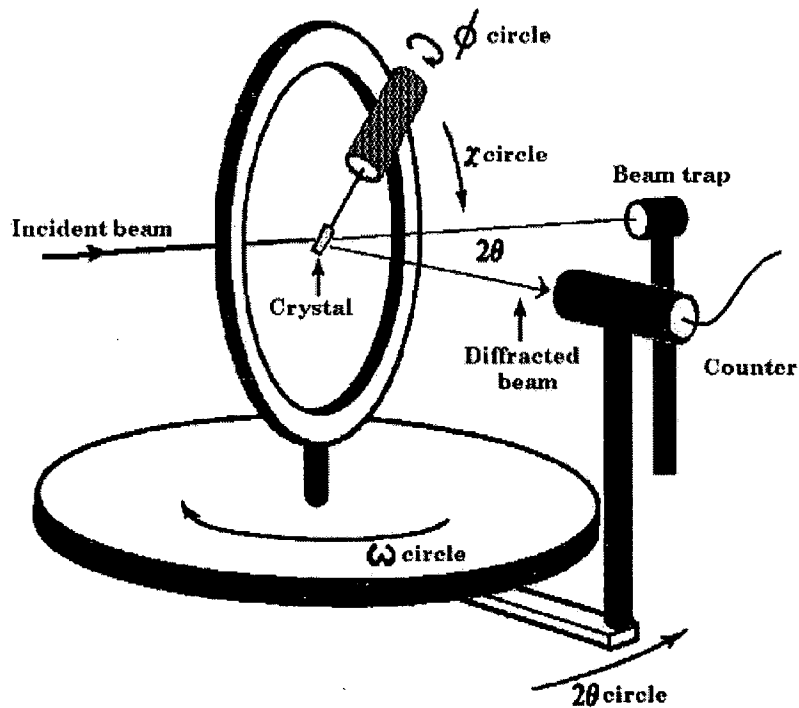


Figure 1.7. A schematic view of a four circle diffractometer.

In an X-ray diffraction experiment, the crystal is bathed in the beam produced by the X-ray source and the diffracted beam is measured by the detector (for this work, an area detector was used) while remainder of direct beam is collected by a beam stopper as represented by a schematic in Figure 1.7.

For a good structure determination, the crystal must be single, not cracked or twinned. This can be checked by examining the crystal under a polarising microscope. There is no hard and fast rule for the size of the crystal. Ideally, the crystal should be completely bathed by X-rays, the larger the crystal the greater the intensity of diffraction, but on the other hand, a larger crystal can absorb X-rays, which reduces the intensity and leads to errors in the data collected. The X-ray beams are collimated to approximately 0.8 mm in diameter and usually a crystal of less than 0.5 mm in any direction is used.

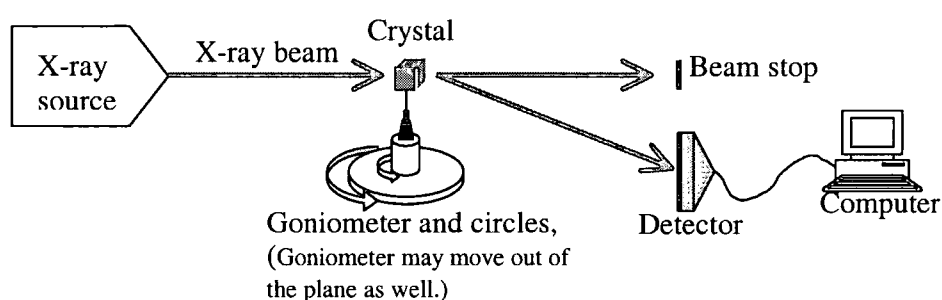


Figure 1.8. A general flow chart of the diffractometer set-up.

1.6.1. Diffractometer

Three different diffractometers, namely, SMART-1000, SMART-6000 and Apex Microsource¹⁸ are used for the experiments of this thesis. All three of these diffractometers are fitted with a charged couple device (CCD) area detector and use Mo-K α radiation with a mean wavelength of 0.71073 Å. However there are two major differences between the SMARTs and Microsource. Firstly, a phosphor coupled through fibre optics to the CCD chip is used for SMARTs, while for the Microsource the

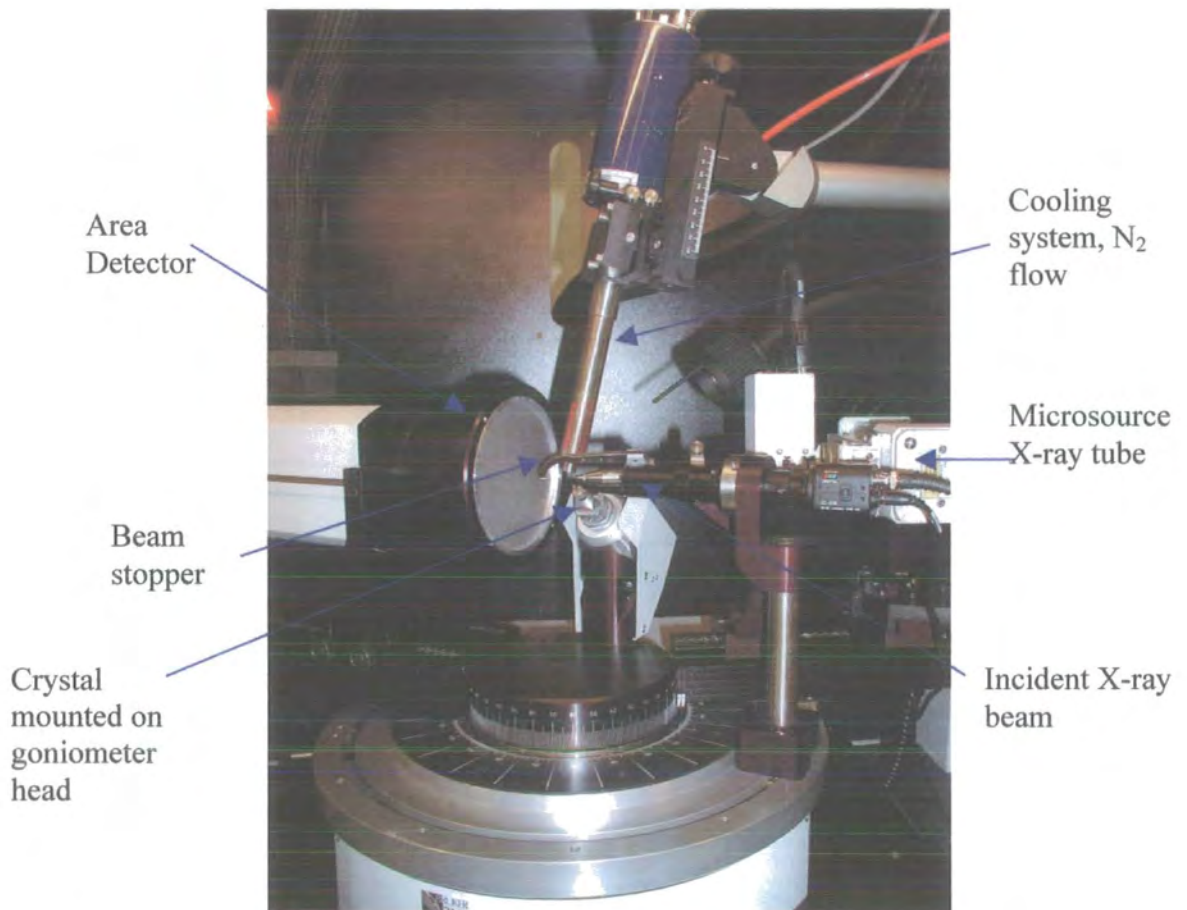
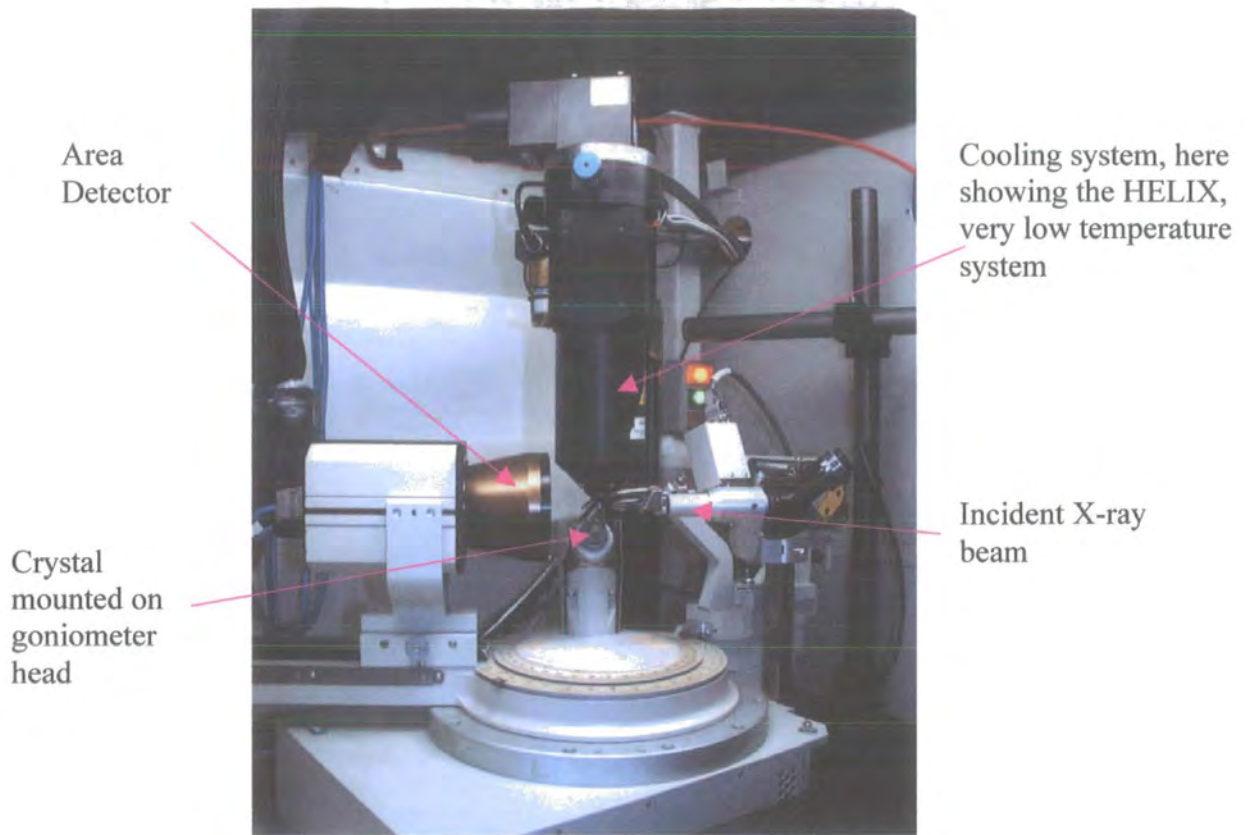


Figure 1.9. (top) SMART-1000 and (bottom) Apex Microsource diffractometer.

absence of a phosphor allegedly reduces the noise level considerably. The major difference between these two types of diffractometer is the X-ray generation. Unlike conventional X-ray tubes where the electron beam current is controlled by the current supplied to the filament, in the microsource the beam current is controlled by means of the potential difference between the cathode and an intermediate electrode, the Wehnelt or 'grid'¹⁹. The following pictures show SMART-1000 and Apex Microsource experiment set-up respectively.

1.6.2. The Cooling System:

Atomic positions can be determined more accurately by cooling the crystal during data collection. At lower temperature the vibration of atoms will be less, hence more precise position of the atoms can be achieved which in effect will give rise to higher intensity data. Again cooling is highly important for crystals with lower stability, or for solvates. For solvates, cooling can put a break on the most common problem, i.e., the loss of the solvent molecule from the lattice, resulting in polycrystalline or opaque material.

For all the work in this thesis, the cooling was obtained using Oxford Cryosystem Cryostream cold nitrogen gas cooler²⁰, which flows a stream of cold nitrogen gas over the crystal to cool it. A crystal can be cooled down to as low as 90 K using a Nitrogen cryostream.

1.7 Experimental Methods:

In all the experiments described here, SAINT+NT program was used to integrate the data and the data were further prepared using XPREP program. The initial trial structure was determined using SHELXS. SHELXL was used for further refinement and SHELXTL and XP was used for generating molecular graphics. Data were corrected for the effects of X-ray absorption where needed, using SADABS²¹.

1.7.1. Indexing:

The indexing and data collection are carried out using mostly automated software SMART. The 'real space method'²² (also known as 'auto-indexing) was used for unit cell determination and indexing. The method involves taking the three shortest non-coplanar reciprocal lattice vectors from the list of reflections and arbitrarily assigning the indices 100, 010, 001 to these basis vectors from which an orientation matrix and cell can be generated. The unit cell thus obtained not necessarily be the correct cell but it must be a sub-cell of the correct lattice as all vectors in the true lattice are also vectors in the sub-cell¹⁶. Once the correct unit cell is obtained, the unit cell parameters are then refined using a far greater number of reflections using least-square methods.

1.7.2 Data Reduction:

Once the final cell is determined, the data were reduced by integration using SAINT package. the process involved converting the raw reflection intensities into structure factor magnitudes using the following expression:

$$|F_{hkl}| = K \sqrt{\frac{I_{hkl}}{(Lp)(Abs)}}$$

Where L is the Lorentz correction, p is the polarisation correction, abs is the absorption correction and K is a scale factor. While Lorentz and polarisation corrections are geometric factors the scale factor is a combination of several factors linked to the crystal and X-ray radiation.

1.7.3. Space Group Determination and Structure Solution:

The space group symmetry of the sample was determined using XPREP programme. The software with the help of cell parameters, Laue symmetry, Bravais lattice and systematic absences, determines the correct space group.

The next step of structure determination is then to convert the structure factors to the electron density distribution $[\rho(xyz)]$ using Fourier synthesis in the following expression:

$$\rho(xyz) = 1/V \sum_h \sum_k \sum_l |F_{hkl}| \cos 2\pi [hx + ky + lz - \alpha(hkl)]$$

where $|F_{hkl}|$ are the amplitudes of the structure factors whereas $[\alpha(hkl)]$ represents the phase information, which can not derived from experimental data. The phase information can be derived by two common methods, namely, direct methods²³ and Patterson method²⁴. For the present work only direct methods are used, a brief working principle of which is described in the following section.

1.7.4. Direct Method:

Direct methods^{23,16} is a statistical method based on two major constraint, (a) non-negative electron density and (b) discrete atomic peaks. Consequently, the trial phases correspond to negative electron density and peaks of closer electron density too close to each other can be rejected. The trial procedure is repeated for the remaining phases and each solution is given a figure of merit. The phases with the best figure of merit is used to generate an electron density map from which the atomic positions can be found. Usually this enables us to determine the non-hydrogen atomic positions. The remainder of the atomic positions or missing atom positions are determined by subtracting the calculated electron density distribution (ρ_{calc}) from that of the observed distribution (ρ_{obs}) using difference Fourier synthesis:

$$\rho_{\text{obs}} - \rho_{\text{calc}} = 1/V \sum_h \sum_k \sum_l |F_{hkl}|_{\text{obs}} - |F_{hkl}|_{\text{calc}} \cos 2\pi [hx + ky + lz - \alpha_{\text{calc}}(hkl)]$$

1.7.5 Structure Refinement:

The model yielded by the structure solution is an approximate arrangement of atoms in the structure, which could be further improved by the refinement process (least squares method). Thus, structure refinement essentially improves the agreement between the observed and calculated structure factor amplitudes $|F_{hkl}|_{obs}$ and $|F_{hkl}|_{calc}$ by improving the accuracy of the atomic coordinates and the atomic thermal displacement parameters. The refinement method or least squares method aims to minimise the sum of squares of the differences between the $|F_{hkl}|_{obs}$ and $|F_{hkl}|_{calc}$ which can be represented as follows

$$D = \sum_{hkl} w_{hkl} (|F_{hkl}|_{obs} - |F_{hkl}|_{calc})^2$$

Where w_{hkl} is the weight of the reflection hkl and is a good indicator of the quality of reflections. The refinement is considered to be complete when the iteration of this process does not bring any significant change in the values of parameters, that is stable refinement has been achieved which could be judged from the R-factor or wR_2 factors.

1.8. Scope of This Thesis:

The work on this thesis can be divided broadly into two parts. The first part involves the crystallographic studies of hydrogen bonds and their role in crystal engineering, whilst the second part deals with the geometrical distortion of three-coordinate metal centres observed in crystal structures retrieved from the Cambridge Structural Database.

The first section can be further subdivided in to two halves, firstly, crystal structure prediction and role of weak hydrogen bonds therein and secondly, the extension of crystal engineering studies to the creation and study of solvates.

In chapter 2, as continuing work on the crystal engineering studies, a series of aminophenols (supraminols) and molecular complexes containing amine and hydroxy groups were investigated. The prime aim of this work was to cross check the mutual linear relationship between C-O and C-N vectors as a prerequisite for forming β -As sheet type networks. We studied crystal structures of different positional isomers where C-O and C-N vectors are not parallel. A series of molecular complexes were designed to study the much ignored area of structural homology in crystallography. And finally, novel network structures observed for this aminophenol series are described.

Chapter 3 deals with one of the most controversial topics, acceptor capabilities of organic halogens. Hydrogen bonds involving organic halogen were always considered as insignificant and of secondary importance. In this chapter, six chloro substituted gem alkynols are reported; each of these structures shows a significant and consistent O-H...Cl interaction. The attractive nature of these interactions can be corroborated by the NMR spectra. From crystal engineering points of view, the O-H...Cl shows a dominant structure-determining role and changes the supramolecular synthon in an interesting, but perfectly comprehensible manner.

The content of the Chapter 4 is somewhat different, it's more like a bridge between crystal engineering and pseudopolymorphism. The title molecule shows a unique crystallographic property. The molecule crystallised with less than optimum hydrogen bonding, which is one of the major driving forces for forming pseudopolymorphs. In the second part, six different solvates are reported.

Chapter 5 represents some rare events, namely, trapping both a higher energy conformation of a solvent, as well as a stable conformation of it in the same host. Two

different conformers, staggered and gauche conformers of diethylamine were trapped in the cis isomer of the title molecule of Chapter 4, while the diethylamine solvate with the trans isomer shows crystal structures reminiscent of the aminophenols. We also reported a discussion about the nomenclature dilemma, and supporting the term “conformation pseudopolymorphism”.

Chapter 6 is the third part of this ongoing project on pseudopolymorphism. In order to have a detailed and complete knowledge of pseudopolymorphism, we crystallised the title molecule from different amine solvents varying the size, shape number of donor amine hydrogen atoms (primary, secondary and tertiary amines). Sixteen different amine solvates are reported here showing predominantly three major supramolecular synthons, very close to those adopted by the aminophenols. The synthon that corresponds to gem-alkynol family was also observed. Several crystal engineering aspects are also discussed with an aim to bridge between main stream crystal engineering and solvates.

On the contrary, Chapter 7 deals with a completely different topic, namely the database study of the coordination spheres of metal complexes. Symmetry-modified principal component analysis has been used to visualise the geometrical distortions of three-coordinate metal centres observed in crystal structures retrieved from the *Cambridge Structural Database*. Results show that 90% of three coordinate species are accounted for by the five elements Cu, Ag, Hg, Au and Zn. Among the three major types of geometries, trigonal planar geometries dominate the data sets, with smaller contributions for Y- and T-shaped structure. For Hg^{II} complexes, a possible reaction pathway for a ligand addition reaction from the T-shaped geometries to trigonal planar is discussed in detail.

1.9. References:

1. J. Maddox, *Nature* 1988, **335**, 201,
2. J. D. Dunitz, *Pure Appl. Chem.* 1991, **63**, 177
3. J.-M. Lehn, *Angew. Chem. Int. Ed. Engl.* 1988, **27**, 89, *ibid.* 1990, **29**, 1304.
4. G. Schmidt, *Pure Appl. Chem.*, 1971, **27**, 647.
5. 'Minutes of the meeting held at Mexico City, Mexico, August 29-31, 1955', *Physical review*, 1955, **100**, 952-953.
6. D. Braga, *Chem. Comm.* 2003, 2751-2754.
7. G. R. Desiraju, *Angew. Chem. Int. Ed. Engl.*, 1995, **34**, 2311-2327. (b) G. R. Desiraju, *Crystal Engineering: The Design of Organic Solids*; Elsevier: Amsterdam, 1989.
8. (a) R. J. Davey, K. Allen, N. Blogden, W.I. Cross, H. F. Lieberman, M. J. Quayle, S. Righini, L. Seton, G. J. T. Tiddy, *CrystEngComm*, 2002, **4**, 257-264.
(b) J. A. R. P. Sarma and G. R. Desiraju, *Cryst. Growth Des.* 2002, **2**, 93-100.
(c) P. K. Thallapally, A. K. Katz, H.L. Carrell, G. R. Desiraju, *Chem. Comm.* 2002, 344-345.
9. (a) E. J. Corey, *Pure Appl. Chem.* 1967, **14**, 19, (b) E. J. Corey, *Chem. Soc. Rev.*, 1988, **17**, 111. (c) E. J. Corey, X.-M. Cheng, *The Logic of Chemical Synthesis*, Wiley, New York, 1989.
10. R. K. Harris, lecture presented at International School of Crystallography, Erice, Italy, June 9-20. 2004.
11. G. A. Jeffrey, *An Introduction to Hydrogen Bonding*, Oxford University Press, Oxford, UK, 1997
12. F. H. Allen, *Crystallography Reviews*, 2004, **10**, 3-15
13. (a) F. H. Allen, O. Kennard, *Chem.Des.Autom.News.*1993, **8**, 30-37, (b) F. H. Allen, *Acta. Cryst.* 2002, **B58**, 380-388.

14. F. H. Allen, R. Mondal, N. A. Pitchford, J. A. K. Howard, *Helv. Chim. Acta*, 2003, **86**, 1129-1139.
15. (a) J. P. Glusker, K. N. Trueblood. *Crystal Structure Analysis, A Primer*. New York, Oxford: Oxford University Press. 1985. (b) J. P. Glusker, M. Lewis, M. Rossi. *Crystal Structure Analysis for Chemists and Biologists*. New York, Wienheim, Cambridge: VCH Publishers. 1994. (c) C. Giacovazzo, ed. *Fundamentals of Crystallography*. New York, Oxford: International Union of Crystallography, Oxford University Press, 1992
16. Notes from: The Ninth BCA Intensive Teaching School in X-Ray Structure Analysis. University of Durham. April 6th–15th, 2003.
17. SMART-1000, SMART-6000 CCD, Bruker AXS, Madison, Wisconsin, U.S.A.
18. Microsource X-ray generator, Bede Scientific Instrument Limited, Durham, UK.
19. Microsource X-ray generator manual, Bede Scientific Instrument Limited, Durham, UK.
20. Cryostream Cooler, Oxford Cryosystems Ltd, Oxford, UK.
21. G.M. Sheldrick, (1997). SHELXS-97, SHELXL 97. Program for the Refinement of Crystal Structures. University of Göttingen, Germany. G. M. Sheldrick, (1998). SHELXTL Version 5.1. Bruker AXS., Madison, Wisconsin, U.S.A.
22. (a) W. Clegg, *J. Appl. Cryst.*, 1984, **17**, 334. (b) R. A. Sparks, *Crystallographic Computing Techniques*, ed. F.R.Ahmed, Munskgaard, Copenhagen, 1976, 267-452, (c) R. A. Sparks, *Crystallographic Computing*, ed. D. Sayre, Clarendon Press, Oxford, 1982, 1-18.
23. (a) D. Harper, J. S. Kasper, *Acta. Cryst.*, 1948, **1**, 70. (b) J. Karle, H. Hauptmann, *Acta. Cryst.*, 1950, **3**, 181. (c) D. Sayre, *Acta. Cryst.*, 1952, **5**, 60.
24. A. L. Patterson, *Phys. Rev.* 1934, **46**, 372-376.

Chapter 2

**Molecular Recognition Among Alcohols and Amines. Novel
Carborundum Network in a Supramolecular Homologous
Series.**

2.1. Introduction

One of the major aims of crystal engineering is to draw some correspondence between molecular functionality and the crystal structures¹. Unlike in molecular chemistry, crystal structures do not follow any explicit relationship with molecular functionality. The relationship is implicit and arises from the complementary nature of molecular recognition, wherein the supramolecular behaviour not only depends on the functional group but also on the position and location of the other functionalities. Crystal structures can be perceived as a result of complex convolution of recognition effects². Structural chemists, in order to simplify this complexity, attempt to identify the small structural unit made of robust and reproducible interaction patterns, better known as the 'supramolecular synthon'³. Once identified, crystal packing can be described more accurately and efficiently utilizing the concept of supramolecular synthon, rather than tediously accumulating the knowledge of individual interaction patterns and consequently their roles towards the crystal packing. Indeed, usage of supramolecular synthons adds a whole new dimension to those of existing contemporary methodologies for exploration of crystal packing.

The Cambridge Structural Database (CSD)⁴, with a huge pool of 'ready-made' crystal structures, evolves as the most useful tool for the characterisation of supramolecular synthons, and for most of the functional groups or sets of functional groups they are now well documented.

2.2. Amine-Alcohol recognition

The family of aminophenols or supraminols, because of their unique complementary nature, offers enough supramolecular diversity to explore the relationship between molecular functionality and crystal packing. With one hydrogen bond donor and two acceptor sites, -OH group is the perfect complementarily to the -NH₂ group that

contains two hydrogen bond donor and one acceptor site⁵. This permits a complete saturation of hydrogen bonding sites, resulting in a supertetrahedral network as elegantly pointed out by Ermer and Eling⁵ and independently by Hanessian and co-workers⁶. It has been noticed immediately that stoichiometry of the amine and hydroxyl group is also an important factor. In principle, for a 1:1 alcohol-amine complexes there could be 50% increase in the number of hydrogen bonds compared to that of uncomplexed constituents. That is, while individually two amine groups or two hydroxyl groups can fulfil potential of two hydrogen bonds, a binary mixture of 1:1 supraminols can form up to three hydrogen bonds with complete saturation of hydrogen bond potential. In compounds like archetypal 4-aminophenol⁵, such a saturation of hydrogen bonds form a sheet type structure where N-H...O and O-H...N [or N(H)O] bonds are arranged in a hexagonal manner, which can also be perceived as the chair form of a cyclohexane ring (Figure 2.1). The phenyl rings or the aryl rings, connect these sheets to complete the structure. This kind of network, due to its very close topological resemblance to the sheet type structures of β -arsenic, is often referred to as the β -As sheet or network, and henceforth we will use the same description. Even though some other supramolecular synthons are also observed for supraminols, the β -As sheet remains the most interesting one, mainly because of the 50% increase in hydrogen bonds resulting from the more hierarchical arrangement and less structural interference between molecular functionalities⁷.

Recently we have investigated a series of aminophenols⁸, varying the length of the linker group (-CH₂) between the two benzene rings and varying the position of the functional groups, in order to study in-depth relationship between the molecular structures and the packing pattern. Out of several interesting findings, we observed an interesting relationship between the length of the linker group (CH₂-) and the structural type adopted by the molecule. The β -As network was observed for those molecules

containing an even number of linker group, but not for odd numbers. A closer investigation into this intriguing observation revealed that, while for the molecule with even numbers of linker groups the orientation of the amine and hydroxyl groups becomes almost linear, they are considerably bent for molecules with an odd numbers of linker groups. In other words, the saturation of hydrogen bond potential and therefore resulting β -As networks appeared for those supraminols wherein the C-O and C-N vectors are nearly parallel in the molecular structures, just as in 4-aminophenol. On the contrary, when C-O and C-N vectors are not parallel, with odd numbered linker group, crystal packing become much more complex in nature and less predictable. For these kind of molecular systems an infinite cooperative arrangement of O-H...N-H...O or a centrosymmetric square motif with N(H)O bonds often appears to

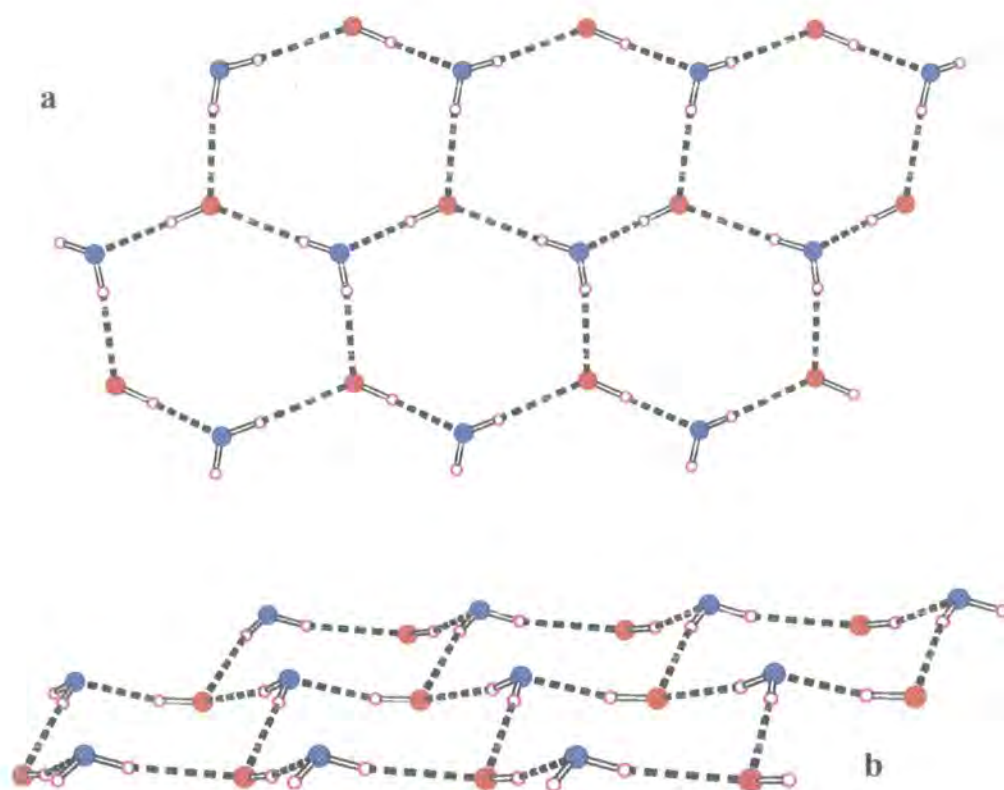


Figure 2.1. β -As Sheets in (a) hexagonal (b) cyclohexane chair network formed by the complete saturation of hydrogen bond potential of amine and hydroxyl groups.

be the dominant interaction pattern. Saturation of hydrogen bond potential seldom occurred for these molecules and often some weaker interactions like N-H... π is observed⁹.

Although for most of the supraminols the β -As network is formed when the C-N and C-O vectors are linear, we found the crystal structure of 4-(4-aminophenoxy) phenol (**1**) to be an exception. It forms a β -As network even though it's a bent molecule with an angle of 141° between C-N and C-O vectors⁸. A considerable amount of out-of-plane (of the phenyl rings) displacement of oxygen atoms as well as amine and hydroxyl groups, force it to shift from the expected 120° for the C-O-C bond. This observation is further supported by the presence of relatively strong C-H...O bonds, that are usually absent or insignificant for supraminols.

The crystal structure seemed to be unique and to deserve further investigation and hence prompted this study. However, compound **1** itself does not provide much scope for further studies. To bypass this difficulty we took help from so-called supramolecular equivalents, which would enable us to manipulate interaction similarities with topologically equivalent functional groups¹⁰.

It has been noted earlier that when dianilines and diphenols form stoichiometric binary crystals, the resultant structures are primarily governed by the principles of amine-hydroxy recognition rather than precise location of the functional groups.

For example, the 1:1 molecular complex of hydroquinone and p-phenylene diamine forms a similar β -As network to the 4-aminophenol. Similarly, the 4,4'-dihydroxybiphenyl and 4,4'-diaminobiphenyl 1:1 molecular complex, adopts a crystal structure closely resembling 4-hydroxy-4'-aminobiphenyl^{5,6}.

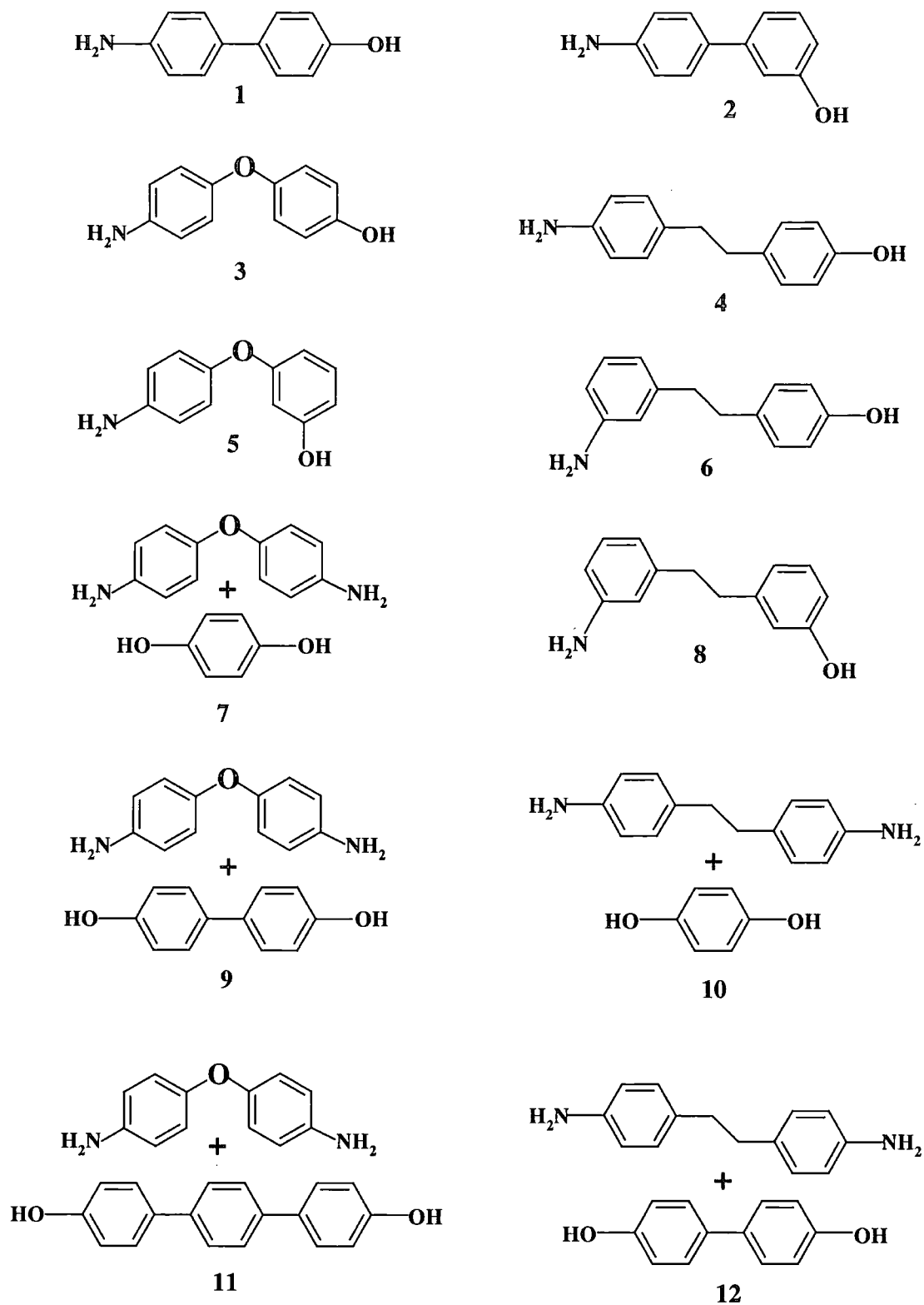
Keeping this in mind, we carried out co-crystallisation experiments of dianiline and diphenols, with an expectation of similar crystal packing (**Scheme 2.I**). Consequently the results of this particular study are important for the three following points, as will be

discussed in subsequent sections.: (1) crystal structure prediction, (2) structural homology and (3) novel network structures.¹¹

2.3. Crystal structure prediction:

Are crystal structures predictable?¹² Although the answer is far from being affirmative¹³, it single-handedly produced more areas of research than anything else in the crystallographic field, namely crystal engineering, crystal designing and so on. Among the numerous events and workshops on crystal structure predictions, the Cambridge Crystallographic Data Centre (CCDC) every alternate year organizes a 'blind test' on three unknown compounds. In these tests, some selected experts in the field are given a task to predict the crystal structures. Even with the most advanced automation and methodologies, the success rate of these predictions, predictably turns out to be a long way off from consistent or reliable predictions¹⁴.

On the contrary, among some of the optimistic aspects, it has been found that under some highly specified conditions crystal structure can be predicted or at least some of the predictions do appear to be true. One such structural prediction of Ermer and Elling is directly related to the present study. They show for some simpler aminophenols, wherein the C-O and C-N vectors are nearly parallel, the β -As structure is formed. Further research on supraminols¹⁵ upholds a general guideline that any aminophenol OH-Ar-NH₂ that forms a β -As sheet structure may be expanded into a 1:1 binary molecular complex of diphenol (OH-Ar-OH) and dianiline (H₂N-Ar-NH₂). Apparently, we are dealing with two different sets of molecules (**Scheme 2.I**), a set of supraminols (H₂N-Ar-OH) and 1:1 molecular complexes of dianilines and diphenols (HO-Ar-OH & H₂N-Ar-NH₂). In this work, we attempt to find out whether aminophenols form β -As networks when C-O and C-N vectors are not parallel, and for molecular complexes, again our aim is to find out whether the above-mentioned guidelines hold.



Scheme 2.I Schematic representation of the supraminols and the 1:1 molecular complexes of interest for these studies.

In our earlier studies⁸, we found a β -As network for 4-hydroxy-4'-aminobiphenyl, **1** and **3**. In order to cross check the precondition of mutually parallel donor acceptor vectors, we studied aminophenols (**2**, **5**, **6**, **8**) where the functional groups are not in their usual *para* position and henceforth are not parallel.

As expected, none of these structures adopt the β -As network nor do the saturation of hydrogen bond potentials take place. Crystal structure of **2** immediately shows the importance of the mutual linearity of C-O and C-N vectors for adopting β -As network;

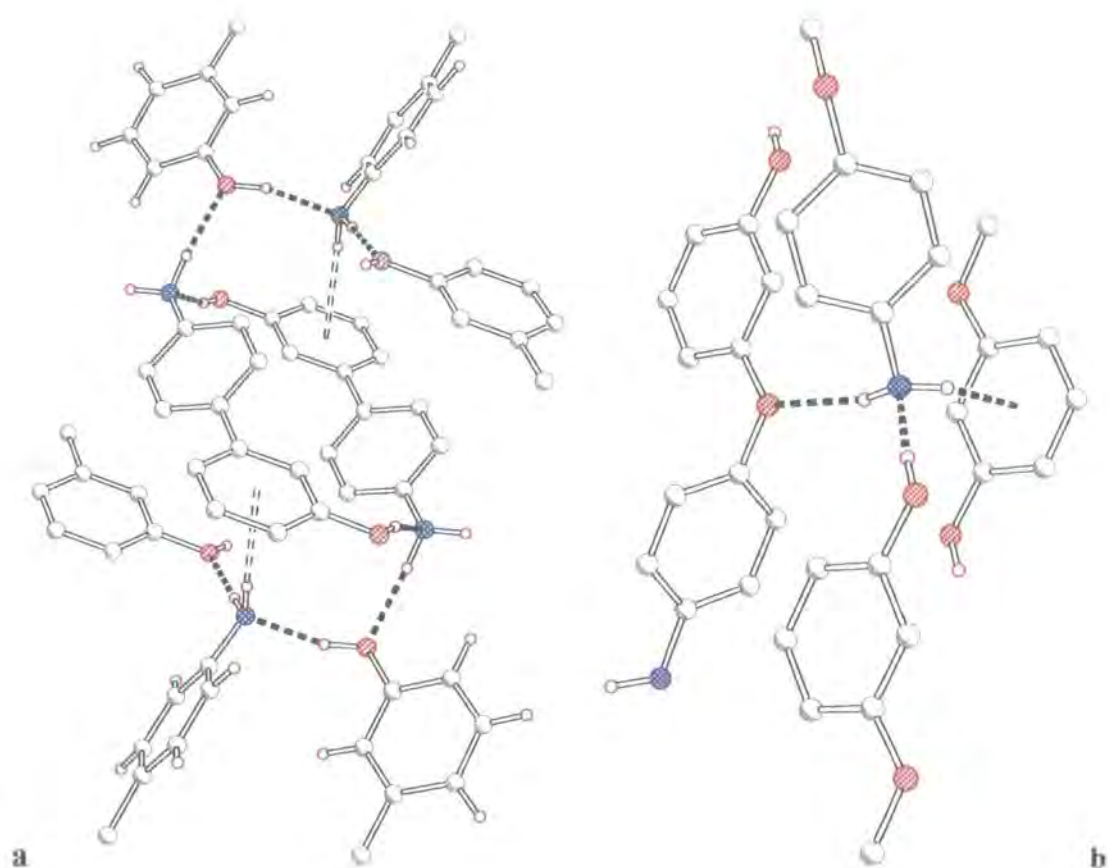


Figure 2. 2 (a) crystal structure of **2** showing infinite cooperative network of N-H...O-H...N, supported by N-H... π interaction. (b) Crystal structure of **5**, where the amine group forms a N-H...O bond with the phenoxy group and not with the hydroxy group. Note that for clarity, all the full molecules were not shown in the pictures and some hydrogen atoms were omitted.

while both 4-aminophenol and **1** both adopt a β -As network, for **2** it shows a infinite cooperative network of O-H...N-H...O bonds⁸, with a second amine hydrogen forming a weak N-H... π bond (Figure 2. 2a). Although crystal packing of **5** is closely related to **2**, nonetheless, there are some subtle differences. The major reason attributed for **3** forming the β -As network, a supporting C-H...O bond, is absent here. Instead the amine group forms a N-H...O bond with the phenoxy oxygen and not with the hydroxy oxygen (Figure 2.2b), which then immediately rules out the mutual saturation of hydrogen bond potential of the supraminol moiety.

Crystal structures of **6** and **8** further vindicate the mutual relationship between linearity of C-O and C-N vectors and saturation of hydrogen bond potential of the supraminol moiety. Likewise in **2** and **5**, again in **6** and **8** are two positional isomers of **4**, that show complete saturation of hydrogen bonds. While in **6** the amine group is at the *meta* position with respect to the linker group, in **8** both the hydroxy and the amine groups are at *meta* positions to the linker group. The change in crystal structures brought about by the change in position of the functional group, is clearly evident from the corresponding crystal structures. Unlike **4**, neither **6** nor **8** show the β -As network in their crystal packing. The crystal structure of **6** is analogous to that of **2** with a similar infinite cooperative N-H...O-H...N bond alongside a weaker N-H... π interaction. The crystal packing of **8**, on the other hand is totally different, wherein a centrosymmetric square synthon⁸ dominates the packing with a supportive N-H... π interaction (Figure 2.3). It is interesting to observe how some simple changes of the functional groups in these three positional isomorphs, result in three wildly different crystal packing arrangements.

In all these aminophenol structures, the less than predictable crystal packing and the absence of the β -As network, vindicate the prerequisite linearity of C-O and C-N vectors for easy crystal structure prediction.

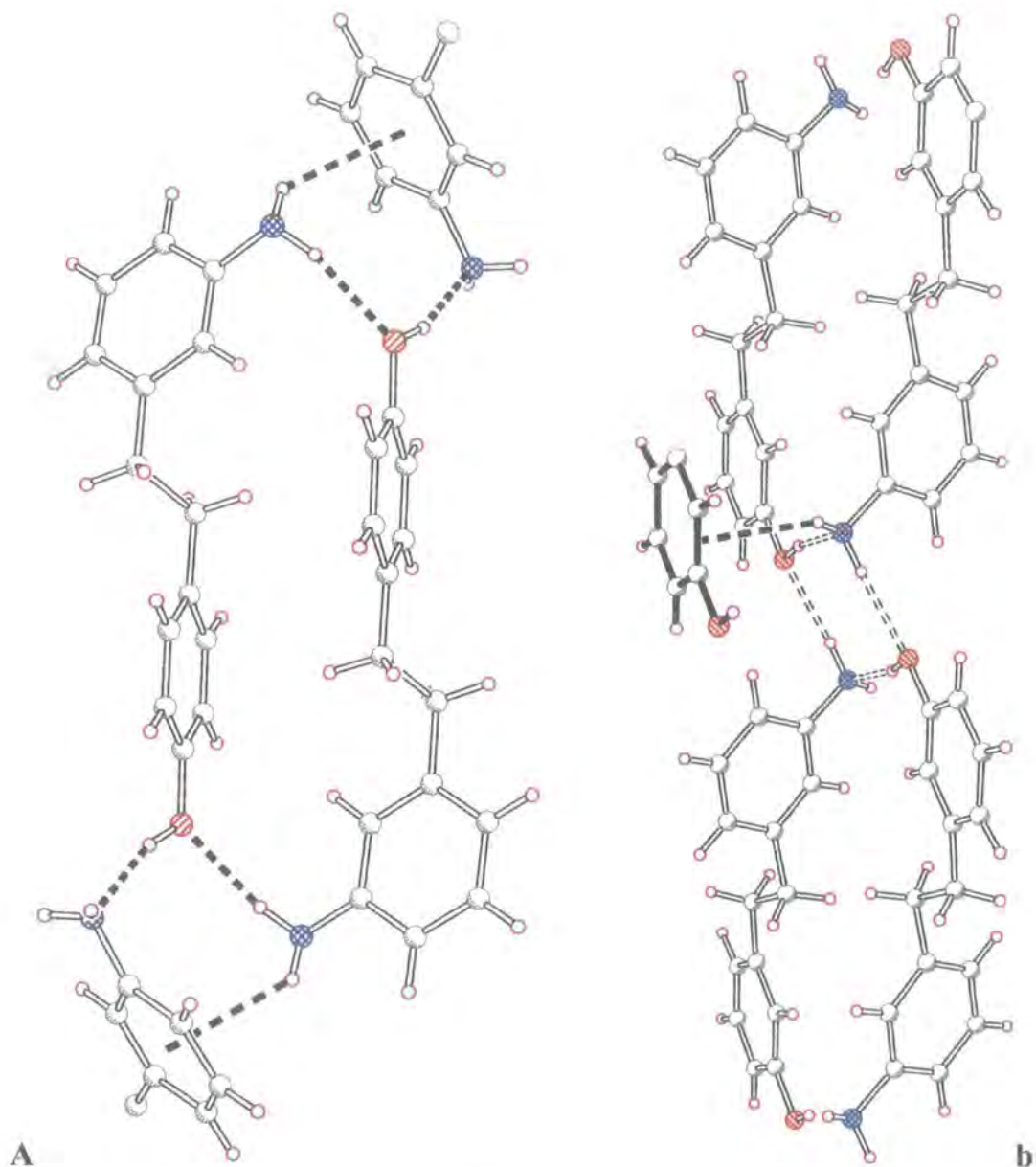


Figure 2.3. (a) crystal structure of **6** showing an infinite cooperative network of N-H...O-H...N, supported by N-H... π interaction. (b) crystal structure of **8**, showing a supramolecular square synthon with N-H... π interaction

Attention was shifted therefore to the binary molecular complexes, to investigate whether the β -As network can be extended into molecular complexes of diphenol and dianilines, if it appears for the corresponding aminophenols.

It is astonishing to see that all the binary complexes (**7**, **9-12**) form β -As sheet structures corroborating our earlier supposition. What is more impressive about the binary complexes is that structural repetitivity is observed in much more unusual supraminols

Table 2.1. Crystallographic data and structure refinement parameters of aminophenols.

	2	5	6	8
Empirical formula	C ₁₂ H ₁₁ O N	C ₁₂ H ₁₁ O ₂ N	C ₁₄ H ₁₅ O N	C ₂₈ H ₃₀ N ₂ O ₂
Formula wt.	185.22	201.22	213.27	426.54
Crystal System	Monoclinic	Monoclinic	Monoclinic	Triclinic
Space group	C2/c	P2(1)/c	P2(1)/c	P-1
<i>a</i> [Å]	32.3064(10)	8.2533(2)	5.9323(3)	5.3735(4)
<i>b</i> [Å]	6.0512(2)	9.0448(2)	22.7220(12)	8.6715(7)
<i>c</i> [Å]	24.6972(8)	13.7207(3)	8.3110(5)	12.6645(10)
α [°]	90	90	90	90.196(3)
β [°]	130.022(3)°	98.961(1)	96.746(2)	98.620(3)
γ [°]	90	90	90	94.567(4)
<i>Z</i> '	1	1	1	1
Volume [Å ³]	3697.4(2)	1011.74(4)	1112.51(11)	581.53(8)
D _{calc} [g/cm ³]	1.331	1.321	1.273	1.218
μ [mm ⁻¹]	0.085	0.091	0.080	0.077
2 θ [°]	3.30 to 55	5.415 to 55	3.58 to 55	4.72 to 55
Range <i>h</i>	-41 to 41	-10 to 10	-7 to 7	-6 to 6
Range <i>k</i>	-7 to 7	-11 to 11	-29 to 29	-11 to 11
Range <i>l</i>	-32 to 32	-17 to 17	-10 to 10	-16 to 16
Reflns. collected	20625	10899	11494	7923
Unique reflns.	4235	2327	2557	2653
Obs. reflns.	3225	1938	1686	1503
<i>R</i> ₁ [<i>I</i> > 2 σ (<i>I</i>)]	0.0391	0.0366	0.0442	0.0466
w <i>R</i> ₂ [all]	0.0955	0.0884	0.0934	0.1205
Goodness-of-fit	1.028	1.042	0.977	0.928
Crystal size mm ³	0.40 x 0.18 x 0.08	0.32 x 0.26 x 0.08	0.18 x 0.08 x 0.04	0.32 x 0.26 x 0.18
Largest diff. peak and hole (e.Å ⁻³)	0.263 and -0.220	0.216 and -0.193	0.271 and -0.248	0.159 and -0.145

(7, 9, 11), which are far from being linear. Interestingly, the reason that was ascribed for the stabilization of the β -As structure in 3 (C-H...O hydrogen bonds) is also valid for 7, 9 and 11. All of them have relatively strong C-H...O bonds of (d , θ) 2.51 Å, 135°, 2.48 Å, 136° and 2.50 Å, 135° respectively, within the dianiline component. This result indicates that insulation of hydrogen bonded and hydrophobic regions is a valuable attribute and can lead to easy crystal structure prediction. As in the present case, the hydrocarbon regions act as the spacers between β -As sheets and lead to distinct structural insulation from each other and in the end it matters little whether the ends of the molecules have two -OH groups, two -NH₂ groups or one -OH and one -NH₂ group.

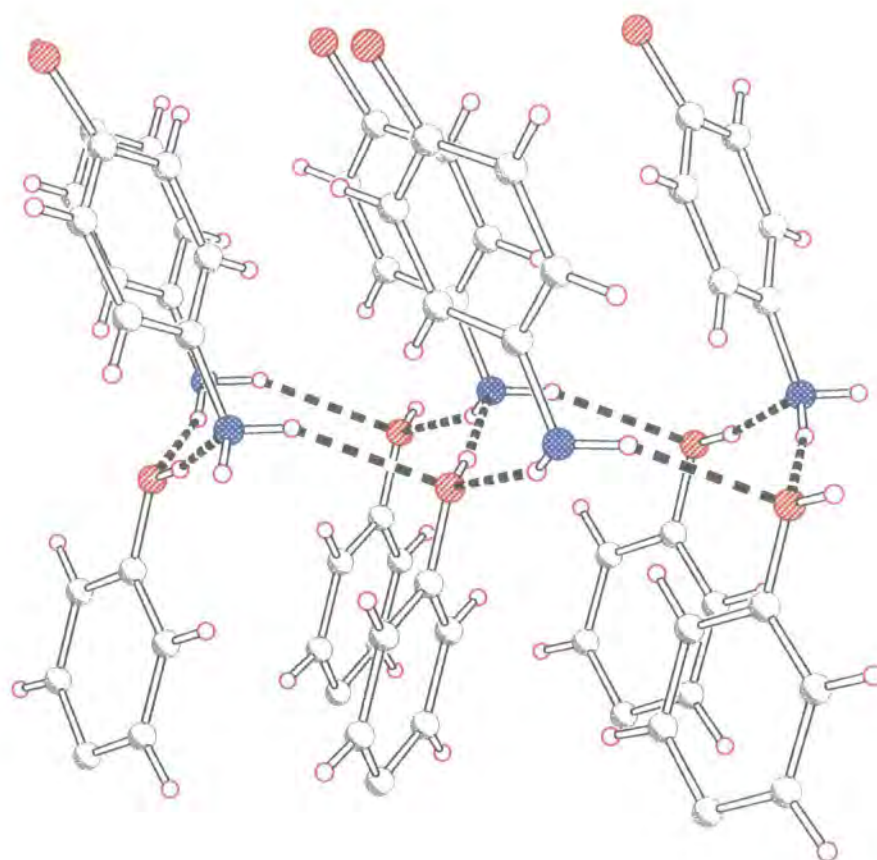


Figure 2.4 Crystal packing of 9. Notice cyclohexane chair network of β -As sheets by complete saturation of the hydrogen bond potential of the diamine and diphenol component

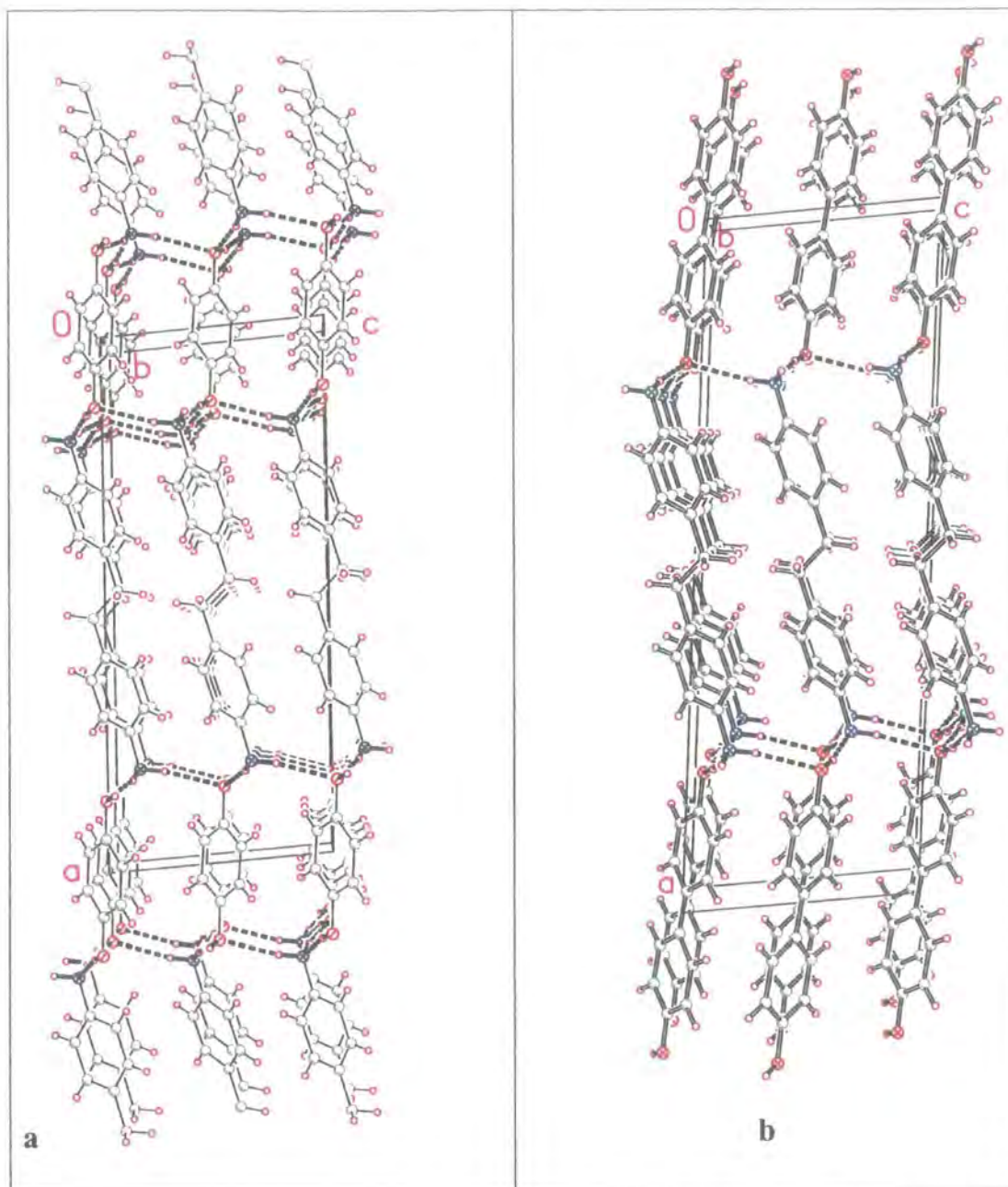


Figure 2.5 crystal packing of (a) **10** and (b) **12** showing β -As structure, Notice the zinc blende network (Section 2.5) formed by both molecules.

2.4. Structural homology:

Structural homology in organic molecules is a well known and much studied phenomenon. On the other hand, supramolecular homology in molecular solids has been discussed ever since the beginnings of X-ray crystallography albeit there are

surprisingly few well-documented examples¹⁶. One such example would be the attempt made by Desiraju and Gavezzotti¹⁷, wherein they analysed the crystal structures of a group of 32 polynuclear hydrocarbons. Among the other findings, they highlighted three important points, (i) based on their shortest crystallographic axis (those 32 hydrocarbons may be classified into four different groups, (ii) the relative contribution of carbon and hydrogen atoms to the molecular surface area play a crucial role in determining the packing type and (iii) it is possible to predict the packing type for any pure polynuclear hydrocarbon from its structural formula alone. Out of those 32 polynuclear polyhydrocarbons, three molecules that form a homologous series (benzene, diphenyl and p-terphenyl) are directly relevant to the present study. These compounds are analogous to the diphenol components in **7**, **9-12**. The idea is to keep one of the components of the binary complexes the same while changing the other component that could form a homologous series. We tried with two different series, one with **7**, **9** and **11**, another with **10,12**. So far we were unable to produce crystals for the molecular complex with p-terphenyl of the second group.

The present work is in a remarkable agreement to the supposition of Desiraju and Gavezzotti, that for a homologous series, the unit cell parameters, in particular one of the cell axes is a unique indicator and regulator. For **7**, **9** and **11**, all the three crystals show some unique resemblances, namely, all of them grew in space groups Pbcn, with the diphenol component lying on a $\bar{1}$ position and the dianiline molecule on a 2-axis. From the cell parameter point of view, the *a* and *b* axial values are almost same in the three cases leaving the *c* axis as the possible unique indicator of homologous series. The *c* axis values increase from 35.145 Å to 43.441 Å to 51.773 Å for **7**, **9** and **11** respectively. This equal amount of increase in *c* axis by ~8.3 Å can be attributed to the increase in length of the corresponding phenylene spacer. In the other series, **10** and **12**, both of them were crystallised in space group P2₁/n. Amazingly, the *b* and *c* axis values

are almost same and they are the same as the values of *a* and *b* axis of the first series (**7**, **9** and **11**). Effectively the unique regulator of the homologous series turn out to be the *a* axis, which increases from 19.487 Å to 23.712 Å, corresponding to the increase in phenylene spacer. We expect that the third compound of this series would crystallise in the same space group with an *a* axis of ~28 Å, and with similar *b* and *c* axes to **10** and **12**.

The observation is highly unusual. A simple search on CSD will place this unusual result in perspective. We searched for molecular complexes that contain diphenols corresponding to those in **7**, **9** and **11**. There is no reported adduct of the diphenol contained in **11**. Five pairs of molecular complexes were observed for two other diphenols. Out of them, no structural homology was observed in three pairs (COHWIF/NISLOQ, FOQHEY/FOQHOI, GUSSES/GUSRER). Interestingly, two other pairs (PITYAS/PITYIA, PITYEW/PITYOG) that do show homology are from the aminophenol family and have the β -As sheet structures! These revelations once again bring in the topic of insulation of hydrogen bonded groups by the hydrocarbon spacer groups. As we have witnessed earlier, the structural insulation is an important criterion for the β -As network to be formed and the supramolecular homology clearly follows from this structural insulation. Only if the hydrocarbon and hydrogen bonded regions in these crystals were well insulated would such phenyl \rightarrow biphenyl \rightarrow terphenyl homology be possible. Apparently, the hydrocarbon regions of the spacer groups of aminophenols crystal packing, reciprocate to that of the pure hydrocarbons. To conclude, since benzene, biphenyl and p-terphenyl form a structural homologous series¹⁷, the same hold true for **7**, **9** and **11**. We expect the third compound of **10** and **12** series to follow the trend and the same should be true as well.

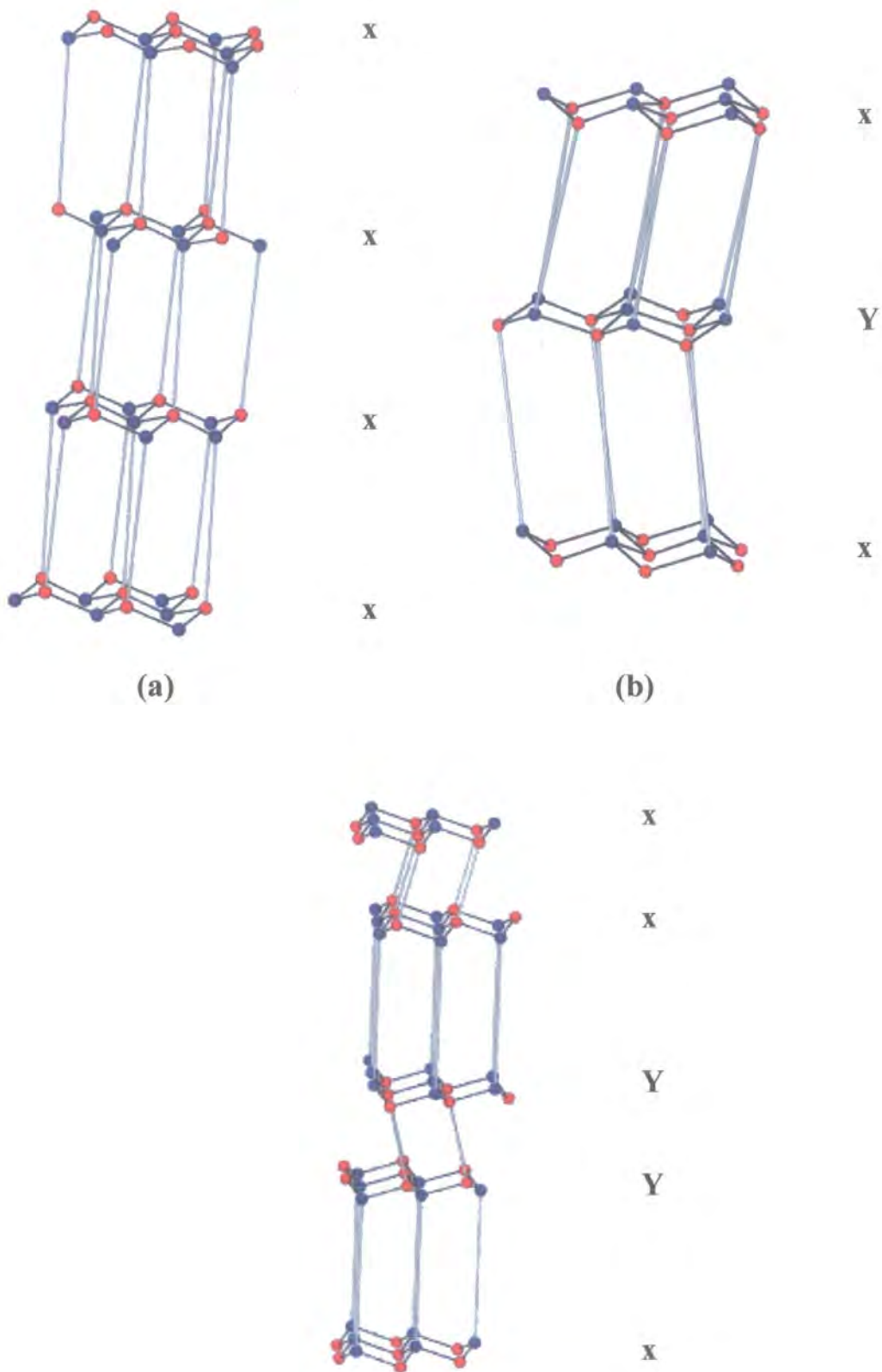


Figure 2.6. Network depictions of (a) Aminophenol 3 (and 10, 12), zinc blende; (b) 4-Hydroxy-4'-aminobiphenyl 1, wurtzite; (c) Molecular complexes (7, 9 and 11), carborundum III. Hydrogen bonds are shown as dark lines and the molecular connections are shown in grey. Notice the X and Y designations of the hydrogen bonded β -As sheets.

2.5. Aminophenols show novel network structures:

Drawing analogies between organic and inorganic crystal structures in terms of network properties has proved often to be useful for crystal engineering studies¹⁸. With the help of a recognised network, it is often easier to rationalise a crystal structure which otherwise may be highly complex in nature. Extensive usage of the diamondoid or β -As network in crystal packing descriptions only further emphasizes this.

In the present context, for aminophenols, the spatial relationship between the β -As sheet structures offers enough diversity for different possible networks. As shown in Figure 2.6, the hexagonal networks (as designated by **X** and **Y**) are based on the conformational preference of the “supramolecular chair cyclohexane” of hydrogen bonds. For example, the zinc blende (cubic ZnS) network is obtained when **X** sheets are arranged in offset manner, while the far less common wurzite (hexagonal ZnS) network arises when **X** and **Y** sheets alternate in an eclipsed manner¹⁹. Previously, the zinc blende network was obtained for **3**⁸, while the wurzite network was seen for **1**. In the present work, again, zinc blende network appeared for **10** and **12** (Figure 2.5). However, for the other series, **7**, **9** and **11**, a unique network is observed, wherein alternation of two **X** sheets and two **Y** sheets create a network that contains both zinc blende and wurzite topologies within the same structures (Figure 2. 7). Most of the networks for organic molecules mimic either zinc blende or wurzite topologies, but the presence of both in the same molecule has not hitherto been observed. This kind of network corresponds to the carborundum III polytype of SiC²⁰, notwithstanding, such a network is unprecedented in molecular solids. So why does such an unusual network arise? A closer investigation suggests that the occurrences of the carborundum network in the crystal structures are predominantly symmetry controlled. Crystallographically, the

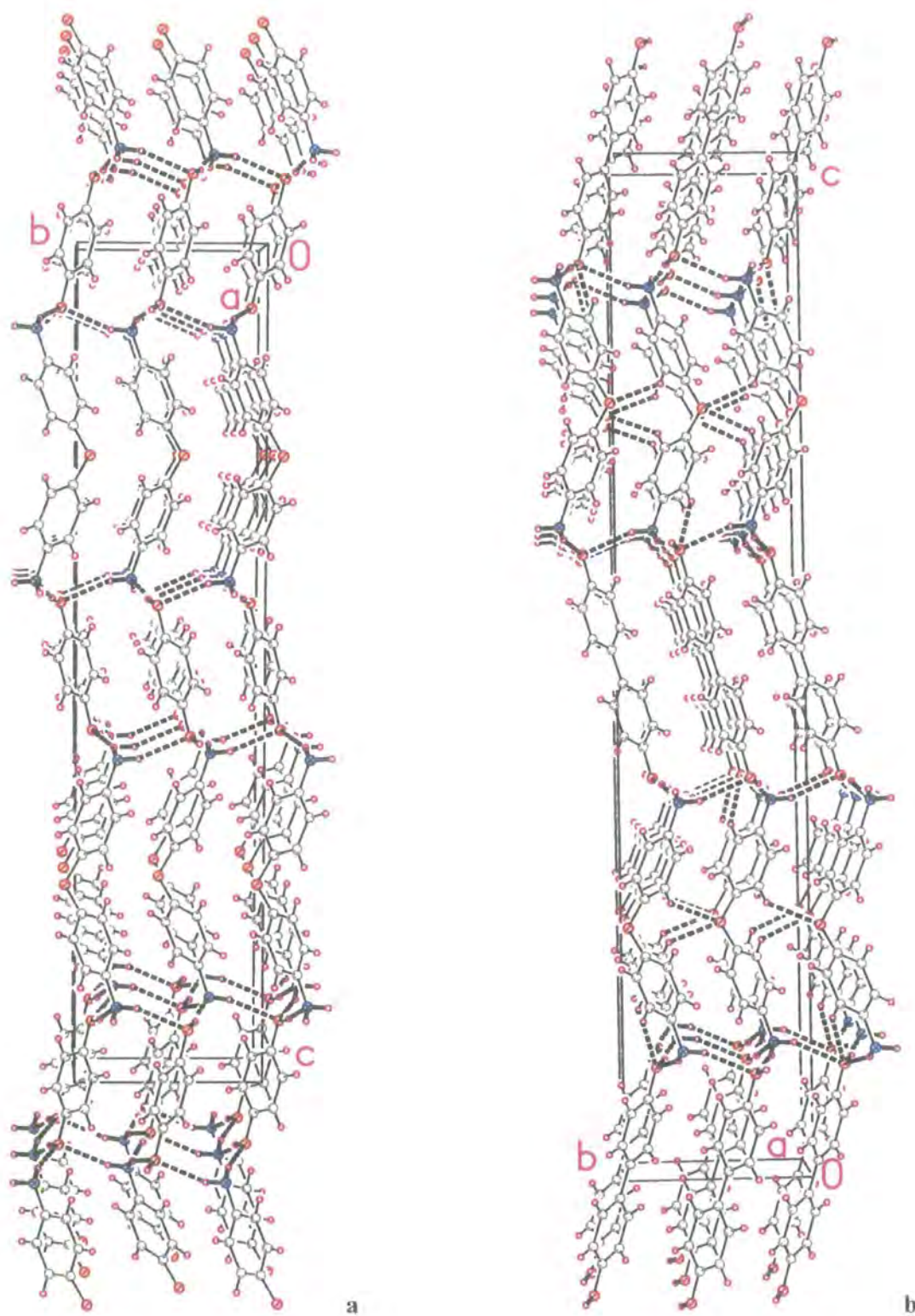
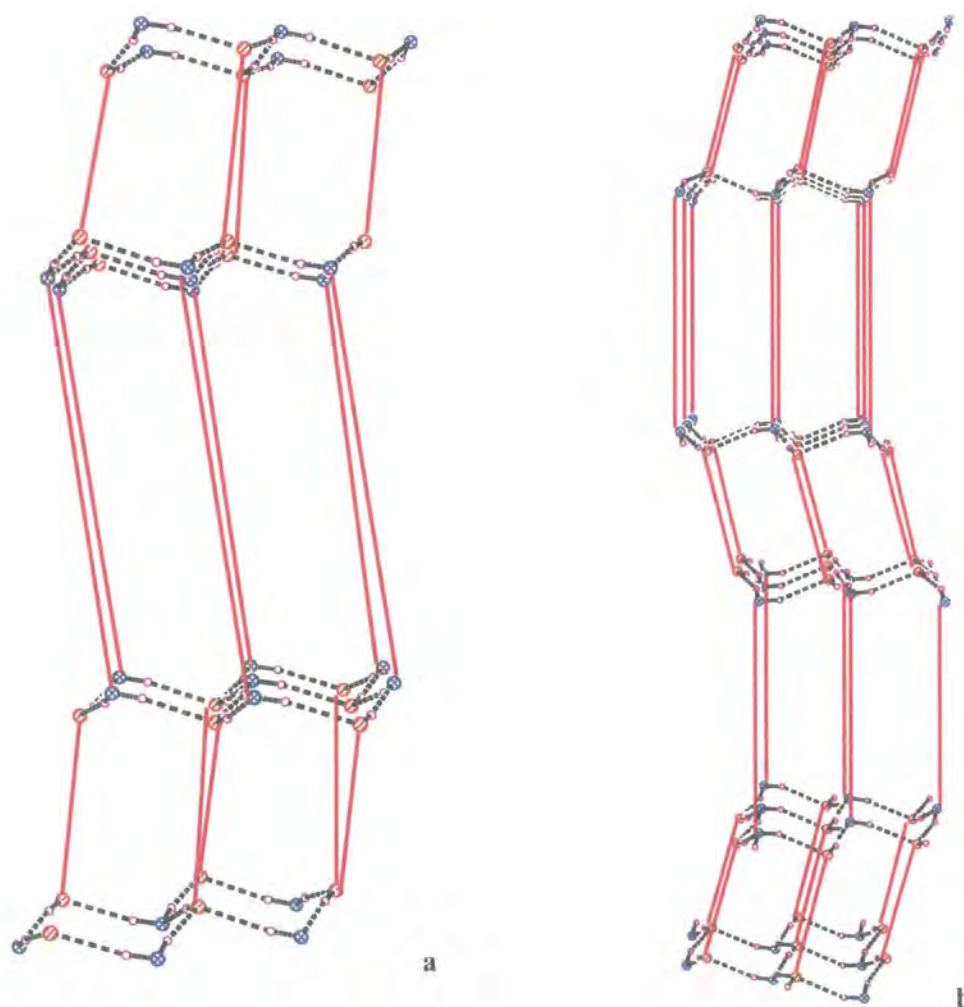


Figure 2.7 Crystal packing of (a) **7** and (b) **9** showing carborundum III type network. Notice that C-H...O bond between the diamines in **9**, which is not shown in **7** for clarity.

major difference between the two series (7,9 and 11 with 10, 12) is that while in 10 and 12 both the components are centrosymmetric, for the other series only the diphenols are centrosymmetric and not dianilines. On the other hand, from symmetry point of view, while zinc blende network is centrosymmetric wurtzite is not. This could lead to a rationalisation for the appearance of the novel carborundum network by drawing a symmetry correlation between two networks and the corresponding molecules involved.



Scheme 2.11 A vis-à-vis comparison of zinc blende and carborundum III network as observed in crystal structures 10 and 7 respectively. The molecular linker groups (phenyl, biphenyl and biphenylether) between the networks are replaced by bars.

Table 2.2. Crystallographic data and structure refinement parameters of molecular complexes.

	7	9	11	10	12
Empirical formula	C ₁₈ H ₁₈ O ₃ N ₂	C ₂₄ H ₂₂ N ₂ O ₃	C ₃₀ H ₂₆ O ₃ N ₂	C ₁₀ H ₁₁ O N	C ₁₃ H ₁₃ O N
Formula wt.	310.34	386.44	462.53	161.20	199.24
Crystal System	Orthorhombic	Orthorhombic	Orthorhombic	Monoclinic	Monoclinic
Space group	Pbcn	Pbcn	Pbcn	P2(1)/c	P2(1)/c
<i>a</i> [Å]	5.4523(2)	5.4647(1)	5.4581(2)	19.4874(5)	23.7415(11)
<i>b</i> [Å]	7.9556(2)	7.9338(2)	7.9851(3)	5.2324(1)	5.3008(2)
<i>c</i> [Å]	35.1453(11)	43.4412(10)	51.7327(16)	8.1805(2)	8.0833(4)
α [°]	90	90	90	90	90
β [°]	90	90	90	94.584(1)	97.162(2)
γ [°]	90	90	90	90	90
<i>Z</i>'	0.5	0.5	0.5	0.5	0.5
Volume [Å³]	1524.47(8)	1883.43(7)	2254.69(14)	831.46(3)	1009.34(8)
D_{calc} [g/cm³]	1.352	1.363	1.363	1.288	1.311
μ [mm⁻¹]	0.093	0.091	0.088	0.084	0.083
2θ [°]	4.64 to 55	3.67 to 55	7.54 to 52	4.20 to 55	3.56 to 55
Range <i>h</i>	-6 to 7	-7 to 7	-6 to 6	-25 to 25	-30 to 29
Range <i>k</i>	-10 to 10	-9 to 10	-9 to 9	-6 to 6	-6 to 6
Range <i>l</i>	-44 to 45	-53 to 56	-63 to 63	-10 to 10	-10 to 10
Reflns. collected	12094	15236	15411	8825	10379
Unique reflns.	1754	2165	2201	1913	2322
Obs. reflns.	1480	1801	1638	1719	2076
<i>R</i>₁ [<i>I</i> > 2 σ(<i>I</i>)]	0.0387	0.0417	0.0511	0.0371	0.0393
wR_2 [all]	0.1069	0.1114	0.1415	0.0975	0.1061
Goodness-of-fit	1.166	1.046	1.106	1.055	1.044
Crystal size (mm³)	0.38 x 0.28 x 0.10	0.4 x 0.38 x 0.10	0.20 x 0.18 x 0.08	0.28 x 0.24 x 0.16	0.24 x 0.22 x 0.12
Largest diff. peak and hole (e.Å⁻³)	0.223 and -0.252	0.310 and -0.205	0.312 and -0.344	0.365 and -0.152	0.272 and -0.261

That is for **7**, **9** and **11**, while the centrosymmetric diphenol molecules form the zinc blende topology on either side of the β -As sheets, the noncentrosymmetric dianiline molecules on the other hand show the wurtzite topology.

Although this kind of correlation can have a far-reaching impact on crystal engineering, namely, acquiring a strategic control of a desired molecular network, any such 'rule' should be adopted with caution and further consideration. For example, compound **3** which does not have $\bar{1}$ symmetry, and could be considered as the supramolecular equivalent to the corresponding binary complexes, still adopts the zinc blende network. To conclude, the aminophenol family does show an incredible amount of diversity and represents a storehouse for various field of studies, be it structural homology, network properties or general crystal engineering interest.

2.6. References:

1. (a) G. R. Desiraju, *Stimulating Concepts in Chemistry*, eds. F. Vögtle, J. F. Stoddart, and M. Shibasaki, Wiley-VCH; Weinheim, 2000. (b) The Crystal as a Supramolecular Entity. *Perspectives in Supramolecular Chemistry*, Vol. 2, eds., G. R. Desiraju, Wiley, Chichester, 1996.
2. (a) R. J. Davey, K. Allen, N. Blogden, W.I. Cross, H. F. Lieberman, M. J. Quayle, S. Righini, L. Seton, G. J. T. Tiddy, *CrystEngComm*, 2002, **4**, 257-264. (b) J. A. R. P. Sarma and G. R. Desiraju, *Cryst. Growth Des.*, 2002, **2**, 93-100. (c) P. K. Thallapally, A. K. Katz, H.L. Carrell, G. R. Desiraju, *Chem. Comm.*, 2002, 344-345.
3. G. R. Desiraju, *Angew. Chem.; Int. Ed. Engl.*, 1995, **34**, 2311-2327. A. Nangia, G. R. Desiraju, *Topics in Current Chemistry*, 1998, **198**, 57.
4. (a) F. H. Allen, O. Kennard, *Chem.Des.Autom.News.*, 1993, **8**, 30-37, (b) F. H. Allen, *Acta. Cryst.*, 2002, **B58**, 380-388.
5. O. Ermer, and A. Eling, *J. Chem. Soc., Perkin Trans.*, 2, 1994, 925-944
6. (a) Hanessian, S.; Gomtsyan, A.; Simard, M.; Roelens, S. *J. Am. Chem. Soc.*, 1994, **116**, 4495-4496, (b) Hanessian, S.; Simard, M.; Roelens, S. *J. Am. Chem. Soc.*, 1995, **117**, 7630-7645. (c) Hanessian, S.; Saladino, R.; Margarita, R.; Simard, M., *Chem. Eur. J.*, 1999, **5**, 2169-2183. (d) Hanessian, S.; Saladino, R in *Crystal Design, Structure and Function, Perspective in Supramolecular Chemistry*, Ed. G. R. Desiraju, Wiley, New York, 2003, **7**, 77.
7. (a) G. R. Desiraju, *Nature*, 2001, **412**, 397-400, (b) N. N. L. Madhavi, C. Bilton, J. A. K. Howard, F.H. Allen, A. Nangia, G. R. Desiraju, *New J. Chem.*; 2000, **24**, 1-4

8. V. R. Vangala, B. R. Bhogala, A. Dey, G. R. Desiraju, C. K. Broder, P. S. Smith, R. Mondal, J. A. K. Howard and C. Wilson, *J. Am. Chem. Soc.*, 2003, **125**, 14495-14509.
9. Allen, F.H.; Hoy, V.J.; Howard, J.A.K.; Thalladi, V.R.; Desiraju, G.R.; Wilson, C.C.; McIntyre, G.J; *J. Am. Chem. Soc.*, 1997, **119**, 3477-3480.
10. (a) T. Steiner, *J. Chem. Soc., Chem. Comm.*, 1995, 95-96. (b) H.-C. Weiss, R. Boese, H. L. Smith, M. M. Haley, *Chem. Comm.*, 1997, 2403-2404. (c) J. M. A. Robinson, B. M. Kariuki, K. D. M. Harris, D. Philip, *J. Chem. Soc. Perkin Trans. 2*, 1998, 2459-2470. (d) E. Gallopini, R. Gilardi, *J. Chem. Soc., Chem. Comm.*, 1994, 173-175. (e) W. Guo, E. Gallopini, R. Gilardi, G. I. Rydja, Y. -H. Chen, *Cryst. Growth Des.*, 2001, **1**, 231-237. (f) G. R. Desiraju, T. Steiner, *The Weak Hydrogen Bond In Structural Chemistry and Biology*, Oxford University Press, Oxford, 1999.
11. A. Dey, G. R. Desiraju, R. Mondal, J. A. K. Howard, *Chem. Comm.*, 2004, in press.
12. J. D. Dunitz, *Chem. Comm.*, 2003, 545-548.
13. (a) A. Gavezzotti, *Acc. Chem. Res.*, 1994, **27**, 309-314. (b) T. Beyer, T. Lewis, S. L. Price, *CrystEngCom*, 2001, **3**(44), 178-212.
14. (a) J. P. M. Lommerse, W. D. S. Motherwell, H. L. Ammon, J. D. Dunitz, A. Gavezzotti, D. W. M. Hoffmann, F. J. J. Leusen, W. T. M. Mooij, S. L. Price, B. Schweizer, M. U. Schmidt, B. P. van Eijck, P. Verwer and D. E. Williams, *Acta. Cryst.*, 2000, **B56**, 697-714. (b) W. D. S. Motherwell, H. L. Ammon, J. D. Dunitz, A. Dzyabchenko, A. Gavezzotti, D. W. M. Hoffmann, F. J. J. Leusen, J. P. M. Lommerse, W. T. M. Mooij, S. L. Price, H. Scheraga, B. Schweizer, M. U. Schmidt, B. P. van Eijck, P. Verwer and D. E. Williams, *Acta. Cryst.*, 2002, **B58**, 647-661

15. Selected references on structural chemistry of supraminols: (a) J. H. Loehlin, M. C. Etter, C. Gendreau, E. Cervasio, *Chem. Mater.*, 1998, **6**, 1218. (b) J. H. Loehlin, K. J. Franz, L. Gist, R. H. Moore, *Acta Cryst.*, 1998, **B54**, 695-704. (c) F. Toda, S. Hyoda, K. Okada, K. Hirostu, *J. Chem. Soc., Chem. Comm.*, 1995, 1531-1532. (d) S. Roelens, P. Dapporto, P. Paoli, *Can. J. Chem.*, 2000, **78**, 723-731. (e) P. Dapporto, P. Paoli, S. Roelens, *J. Org. Chem.*, 2001, **66**, 4930-4933. (f) J. Lewinski, J. Zachara, T. Kopec, B. K. Starawiesky, J. Lipkowski, I. Justyniak, E. Kolodziejczyk, *Eur. J. Inorg. Chem.*, 2001, **5**, 1123. (g) B. O'Leary, T. R. Splading, G. Ferguson, C. Glidewell, *Acta Cryst.*, 2000, **B56**, 273-286.
16. J. M. Robertson, *Proc. R. Soc., London*, 1951, **A207**, 101.
17. G. R. Desiraju and A. Gavezzotti, *J. Chem. Soc., Chem. Comm.*, 1989, 621-623.
18. (a) B. F. Hoskins and R. Robson, *J. Am. Chem. Soc.*, 1990, **112**, 1546-1554; (b) M. J. Zaworotko, *Chem. Soc. Rev.*, 1994, **4**, 283-288; (c) X. Wang, M. Simard and J. D. Wuest, *J. Am. Chem. Soc.*, 1994, **116**, 12119-12120; (d) D. S. Reddy, D. C. Craig and G. R. Desiraju, *J. Chem. Soc., Chem. Comm.*, 1994, 1457-1458; (e) K. A. Hirsch, S. R. Wilson and J. S. Moore, *Chem. Eur. J.*, 1997, **3**, 765-771; (f) E. Galoppini and R. Gilardi, *Chem. Comm.*, 1999, 173-174; (g) O. R. Evans, R.-G. Xiong, Z. Wang, G. K. Wong and W. Lin, *Angew. Chem. Int. Ed.*, 1999, **38**, 536-538; (h) D. S. Reddy, T. Dewa, K. Endo and Y. Aoyama, *Angew. Chem. Int. Ed.*, 2000, **39**, 4266-4268; (i) W. Guo, E. Galoppini, R. Gilardi, G. I. Rydja and Y. -H. Chen, *Cryst. Growth. Des.*, 2001, **1**, 231-237; (j) -Q. Ma, H. -L. Sun and S. Gao, *Chem Comm.*, 2003, 2164-2165
19. O. M. Yaghi, M. O'Keeffe, N. W. Ockwig, H. K. Chae, M. Eddaoudi and J. Kim, *Nature*, 2003, **423**, 705-714.
20. A. R. Verma and P. Krishna, *Polytypism and Polymorphism in Crystals*, Wiley, New York, 1966

Chapter Three

Organic Chlorine as an Hydrogen Bond Acceptor

3.1. Introduction

In crystal engineering, the supramolecular chemist aims to design and control the packing arrangements through the identification of robust and reproducible interaction patterns or supramolecular synthons¹. Initially, the studies of molecular recognition and crystal engineering in organic systems were focused on the strong (energy range 5-15 kcal mol⁻¹) D-H...A (D, A = O, N) hydrogen bonds, the structure defining role of which is now well documented. Other types of interactions such as quadrupole-quadrupole, π - π or weaker bonds such as C-H... π (arene) or C-H... π (alkyne) are now attracting attention. Although these interactions are individually weaker (energy < 5 kcal mol⁻¹) and (geometrically) less conspicuous, their combined effect can be equally important². Recent interest on weaker hydrogen bridges like C-H...O further emphasise this point³. The term 'hydrogen bridge'⁴ was preferred over 'hydrogen bond' for this kind of weak interaction, as in these interactions the hydrogen atom is attached to at least two atoms (more than two for bi-, tri-furcating hydrogen bonds), ergo acts like a bridge between donor and acceptor atoms.

However in a sharp contrast to these, there has always been some scepticism about the acceptor capabilities of organic halogens, C-X (X= F, Cl, Br, I) owing to the occasional involvement in the hydrogen bonding and because of the hard donor-soft acceptor nature of the interaction⁵. Hydrogen bridges of the type O-H...Cl-C occur very rarely, predominantly for sterically hindered acceptor-poor systems, in other words when steric hindrance around the donor group makes it difficult for the acceptor group to be involved in any intermolecular interactions. Toda and co-workers reported an unusual O-H...O-H...Cl-C cooperative network (d, 2.30 Å; D, 3.09 Å; θ 139°) in a ferrocene derivative where an awkward molecular shape makes intermolecular hydrogen bonding less favourable with a tertiary hydroxyl group⁶. Perhaps due to this special precondition, interactions involving halogens are always considered as secondary and less important.

On the contrary, hydrogen bridges of the type O-H...Cl with primary importance were cited as early as the beginning of the last century. This includes some of the classical work of Hantzsch⁷ on dimethyl-3,6-dichloro-2,5-dihydroxyterephthalate and elegant work of Wulf on ortho-halogenated phenols⁸. Later on, Byrn, Curtin and Paul⁹ and independently Dunitz¹⁰ carried out further study on dimethyl-3,6-dichloro-2,5-dihydroxyterephthalate. The molecule has different conformations in three polymorphic forms owing to the twist angle of the ester group which gives rise to different hydrogen bonding patterns. The three polymorphs appeared with different coloured crystals. Interestingly, one of the trimorph results as a direct consequence of an O-H...Cl interaction; a hydroxyl group forms an O-H...Cl hydrogen bridge rather than O-H...O interaction, as observed for the other two. Among other contemporary workers, Burks and coworkers mentioned a relatively strong intramolecular O-H...Cl (d, 2.45 Å, D, 3.11 Å, θ 141°) interaction, originated because of the inaccessibility of the stronger carbonyl acceptors for the crystalline diterpenoid briarein A, wherein the absence of any intermolecular interaction, makes this interaction structure determining¹¹. Although most examples of O-H...Cl-C hydrogen bonding involve sterically hindered donors, crystalline chloramphenicol shows an unexpected intra-cum-intermolecular O-H...O-H...Cl-C pattern that would confound most current efforts at crystal structure prediction¹². Very recently Davey and co-workers reported O-H...Cl-C interactions that have been invoked even in solution and facilitate a formation of different polymorphs of 2,6-dihydroxybenzoic acid during recrystallisation from CHCl₃¹³.

With growing interest in non-conventional interaction patterns, the assessments of acceptor capabilities of halogen become the subject of routine work, rather than individual attempt or accidental discovery. Like any other crystal engineering topics, they were initiated with database studies, too. Howard et.al carried out a detailed database study to evaluate the mimicking capability of fluorine for the bio-organic

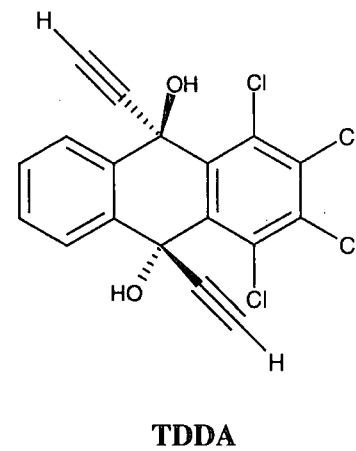
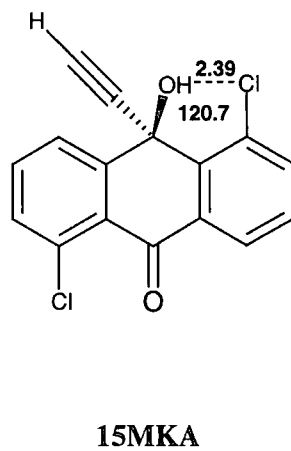
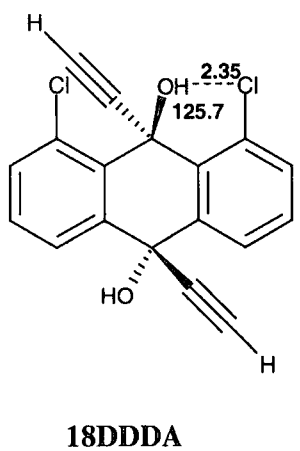
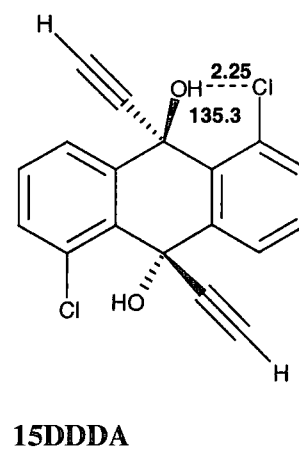
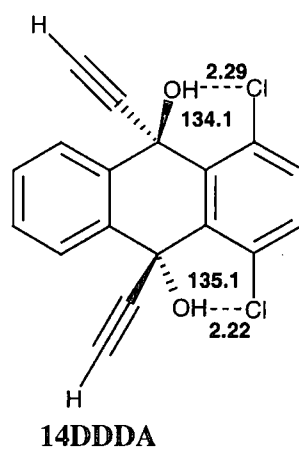
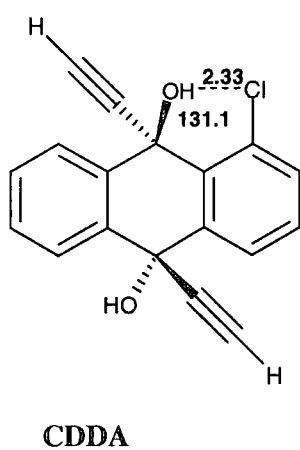
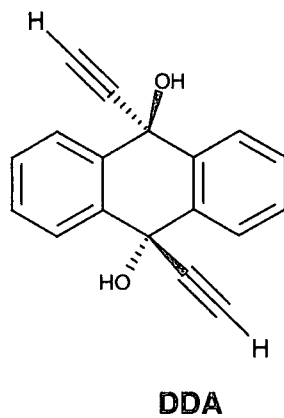
hydroxyl group¹⁴. It was observed that C_{sp3}-F fluorine [Energy C_(sp3)-F...H-O = 2.38 kcal mol⁻¹] atoms are stronger hydrogen bond acceptors than C_{sp2}-F fluorine atoms [Energy C_(sp2)-F...H-O = 1.48 kcal mol⁻¹]. Also fluorine shows a preference for non-acidic hydrogen (i.e. H-C rather than H-O or H-N) for than acidic hydrogen. Later on, Brammer and Orpen pointed out an interesting front on the acceptor capabilities of halogen, viz, the activation of the halogen involved¹⁵. From an analysis of 6624 crystallographically characterized hydrogen bonds containing O-H or N-H fragment as the donor groups, they studied the vis-à-vis acceptor capabilities of Cl⁻, M-Cl (M=transition metal) and C-Cl. Their results show that while organic chlorines are very poor hydrogen bond acceptors, the chloride ion or metal bound chlorines are capable of forming good, anisotropic (for M-Cl) hydrogen bond. Aakeröy¹⁶ and co-workers and later Thallapally and Nangia¹⁷, in what could be perceived as the continuation of the above work carried out a similar study using the CSD for Cl⁻, M-Cl and C-Cl except with C-H as the donor group, devoid of any other interference. The results show that while interactions involving Cl⁻ and M-Cl could be termed as hydrogen bonds, C-H...Cl-C is merely a van der Waals interaction.

In opposition to these rhetoric, in 1997, Jack Dunitz and Taylor⁵ put forward their somewhat more pessimistic conclusion as “*organic fluorine hardly ever accepts hydrogen bonds*”. Two years later Strauss and co-workers¹⁸ identified the strongest and significant inter- and intramolecular O-H...F-C hydrogen bonding. The presence of a linear and short intermolecular (d=2.01Å, D= 2.971Å, θ=171°) and two intramolecular O-H...F-C (d=2.32, 2.16Å, θ=96 & 100°) hydrogen bonds was further supported by F¹⁹ NMR and IR spectroscopic data. Slowly but steadily, the acceptor capability of fluorine became a subject of considerable interest. Glusker¹⁹ and co-workers have been in the forefront of studying the hydrogen bond properties of organic fluorine. Boese and Desiraju studied a series of compounds containing only C,H and F atoms, in order to

overcome the problem of poor competition of C-F group from strong acceptor groups with N or O atoms. In comparison to other halogens, their result unequivocally shows the preference of F atom to form C-H...F interactions rather than F...F interactions. A clear resemblance between C-H...F and C-H...O or C-H...N interactions make it a potential field for crystal engineering. However, the fact that a C-H...F interaction was prominent only when that carbon acidity was enhanced and the absence of any other strong acceptor group was unable to clear the air of suspicion.²⁰

Application of the weak and reversible nature of C-H...F-C in the field of catalysis was emphasized by Chan and co-workers²¹. Hydrogen bond properties of halogens have always been a subject huge interest for biologist and biochemists. Very recently Parsch and Engels²² reported C-H...F-C interactions stabilizing the duplex formation with RNA having unnatural fluorinated bases. Olsen and co-workers report a strong C-H...F-C ($d=2.1 \text{ \AA}$, $\theta=157^\circ$) bond for a 4-fluorobenzyl moiety at the bonding site of thrombin.²³

Six chloro-substituted compounds (**Scheme 3.1**) of interest here are part of a much greater family of gem-alkynols which were prepared as a part of the crystal engineering studies. The combination of both a weaker and a strong hydrogen bonding functional group creates an interesting challenge to the crystal engineers. The lack of structural repetitivity among the compounds may arise from the close juxtaposition of two pairs of hydrogen bond donors and acceptors. This, in a way, makes the four primarily possible interactions, O-H...O, C \equiv C-H...O, O-H... π and C \equiv C-H... π , highly competitive. Therefore the packing pattern adopted by any compound is extremely sensitive to molecular features and thus generates different networks and interactions like C-H...Cl or O-H...Cl interactions within the crystal structures.



Scheme 3.1. Compounds in this study with the metrics of the solid state O-H...Cl-C interactions marked.

This present chapter²⁴ was prompted by the rare, but consistent, appearances of intramolecular O-H...Cl-C interactions. These organic chlorines (C-Cl) herein neither can hardly be considered as activated halogens nor do the molecules have any significant steric hindrance which rules out any possibility of acceptor-poor system. Unusual NMR spectroscopic data appear to be the manifestation of O-H...Cl interactions, too. So much so, from a crystal engineering point of view the inconsistent hydrogen bonds formed by these molecules than rest of the family can be explain nicely only when O-H...Cl-C interactions are taken into account as a primary and structure determining interactions.

3.2. Result and Discussion

Although there are some reports in the literature, there always has been some scepticism about the O-H...Cl interaction and more importantly its significance towards crystal structure. Such questions were further raised by Rowland and Taylor's²⁵ unusual findings that while the $d(H...A)$ values for (O,N)-H...N(O) interactions are smaller than those for C-H...O(N), the reverse order is true when acceptor is an organic chlorine. In other words, the 'd' values are shorter for interactions between organic halogens (Cl, Br) and non-acidic hydrogen (C-H) rather than OH or NH. The finding though seems to be an illusion, but is in good agreement with fluorine analogues as mentioned earlier. The authors rationalised this apparent confusing reverse trend as the direct consequence of bi-, tri-furcation of hydrogen bond involving acidic hydrogen atoms (O-H or N-H), while most of the non-acidic hydrogen atoms are involved in stand alone interactions. This often turns an O-H...Cl interaction into a minor component with larger d values compared to that of the stand alone C-H...Cl interaction.

A CSD study shows that out of 1194 crystal structures that contain both organic chlorine and hydroxyl groups, only ca. 9% (180) form O-H...Cl interactions. Quite

interestingly, the intramolecular interactions (82) show a sheer domination over the intermolecular interactions (60), which does hint towards the presence of special geometrical conditions or steric hindrance.

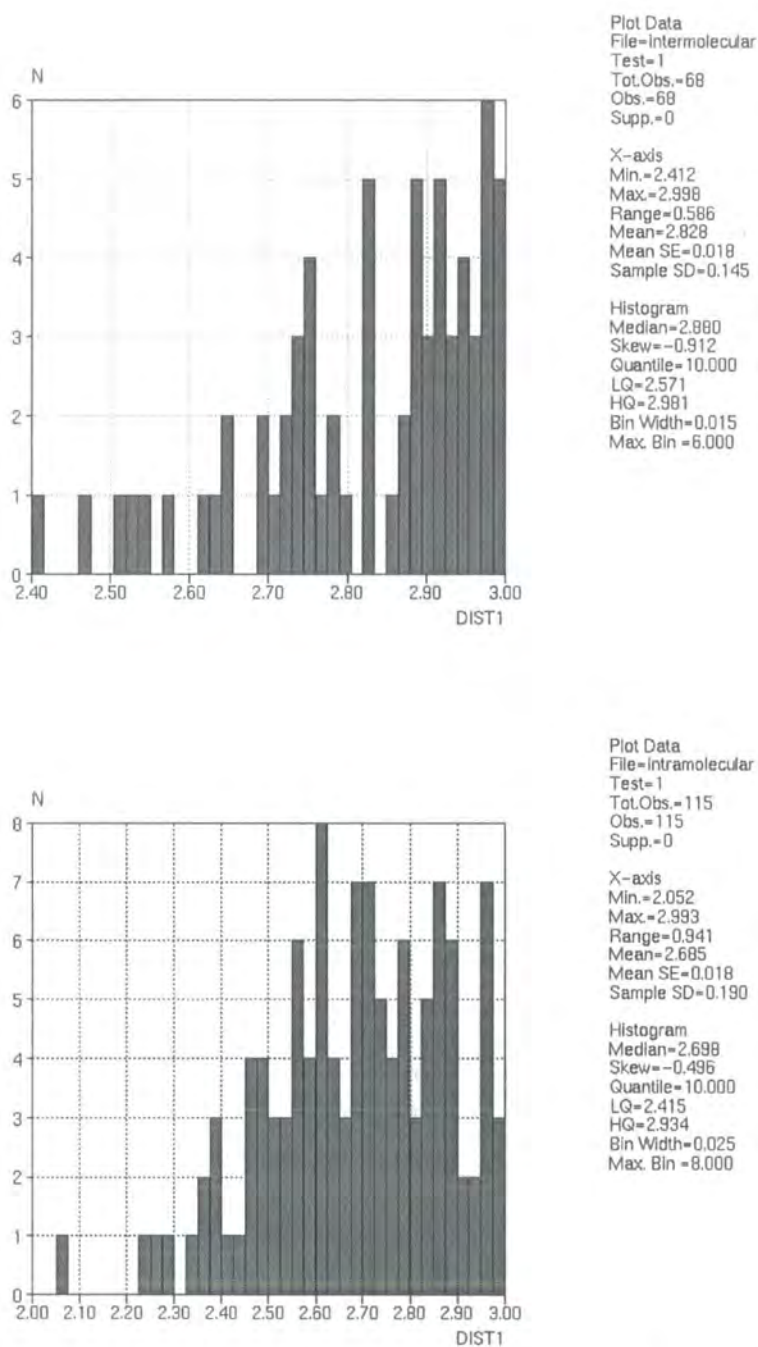


Figure 3.1. Histograms of intermolecular (top) and intramolecular (bottom) O-H...Cl-C interactions.

In this chapter, we will focus our attention on the six chloro substituted gem-alkynols, five of which show O-H...Cl interactions in the solid state (crystal).

The basic approach was to study the changes in crystal structure brought about by the changes in the molecular structure. It has been observed earlier that some changes in the molecular structure may be carried out over a range of substituent groups without perturbing the overall crystal structure type; but at the limit of this range, just a slight change in the molecular structure may change the whole crystal packing²⁶.

We begin with the parent DDA molecule (**Scheme 3.I**) that exhibits cooperative cyclic synthons **V** and **VI** (Scheme 3.2) that are characteristic of this family. Each of these synthons is composed of alternating strong O-H...O & C-H...O or C-H...O & C-H... π bonds. Herein, we have selectively replaced hydrogen atoms by chlorine atoms in this work with an aim to derive some insight about the effects of chlorine atom on the above-mentioned interactions. The structures of interest here therefore can provide the evidence of interference or reinforcement of O-H...O, C-H...O or O-H... π & C-H... π interactions observed in DDA with interactions involving organic chlorine. In other words, this provides the unique opportunity to judge the robustness of the synthon and hydrogen bond acceptor capabilities of halogen at the same time²⁷.

Out of six molecules of interest, TDDA does not form any intramolecular hydrogen bonds in crystalline form. Based on the rest of the structures the main objectives of this chapter are (a) to investigate the geometric as well as the chemical effects of chlorine substitution, consequently how O-H...Cl interactions fit into the hydrogen bonding pattern, (b) an elaborate description of the transition state of supramolecular transformation from unsubstituted compound DDA via a suitable intermediate, (c) evaluation of acceptor capabilities of organic chlorine in terms of O-H...Cl interactions and (d) further evidence from NMR data.

3.3. Hydrogen Bonding Patterns

15DDDA has been discussed in detail in Chapter 4 in a different context. The presence of chlorine atoms in close proximity to gem alkynol groups seems to make it difficult to form short and linear hydrogen bonds, and consequently we found only one from each

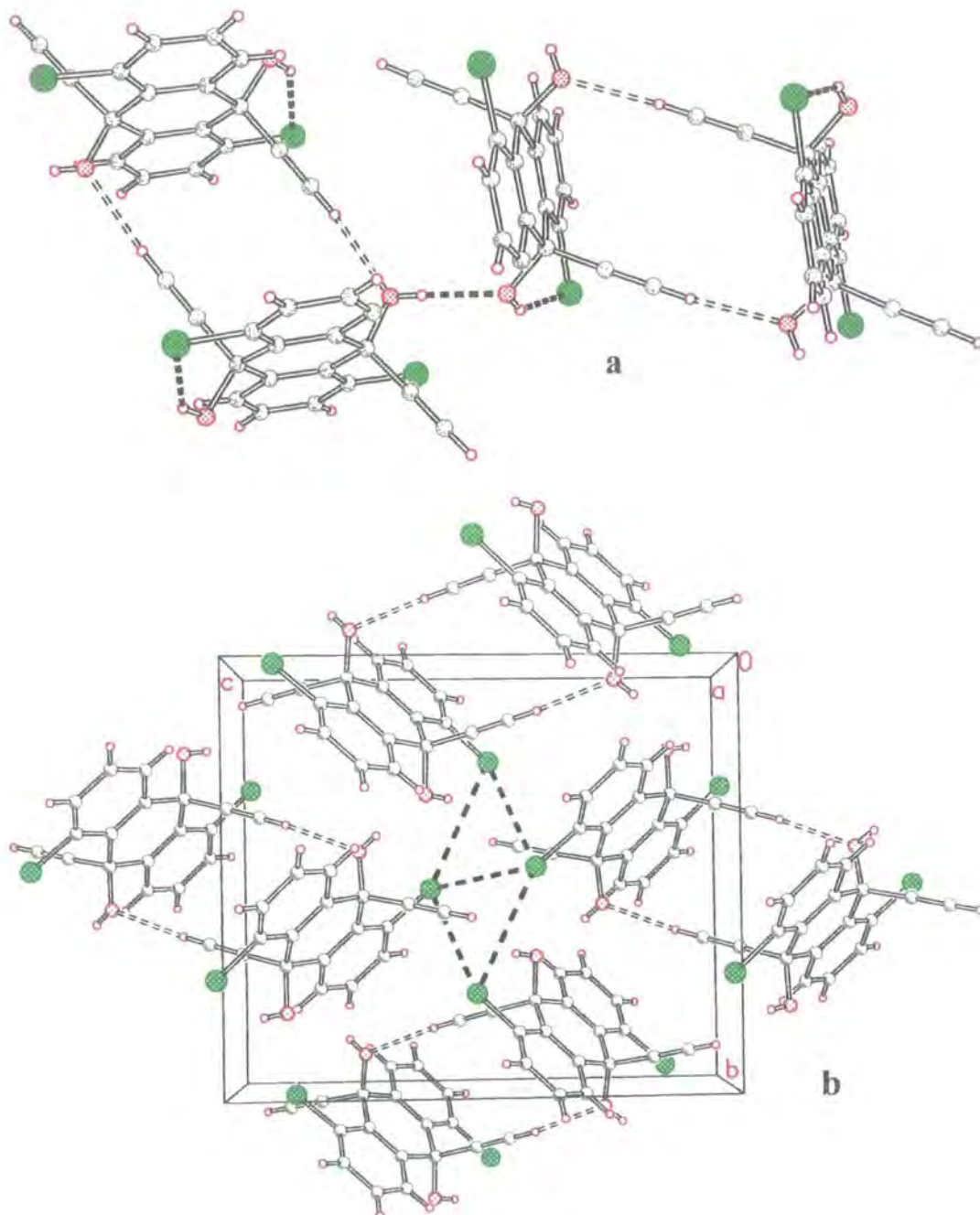


Figure 3.2. Packing diagram of 15DDDA showing (a) Dimer synthon with O-H...O and O-H...Cl interaction (in bold lines) and (b) the planar 'Cl₄' synthon (highlighted) at the position (0.5, 0.5, 0.5), C-H...O dimers are also shown.

of these two hydroxyl and ethynyl groups form strong hydrogen bonds. Two distinct interaction patterns are observed for 15DDDA. The dominant interaction patterns appear to be a cooperative arrangement of three hydrogen bonds, an intermolecular C-H...O (d, 2.44 Å, θ , 164.7°), an intermolecular O-H...O (d, 1.83 Å, θ , 173.8°) and an intramolecular O-H...Cl-C (d, 2.25 Å, θ , 135.4°). Four quasi type-II²⁸ Cl...Cl contacts (d, 3.56, 3.69 Å) and one type-I (d, 3.64 Å) form a tetrachloro supramolecular synthon. The closed loop synthon (V and VI) in DDA has been diminished, instead a C-H...O dimer between two inversion related interactions is observed²⁶ (Figure 3.2)

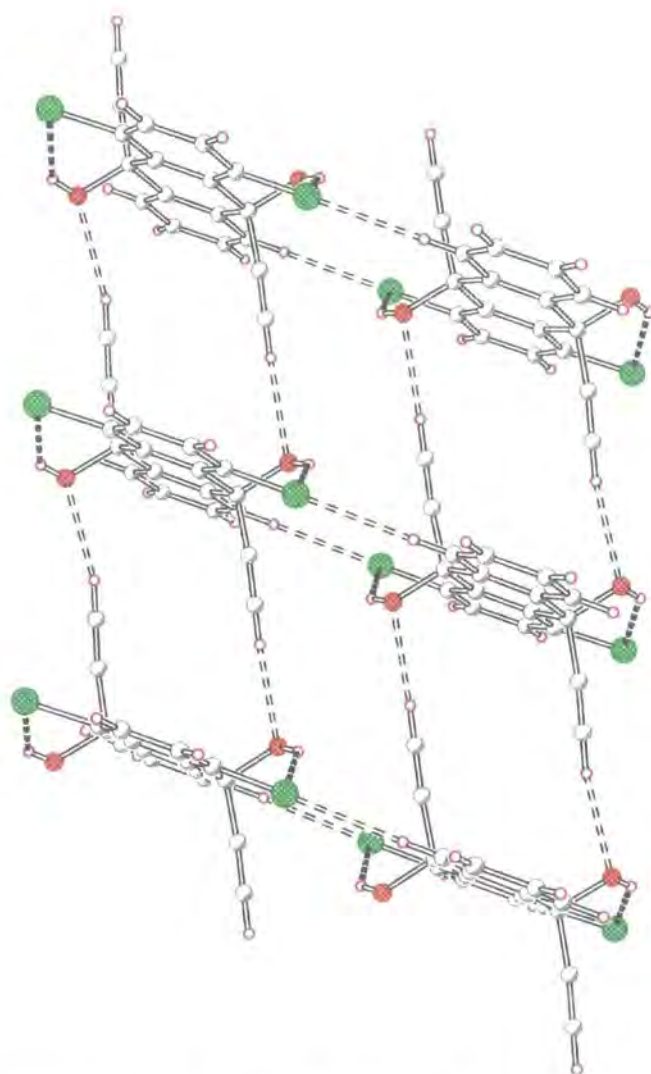


Figure 3.3 Packing diagram of 14DDDA showing O-H...Cl-C interaction and planar C-H...O dimer synthon

A similar kind of C-H...O dimer is also observed for 14DDDA, cooperative with the shortest O-H...Cl (d, 2.22 Å, θ , 135.4°) interaction in this series (**Figure 3.3**). However it's the lack of O-H...O hydrogen bonding that makes it unique from the rest of the series. This particular crystal packing once again clearly proves the hypothesis that collectively weaker hydrogen bonds can outweigh the stronger interaction like O-H...O from primary or structure determining role. At the same time, absence of any significant extra steric bulk than DDA or 15DDDA does make a strong case for upgrading the O-H...Cl as interaction of primary importance. The main structural deviation from DDA

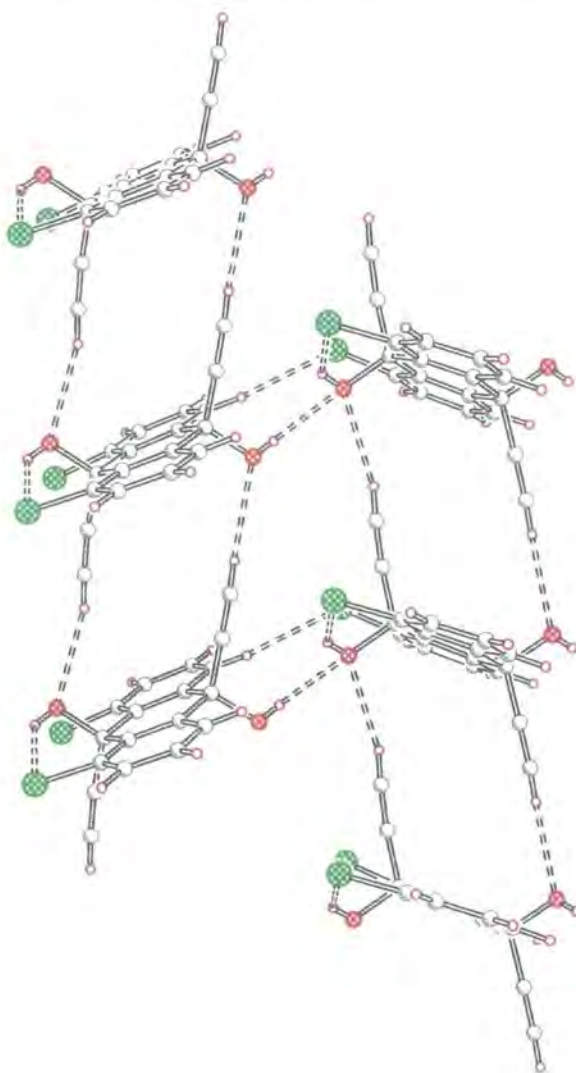


Figure 3.4 Packing diagram of 18DDDA with the similar planar dimer synthon.

to 14DDDA is not only the extinction of the supramolecular loop synthon, but a definite change of packing pattern to a recurring one based on entirely a 'strong' de-facto weaker interaction.

For 18DDDA, the dimer reappears, however unlike 14DDDA, spatial orientation is more converging than parallel. The most probable reason for this distortion in orientation could be attributed to the fact that the dimer has to accommodate a rather weak O-H...O interaction that was absent for 14DDDA. However like in 14DDDA, the cooperative arrangement of the type C-H...O-H...O-H....Cl-C (inter, inter, intramolecular) appears to be the dominant interaction pattern.(Figure 3.4)

Table 3.1 Hydrogen bond table for the 14DDDA

D-H...A	d(D-H)	d(H...A)	d(D...A)	<(DHA)
O ₁ -H ₁ ...Cl ₁	0.84	2.39	3.055(5)	136.5
O ₂ -H ₂ ...Cl ₂	0.84	2.33	3.000(5)	137.7
C ₁₆ -H ₁₆ ...O ₁	0.95	2.52	3.436(8)	161.1
C ₁₈ -H ₁₈ ...O ₂	0.95	2.56	3.453(8)	157.3

The above discussion shows that except TDDA (which does not form any O-H...Cl interaction in solid state), an intramolecular O-H...Cl-C dictates the hydrogen bonding pattern and hence the crystal packing. As we will see in the next section these O-H...Cl interactions are 'strong' enough to disrupt the well established supramolecular synthons and can play a crucial role of de-facto structure determining interactions. The consistent appearance of O-H...Cl interactions and consequently the C-H...O dimer synthon in all three structures thus created, shows a general resemblance of overall packing.

Table 3.3. Crystallographic data and structure refinement parameters.

	CDDDA	14DDDA	18DDDA
Solvent of Crystallization	EtOH/benzene (1:1)	EtOH/benzene (1:1)	CHCl ₃ /benzene (1:1)
Empirical formula	C ₁₈ H ₁₁ O ₂ Cl	C ₁₈ H ₁₀ O ₂ Cl ₂	C ₁₈ H ₁₀ O ₂ Cl ₂
Formula wt.	294.72	329.16	329.16
Crystal System	Triclinic	Triclinic	Monoclinic
Space group	$P\bar{1}$	$P\bar{1}$	$C2/c$
<i>a</i> [Å]	8.4500(17)	6.7496(4)	27.597(6)
<i>b</i> [Å]	9.2334(18)	7.2021(4)	6.8419(14)
<i>c</i> [Å]	14.108(3)	15.5160(8)	15.099(3)
α [°]	84.52(3)	76.992(2)	90
β [°]	89.85(3)	87.075(2)	101.48(3)
γ [°]	73.53(3)	74.353(2)	90
<i>Z</i> '	1.5	1	1
Volume [Å ³]	1050.4(4)	707.63(7)	2793.8(10)
F (000)	456	336	1344
ρ_{calc} [g/cm ³]	1.398	1.545	1.565
μ [mm ⁻¹]	0.273	0.462	0.468
2θ [°]	4.623 to 54.940	2.70 to 58.10	5.506 to 54.993
Range <i>h</i>	-10 to 10	-9 to 9	-35 to 35
Range <i>k</i>	-11 to 11	-9 to 9	-8 to 8
Range <i>l</i>	-18 to 18	-21 to 21	-19 to 19
Reflns. collected	12642	8590	15923
Unique reflns.	4803	3693	3211
Observed reflns.	3970	3175	2886
R_1 [$I > 2\sigma(I)$]	0.0408	0.0969	0.0350
WR_2	0.1025	0.2786	0.0999
Goodness-of-fit	1.028	1.238	1.058
<i>T</i> [K]	120(2)	120(2)	120(2)
CCDC deposition No.	224902	224905	224903
Crystal size (mm ³)	0.44 x 0.32 x 0.08	0.34 x 0.28 x 0.08	0.32 x 0.22 x 0.16

Table 3.3a Crystallographic data and structure refinement parameters.

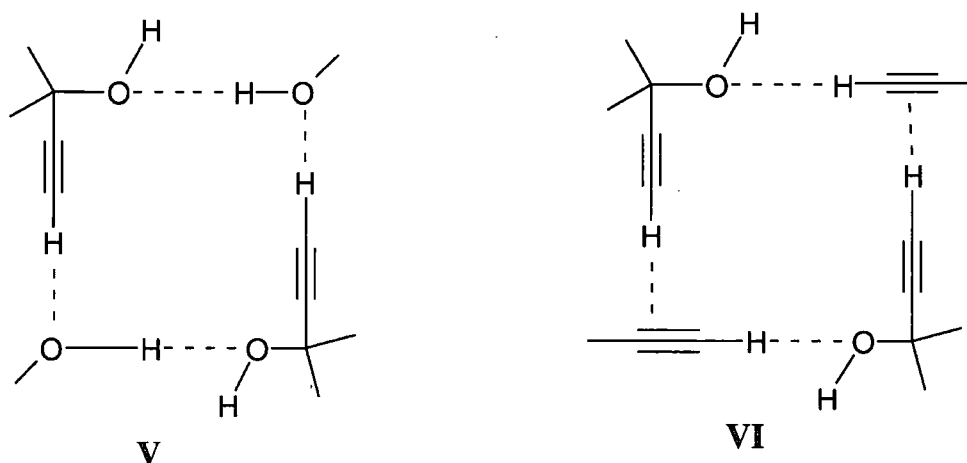
	15MKA	TDDA	DDDA
Solvent of Crystallization	CHCl ₃ /benzene (1:1)	CHCl ₃ /benzene (1:1)	EtOH/Benzene (1:1)
Empirical formula	C ₁₆ H ₈ O ₂ Cl ₂	C ₁₈ H ₈ O ₂ Cl ₄	C ₁₈ H ₁₀ Cl ₂ O ₂
Formula wt.	303.12	398.04	329.16
Crystal System	Monoclinic	Monoclinic	Monoclinic
Space group	<i>P</i> 2 ₁ / <i>n</i>	<i>P</i> 2 ₁	<i>P</i> 2 ₁ / <i>n</i>
<i>a</i> [Å]	7.2693(2)	9.3730(5)	7.4205(2)
<i>b</i> [Å]	11.5276(3)	9.5301(5)	12.7571(4)
<i>c</i> [Å]	15.4191(4)	10.3102(5)	14.8695(4)
α [°]	90	90	90
β [°]	98.775(1)	114.559(2)	93.382(1)
γ [°]	90	90	90
<i>Z</i> '	1	1	1
Volume [Å ³]	1276.96(6)	837.65(7)	1405.16(7)
F(000)	616	400	
ρ_{calc} [g/cm ³]	1.577	1.578	1.556
μ [mm ⁻¹]	0.504	0.714	0.465
2θ [°]	5.346 to 55.002	4.341 to 57.977	4.20 –57.98
Range <i>h</i>	-9 to 9	-12 to 12	-10 to 9
Range <i>k</i>	-14 to 13	-13 to 13	-17 to 17
Range <i>l</i>	-19 to 20	-14 to 13	-20 to 20
Reflns. collected	12801	10227	16581
Unique reflns.	2925	4398	3207
Observed reflns.	2436	4344	2702
<i>R</i> ₁ [<i>I</i> > 2 σ (<i>I</i>)]	0.0348	0.0283	0.0328
WR ₂	0.0912	0.0748	0.0853
Goodness-of-fit	1.052	1.057	1.031
<i>T</i> [K]	100(2)	120(2)	120(2)
CCDC deposition No.	224904	224901	200403
Crystal size (mm ³)	0.22 x 0.18 x 0.06	0.58 x 0.28 x 0.12	0.40 x 0.18 x 0.08

Table 3.2 Hydrogen bond table for the 18DDA

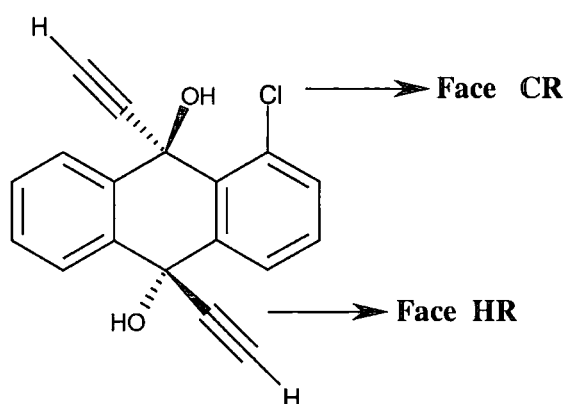
D-H...A	d(D-H)	d(H...A)	d(D...A)	<(DHA)
O ₁ -H ₁ ...Cl ₁	0.75(3)	2.49(2)	3.0210(13)	129(2)
O ₂ -H ₂ ...O ₁	0.73(3)	2.32(3)	2.8943(16)	137(2)
C ₁₆ -H ₁₆ ...O ₁	0.90(3)	2.68(3)	3.525(2)	156(2)
C ₁₈ -H ₁₈ ...O ₂	0.90(3)	2.72(3)	3.581(2)	162(2)

3.4. Synthons Disruptions

In crystal engineering, the supramolecular chemist aims to design and subsequently control the packing arrangements, which are invaluable important for designing crystals with desired properties. The identification of robust and reproducible interaction patterns or supramolecular synthons is a major aim of these studies, which in effect enables us to establish the correspondence between molecular and crystal structures. It has been noted earlier that supramolecular synthons play the same role in the crystal packing, as does the molecule. Hence, the strategic control over robust and reproducible supramolecular synthons can contribute to the control over crystal packing²⁶.

**Scheme 3.2.** Schematic representation of supramolecular synthon V and VI.

Supramolecular synthons based on strong and weak hydrogen bonds have been well documented and the most common patterns formed by such bonds have been characterized using Cambridge Structural Database (CSD). The representative synthons for the parent DDA are V and VI (Scheme 3.2). As mentioned earlier, the main idea of replacing aromatic hydrogen by chlorine was to investigate the effects on the supramolecular synthon and to test their robustness. In the present context, we have started with one distinct array of supramolecular synthons and ended up with excellent layer and pillar networks by rupturing two previous supramolecular arrays. Quite interestingly, this apparently irrelevant packing pattern or sudden supramolecular transformation from non-chlorinated DDA to those of dichlorinated 14DDDA, 15DDDA and 18DDDA does not take place in one-step transformation but in stepwise manner and can be rationalised via the mono-chlorinated CDDA. To the best of our knowledge, we are the first to report this kind of supramolecular ‘reaction’¹ via an intermediate crystal structure, which could be perceived as a transition state. It is therefore imperative to discuss this latter compound in detail.



Scheme 3.3. Schematic representation of the two different faces in CDDA.

The molecule, CDDDA can be visualised as having two distinct faces, namely, chlorine rich (**CR**) and hydrogen rich (**HR**) faces (Scheme 3.3) in its self assembly to the crystal ($P2_1$, $Z' = 1.5$). Effectively, for the two gem-alkynol groups there are two different local environments. While one would expect a normal behaviour from face **HR**, presence of

the chlorine atom on the contrary should provide a vis-à-vis effect of chlorine atoms on face **CR**. The effect of maiden chlorine is clearly evident in term of faces as shown in Fig. 3.5. In an unprecedented occurrence, face **HR**, devoid of any perturbation forms synthon **VI** and retains the synthon **V** characteristics of the unsubstituted DDA. Face **CR** on the other hand facilitates the O-H...Cl bonding and consequently partially disturbs the formation of synthon **V**. The loss of strong O-H...O hydrogen bonding is counterbalanced by the formation of a dimer with relatively weak C-H...O bonds, which is present in all dichloro derivatives.

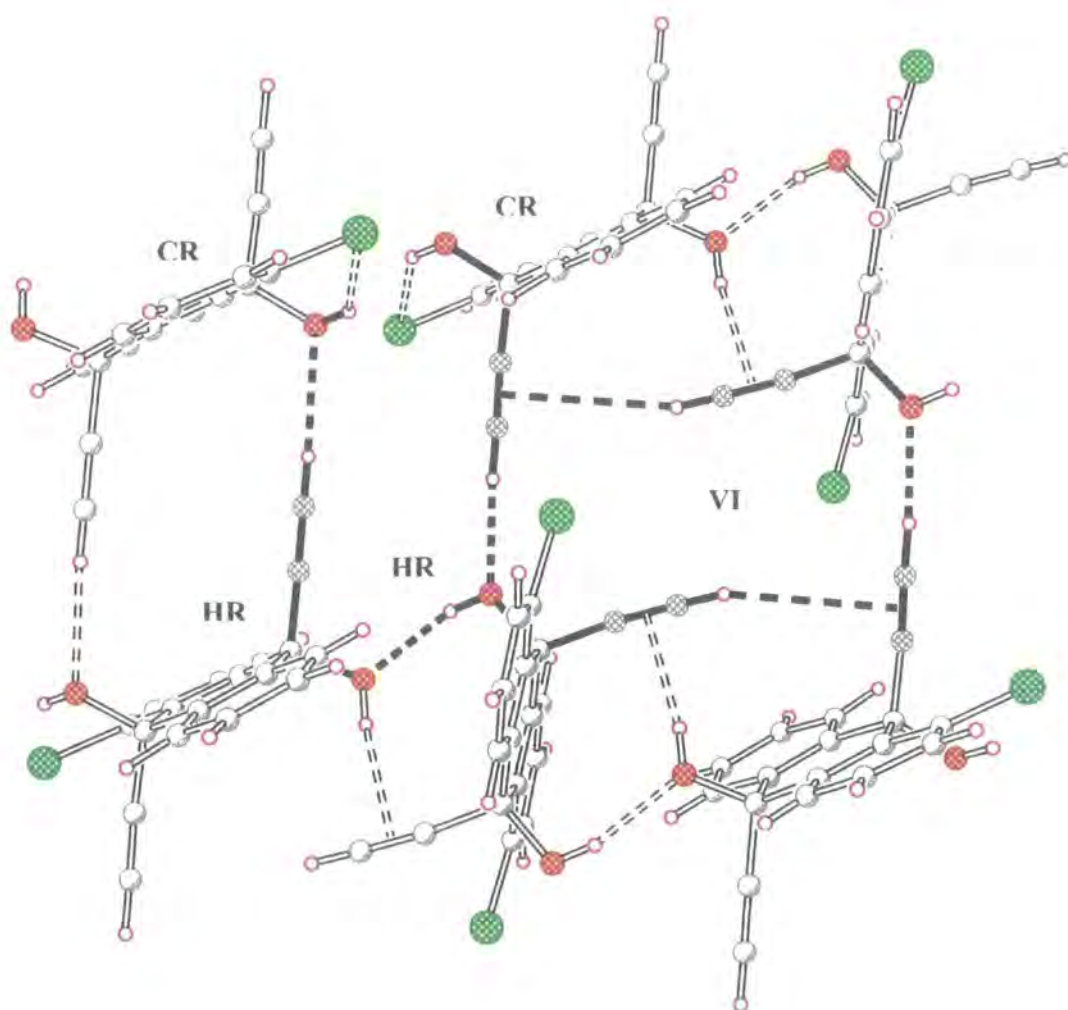
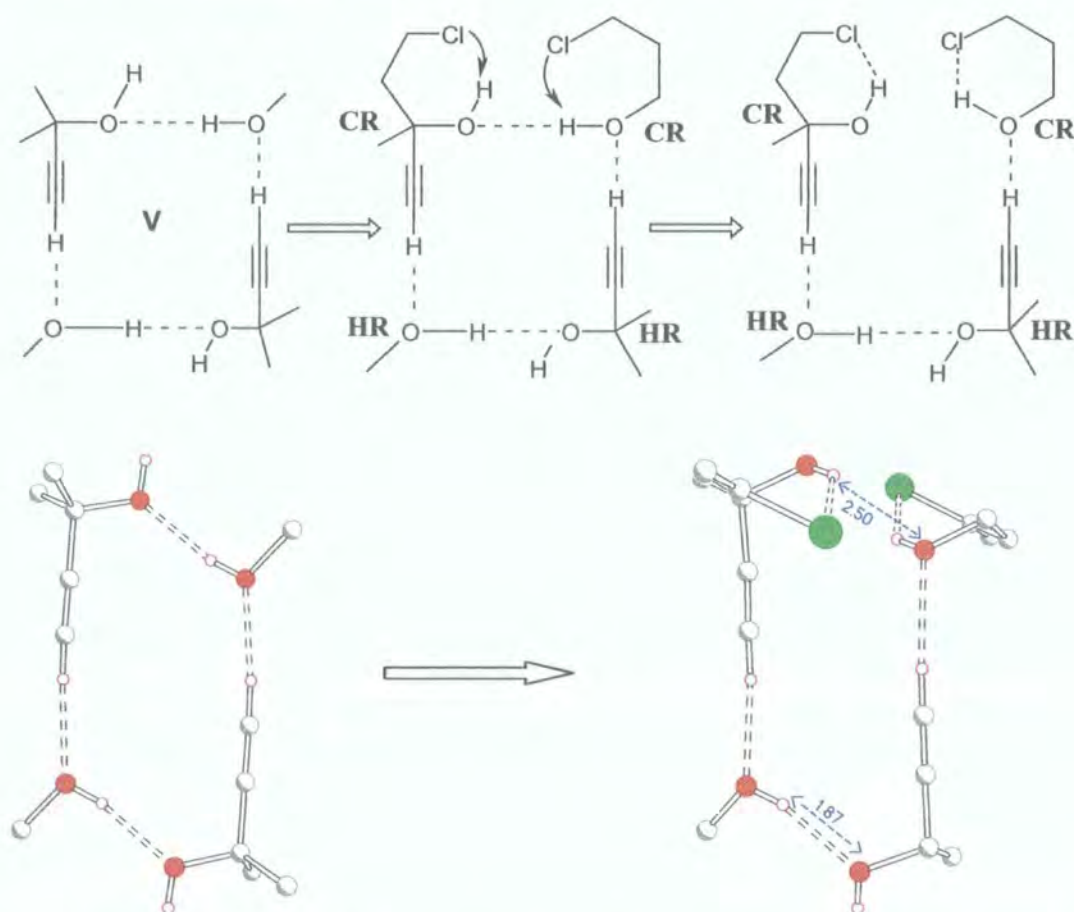


Figure 3.5. Packing diagram of CDDA. Notice how the O-H...Cl interaction is disrupting the synthon **V**, leaving synthon **VI** intact (highlighted). The planar C-H...O dimer synthon, seen in all three dichloro isomers, generated by disrupting Synthon **V**, is also shown.

Table 3.4 Hydrogen bond table for the CDDA

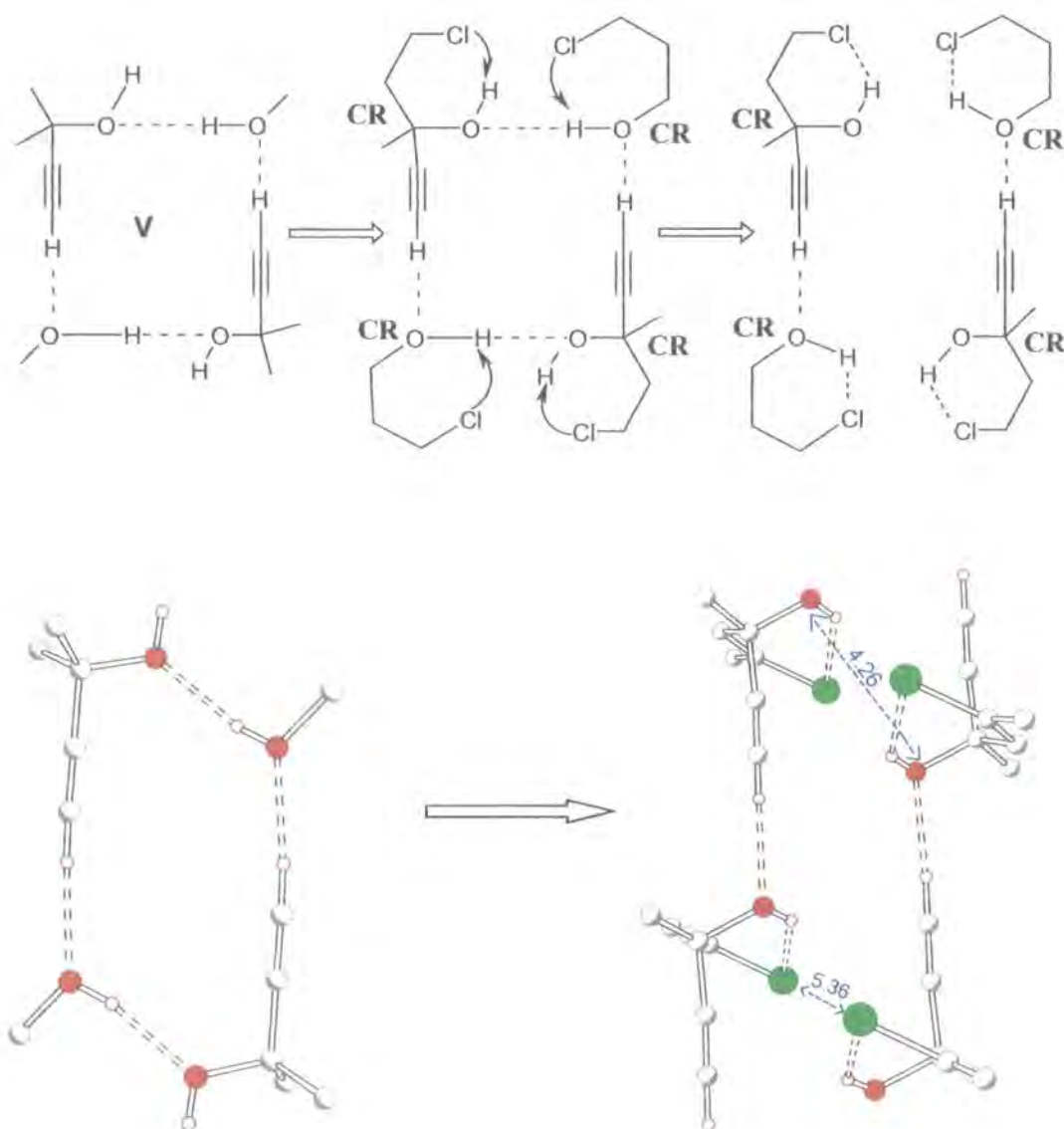
D-H...A	d(D-H)	d(H...A)	d(D...A)	<(DHA)
O ₁ -H ₁ ...Cl ₁	0.73(3)	2.50(3)	3.0728(15)	137(3)
O ₁ '-H ₁ '...O ₂	0.78(3)	2.06(3)	2.822(2)	163(3)
C ₁₆ -H ₁₆ ...O ₁ '	0.99(3)	2.12(3)	3.105(3)	176(2)
C ₁₈ -H ₁₈ ...O ₁	0.91(2)	2.51(2)	3.376(3)	159.0(19)

In a groundbreaking introduction of the 'Supramolecular Synthons', Desiraju¹ put forward an analogy between crystal engineering and organic synthesis by addressing molecular and intermolecular forces as the building block of a crystal, just as atoms and interatomic bonds build up molecules.



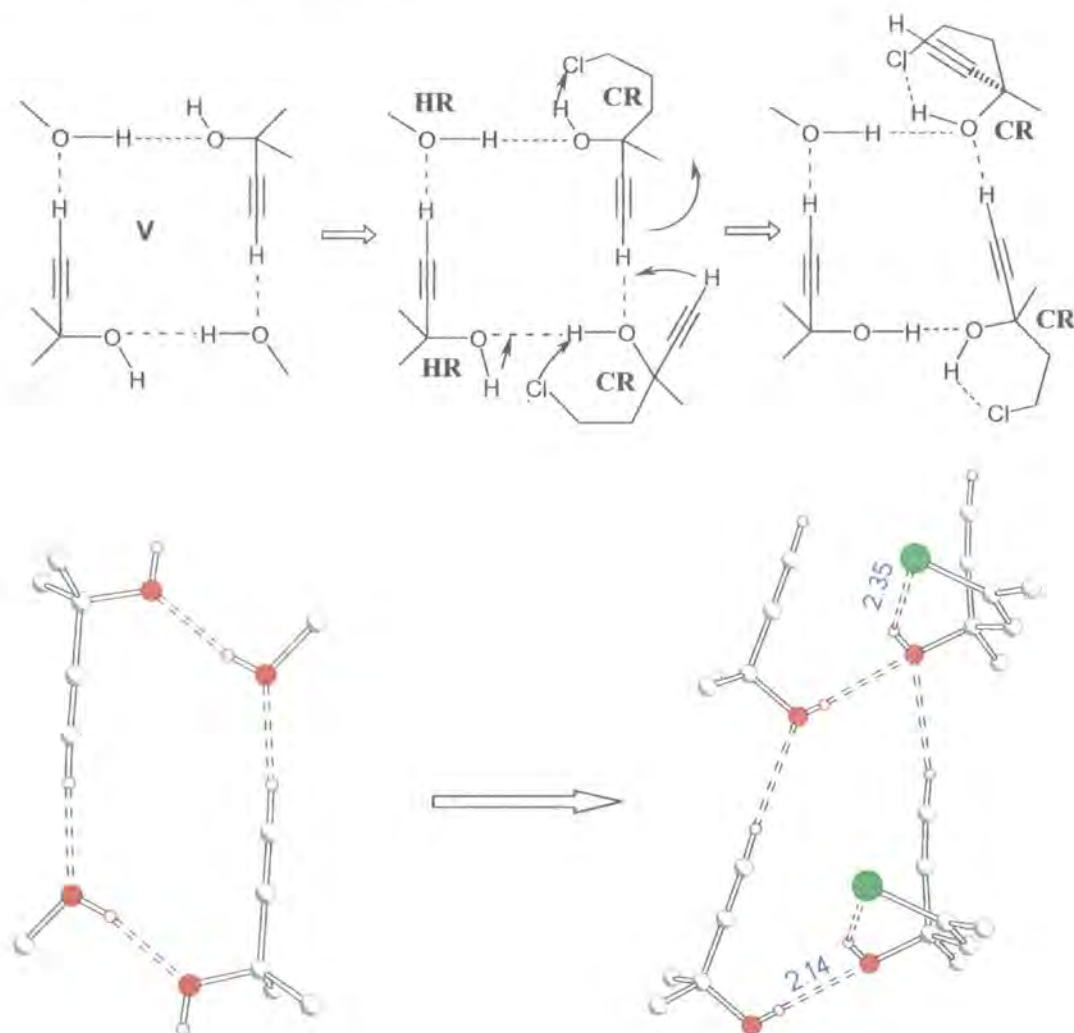
Scheme 3.4. Supramolecular distortion of synthon **I** by the chloro group via intramolecular hydrogen bonding. Note how the vestigial synthon on the hydrogen rich side **B** of the molecule retains its original identity.

Based on this theory, change over (disruption) from synthon **V** and **VI** to dimer can be considered as a supramolecular reaction pathway with CDDA crystals as an intermediate or transition state as shown in Scheme 3.4. The crystal packing further highlights the importance of O-H...Cl interaction toward the structure determination. Had O-H...Cl interaction been a force contact, one would expect synthon **VI** with weaker C-H... π interaction to be more vulnerable to disruption than synthon **V**, composed of stronger bonds.



Scheme 3.5. Supramolecular distortion of synthon **V** by two Cl-groups in 14DDDA.

The supramolecular reaction, considering unsubstituted DDA as the starting compound and monochlorinated CDDA as the intermediate state, not surprisingly, can only be completed with the dichloro derivative playing the role of product. In order to study the complete 'reaction mechanism', dichlorinated compounds therefore immediately draw our attention. In principle, two chlorine atoms, next to the gem alkynol groups can be introduced as many as three different ways, and the corresponding molecules would be, 14DDDA, 18DDDA and 15DDDA.



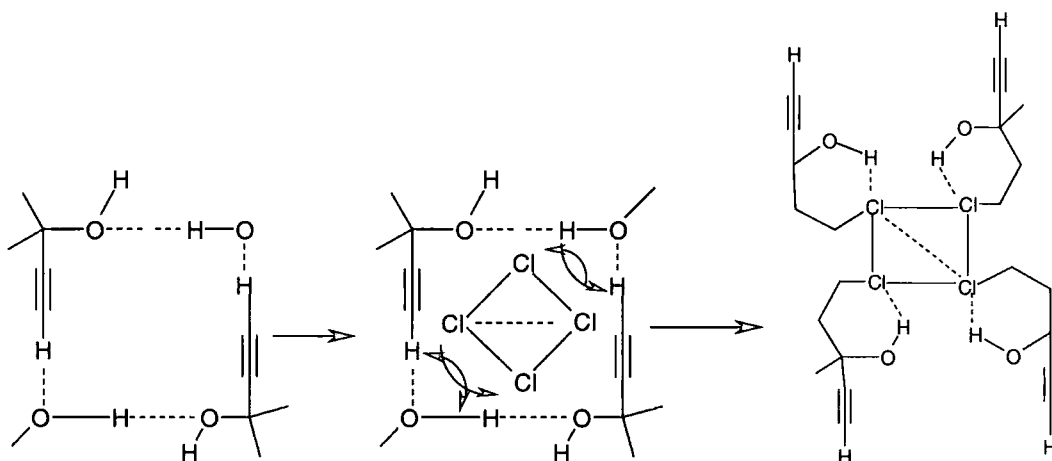
Scheme 3.6. Supramolecular distortion of synthon V by two Cl-groups in 18DDDA

In continuation of our discussion so far, two chlorine groups in 14DDDA make both faces chlorine rich (CR), as a result of that, as expected, both the O-H...O bonds of synthon V are transformed into the O-H...Cl interaction on either side. With an

excellent agreement to our prediction this brings a total disruption of the synthon ∇ (Scheme 3.5).

Supramolecular transformation from DDA to 18DDDA can also be analysed in the similar fashion. Unlike 14DDDA or 15DDDA, 18DDDA resembles more CDDDA with the presence of CR and HR faces. Again there are two geometrically and chemically different faces, a portion surrounded by not one, but two chlorine atoms, while the opposite portion is devoid of any such perturbation. In a remarkable agreement with earlier observation for CDDDA and 14DDDA, half of the synthon remains intact, while on the CR face, once again the O-H...Cl interaction dominates and modifies the O-H...O bonding. The transformation, as shown in the schematic diagram (Scheme 3.6), is slightly different with a long O-H...O bond cooperative with O-H...Cl interaction.

The crystal packing of 15DDDA is quite unusual even though it is in accord with the context of the present chapter. The effect of chlorine atoms can be perceived clearly from the packing and a simple comparison with DDA. Both the molecules are centrosymmetric, and whereas in DDA the molecule occupies a special position, the



Scheme 3.7. Supramolecular distortion of synthon ∇ by two Cl-groups in 15DDDA

15DDDA molecules are in general positions in the unit cell. The major structural feature of 15DDDA is the incorporation of the 'Cl₄' synthon (Figure 3.2) in the middle of synthon V, which apparently breaks up into pieces by the intramolecular interaction of two chlorine atoms with the OH groups. Again the absence of synthon V and VI can be ascribed to the presence of O-H...Cl interactions as shown in Scheme 3.7.

3.5. Competition between organic chlorine and a strong acceptor

With the discussion so far, even though we can easily come to a conclusion on the effectiveness of organic chlorine as a hydrogen bond acceptor, one can argue about the competitiveness of the O-H...Cl interaction in the absence of any stronger acceptor than O-H, such as keto group. To clear any air of confusion or nagging doubt, we studied 15MKA, which contains both hydroxyl and keto groups, hence an ideal molecule for the comparison of organic chlorine with strong and moderately strong acceptors under almost identical geometrical and chemical environments.

Table 3.5 Hydrogen bond table for the 15MKA

D-H...A	d(D-H)	d(H...A)	d(D...A)	<(DHA)
O ₁ -H ₁ ...Cl ₂	0.74(2)	2.53(2)	3.0172(13)	125(2)
O ₁ -H ₁ ...O ₂	0.74(2)	2.23(2)	2.8008(16)	135(2)
C ₁₆ -H ₁₆ ...O ₁	0.91(2)	2.55(2)	3.254(2)	134.0(19)
C ₁₆ -H ₁₆ ...O ₂	0.91(2)	2.56(2)	3.331(2)	142.8(19)

Considering the acceptor capability hierarchy, one would expect a strong O-H...O=C bond to dominate the interaction pattern, on the other hand, the presence of any significant O-H...Cl interaction would be enough to set up organic chlorine as a viable hydrogen bond acceptor. In continuation of the uniqueness of the topic, in the crystal structure of 15MKA both the keto group and Cl atom compete for a single available

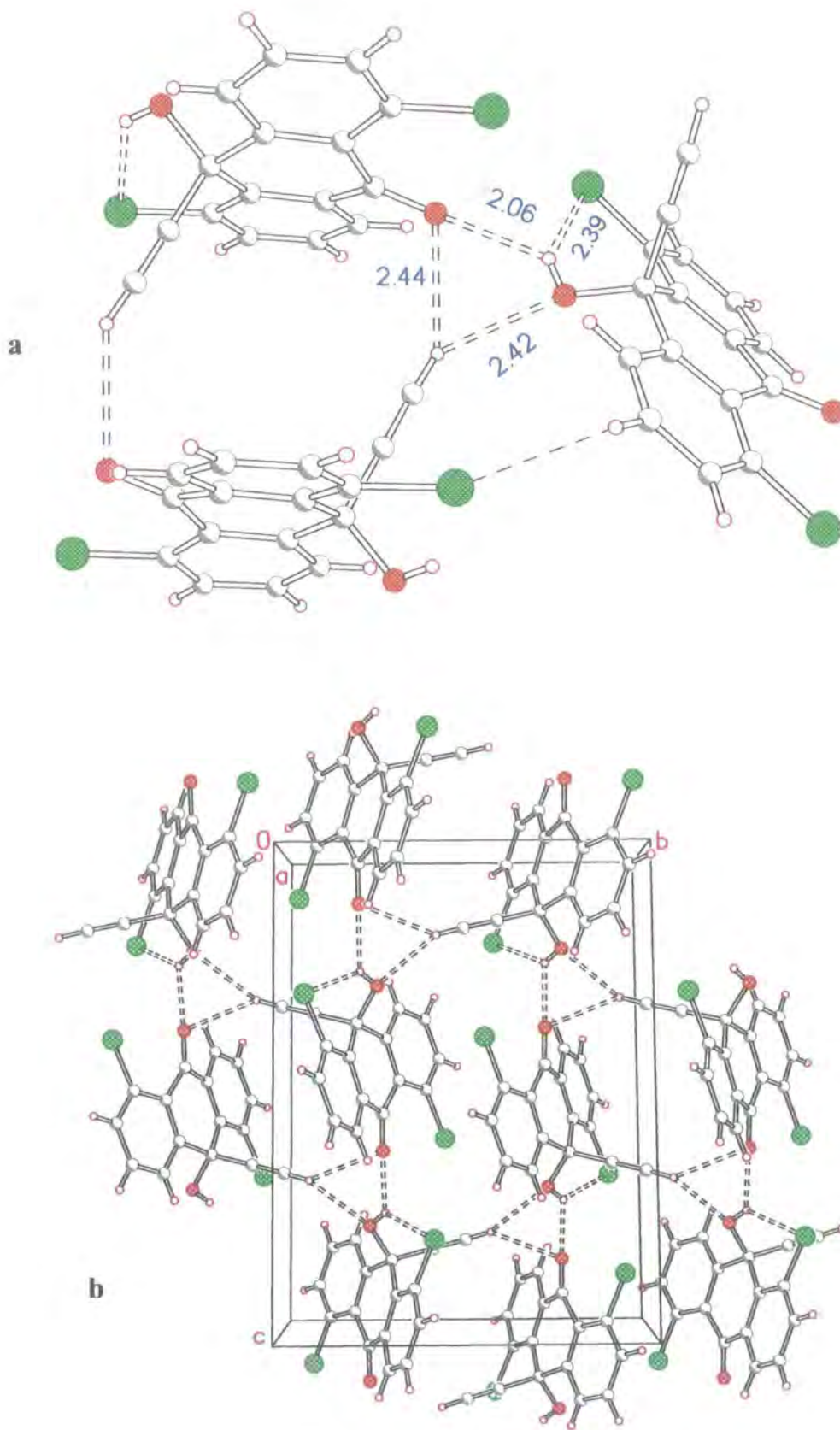


Figure 3.6. (a) Interaction hierarchy of 15MKA, Notice the four distinct hydrogen bridges, the numbers are hydrogen bonding distances in Å, (b) Packing diagram of 15MKA. Cl-atoms are shown in green and O-atoms in red.

donor atom (OH), resulting a bifurcated hydrogen bond. It is difficult to say whether the relatively weak and long O-H...O=C interaction (d, 2.23 Å, θ , 130.1°) with a strong acceptor is more important than a short intramolecular O-H...Cl-C interaction (d, 2.53 Å, θ , 120.7°) with a 'poor' acceptor. To make this unique interaction pattern even more interesting, another bifurcated hydrogen bond involving the ethynyl hydrogen takes place as if to satisfy the 'unfulfilled' acceptor capabilities of the keto group (d, 2.42 Å, θ , 140.4°), with the OH group being the other acceptor group.

It is indeed difficult to decide which one among these four interactions is more important for the structure. To conclude, it may not be clear-cut evidence, but the presence of relatively strong O-H...Cl interaction in crystal packing is a testament to the credible acceptor capabilities of organic halogen.

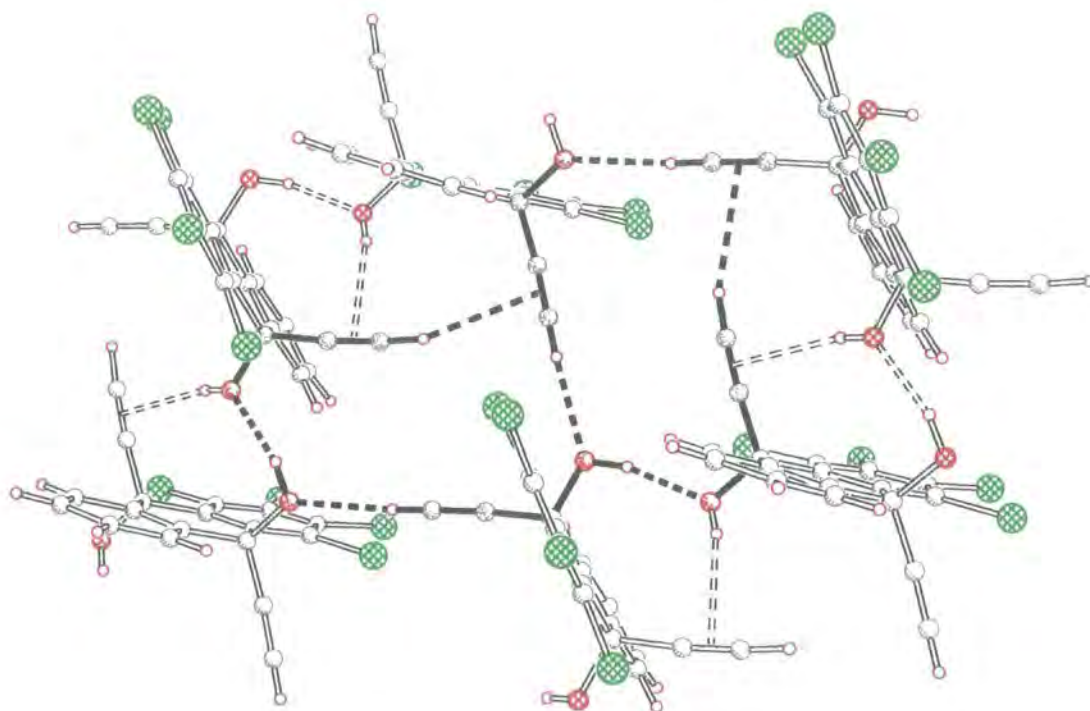
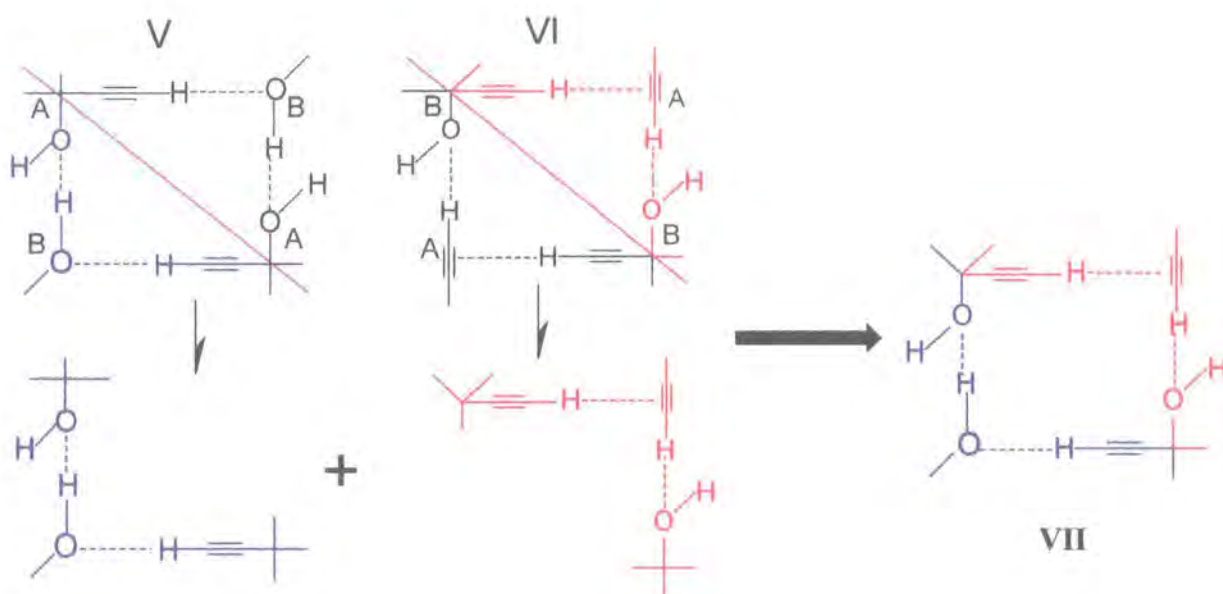


Figure 3.7 Packing diagram of TDDA, note both hydroxyl groups form strong O-H...O, with the new synthon VII (highlighted).

3.6. Novel Synthron Creation:

The above discussion does show that organic chlorine can form strong and structure determining hydrogen bonds that could mould a recognised supramolecular synthron in some comprehensible manner. Notwithstanding, the unique crystal structure of TDDA that does not form any O-H...Cl bond in the solid state shows that chlorine can still geometrically effect the crystal packing. Previous work on this family shows that two major supramolecular synthrons, **V** and **VI** dominate crystal packing. In an unprecedented occurrence, TDDA forms a synthron (**VII**) that is nothing but the 1:1 linear combination of synthron **V** and **VI** as shown in Scheme 3.8. This is first time we found a supramolecular synthron formed from the combination of two other existing synthrons of the family. Although we can draw a preliminary conclusion that this is due to the geometrical effects of four chlorine atoms, this unusual but useful observation deserves further attention and the molecule is still under investigation.



Scheme 3.8. Formation of synthron **VII** from the 1:1 linear combination of **V** and **VI**

3.7. Reinforcement from NMR Data

Evidence of hydrogen bonding is often corroborated by other techniques, among the other techniques IR spectroscopy and solid state NMR spectroscopy²⁹ are most commonly used tools. Herein, the notion of an intramolecular O-H...Cl interaction was further reinforced by the solution NMR data (CDCl_3) of all the six molecules. Data for all seven (with parent DDA) are provided in **Table 3.6**.

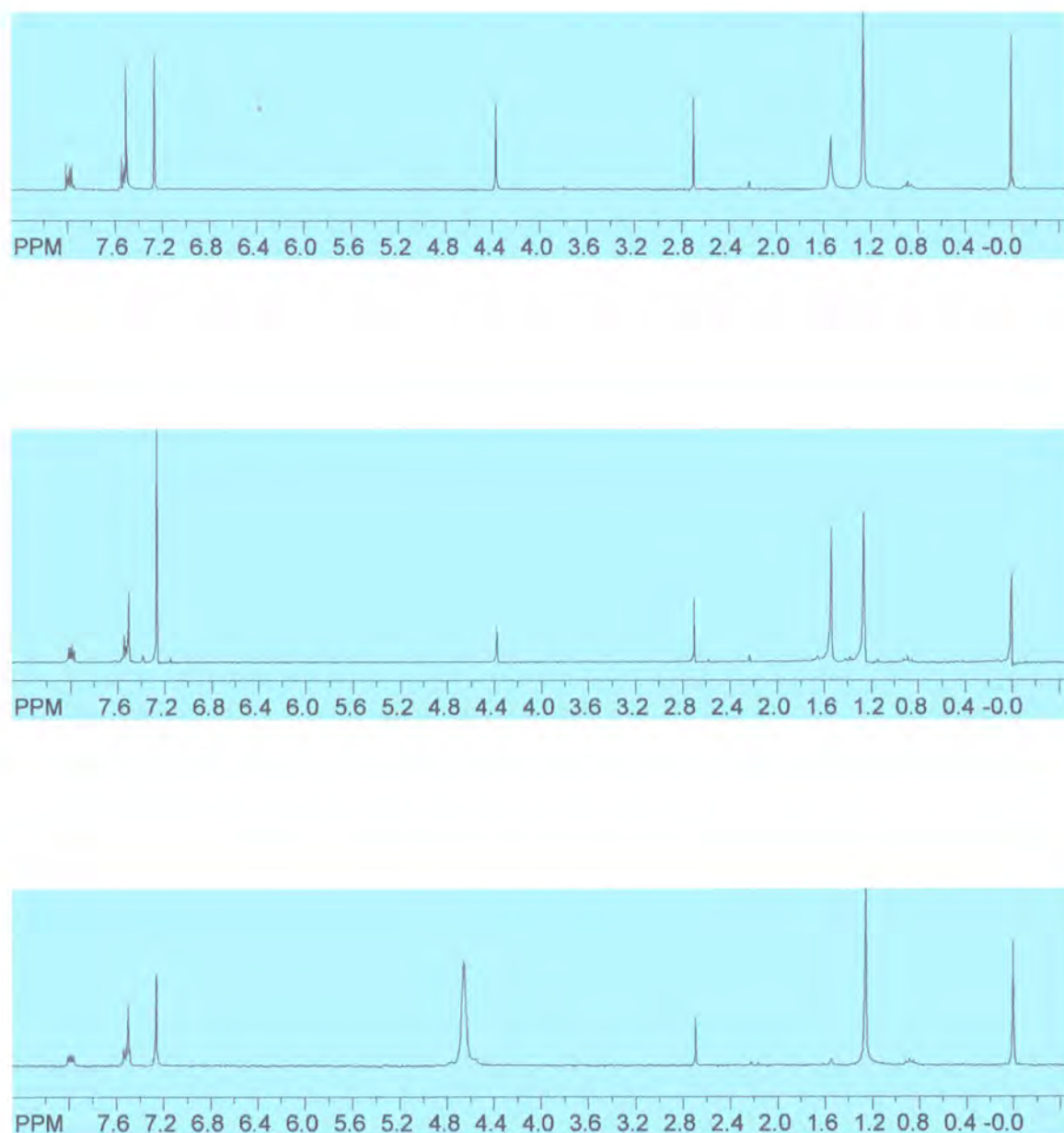


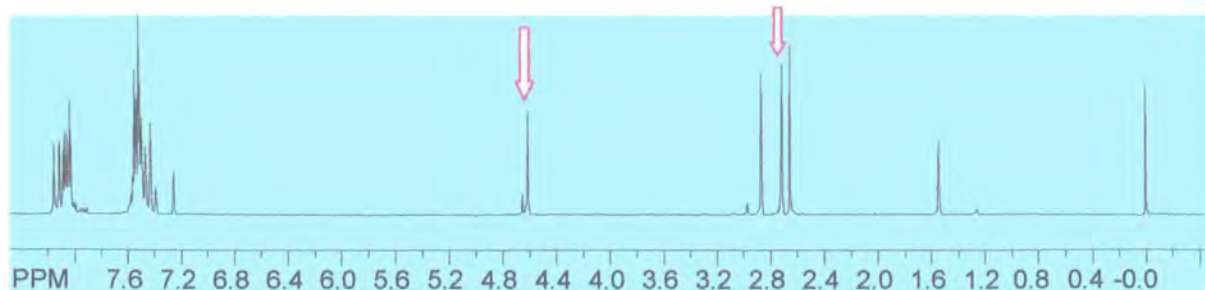
Figure 3.8. ^1H NMR spectra of 14DDDA (CDCl_3). Top: Initial spectrum; Middle: twice diluted; Bottom: D_2O added.

There are some common and consistent trends among the compounds that were sometime missing in the solid state. All those O-H group that possibly can participate in intramolecular O-H...Cl interaction, do so. It is interesting to note here that such interactions were absent for both the OH groups of TDDA and for one OH group of 15DDDA in the solid state. Three important points were emphasized that were emerged the NMR experiments, (a) the intramolecular nature of the interaction, (b) the hydrogen atoms of interest belong to the hydroxyl group and (c) the attractive nature of the interaction.

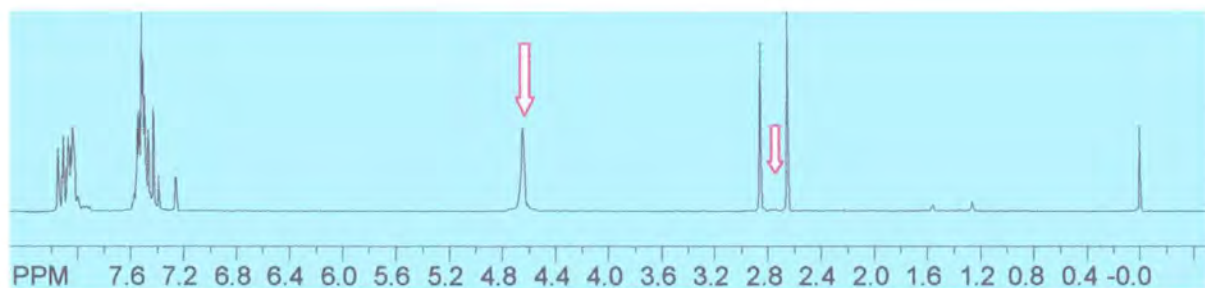
The typical peaks for hydroxyl hydrogen atom routinely shift from $\delta 2.6$ to around $\delta 4.5$ for those containing an adjacent chlorine group, apparently due to the formation of an O-H...Cl interaction. Upon dilution with CDCl_3 , there was no further change in the intensity or the peak position, as shown in Figure 3.8 for 14DDDA, which confirms the intramolecular nature of the interaction. Again the proton exchange reaction with D_2O and subsequently the disappearance of the peak at $\delta 4.5$ further confirms that the exchanged hydrogen atom indeed belongs to the hydroxyl group.

Table 3.6. ^1H NMR Chemical shifts of hydroxyl H-atoms in *gem*-alkynols showing the existence of intramolecular O-H...Cl-C interactions.

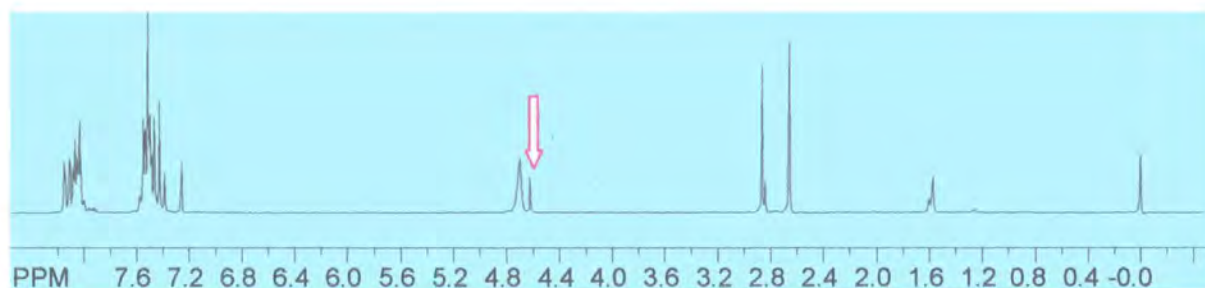
Compound	$\delta(\text{O-H}\dots\text{Cl-C})$ hydrogen bonded hydroxyl proton (ppm)	δ (free O-H) (ppm)
DDA	—	2.80
CDDA	4.61	2.78
14DDDA	4.39	—
15DDDA	4.46	—
18DDDA	4.51	2.79
TDDA	4.40	—
15MKA	4.71	—



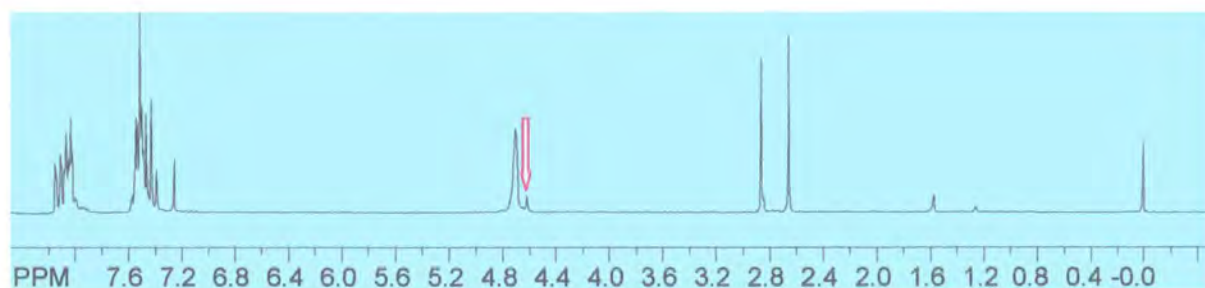
0 sec



40 sec



120 sec



1 hour

Figure 3.9. Time resolved D_2O exchange NMR spectra of CDDA. Note that the intramolecular O–H...Cl hydrogen bonded proton (δ 4.61) exchanges slowly when compared with the ‘free’ hydroxyl proton at δ 2.78 which exchanges immediately.

The intramolecular as well as the attractive nature of the interaction was further unfolded from an experiment with CDDA. Recalling the faces **CR** and **HR** for CDDA, which contain two non-equivalent O-H groups, wherein only one OH group, belonging to the **CR** face can only form an O-H...Cl interaction and not the other one. We tried to exploit this sharp contrast in the local environment and the result is a clear manifestation of two distinct hydroxyl groups' behaviour. Upon addition of D₂O, while the 'free' OH group undergoes hydrogen exchange almost instantly, the hydroxyl hydrogen involving the O-H...Cl interaction, dramatically retards the process. The complete exchange of hydrogen, as shown in Figure 3.9, took place in almost one hour. These findings are of enormous importance and speak in favour of viable acceptor capabilities of organic halogens. The acceptor capabilities of organic halogen have never been above controversy and were always considered as sterically induced in order to accommodate a special geometry (intramolecular), or as secondary interactions arising from close packing considerations (intermolecular) and lacking in stabilising characteristics. However, the gradual exchange of the proton does prove that the O-H...Cl interaction herein is of attractive in nature and not arising from any forced contact.

3.8. References:

- [1] G. R. Desiraju, *Angew. Chem. Int. Ed. Engl.*, 1995, **34**, 2311-2327.
- [2] G. R. Desiraju, T. Steiner, *The Weak Hydrogen Bond in Structural Chemistry and Biology*, Oxford University Press, Oxford, 1999.
- [3] T. Steiner, *Chem. Comm.*, 1997, 727-734.
- [4] a) G. R. Desiraju, *Acc. Chem. Res.*, 2002, **35**, 565-573; b) T. Steiner, *Angew. Chem.*, 2002, **114**, 50-80, *Angew. Chem. Int. Ed. Engl.*, 2002, **41**, 48-76. c) T. W. Martin, Z. S. Derewenda, *Nature Structural Biology*, 1999, **6**, 403-405.
- [5] J. D. Dunitz, R. Taylor, *Chem. Eur. J.*, 1997, **3**, 89-98.
- [6] F. Toda, H. Liu, I. Miyahara, K. Hirotsu, *J. Chem. Soc. Perkin Trans. 2*, 1997, **218**, 85-88.
- [7] A. Hantzsch, *Chem. Ber.*, 1915, **48**, 797-816.
- [8] O. R. Wulf, U. Liddel, S. B. Hendricks, *J. Am. Chem. Soc.*, 1936, **58**, 2287-2293.
- [9] a) D. Y. Curtin, S. R. Byrn, *J. Am. Chem. Soc.*, 1969, **91**, 1865-1866; b) D. Y. Curtin, S. R. Byrn, *J. Am. Chem. Soc.*, 1969, **91**, 6102-6106; c) S. R. Byrn, D. Y. Curtin, I. C. Paul, *J. Am. Chem. Soc.*, 1972, **94**, 890-898;
- [10] a) Q. -C. Yang, M. F. Richardson, J. D. Dunitz, *J. Am. Chem. Soc.*, 1985, **107**, 5535-5537; b) Q. -C. Yang, M. F. Richardson, J. D. Dunitz, *Acta Cryst.*, 1989, **B45**, 312-323; c) M. F. Richardson, Q. -C. Yang, E. N. Bregger, J. D. Dunitz, *Acta Cryst.*, 1990, **B46**, 653-660.
- [11] J. E. Burks, D. van der Helm, C.Y. Chang, L.S. Ciereszko, *Acta Cryst.*, 1977, **B33**, 704-709.
- [12] K. R. Acharya, D. S. S. Gowda, M. Post, *Acta Cryst.*, 1979, **B35**, 1360-1363.
- [13] R. J. Davey, N. Blagden, S. Righini, H. Alison, M. J. Quayle, S. Fuller, *Cryst. Growth Des.*, 2001, **1**, 59-65.

- [14] J. A. K. Howard, V. J. Hoy, D. O'Hagan, G. T. Smith, *Tetrahedron*, 1996, **52**, 12613-12622.
- [15] a) G. Aullón, D. Bellamy, L. Brammer, E. A. Bruton, A. G. Orpen, *Chem. Comm.*, 1998, 653-654. b) L. Brammer, E. A. Bruton, P. Sherwood, *Cryst. Growth Des.*, 2001, **1**, 277-290;
- [16] C. B. Aakeröy, T. A. Evans, K. R. Seddon, I. Pálinkó. *New J. Chem.*, 1999, **23**, 145-152
- [17] P. K. Thallapally, A. Nangia, *CrystEngComm.*, 2001, **27**, 1-6.
- [18] T. J. Barbarich, C. D. Rithner, S. M. Miller, O. P. Anderson, S. H. Strauss, *J. Am. Chem. Soc.*, 1999, **121**, 4280-4281.
- [19] a) P. Murray-Rust, W. C. Stallings, C. T. Monti, R. K. Preston, J. P. Glusker, *J. Am. Chem. Soc.*, 1983, **105**, 3206-3214. b) L. Shimoni, J. P. Glusker, *Struct. Chem.*, 1994, **5**, 383-397.
- [20] V. R. Thalladi, H. -C. Weiss, D. Bläser, R. Boese, A. Nangia, G. R. Desiraju, *J. Am. Chem. Soc.*, 1998, **120**, 8702-8710.
- [21] S. C. F. Kui, N. Zhu, M. C. W. Chan, *Angew. Chem.*, 2003, **115**, 1666-1670; *Angew. Chem. Int. Ed. Engl.*, 2003, **42**, 1628-1632.
- [22] J. Parsch, J. W. Engels, *J. Am. Chem. Soc.*, 2002, **124**, 5664-5672.
- [23] J. A. Olsen, D. W. Banner, P. Seiler, U. O. Sander, A. D'Arcy, M. Stihle, K. Müller, F. Diederich, *Angew. Chem.*, 2003, **115**, 2611-2615; *Angew. Chem. Int. Ed. Engl.*, 2003, **42**, 2507-2511
- [24] R. Banerjee, G. R. Desiraju, R. Mondal, J. A. K. Howard *Chem. Eur. J.*, 2004, **10**, 3373-3383.
- [25] R. S. Rowland, R. Taylor, *J. Phys. Chem.*, 1996, **100**, 7384-7391.
- [26] R. Banerjee, G. R. Desiraju, R. Mondal, A. S. Batsanov, C. K. Broder, J. A. K. Howard, *Helv. Chim. Acta.*, 2003, **86**, 1339-1351.

- [27] a) N. N. L. Madhavi, G. R. Desiraju, C. Bilton, J. A. K. Howard, F. H. Allen, *Acta Cryst.*, 2000, **B56**, 1063-1070; b) C. Bilton, J. A. K. Howard, N. N. L. Madhavi, A. Nangia, G. R. Desiraju, F. H. Allen, *Acta Cryst.*, 2000, **B56**, 1071-1079; c) N. N. L. Madhavi, C. Bilton, J. A. K. Howard, F. H. Allen, A. Nangia, G. R. Desiraju, *New J. Chem.*, 2000, **24**, 1-4; d) F. H. Allen, J. A. K. Howard, V. J. Hoy, G. R. Desiraju, D. S. Reddy, C. C. Wilson, *J. Am. Chem. Soc.*, 1996, **118**, 4081-4084.
- [28] R. Parthasarathy, G. R. Desiraju, *J. Am. Chem. Soc.*, 1989, **111**, 8725-8726.
- [29] A. E. Aliev, K. D. M. Harris, *Structure and Bonding*, 2004, **108**, 3-48.

Chapter 4

Correlation Between the Molecular Symmetry and Crystallographic Symmetry in Gem-Alkynol Family and their Pseudopolymorphs

4.1. Introduction

One of the major aims of crystal engineering is to obtain crystals that have or lack a particular symmetry element¹. Based on this, the relationship between molecular and supramolecular (crystal) symmetry can be categorized either as (1) the symmetry of the molecule is lowered in the crystal, (2) the crystal symmetry is higher than the molecular symmetry or (3) the molecular and crystal symmetries are matched. The first of these is most common and closely relates to the Kitaigorodski's close packing theory.

The theory of close-packing forms the basic framework of our understanding of the ways in which organic molecules assemble into crystals. The underlying reason for preference of molecules to form a particular crystal structure and the reliable correlation between molecular symmetry and crystallographic symmetry is of great importance for crystal structure prediction and crystal engineering. One approach could be drawing statistical correlation from the existing crystal structures. Such efforts have been made as early as the 1940s when Nowacki² and later Kitaigorodski³ outlined several consequences of the close-packing principles as applied to organic molecular solids. In general, it was observed that only 20 of the possible 230 space groups are commonly adopted.

Out of several consequences of the close packing principles in organic molecular solids as pointed out by Kitaigorodski in his book³, those relevant to this work are (1) centrosymmetric space groups are preferred, (2) space groups that contain translational symmetry like screw axis and glide planes are preferred, (3) the inversion centre is the only molecular symmetry element that is routinely carried into the crystal structure. In other words, molecules that have the symmetry element i usually adopt a $\bar{1}$ site in the crystal.

Very recently the Cambridge Structural Database (CSD)⁴ put forward a relational database, CSDSymmetry⁵, which enables us to draw the definitive relationships from existing crystal structures, between point group and space group for small molecule crystal structures.

Special features in the crystal structure and pseudopolymorphism are apparently two distinctly different issues of crystal engineering, yet they are often found closely interrelated.

In 1995, Threlfall⁶ introduced the term pseudopolymorphism to describe two or more solvated crystalline forms of a compound, which have different crystal structures and/or differ in the nature and stoichiometry of the included solvent. The usage of the two terms, solvate and pseudopolymorphs are user-dependent, otherwise chemically synonymous. While most chemists prefer the term solvate, pseudopolymorph is more popular in the pharmaceutical circle⁷. This term was further mentioned and defined by Byrn⁸ and Bernstein⁹ in their respective books on the solid state chemistry of drugs and polymorphism.

Unlike polymorphs, until recently pseudopolymorphs have not been treated systematically. Usually inclusion of solvent has been considered as a nuisance and studied only out of general interest. The whole perception of solvates however changed significantly over the last decade, with growing interests in the crystal engineering fuelling more interests on the other aspects of crystal structures. Invariably the role of solvents in the crystal structure was imperative interest for some early studies. Solvents can play three important roles in the crystal by (1) taking part in hydrogen-bonded networks, (2) filling the spaces or cavities without any strong interaction, and (3) acting as a ligand to coordinate with metal atom for inorganic crystal structures¹⁰.

However, solvent inclusion is not common especially for organic crystal structures, and any such occurrence always suggests some special reason, such as unsatisfied hydrogen bonds, inadequate packing, etc. A recent study revealed that only 15% of organic compounds in the CSD are pseudopolymorphs, i.e., include solvent molecules in the respective crystal structure. Detailed 'knowledge-mining' from CSD shows that 20 common solvents appear at least 50 times in different organic crystal structures¹¹. A multi-point hydrogen bonding

model between solvate and solvent molecules was put forward by Nangia and Desiraju¹² in order to explain the tendency/reluctance of solvent molecules to form solvates. The model was broadly based on two thermodynamic parameters, entropy and enthalpy, which act as the driving force for the nucleation and crystallisation process. As crystallisation begins, solvent molecules come out of the aggregate and go to the bulk solution with increasing entropy, this is coupled with the enthalpic gain which comes from the formation of robust supramolecular synthon within the stable solute species. The simultaneous occurrence of these two energetically favourable processes is the prime reason why 85% of organic crystals are unsolvated. Conversely there might be an '*interruption*'¹³ to these 'normal' sequences of crystallisation to an unsolvated form by the formation of either strong O/N-H...O/N or weak C-H...O hydrogen bonds between solvent and solute molecule in a multi point manner. This, in effect, makes extraction of solvent molecule from the aggregate to the bulk enthalpically disadvantageous enough to lead to solvate formation.

Most of the solvates fit nicely with this multi point recognition model. One such example would be the solvates of 3,5-dinitrosalicylic acid, wherein out of seven solvates, four are with dioxane, owing to the double acceptor capabilities of the two oxygen atoms of the dioxane molecule¹⁴.

As a compliment to these studies, detailed studies have been made on developing host molecules of different steric bulk and functionality as a part of host-guest complexes, where most of the time, common solvents appear to be the guest molecule. Weber¹⁵ and Toda¹⁶ are among the front-runners in reporting these kind of studies. According to Weber, a successful host molecule should be bulky, rigid and should contain functional groups capable of forming host-guest specific interaction¹⁷.

Nonetheless, it is an indisputable fact that the guest inclusion properties of a large number of host molecules have been discovered by chance rather than by design. One such example

would be tetrakis (4-nitrophenyl) methane, wherein for the first time a robust diamonoid built with weak C-H...O, π ... π interactions was observed in some of the solvates¹⁸. Elegant work by Bishop and co workers on the diquinoxaline lattice inclusion host reveals a preference to trap small polychloroalkane guests through rather weak C-H...N hydrogen bonds¹⁹. Very recently, Boese and Desiraju²⁰, while studying pseudopolymorphism of sym-trinitrobenzene (TNB), point out the subjective limitation of the terms like solvate, pseudopolymorphs. For solvents like toluene and benzene where the driving force is π ... π stacking, they prefer to use the term donor-acceptor complex rather than pseudopolymorph or molecular complex⁷.

Any new term's entry in the literature brings home some new controversy with it; at the same time some terms are too common to discard or modify^{21, 22}. Boese and Desiraju cited a well-known example of this kind of murkier definition of TNB-anthracene crystal structure⁷. The authors argue "molecular complexes" would be a more aptly chosen term than "pseudopolymorph", as the anthracene was used in a solid form and not in a liquid form, on the contrary "pseudopolymorph" would be the more appropriate if liquid anthracene (at elevated temperature) was used. Even though the term pseudopolymorph is not entirely unambiguous and the legality of polymorph is same as pseudopolymorph¹⁴, it is difficult to displace with a new term and hereafter we will use solvate or pseudopolymorph to avoid any confusion.

4.2. Result and Discussion:

This particular work²³ was prompted by the 'unusual' observation that the title molecule, 1,5-dichloro-trans-9,10-diethynyl-9,10-dihydroanthracene-9,10-diol (DDDA), belongs to C_i point group but does not occupy this site symmetry in the crystal.

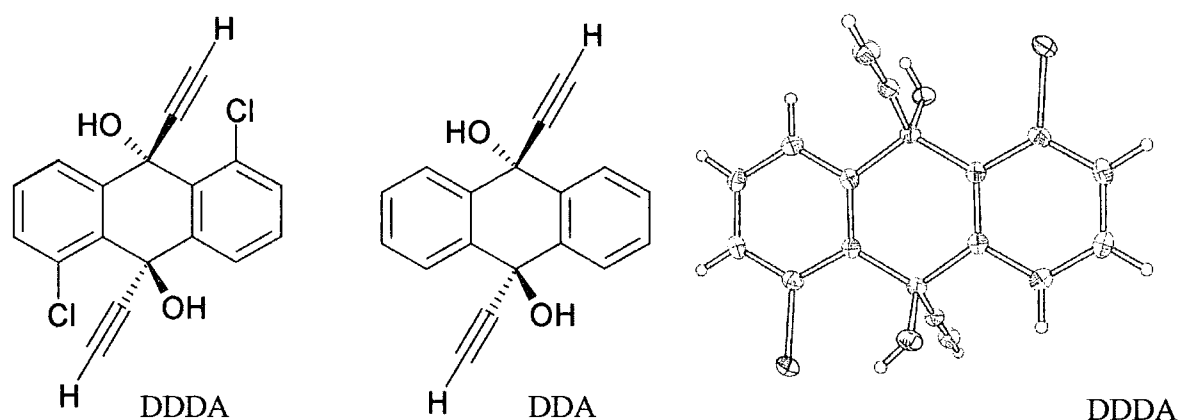
The molecule lies on a general position in the unit cell though it adopts a centrosymmetric space group. This occurrence is contrary to the observation of Kitaigorodski stated earlier and deserved a more detailed study because of its deemed unusualness.

At the same time it raises another question, how uncommon is such an occurrence? To answer this question, we start with most the conventional approach, viz., deriving statistical data from the existing crystal structures. We used CSDSymmetry⁵, an algorithm that perceives molecular symmetry and has been applied to ca. 200,000 entries from CSD. The perceived point group, as well as crystallographic properties such as the space group, occupied Wyckoff positions and the number of residues in the asymmetric unit has been placed for each molecule in the relational database, CSDSymmetry. Queries may be posed to this database to obtain information on the relationship between molecular and crystal symmetry.

For the present case, we found that out of 18,008 molecules belonging to the point group containing the symmetry element *i*. 17,152 molecules (95.2%) crystallise in a space group containing a Wyckoff position of symmetry *i*, again 15156 (88.4%) molecules of these lie on a crystallographic inversion centre. When an additional constraint such as *i*, is the only molecular symmetry (same as DDDA) applied, 99% of such molecules lie on an inversion centre in the crystal. So much so, such behaviour was not observed for any other symmetrical gem-alkynol studied by us or/and in nearly 135 existing entries in CSD. These compelling numbers led us to a preliminary conclusion: although the behaviour of the title molecule is not unprecedented, it is certainly unusual.

We took the opportunity to compare this structure to the non-chloro analogue, trans-9,10-diethynyl-9,10-dihydroanthracene-9,10-diol (DDA)²⁴, which lies on an inversion centre in space group $P\bar{1}$. Vis-à-vis correlation between changes in crystal structure brought about by changes in the molecular structures yields a few important points. (1) Chemical as well as

geometrical effects of the substituent groups in a molecule are manifested in the crystal packing adopted. (2) Positioning of the substituent in the molecule is also important, not only the nature of the substituent. (3) Up to a certain limit, changes in the molecular structure may be carried out over a range of substituent groups without perturbing the crystal structure. But at the limit of the range, a slight change in the molecular structure may change the whole crystal packing. In the present context, two chloro groups in a close juxtaposition to the already crowded alkynol functionality in DDDA result in different crystal packing than non-chloro analogue of DDA.



Scheme 4.1. Schematic diagram and single molecule of DDDA and DDA.

Thermodynamically, centrosymmetric molecules tend to lie on inversion centre in the crystal so that the largest number of atoms are then able to aggregate with the shortest possible separations; this will reduce the free energy which is in accord with the theory that any observed crystal structure is a free energy minimum³. Therefore it may be presumed

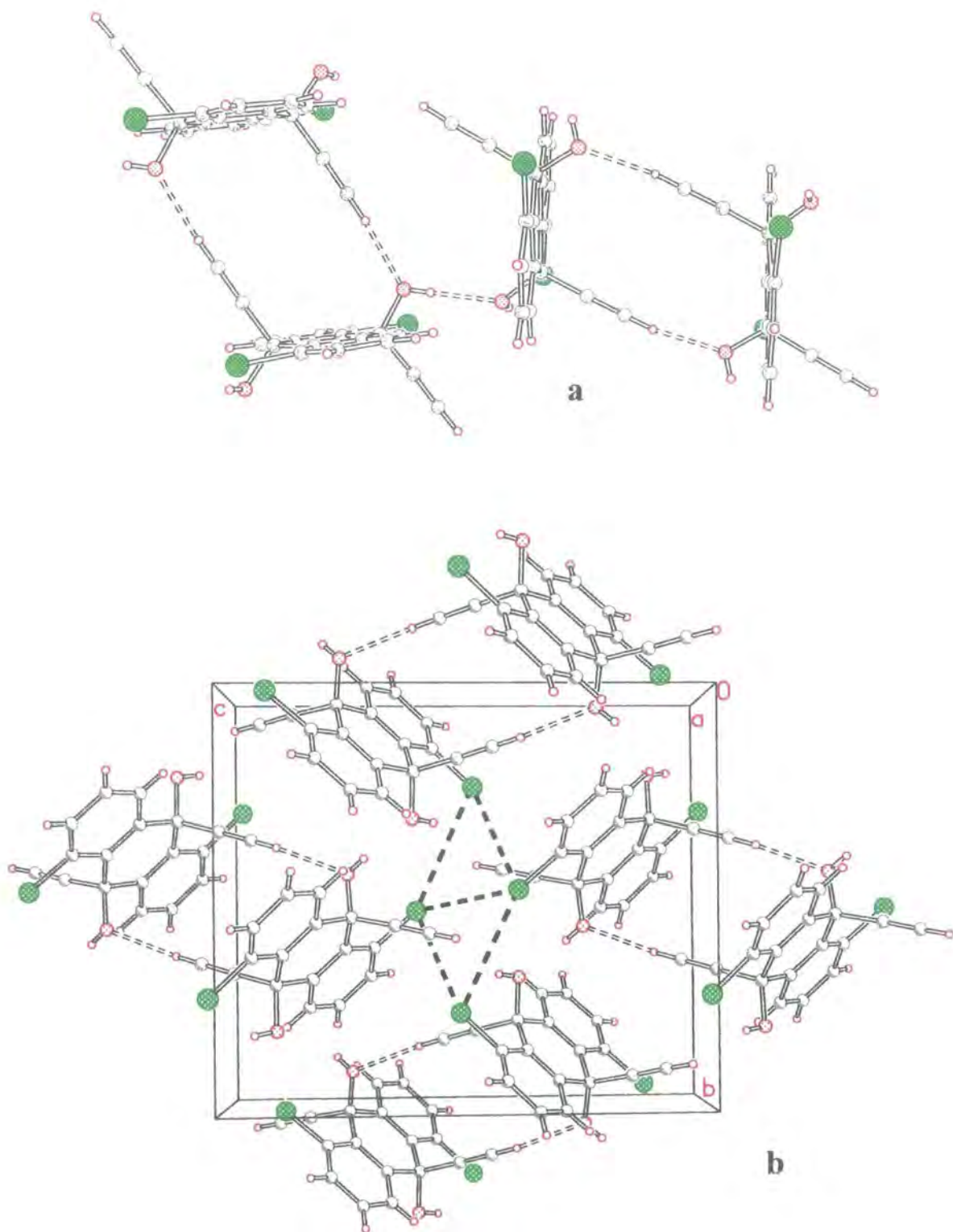


Figure 4.1. a) Dimer synthon formed by the DDDA, Notice the two dimer is linked with O-H...O bond. b) . Packing diagram of DDDA. Notice the planar Cl₄ synthon (highlighted) at the position (0.5, 0.5, 0.5). C-H...O hydrogen bridges are also shown.

that there are other compensating factors to reduce the free energy for this unusual packing, where a centrosymmetric molecule lying on a crystal inversion centre is absent.

This invariably draws more attention towards the hydrogen bonds and other intermolecular interactions in the crystal structure of DDDA. Two major interaction patterns are observed. One with a cooperative arrangement of three hydrogen bonds, an intermolecular $C\equiv C-H\dots O$ ($d= 2.44 \text{ \AA}$, $\theta= 164.7^\circ$), an intermolecular $O-H\dots O$ ($d=1.83 \text{ \AA}$, $\theta= 173.8^\circ$), and a weak $O-H\dots Cl$ ($d= 2.25 \text{ \AA}$, $\theta= 135.4^\circ$) interaction. [Figure 4.1(a)].

Lack of local symmetry is also evident from these interaction patterns. While one of the hydroxyl groups is engaged in an $O-H\dots O$ bond the other one is relegated to a weaker $O-H\dots Cl$ interaction. Only one of the ethynyl group forms hydrogen bond, the other one is apparently 'free'.

The second interaction pattern can be derived from four chlorine atoms. This 'Cl₄' synthon built up with four quasi type-II $Cl\dots Cl$ contacts ($d, 3.56, 3.69 \text{ \AA}$) and one type-I $Cl\dots Cl$ contact ($d, 3.64 \text{ \AA}$)²⁵. [Figure 4.1(b)]. A $C-H\dots O$ dimer between two inversion related interactions could be derived as a third synthon from the first type of interactions.

Out of these, the densely packed and symmetrical (planar) four-atom 'Cl₄' supramolecular synthon appears to be the dominant interaction pattern. This synthon lies on the inversion centre in the crystal which provides the opportunity for largest number of atoms to aggregate with shortest possible separations. This is precisely the reason why centrosymmetric molecules tend to lie on inversion centres in the crystal.

In the context of crystal engineering, it has been noted earlier that organic crystal structure can well be simplified to a network wherein the molecules are the nodes and the supramolecular synthons are node connections¹, that is, supramolecular synthons can be considered as being equivalent to molecules. In other words crystal symmetry may be

analysed as a convolution of molecular symmetry and supramolecular synthon (or void) symmetry²⁶.

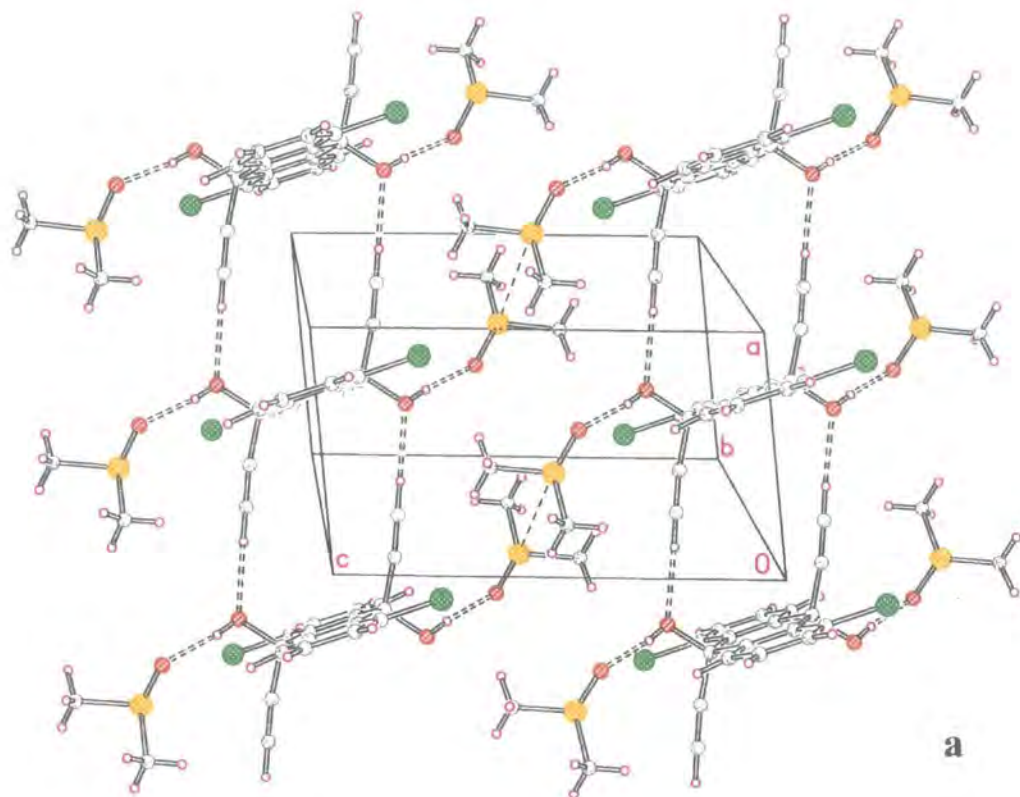
In the present context, the 'Cl₄' supramolecular synthons are playing the same role in the crystal packing as normally does a molecule and it has turned the packing 'inside out'. This particular molecule thus provides us an unique crystal structure where all the special positions are occupied by voids and the molecules lie at the general positions in the unit cell. Although we could explain the observed packing and is not particularly unfavourable, nonetheless it still posed a question about its unusual nature. For most of the gem-alkynol structures cooperative chains of O-H...O hydrogen bond and/or loops of weak and strong hydrogen bonds (synthon V, VI and VII in chapter 3) are the dominant interaction patterns²⁴. We suggest that the already crowded environment in the gem-alkynol group is made even more hindered by the close juxtaposition of two chlorine atoms, which prevent formation of extensive hydrogen bonding networks, that otherwise has been observed for this family. The disruption of the extensive hydrogen bonding is evident from the hydrogen bonding patterns, as one hydroxyl group forms an O-H...O bond, the other an O-H...Cl interaction, while one ethynyl group forms a C-H...O bond and the other one is apparently 'free'. In order to check the viability of our crystal packing pattern we searched for 'Cl₄' units in the CSD (Conquest 1.4, version 5.23, April 2002). The result further strengthens our suggestion. Out of 2918 chloro-substituted aromatic entries, 298 cases were observed where formation of 'Cl₄' tetramer appears to play an important role. This number is supportive enough to make this synthon structure determining.

4.3. Pseudopolymorphism

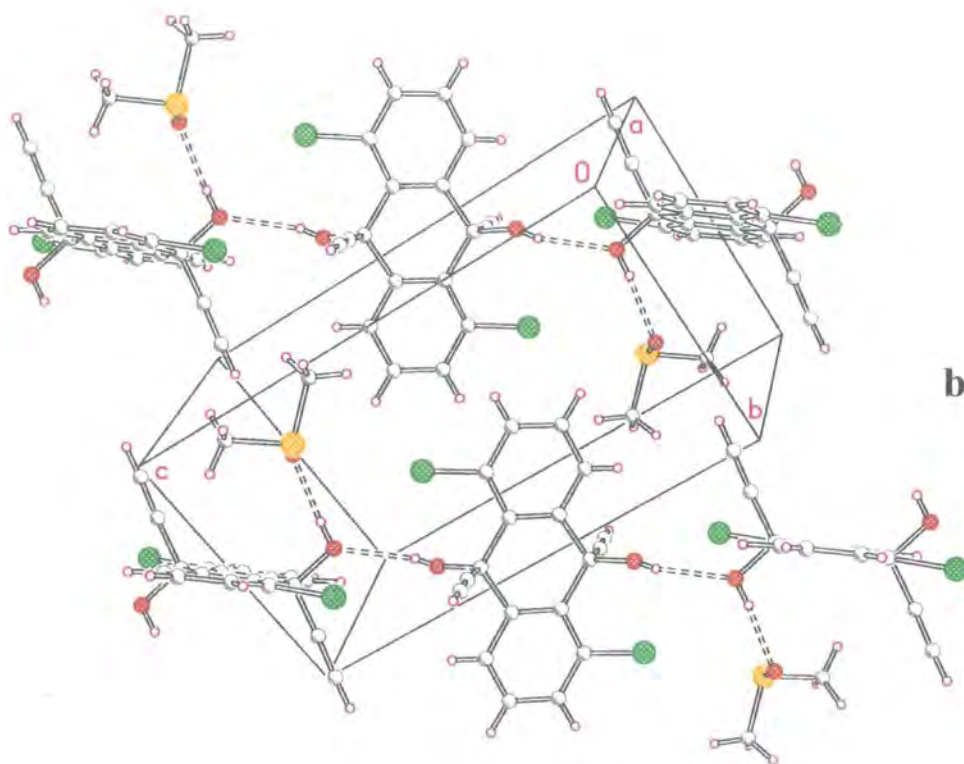
One of the interesting features of DDDA crystal packing was the lack of local symmetry. The presence of two chlorine atoms in close proximity to the gem-alkynol group, make it difficult to form short and linear hydrogen bonds, as we found that only one out of the two hydroxyl and the two ethynyl groups form strong hydrogen bonds. This clearly suggests the hydrogen bonds formed did not fulfil their potential. It has been noted earlier that systems with unsatisfied hydrogen bond potential, originating from the absence of robust supramolecular synthons tend to form pseudopolymorphs. Keeping that in mind, we carried out crystallisation from some dipolar aprotic solvents solvents that are well known for their tendencies to lead to pseudopolymorph formation.

We were successful beyond our most optimistic expectations. Four common solvates, viz., dimethyl sulfoxide (DMSO), N-methyl pyrrolidone (NMP), hexamethylphosphoramide (HMPA) and N,N-dimethylformamide (DMF) were used for this study. In the following section five of these solvates, (DDDA).(DMSO), (DDDA).(DMSO)₂, (DDDA).(NMP)₂, (DDDA).(HMPA)₂ and (DDDA).(DMF)₂, will be described.

(DDDA).(DMSO)₂ : This crystal structure clearly proves the hypothesis that unsolvated DDDA molecules adopt an unusual packing arrangement because of inadequate short and linear hydrogen bonds. The small size and good hydrogen bonding ability of DMSO is easily able to overcome the steric hindrance and is able to make a linear approach in order to form a strong O-H...O bond. The DDDA molecule lies on an inversion centre and an O-H...O mediated 1:2 solute-solvent module is observed. The dimer synthon is retained here and is cooperative with the O-H...O bonds, and these constitute an excellent 3D- layer and pillar network. Quite clearly the small size and good hydrogen bonding ability allows the



a



b

Figure 4.2. (a) Packing diagram of (DDDA).(DMSO)₂. Notice the O-H...O bond and the C-H...O dimer retained here. (b) Packing diagram of (DDDA).(DMSO). Notice the O-H...O bond.

directed inclusion of DMSO molecules and changes the ‘unusual’ crystal packing of DDDA towards a more ‘normal’ one. [Figure 4.2 (a)]

(DDDA).(DMSO) : This structure is a ‘polymorph of a pseudopolymorph’ of (DDDA).(DMSO)₂ with an ‘extra’ molecule of DDDA interleaved between the 1:2 solute-solvent module via an O-H...O bond to give a host rich structure. As a result, the ethynyl group becomes ‘free’ and no C-H...O dimer synthon is formed. [Figure 4.2 (b)]. A typical C-H...O bond is observed between the activated methyl group of DMSO and hydroxy group of DDDA¹².

Table 4.1. Selected hydrogen bond table for the solvates

Solvent	Interaction	<i>d</i> (Å)	<i>D</i> (Å)	θ (°)
DMSO (I)	C-H...O	2.32	3.258(2)	142.9
	C-H...O	2.45	3.491(2)	159.1
	O-H...O	1.76	2.733(2)	169.5
	O-H...O	1.96	2.853(2)	149.8
DMSO (II)	C-H...O	2.14	3.184(2)	163.9
	C-H...O	2.42	3.538(2)	167.2
	O-H...O	1.71	2.682(2)	172.4
NMP	C-H...O	2.41	3.277(2)	135.3
	C-H...O	2.45	3.443(2)	150.9
	C-H...Cl	2.67	3.752(1)	172.4
	O-H...O	1.74	2.726(2)	172.4
HMPA	C-H...O	2.27	3.274(5)	153.2
	C-H...O	2.36	3.343(5)	149.9
	O-H...O	1.70	2.667(4)	165.9
	O-H...O	1.71	2.667(4)	161.4
	C-H...Cl	2.62	3.706(6)	176.1
DMF	C-H...O	2.19	3.227(5)	159.3
	C-H...O	2.30	3.312(5)	154.3
	O-H...O	1.70	2.689(5)	176.1
	O-H...O	1.71	2.695(4)	173.8

(DDDA).(NMP)₂, (DDDA).(HMPA)₂: For these two crystal structures, again a 1:2 solute-solvent module is the recurring theme, however here DDDA molecules are connected by C-H...Cl bonds. From the packing point of view these two crystal packings are identical. **[Figure 4.3]**

(DDDA).(DMF)₂ : This structure is pseudo-centrosymmetric and the similar 1:2 solute-solvent module lies on an pseudo-inversion centre. Like the DMSO solvate, the DDDA molecules appear to be linked with C-H...O hydrogen bonds, however no dimer synthon is formed here. Instead a 'tetramer' of DDDA is formed with C-H...O bonds and two DMF molecules nicely fit into the cavity. **[Figure 4.4]**

Table 4.2. A comparison of the five solvates with regard to selected solvent and crystal properties.

Solvent	Host/ Guest ratio	Space group	Packing Coefficient	Solvent Surface Area Å ² /u.c	Solvent Volume Å ³ /u.c	Acceptor Strength	
						Electrostatic	Mulliken
DMSO	1:1	P $\bar{1}$	73.0	101.04	72.05	-0.521	-0.784
DMSO	1:2	P $\bar{1}$	70.6	101.04	72.05	-0.521	-0.784
NMP	1:2	P $\bar{1}$	70.2	134.45	102.72	-0.622	-0.620
HMPA	1:2	P $\bar{1}$	68.7	221.53	179.35	-0.702	-0.579
DMF	1:2	P2 ₁ (pseudo P2 ₁ /n)	72.5	108.40	78.65	-0.553	-0.579

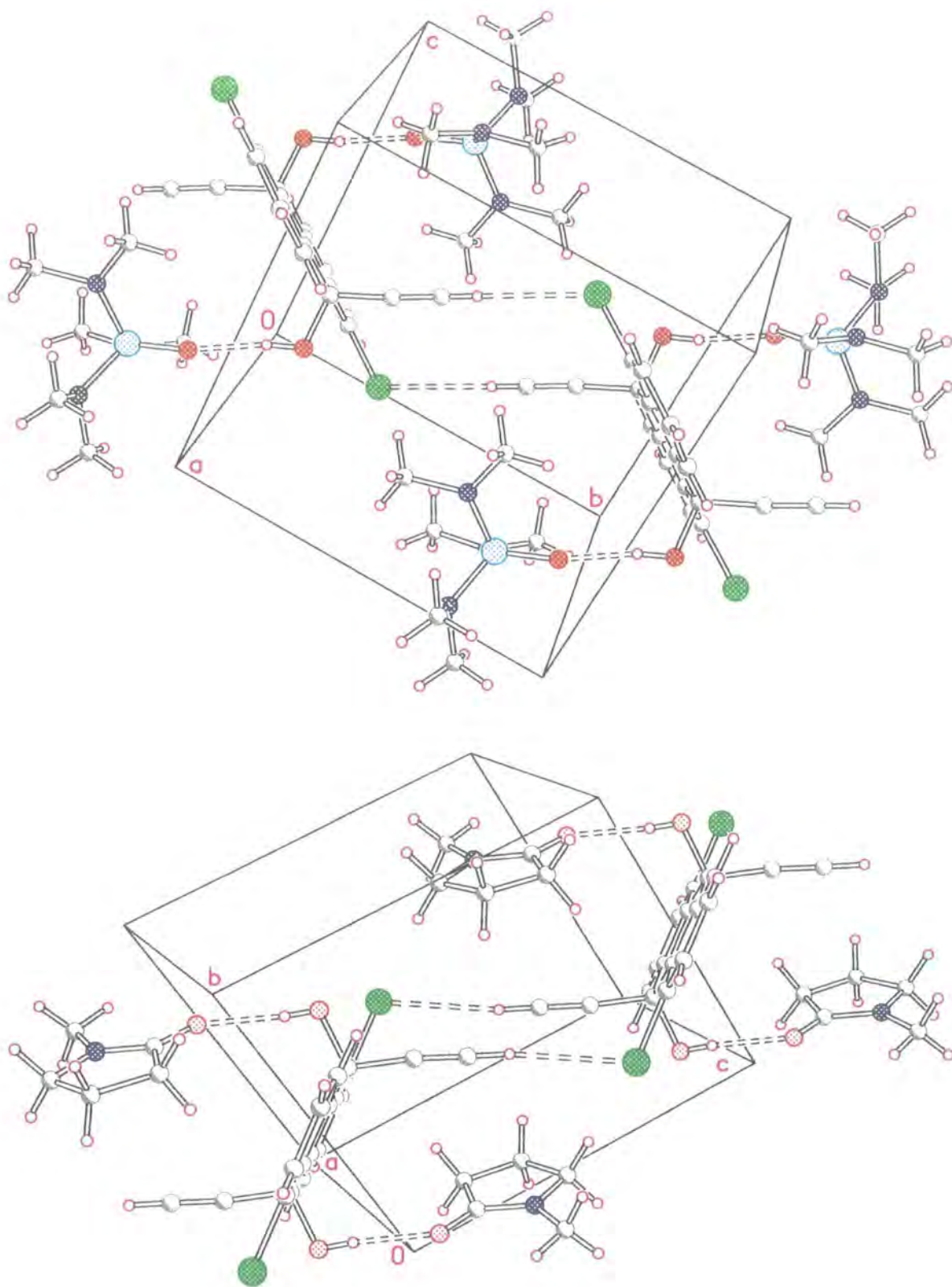


Figure 4.3. (a) Packing diagram of (DDDA).(HMPA)₂, Notice the O-H...O bond and the C-H...Cl bond. (b) Packing diagram of (DDDA).(NMP)₂, Notice the O-H...O bond, C-H...Cl dimer retained here.

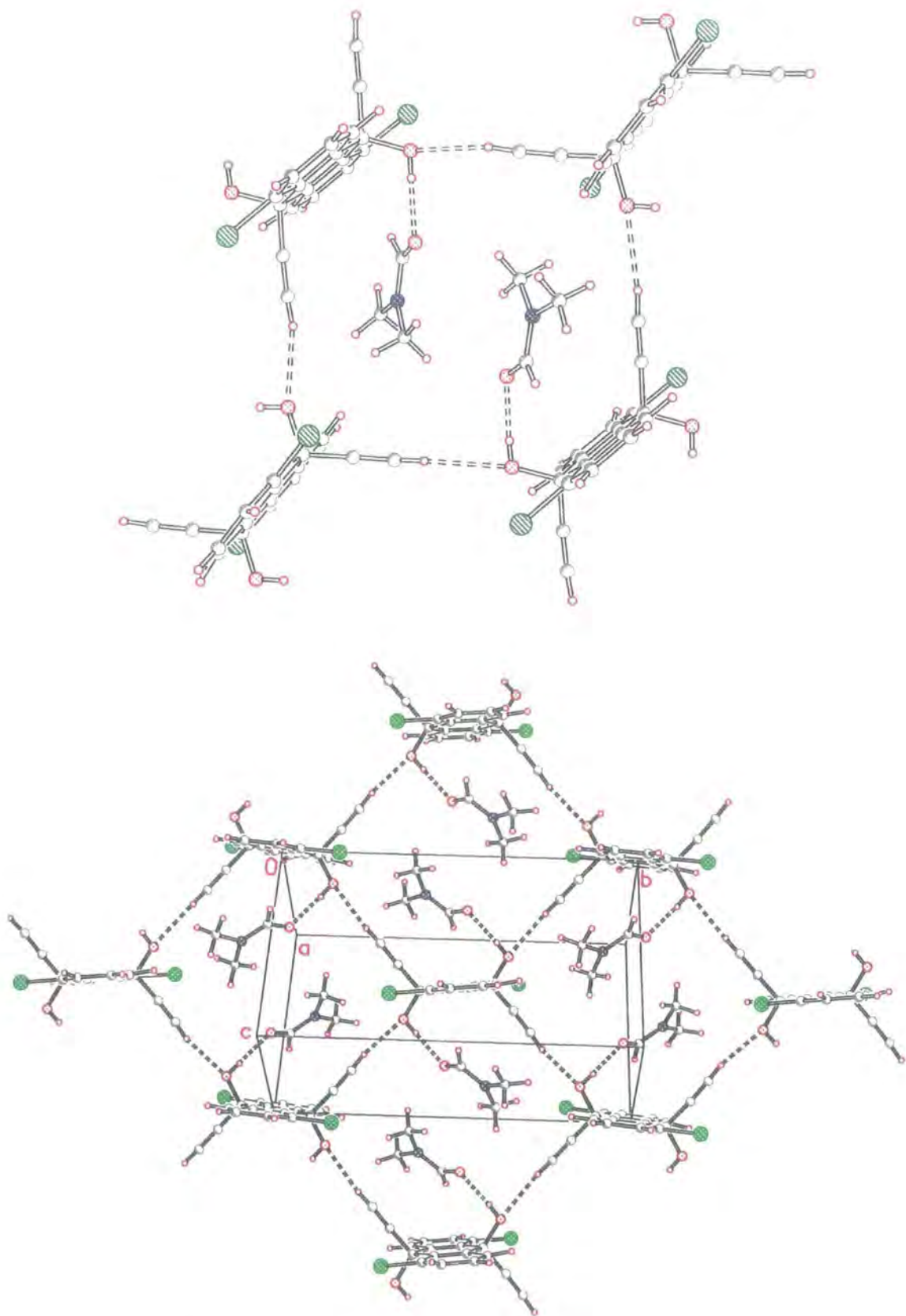


Figure. 4.4 Packing diagram of (DDDA)(DMF)₂.

Table 4.3. Crystallographic data and structure refinement parameters.

Identification code	DDDA	DDDA (DMSO) ₂	DDDA.DMSO
Solvent	EtOH/Benzene (1:1)	DMSO	DMSO/DMF (1:1)
Empirical Formula	C ₁₈ H ₁₀ Cl ₂ O ₂	(C ₁₈ H ₁₀ Cl ₂ O ₂) ·(C ₂ H ₆ OS) ₂	(C ₁₈ H ₁₀ Cl ₂ O ₂) C ₂ H ₆ OS
Formula wt.	329.16	485.42	407.29
Crystal System	Monoclinic	Triclinic	Triclinic
Space group	<i>P</i> 2 ₁ / <i>n</i>	<i>P</i> $\bar{1}$	<i>P</i> $\bar{1}$
<i>a</i> [Å]	7.4205(2)	6.6307(5)	7.3174(15)
<i>b</i> [Å]	12.7571(4)	7.6581(5)	9.3646(19)
<i>c</i> [Å]	14.8695(4)	11.9717(7)	14.222(3)
α [°]	90	79.613(2)	81.14(3)
β [°]	93.3820(10)	84.232(2)	89.16(3)
γ [°]	90	67.037(2)	67.56(3)
<i>Z</i> '	1	0.5	1
Volume [Å ³]	1405.16(7)	550.26(6)	889.0(3)
F (000)	672	252	420
D _{calc} [g/cm ³]	1.556	1.465	1.522
μ [mm ⁻¹]	0.465	0.512	0.501
2 θ [°]	4.20 – 57.98	3.90 – 54.98	4.76 – 54.98
Crystal size	0.40 x 0.18 x 0.08	0.36 x 0.32 x 0.1	0.48 x 0.35 x 0.18
Index Range	-10 ≤ <i>h</i> ≤ 9, -17 ≤ <i>k</i> ≤ 17 -20 ≤ <i>l</i> ≤ 20	-8 ≤ <i>h</i> ≤ 8 -9 ≤ <i>k</i> ≤ 9 -15 ≤ <i>l</i> ≤ 15	-9 ≤ <i>h</i> ≤ 9 -12 ≤ <i>k</i> ≤ 11 -18 ≤ <i>l</i> ≤ 18
Reflns. Collected	16581	6206	10782
Unique reflns.	3207	2530	4079
Observed reflns.	2702	2385	3749
<i>R</i> ₁ [<i>I</i> > 2 σ (<i>I</i>)]	0.0328	0.0388	0.0325
<i>wR</i> ₂ [all]	0.0853	0.0948	0.0895
Goodness-of-fit	1.031	1.061	1.059
CCDC deposition No.	200403	200399	200400

Identification code	DDDA.(NMP) ₂	DDDA.(HMPA) ₂	DDDA.(DMF) ₂
Solvent	NMP	HMPA	DMF
Empirical formula	(C ₁₈ H ₁₀ Cl ₂ O ₂). (C ₅ H ₉ NO) ₂	(C ₁₈ H ₁₀ Cl ₂ O ₂). (C ₆ H ₁₈ N ₃ OP) ₂	(C ₁₈ H ₁₀ Cl ₂ O ₂). (C ₃ H ₇ NO) ₂
Formula wt.	527.42	687.57	475.35
Crystal System	Triclinic	Triclinic	Monoclinic
Space group	$P\bar{1}$	$P\bar{1}$	$P2_1$
<i>a</i> [Å]	7.4173(15)	8.5057(2)	7.3834(3)
<i>b</i> [Å]	9.1696(18)	9.7689(2)	15.3739(8)
<i>c</i> [Å]	9.6472(19)	10.7323(2)	10.3430(5)
α [°]	103.40(3)	86.9450(10)	90
β [°]	90.46(3)	77.4350(10)	102.497(2)
γ [°]	102.70(3)	84.8540(10)	90
<i>Z</i> '	0.5	0.5	1
Volume [Å ³]	621.5(2)	866.37(3)	1146.23(9)
F (000)	276	364	496
λ [Å]	0.71073	0.71073	0.71073
<i>D</i> _{calc} [g/cm ³]	1.409	1.318	1.377
μ [mm ⁻¹]	0.300	0.323	0.317
2 θ [°]	4.34 –54.98	3.90 –54.98	4.04 –54.96
Crystal size	0.44 x 0.32 x 0.30	0.42 x 0.32 x 0.16	0.38 x 0.35 x 0.20
Index Range	-9 ≤ <i>h</i> ≤ 9 -11 ≤ <i>k</i> ≤ 11 -12 ≤ <i>l</i> ≤ 12	-11 ≤ <i>h</i> ≤ 11 -12 ≤ <i>k</i> ≤ 12 -13 ≤ <i>l</i> ≤ 13	-9 ≤ <i>h</i> ≤ 9 -19 ≤ <i>k</i> ≤ 19 -13 ≤ <i>l</i> ≤ 13
Reflns. Collected	7131	9911	11510
Unique reflns.	2848	3965	4895
Observed reflns.	2701	3727	4233
<i>R</i> ₁ [<i>I</i> > 2 σ (<i>I</i>)]	0.0322	0.0325	0.0576
<i>wR</i> ₂ [all]	0.0871	0.0886	0.1539
Goodness-of-fit	1.031	1.041	1.182
CCDC deposition No.	200401	200402	200398

All these five crystal structures show one common trend, usually a 1:2 solute-solvent module mediated by an O-H...O bond as the dominant interaction pattern. For each solvate, the module lies on an inversion centre (or pseudo-inversion centre). This justifies our earlier hypothesis of an unsatisfactory hydrogen bonding model for the unsolvated DDDA molecule, which is outweighed by the inclusion of a smaller guest molecule with a shorter and more nearly linear O-H...O bonding

Competition experiments were carried out in order to find out the preference for solvent molecule inclusion. As a part of that, DDDA was crystallized from DMSO+DMF, DMSO+HMPA, HMPA+DMF, NMP+HMPA and NMP+DMF solvent mixtures. At least 6 crystals were selected and checked on diffractometer, only one pseudopolymorph was obtained for each set of solvent mixtures. For the above mentioned solvent mixtures the pseudopolymorphs obtained are respectively, DMSO, DMSO, HMPA, NMP and NMP. This results suggest the preference for solvent inclusion in the system follows the order DMSO>NMP>HMPA>DMF. This order can be rationalised on the basis of size and the hydrogen bonding ability of the solvent molecule. In general practice, inclusion of solvent molecule in the lattice is favoured by smaller size and better hydrogen bonding ability. The above mentioned order of solvent inclusion fits perfectly with the Table 4.1 & 4.2 data, which indicate that both the chemical and the geometrical factors are important for the stabilisation of the crystal.

4.4. References:

1. P. K. Thallapally, K. Chakraborty, A. K. Katz, H. L. Carrell, S. Kotha and G. R. Desiraju *CrystEngComm*, 2001,**31**, 1-3.
2. a) W. Nowacki, *Helv. Chim. Acta.*, 1942, **25**, 863;
b) W. Nowacki, *Helv. Chim. Acta.*, 1943, **26**, 459.
3. A. I. Kitaigorodskii, '*Molecular Crystals and Molecules*', Academic Press, New York, 1973.
4. (a) F. H. Allen, O. Kennard, *Chem. Des. Autom. News*, 1993, **8**, 30-37, (b) F. H. Allen, *Acta Cryst.* 2002, **B58**, 380-388.
5. J. W. Yao, J. C. Cole, E. Pidcock, F. H. Allen, J. A. K. Howard, W. D. S. Motherwell, *Acta Cryst.*, 2002, **B58**, 640-646.
6. Threlfall, T. L., *Analyst*, 1995, **120**, 2435-2460.
7. R. K. Jetti, R. Boese, P. K. Thallapally, G. R. Desiraju, *Cryst. Growth Des.*, 2003, **3**(6), 1033-1040
8. S. R. Byrn, *Solid-State Chemistry of Drugs*, Academic Press, New York, 1982.
9. J. Bernstein, *Polymorphism in Molecular Crystals*, Clarendon: Oxford, 2002.
10. C. H. Görbitz and H.-P. Hersleth, *Acta Cryst.*, 2000, **B56**, 526-534
11. G. R. Desiraju, *Chem. Comm.*, 1991, 426-428.
12. A. Nangia, G. R. Desiraju, *Chem. Comm.*, 1999, 605-606
13. G. R. Desiraju in '*Simulating Concepts in Chemistry*', Eds. S. Shibasaki, J. F. Stoddart, F. Vogtle, Wiley, Chichester, 2000, pp 293.
14. V. S. S. Kumar, S. S. Kuduva, G. R. Desiraju, *J. Chem. Soc., Perkin Trans.*, 2, 1999, 1069-1073
15. E. Weber, S. Nitsche, A. Weirig, I. Csöreg, *Eur. J. Org. Chem.*, 2002, 856-872

16. a) F. Toda, K. Tanaka, , R. Kuroda, *Chem. Comm.*, 1997, 1227-1228, b) M. R. Caira, L. R. Nassimbeni, F. Toda, D. Vujovic, *J. Am. Chem. Soc.*, 2000, **122**, 9367-9372, c) F. Toda, K. Tanaka, R. Kuroda, *Chem. Comm.*, 1997, 1227-122, b) M. R. Caira, L. R. Nassimbeni, F. Toda, D. Vujovic, *J. Chem. Soc., Perkin Trans.*, 2, 2001, 2119-2124. d) M. R. Caira, A. Jacobs, L. R. Nassimbeni, F. Toda, *CrystEngComm*, 2003, **5** (28), 150-153
17. E. Weber, in *Inclusion Compounds*, J. L. Atwood, J. Davies, D. D. Macnicol, Eds; Oxford University Press, Oxford, 1991, vol. **4**, pp. 188-262
18. R. Thimattam, F. Xue, J. A. R. P. Sarma, T. C. W. Mak, G. R. Desiraju, *J. Am. Chem. Soc.*, 2001, **1230**, 4432-4445
19. a) C. E. Margi, R. Bishop, D. C. Craig, M. L. Scudder, *Eur. J. Org. Chem.*, 2001, 863-873, b) C. E. Margi, R. Bishop, D. C. Craig, M. L. Scudder, *Eur. J. Org. Chem.*, 2003, 72-81.
20. P. K. Thallapally, A. K. Katz, H. L. Carrell, G. R. Desiraju, *CrystEngComm*, 2003, **5**(18), 87-92
21. G. R. Desiraju, *CrystEngComm*, 2003, **5**(82), 466-467
22. J. D. Dunitz, *CrystEngComm*, 2003, **5**(9), 506-506.
23. R. Banerjee, G. R. Desiraju, R. Mondal, A. S. Batsanov, C. K. Broder, J. A. K. Howard, *Helv. Chim. Acta.*, 2003, **86**, 1339-1351.
24. a) C. Bilton, J. A. K. Howard, N. N. L. Madhavi, A. Nangia, G. R. Desiraju, F. H. Allen, *Acta Cryst.*, 2000, **B56**, 1071-1079; b) N. N. L. Madhavi, G. R. Desiraju, C. Bilton, J. A. K. Howard, F. H. Allen, *Acta Cryst.*, 2000, **B56**, 1063-1070; c) N. N. L. Madhavi, C. Bilton, J. A. K. Howard, F. H. Allen, A. Nangia, G. R. Desiraju, *New J. Chem.*, 2000, **24**, 1-4; d) F. H. Allen, J. A. K. Howard, V. J. Hoy, G. R. Desiraju, D. S. Reddy, C. C. Wilson, *J. Am. Chem. Soc.*, 1996, **118**, 4081-4084.
25. R. Parthasarathy, G. R. Desiraju, *J. Am. Chem. Soc.*, 1989, **111**, 8725-8726.
26. a) D. S. Reddy, D. C. Craig, G. R. Desiraju, *J. Am. Chem. Soc.*, 1996, **118**, 4090-4093, b) G. R. Desiraju, *Angew. Chem. Int. Ed. Engl.*, 1995, **34**, 2311-2327.

Chapter 5

Conformational Pseudopolymorphism :

Unprecedented Observation of Both Gauche and Staggered

Forms of Diethylamine in Solvates With the Same Host

5.1. Introduction:

The field of inclusion complexes, clathrates (lattice inclusion), pseudopolymorphism, host-guest chemistry has grown dramatically in recent years; owing to their great potential for a variety of fundamental and practical aspects. As a direct manifestation of this, the number of chemical abstracts under the terms “clathrate” and “inclusion compounds” has increased up to a massive 1025 in 2001 from a mere 60 in 1970¹. The majority of the inclusion compounds result from multipoint hydrogen bonding with a pre-formed host receptor.

Molecular recognition lies at the heart of inclusion compounds and indeed, during the last decade or so, the major part of the crystal engineering studies associated with pseudopolymorphism involved designing host molecules of different steric bulk, shape and functionality. Weber, one of the pioneers of this field, outlined a successful host molecule as bulky, rigid and preferably containing functional groups capable of forming specific host-guest interactions².

Pseudopolymorphism is not a common phenomenon for organic compounds, being observed only for 15% cases³. It was noted that solvation occurs only when enthalpic gain from the solute-solvent multipoint interactions outweigh the combined effect of entropy gain by solvent extrusion during nucleation and enthalpic gain from forming robust supramolecular synthon among the solute molecules. This invariably suggests solvents with stronger hydrogen bonding capability stand more chance to form solvates than non-polar hydrocarbon solvents, at least for host molecules containing potential hydrogen bonding functional groups and not chosen for mere space-filling.

Unlike host molecules, solvent molecules, however, have seldom received any special attention and most of the time solvates are obtained by trial and error methods rather than strategically chosen because of some specific important characteristic of a particular solvent. A recent CSD study shows that only 20 common solvents are

incorporated in crystal structures more than 50 times³. Not surprisingly, solvents containing oxygen atoms dominate the list supporting the multi-point recognition model. However, it is surprising enough to note that not a single amine solvent secures a place in the list, given the fact that amines are one of the most extensively studied functional groups in crystal engineering field. This is perhaps due to the hostile environment associated with amines and the unstable nature of the amine solvates.

The host molecule (1,5-dichloro-*trans*-9,10-diethynyl-9,10-dihydroanthracene-9,10-diol, **Figure 5.1.**) of this work has shown some unusual tendency to form solvates⁴ with different solvents including amines, due to the unsatisfied hydrogen bonds formed in the unsolvated crystal structures. A detailed discussion about amine solvates and the supramolecular synthons therein is beyond the scope of this chapter and will be discussed in next chapter. In this chapter we will solely concentrate on a rare occurrence where the crystal lattice of a solute molecule (host) traps a conformationally flexible solvent molecule (guest) in one of its higher energy conformations.

The conformations of simple acyclic molecules have been the prime interest of many researchers from very early years and have been extensively studied theoretically as well as spectroscopically⁵. On the contrary only a handful of examples are known in the literature where they have been studied crystallographically, namely “freezing” out different conformations of solvents.

Toda and coworkers were able to trap a nearly eclipsed chiral rotamer of 1,2-dichloroethane in a pure state as an inclusion complex crystal with another chiral host compound⁶. They claimed to be the first group to isolate a conformation between gauche and eclipsed form with a dihedral angle between two chlorine atoms of 36°. Further crystallographic investigation shows that two chlorine atoms in trans position cannot be accommodated in the cavity and a favourable accommodation can only be obtained with a sterically unfavourable eclipsed form.



In another excellent piece of work they report the successful isolation of different tautomers of imidazole derivatives in a pure state by inclusion complexation with host compounds⁷. Recently Kumar and Nangia while studying with a clay mimic organic host, report an n-hexane solvate, where the solvent is disordered over two different orientations⁸.

The existence of different conformers or conformations and their interconversion were known from theoretical work and have been studied spectroscopically, especially with more sophisticated instrumentation, and techniques such as dynamic NMR have emerged as one of the most powerful tools for these kind of studies⁹. For instance, recently, for the first time the existence of bispidinone system in chair-boat conformer was established both by ¹H and ¹³C NMR as well as X-ray crystallography, while in solution a rapid interconversion with boat-chair was revealed by variable temperature NMR studies¹⁰.

For biological systems, conformational changes of different polypeptides, amino acids and proteins and the role of solvents were studied from very early days by different renowned crystallographers. Trapping different conformations as intermediate states is a routine practice and a highly successful tool for biological systems, especially in the study of protein folding. The relationship between conformational parameters of different amino acids was studied in detail by the great G. N. Ramachandran, and was later formulated as the famous *Ramachandran plot*¹¹.

Isolation of a particular conformer by diastereomeric or enantiomeric reactions are routinely carried out for chiral molecules using some chiral base or acid. Many of them are used for mapping chemical reaction by considering them as the transition state which could be useful to deduce the reaction mechanism.

Nonetheless, such studies are not common for chemical and rare for crystal engineering studies. One of my predecessor's work is important in this regard. Trans-1,4-

diethynylcyclohexane-1,4-diol, which is the first bis-gem-alkynol studied in this series, represents a unique example of the simultaneous occurrence of both conformational polymorphism and conformational isomorphism¹². The compound crystallises in two distinctly different modifications both in space group $P\bar{1}$ with three symmetry independent molecules occupying distinct inversion centres. While one crystal structure contains two molecules with diaxial hydroxy groups and one molecule with diequatorial OH group, the other crystal structure comprised of two molecules with diequatorial and one with diaxial OH groups. Interestingly, one pseudopolymorphic 1:1 monohydrate of diequatorial OH conformers crystallise with an identical O-H...O helical trimeric supramolecular synthon to the two other unsolvated structures.

5.2. Result and Discussion:

In this chapter we will discuss one even more rare event, namely the trapping a guest molecule in a high energy conformation in a host molecule. There is precedent for trapping one conformation in a host molecule, but trapping both a higher energy conformation of a solvent, as well as a stable conformation of it in the same host has not hitherto been seen. To our best knowledge, we are the first to report herein the unprecedented observation of two distinct 1:1 solvates of diethyl amine in both gauche

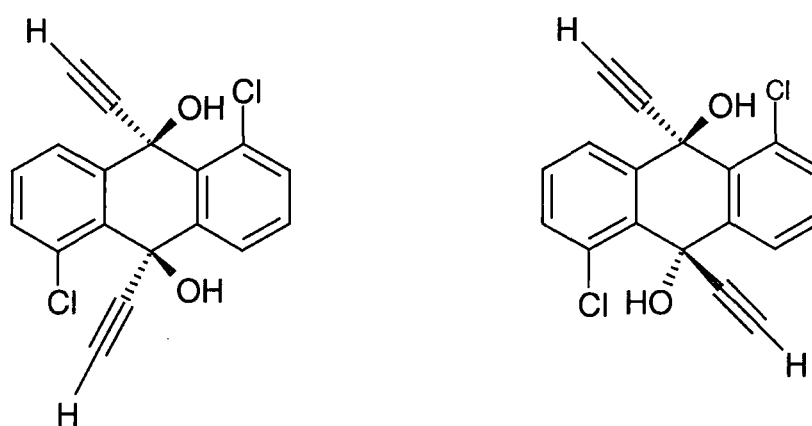
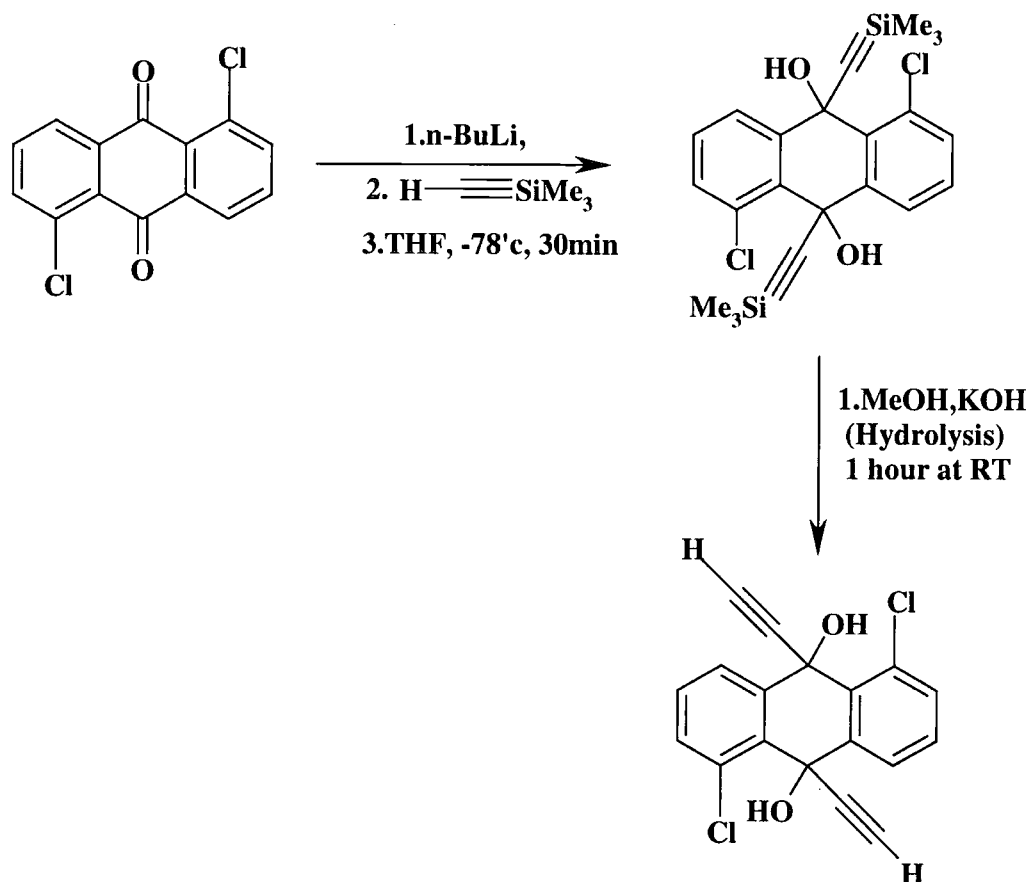


Figure 5.1. Schematic diagram of *cis*- and *trans*- 1,5-dichloro-*cis*-9,10-diethynyl-9,10-dihydroanthracene-9,10-diol

and more stable staggered rotamers with the host compound 1,5-dichloro-*cis*-9,10-diethynyl-9,10-dihydroanthracene-9,10-diol. Also the staggered form of the amine trapped in the *trans* form will be reported here.



Scheme 5.I. Schematic representation of two step synthetic strategy of the host molecule.

5.3. The *Cis* isomer

In the previous chapter (Chapter 4) we have witnessed the '*unusual*' behaviour of the *trans* isomer of the host molecule with serendipitous solvates and with polar aprotic solvents with more '*normal*' behaviour. Isolation of the *cis* isomer was unexpected and was achieved only with very careful experimentation with the aim of any new polymorph with '*normal*' behaviour. The strategy for synthesis of gem-alkynols is

important in this regard (**Scheme 5.I**). The diol was synthesized by the hydroxy ethynylation of 1,5-dichloroanthraquinone by a two step reaction, by adding $\text{TMSC}\equiv\text{C-Li}$ to the diketone followed by the hydrolysis of the TMS groups by KOH, with *trans* isomer as the preponderant product and a trace of *cis* isomer being formed. The yield of the *cis* isomer being so small that it could never be separated satisfactorily via column chromatography. Crystallisation of the crude product from EtOH/benzene (1:1) yields *trans* isomers in needle form. In search of any new polymorph, the crude material was crystallized from many different solvent systems, however without success except with acetone/benzene. The crude product exhibits concomitant crystallisation from acetone/benzene giving two crystalline morphologies, prism and needles corresponding to almost similar unit cells with only the 'c' axis being 2Å larger for the former, than in the previously reported structure (Table 5.3). The crystal structure determined was shown to correspond to the unsolvated forms of the *cis* and *trans* isomer respectively.

We have noted previously for the *trans* diol that there is an unsatisfactory hydrogen bonding pattern, brought about by the steric hindrance of the two chlorine groups juxtaposed to the hydrogen bond donor and acceptor groups in the molecule⁴. In principle, the sterically constrained environment of the hydroxyl and ethynyl group should be present for the *cis* isomer also. This draws our attention immediately to the packing of *cis* isomers. On the face of it, the first question arises, "does the molecule follow a satisfactory hydrogen bonding pattern?" The answer is probably 'No'. The crystal packing comprises varieties of weak hydrogen bonds, and there is most notably an absence of any strong O-H...O (H) hydrogen bonds, typically present for the gem-alkynol family. Instead the molecules show unique crystal packing, which closely resemble different structural motifs rather than gem-alkynol family^{12, 13}.

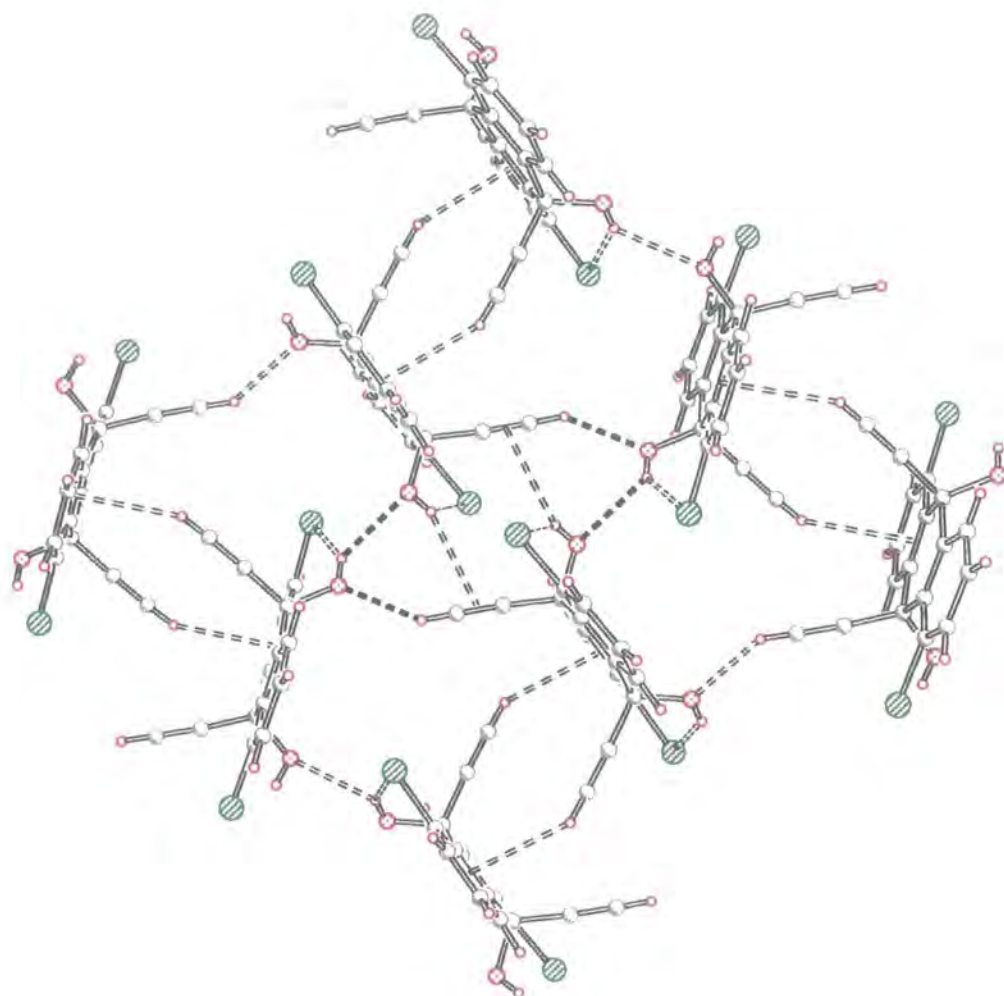


Figure 5.2. Crystal structure of *cis*-diol. Please note the distorted synthon **V** (highlighted with bold bond) at the centre.

Table 5.1. Hydrogen bond parameters for the *cis*-diol.

D-H...A	d(D-H)	d(H...A)	d(D...A)	<(DHA)
O ₁ -H ₁ ...Cl ₁	0.76(4)	2.47(4)	3.040(2)	134(4)
O ₁ -H ₁ ...O ₂	0.76(4)	2.51(4)	2.977(3)	121(4)
O ₂ -H ₂ ...Cl ₂	0.78(4)	2.57(4)	3.071(2)	123(4)
O ₂ -H ₂ ...X1A*	0.78(4)	2.771	3.440(3)	144.5(4)
C ₁₆ -H ₁₆ ...X1B**	0.87(4)	2.827	3.580(4)	145.6(3)
C ₁₈ -H ₁₈ ...O ₁	0.91(3)	2.28(3)	3.084(3)	147(3)

*X1A is the mid point of C17-C18 triple bond, ** X1B is the ring centroid

For most of the compounds in the gem-alkynol family, two representative synthons, made of a loop of strong (O-H...O) and weak (C-H...O and C-H... π) hydrogen bonds dominate the crystal packing. For the *cis* diol, instead of a strong O-H...O bond, one hydroxy group forms an intermolecular O-H... π , which is embedded with the somewhat more distorted synthon V. The distortion arises as the second hydroxy group forms a bifurcated O-H...O hydrogen bridge, accepting also an intramolecular O-H...Cl hydrogen bridge. It is quite interesting to note that while some of the interaction pattern closely resembles the synthon observed with 2-ethynyladamantan-2-ol¹³, at the same time, steric bulk as well as the intramolecular O-H...Cl-C interaction and consequently the disruption of the synthons, was seen previously for the trans analogue and other chloro derivatives¹⁴. The prime difference between the two isomers is that whereas for the trans isomer (Chapter 4) only one hydroxy group engages in an O-H...Cl interaction, both OH groups are involved in O-H...Cl interaction for the *cis* diol, (Figure 5.2) bifurcated by either O-H... π or O-H...O interaction. Again the bifurcated O-H...O hydrogen bridge is almost similar to trans keto-alcohol derivative, (Figure 3.6, Chapter 3), except the keto group is devoid of any donor H atom and could not form any O-H... π interactions, but it can form a C-H... π bond. The other ethynyl hydrogen atom is directed towards an aromatic ring, forming a C-H... π bond to the ring. Out of these interesting blends of structural similarities, it is difficult to pinpoint the most closely related to gem-alkynol family and important one. However, the crystal structure does hint that perhaps not by design but by a trail and error method, we found another host molecule with unsatisfied hydrogen bonding potential.

5.4. Solvates of the cis-diol

We have experienced previously for the trans-diol, (Chapter 4) an awkward hydrogen bond pattern resulting from the sterically constrained environment of hydroxyl and ethynyl groups, and we have shown how this uncomfortable pattern can relax via solvation. Noting further that the cis diol too forms a hydrogen bonding less than optimal, can we expect a similar kind of solvent induced relaxation for the cis diol? Precisely at this point we decided to try some different 'uncommon' solvents. An amine being an organic base should form strong hydrogen bonds, hence promotes the solvation. A detailed discussion about amine solvents is the main objective of the next chapter (Chapter 6) and we will content ourselves here with diethylamine solvates.

The crude mixture of isomers was crystallised from a 1:1 mixture of ethanol and diethylamine solvents. Crystals with two different morphologies were obtained, cube and plate corresponding to the 1:1 solvates of the cis-diol containing gauche and staggered diethylamine conformations respectively (Figure 5.3) and these showed markedly different cell parameters. The trans form was obtained when co-crystallised from acetone + diethylamine (1:1), wherein the diol is found to be disordered with two orientation in a ratio of 9:1, but the amine is ordered.

At first we were quite puzzled with two different modifications of cis diol solvates with apparently similar crystal structures. A closer inspection however reveals that diethylamines are in two different conformations, gauche and staggered. The dihedral angle between the two best planes in gauche conformer is 70° whereas for staggered form it is 178° . To validate this implicitly unusual nature of this occurrence we took the help of the Cambridge Structural Database (CSD)¹⁵. A simple search of the CSD reveals

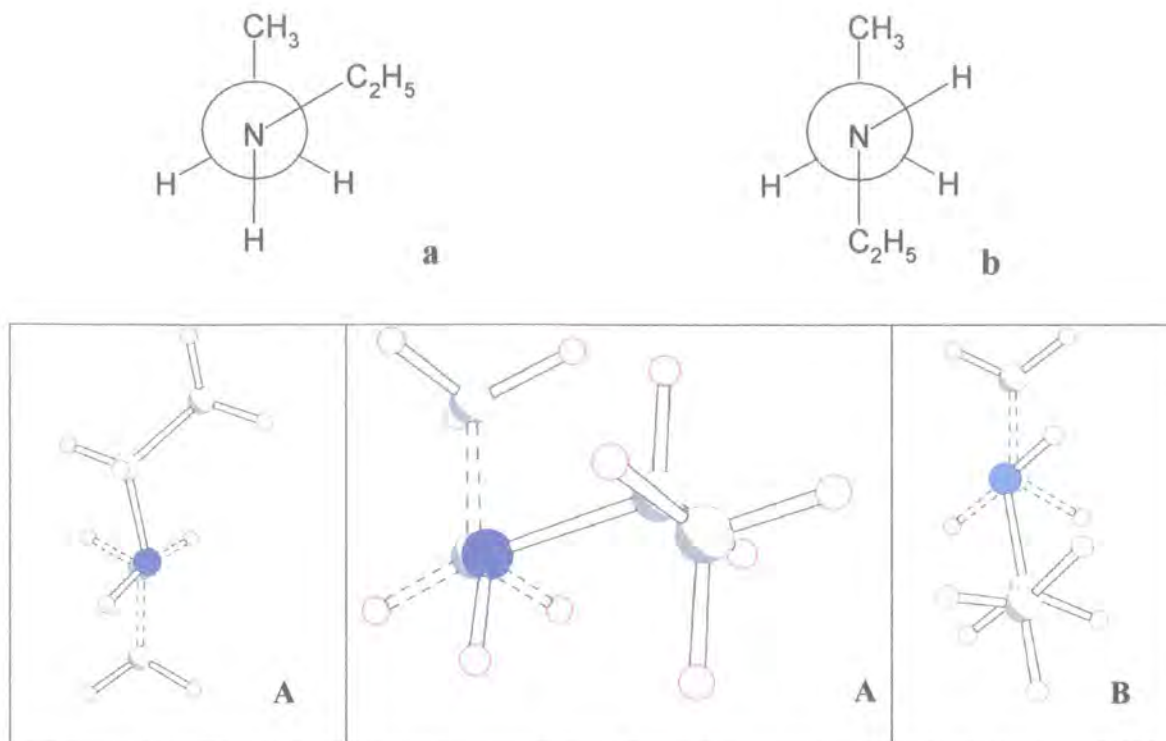
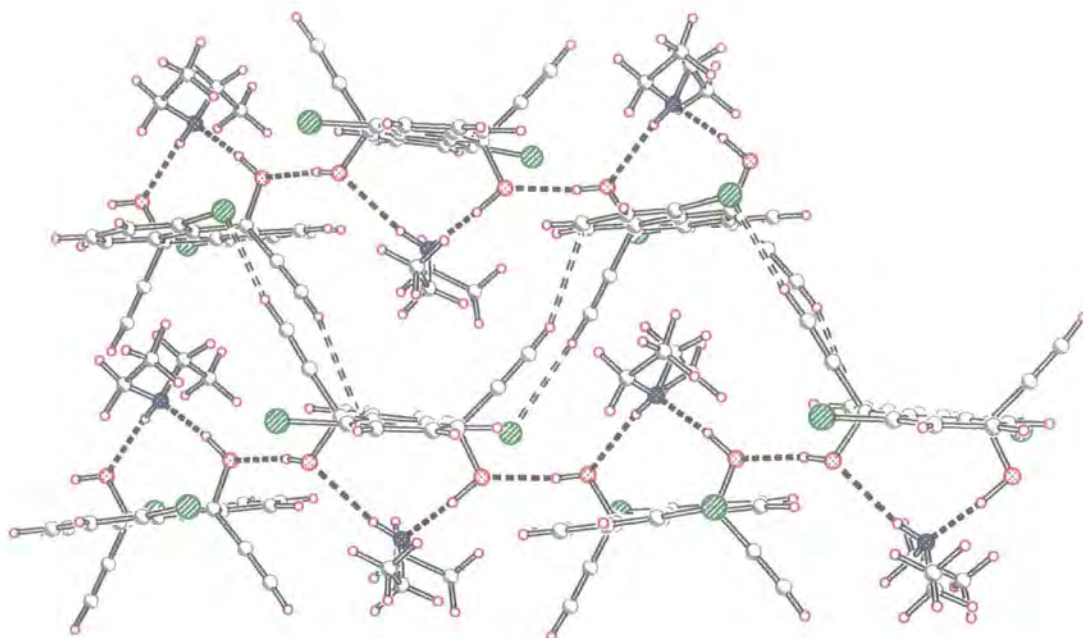


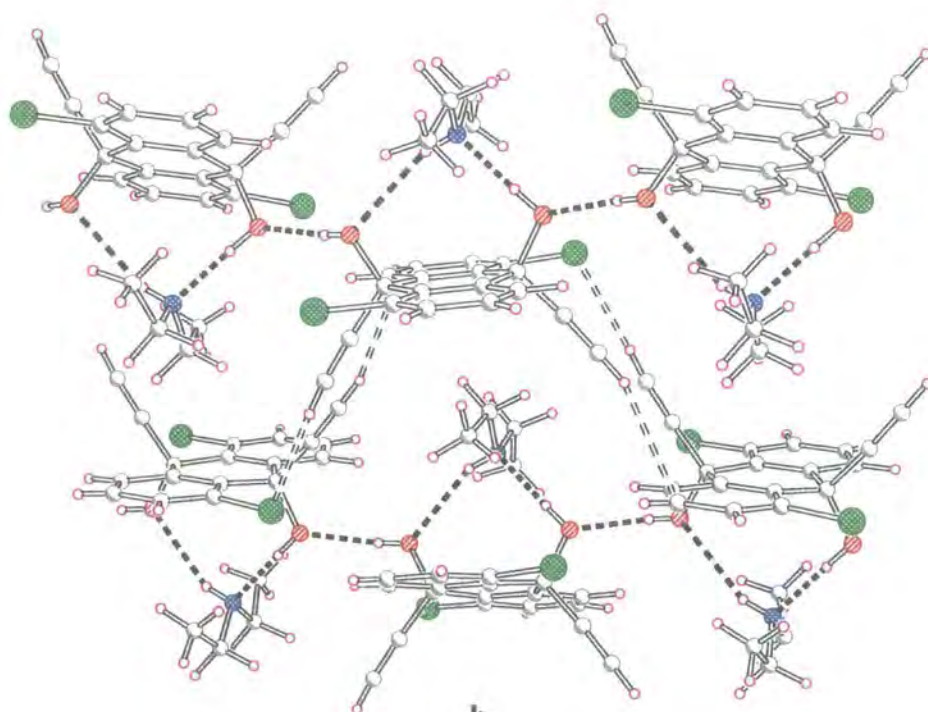
Figure 5.3. Two different views of gauche (A) and one of the staggered (B) conformations of Et₂ NH found in the solvates and their corresponding schematic representations (a & b)

that only seven diethylamine solvates are present in the database and in all of these, the molecule adopts the more stable staggered conformation¹⁶. Again the concomitant crystallisation of the two conformers suggests a small energy difference and indeed the energy difference between the staggered and the gauche conformations was estimated to be 3.26 kJ mol⁻¹ (DFT) and 5.06 kJ mol⁻¹ (HF).

A careful investigation of the crystal packing was undertaken in order to get some more insight into why the two crystal forms were obtained. The two solvates show almost identical crystal packing. As we anticipated earlier, for both the solvates the difficulty in forming short and adequately strong hydrogen bonds has been overcome by active participation of amine group. Both the hydroxyl groups of the cis diol form 'stand-alone' strong hydrogen bond with the amine groups. One of the prime reasons for choosing amines as the solvent was to study the mutual competition/interference of



a



b

Figure 5.4. Crystal structures of solvates of *cis*-diol with (a) gauche (b) staggered conformers of Et_2NH . Please note the infinite cooperative arrangement of $\text{O}\dots\text{H-N}\dots\text{H-O}\dots\text{H-O}\dots\text{H-N}$ interactions.

hydroxyl, amine and ethynyl groups. To our astonishment, we observe that the amine and diol interaction patterns closely follow those of the molecular complexes of the aminols even though amine used herein is secondary with one donor hydrogen atom rather than two for usual aminol studies. The diethylamine molecule links to the intermolecular hydroxyl groups of the diol and there is an infinite cooperative array of O-H...N, N-H...O and O-H...O interactions. The solvent molecule can be imagined as trapped in a cavity formed by C-H...Cl and C-H... π (arene) framework (Figure 5.4). Both the conformers perform the same function and the cooperative array is topologically the same, albeit there are two striking differences. Firstly, while the O-H...N and O-H...O interactions are comparable, the N-H...O bond is distinctly longer for staggered form and secondly while the diols are arranged in parallel fashion for gauche form, they are in a non-parallel, converging orientation for staggered form as shown in Figure 5.5(a,b).

We found these apparently two irrelevant features are linked with each other in a quite unique way via steric hindrance. Figure 5.5(a) suggests that the gauche form causes less steric hindrance than the staggered conformer where the diols have to orient themselves in a converging manner [Figure 5.5(b)] in order to accommodate the solvent molecules inside the cavity. In other words, the lengthening of the N-H...O interaction seems to arise from steric hindrance between one of the ethyl group of the solvent and the aromatic ring of the diol. For the gauche conformation, steric hindrance is reduced when the methyl moiety in the ethyl group swings away from the ring resulting in a optimally shorter N-H...O bond. This helps us to explain the existence of two energetically different conformers in terms of two following complimentary features. We suggest that the N-H...O lengthening in the staggered form is balanced by the solvent being in the most stable conformer, alternatively, the more energetic gauche conformation is stabilized by

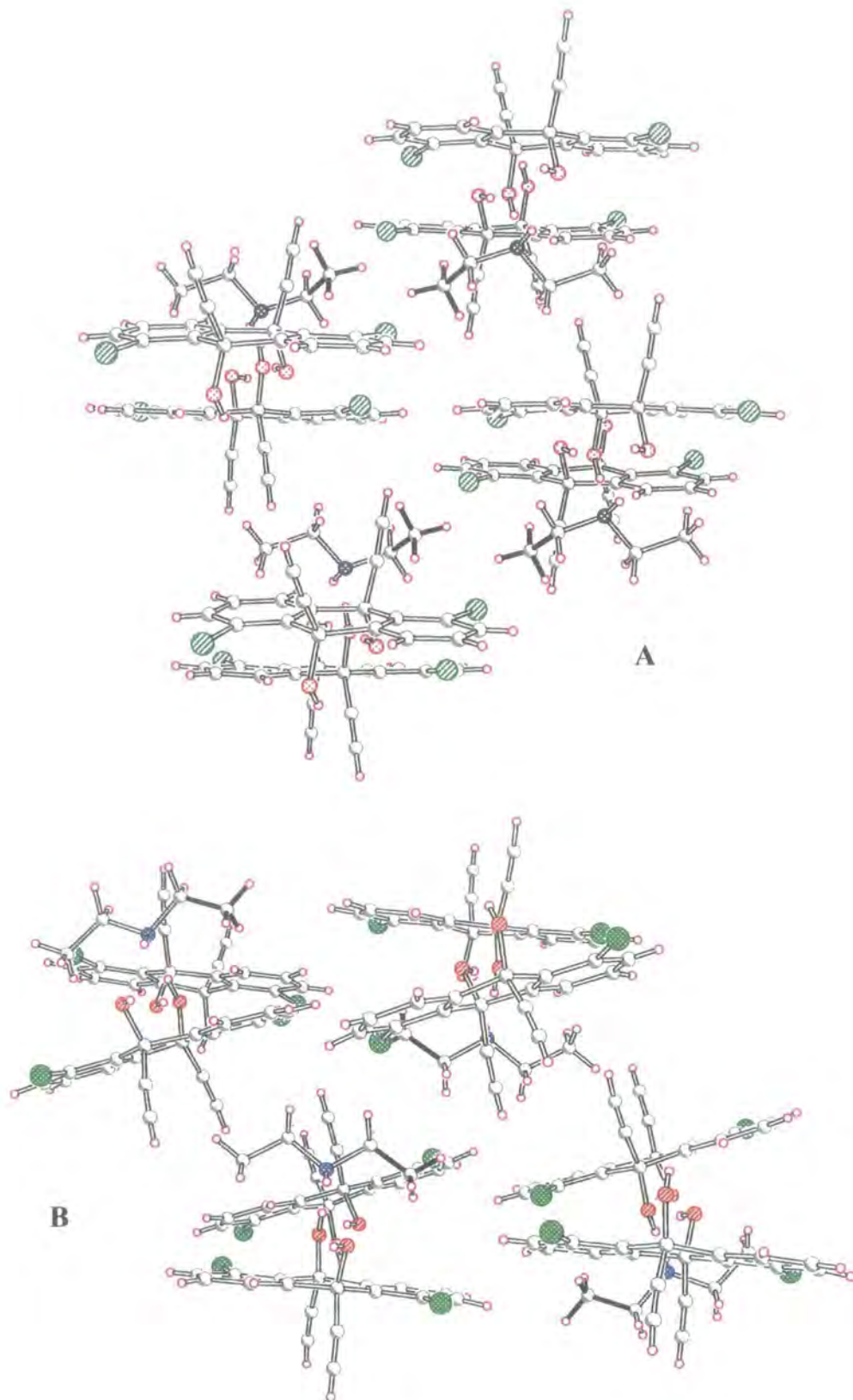


Figure 5.5. orientation of cis diol in two different solvates, please note the methyl fragment in gauche conformation(a) swings away to reduce the steric hindrance compared to the staggered conformation (b)

a better N-H...O bond. All other packing features in the two solvates are nearly comparable and we feel that it is reasonable to equate the energy difference between rotamers of *ca.* 4 kJ mol⁻¹ with a difference of around 0.3 Å in an N-H...O hydrogen bond¹⁷.

Table 5.2. Hydrogen bond parameter for the gauche conformer

D-H...A	d(D-H)	d(H...A)	d(D...A)	<(DHA)
O ₁ -H ₁ ...N ₁	1.01(3)	1.67(3)	2.677(2)	172(3)
O ₂ -H ₂ ...O ₁	0.84(3)	1.95(3)	2.782(2)	171(3)
N ₁ -H ₂₄ ...O ₂	0.91(3)	2.29(3)	3.178(2)	167(3)
C ₁₆ -H ₁₆ ...X*	0.90(3)	2.828	3.675	158.3
C ₁₈ -H ₁₈ ...Cl ₁	0.97(4)	3.015(4)	3.650(3)	155.2(3)

Table 5.3. Hydrogen bond parameter for the staggered conformer

D-H...A	d(D-H)	d(H...A)	d(D...A)	<(DHA)
O ₁ -H ₁ ...O ₂	0.79(4)	1.99(4)	2.774(3)	173(4)
O ₂ -H ₂ ...N ₁	0.88(5)	1.83(5)	2.711(3)	177(5)
N ₁ -H ₁₁ ...O ₁	0.83(3)	2.59(3)	3.362(3)	157(3)
C ₁₈ -H ₁₈ ...Cl ₁	0.87(4)	2.80(4)	3.656(3)	167(3)
C ₁₆ -H ₁₆ ...X*	0.90(3)	2.843	3.790	161.3

* X the mid point of the benzene ring with C-H... π interaction.

5.5. *Trans* Diol Solvate

If the serendipitous findings of the *cis* diol solvates come as a surprise, then the diethylamine solvate with *trans* diol comes nothing short of a strategically important product. The *trans* diol solvate vindicates our strategy for using amine solvents for competitive studies among the amine, hydroxyl and ethynyl groups. We have noted in Chapter 2 that for aminophenols and molecular complexes containing amine and OH

groups, the structural patterns revolve round three major supramolecular synthons, the β -As sheet, the centrosymmetric square motif and the infinite cooperative array of O-H...N-H...O-H...O (as observed for cis diol, Figure 5.4). The diol is found to be disordered [90:10 ratio] but the amine is ordered. The diethylamine molecule appears to be in the more stable staggered conformation with the dihedral angle between the two

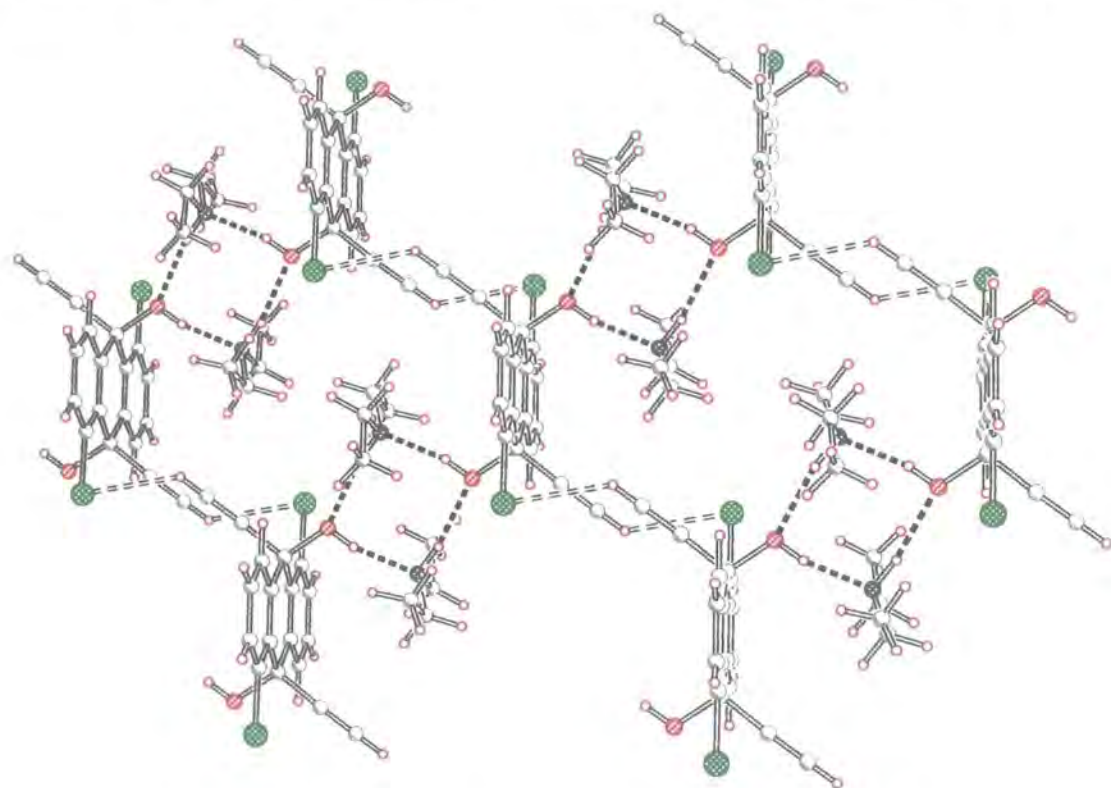


Figure 5.6. Crystal structure of the *trans*-diol solvate showing the square motif.

best planes being 171.5° . Several attempts were made to find the gauche form, however all efforts were in vain. Interestingly the hydrogen bonding pattern is quite different from that seen in the crystals of the amine with the cis isomer earlier, forming the familiar centrosymmetric square O-H...N-H...O-H motif, as seen in the amino-phenol series. [O-H...N = 2.71 Å, 1.95 Å, 166° , N-H...O = 3.13 Å, 2.23 Å, 169.2°] (Figure 5.6) The 3D packing arrangement shows the amine groups forming layers between the diols which show weak C \equiv C-H...Cl interactions. (3.55 Å, 2.91 Å, 134.8°). The diols are oriented in a parallel fashion and we suggest that the formation of a robust

supramolecular synthon eliminates the possibility of the other amine conformer by forming strong hydrogen bonds.-

Table 5.4. Crystallographic data and structure refinement parameters.

	Trans diol	Cis-diol	Cis-Gauche	Cis-staggered	Trans-staggered
Solvent	Ethanol/ Benzene (1:1)	Acetone /Benzene (1:1)	Ethanol/ Diethylamine (1:1)	Ethanol/ Diethylamine (1:1)	Acetone /Benzene/ Diethylamine
Empirical formula	C ₁₈ H ₁₀ Cl ₂ O ₂	C ₁₈ H ₁₀ Cl ₂ O ₂	(C ₁₈ H ₁₀ Cl ₂ O ₂) (C ₄ H ₁₁ N)	(C ₁₈ H ₁₀ Cl ₂ O ₂) (C ₄ H ₁₁ N)	(C ₉ H ₅ ClO) (C ₄ H ₁₁ N)
Formula wt.	329.16	329.16	402.30	402.30	237.72
Crystal System	Monoclinic	Monoclinic	Monoclinic	Orthorhombic	Triclinic
Space group	<i>P2₁/n</i>	<i>P2₁/n</i>	<i>P2₁/n</i>	Pbca	P-1
<i>a</i> [Å]	7.4025(2)	7.4731(2)	8.1794(2)	14.955(3)	8.8625(4)
<i>b</i> [Å]	12.7571(4)	12.5163(3)	13.6483(4)	13.659(3)	8.8881(5)
<i>c</i> [Å]	14.8695(4)	16.2952(5)	18.0272(5)	19.433(4)	9.5190(5)
α [°]	90	90	90	90	109.609(2)
β [°]	93.382(1)	100.565(1)	96.984(1)	90	116.003(2)
γ [°]	90	90	90	90	90.739(2)
<i>Z</i>'	1	1	1	1	0.5
Volume [Å³]	1405.16(7)	1498.34(7)	1997.53(9)	3969.4(14)	623.39(6)
λ [Å]	0.71073	0.71073	0.71073	0.71073	0.71073
D_{calc} [g/cm³]	1.556	1.459	1.338	1.346	1.266
μ [mm⁻¹]	0.465	0.436	0.342	0.344	0.285
2θ [°]	4.20-57.98	5.086 54.806	5.252 54.964	4.550 54.564	4.955 54.977
Range <i>h</i>	-10 to 9	-9 to 9	-10 to 10	-19 to 19	-11 to 11
Range <i>k</i>	-17 to 17	-16 to 16	-16 to 16	-17 to 17	-10 to 11
Range <i>l</i>	-20 to 20	-21 to 21	-22 to 22	-25 to 25	-12 to 12
Reflns. collected	16581	16656	19907	41925	7477
Unique reflns.	3207	3431	3925	4557	2862
Obs. reflns.	2702	2430	3353	3539	2634
<i>R</i>₁ [<i>I</i> > 2 σ(<i>I</i>)]	0.0328	0.0539	0.0460	0.0656	0.0388
wR_2 [all]	0.0853	0.1172	0.1105	0.1230	0.1054
Goodness-of-fit	1.031	1.054	1.105	1.161	1.103
T [K]	120(2)	120(2)	120(2)	95(2)	120(2)
Crystal size	0.40 x 0.18 x 0.08 mm ³	0.24 x 0.22 x 0.14	0.26 x 0.22 x 0.16	0.22 x 0.18 x 0.06	0.28 x 0.08 x 0.04

5.6. Nomenclature

This particular work eventually forced us to face another nomenclature dilemma. As noted by Desiraju¹⁸, “*problems with nomenclature are necessary evils in the development of a new subject*”; in early days of a subject, enthusiasm and inability of the old term to describe new concepts make it easier to coin new names. However, *What is easy is sometimes not what is best*. As we are confronted here with the much used term “pseudopolymorphism”. McCrone¹⁹ originally suggested the term pseudopolymorphism in order to describe two or more solvated forms of the same compound. Solvate and pseudopolymorph are, in principle, two synonymous terms and mainly user dependent. While solvate is more common term in chemical circles, pseudopolymorph has become a standard in the pharmaceutical literature. Both Byrn²⁰ and Bernstein²¹ have discussed the ambiguity of the term in their book. Threlfall²² mentions several difficulties in its usage. The logic behind the usage of pseudopolymorph implies that there are two structures, the unsolvated and solvated forms with different crystal structures but that because the systems being considered are different chemical entities, the ‘polymorphism’ is not real but ‘pseudo’

On the contrary, it has been argued from the very definition of pseudopolymorph, a compound and its solvate must necessarily have different crystal structures and that rule them out of being chemically identical. Since they are not chemically identical it is argued that there is no question of polymorphism, pseudo or otherwise. The literature is confusing, there are several definitions of the term *pseudopolymorph* and the authors of these papers rarely cite each other²³.

Can we refer to these solvates as pseudopolymorphs? Ideally, the term *polymorph* should be restricted to different crystal forms of a single compound. Difficulties seem to arise for multi-component crystals, with too many structural variations²⁴. These may range from a situation wherein one of the components is mostly an innocuous bystander

in a crystal structure that is largely determined by the other, to one wherein both the components are essential for the crystal packing²⁵. The term *polymorphism* seems to be unnecessarily restrictive with regards to the identity of chemical composition *for some types of multi-component crystals*. In this context, the term *pseudopolymorphism* has virtues that need to be considered on a case-by-case basis. This term brings to attention the fact that certain related multi-component crystals, with the same or different chemical composition, have distinct crystal structures. On the other hand, indiscriminate application of the term will result in all polycomponent crystals being called pseudopolymorphs. In the present context, both the solvates of cis diol, in principle, may be called polymorphs according to current definition. However, there are some points that are worthy of attention. The major component, cis diol is virtually the same, the hydrogen bonding and orientation of the aromatic rings result from the minor component. The same conformation of the major component ruled out another possibility of calling them “conformational polymorphs”. Given that it is the minor component in these pseudopolymorphs that has the conformational variations, we believe it will be more appropriate to refer to them as *conformational pseudopolymorphs*.^{26, 27}

5.7. References

1. L. R. Nassimbeni, *Acc. Chem. Res.*, 2003, **36**, 631-637.
2. E. Weber, *Inclusion Compounds*; Ed. J. L. Atwood, J. E. D. Davis and D. D. MacNicol, Oxford University Press, Oxford, 1991, vol. 4, Ch. 5, pp 188-263
- 3 A. Nangia and G. R. Desiraju, *Chem Comm.*, 1999, 605-606.
- 4 R. Banerjee, G. R. Desiraju, R Mondal, A. S. Batsanov, C. K. Broder and J. A. K. Howard, *Helv. Chim. Acta.*, 2003, **86**, 1139-1151.
5. Stereochemistry of Organic Compounds, Ed. E. L. Eliel and S. H. Wilen, Wiley, 1994.
6. Toda, K. Tanaka and R. Kuroda, *Chem Comm.*, 1997, 1227-1228;
7. M. Yagi, S. Hirano, S. Toyota, M. Kato, F. Toda, *CrystEngComm*, 2002, **4**(25), 143-145.
8. V. S. S. Kumar and A. Nangia *Chem Comm.*, 2001, 2392-2393.
9. P. P. Chu, M. Cheng, W. Huang, F. Chang, *Macromolecules*, 2000, **33**, 9360-9366.
10. S.Z.Vatdadzem, D. P. Krutko, N. V. Zyk, N. S. Zefirov, A. V. Churakov, J. A. K. Howard, *Mendeleev Communications*, Vol. **9**, 1999, No.3, pp 103-105
11. *Conformation of Biopolymers*, Vol. 1 & 2, Ed. G. N. Ramachandran, Academic Press, London and New York, 1967.
12. C. Bilton, J. A. K. Howard, N. N. L. Madavi, A. Nangia, G. R. Desiraju, F. H. Allen, C. C. Wilson, *Chem. Comm.*, 1999, 1675-1676.
13. F. H. Allen, J. A. K. Howard, V. J. Hoy, G. R. Desiraju, D. S. Reddy, C. C. Wilson, *J. Am. Chem. Soc.*, 1996, **118**, 4081-4084.
14. R. Banerjee, G. R. Desiraju, R. Mondal, J. A. K. Howard, *Chem. Eur. J.*, 2004, **10**, 3373-3383.
- 15 (a) F. H. Allen, O. Kennard, *Chem. Des. Autom. News*, 1993, **8**, 30-37, (b) F. H. Allen, *Acta. Cryst.*, 2002, **B58**, 380-388

16. E Weber, T. Hens, Q. Li and T. C. W. Mak, *Eur. J. Org. Chem.*, 1999, 1115-1125.
17. D. F. Plusquellic, X.-Q. Tan, D. W. Pratt, *J. Chem. Phys.*, 1992, **96**, 8026-8036.
18. G. R. Desiraju, *CrystEngComm*, 2003, **5** (28), 466-467.
19. W. C. McCrone in *Physics and Chemistry of the Organic Solid State*, Vol. 2, ed. D. Fox, M. M. Labes, A. Weissberger, Wiley Interscience, New York, 1965.
20. S. R. Byrn, *Solid State Chemistry of Drugs*, Academic Press, 1982, New York.
21. J. Bernstein, *Polymorphism in Molecular Crystals*, Clarendon, Oxford, 2002.
22. T. L. Threlfall, *Analyst*, 1995, **120**, 2435-2460.
23. S. Ahn, B. M. Kariuki and K. D. M. Harris, *Cryst. Growth. Des.*, 2001, **1**, 107-111;
- V. S. S. Kumar S. S. Kuduva and G. R. Desiraju, *J. Chem. Soc., Perkin Trans.*, 2, 1999, 1069-1074.
24. R. K. R. Jetti, R. Boese, P. K. Thallapally and G. R. Desiraju *Cryst. Growth. Des.*,
Advanced article.
25. A. I. Kitaigorodskii, *Mixed Crystals*, Springer, Berlin 1983; G. R. Desiraju, *Crystal Engineering. The Design of Organic Solids*, Elsevier, Amsterdam, 1989.
26. M. Yagi, S. Hirano, S. Toyota, M. Kato, F. Toda, *CrystEngComm*, 2002, **2**(25), 143-145.
26. R. Glaser and D. Shiftan *J. Org. Chem.*, 1999, **64**, 9217-9224;
27. P. Prabakaran, B. Umadevi, P. Panneerselvam, P. T. Muthiah, G. Bocelli, L. Right, *CrystEngComm*, 2003, **5**, 487-489.

Chapter 6

**Correspondence between Molecular Functionality and Crystal
Structures: Supramolecular Chemistry of Amine Solvates of a
Gem-Alkynol.**

6.1. Introduction

The field of inclusion complexes, clathrates, pseudopolymorphism, host-guest chemistry has grown dramatically in recent years¹ owing to their great potential for variety of fundamental and practical aspects. Such importance of pseudopolymorphism was explored by Byrn, Bernstein, Desiraju and others² in their respective books and works. Molecular recognition lies at the heart of the inclusion compounds and indeed during the last decade or so, the major part of the crystal engineering studies associated with pseudopolymorphism, involve designing host molecules with different shape, steric bulk and functionality². Weber, one of the pioneers of this field, outlined a successful host molecule as bulky, rigid and preferably containing host-guest interaction-specific functional groups³. On the face of it, undisputedly most of the host molecules were discovered accidentally rather than from a premeditated design⁴.

Solvent inclusion in organic crystals is quite uncommon, being observed only for 15% of cases. A detailed knowledge mining from the Cambridge Structural Database (CSD) and subsequently reluctance/tendency of the solvent molecules to be included in the crystal, was rationalized by a multi-point recognition model, put forward by Desiraju and Nangia⁵. Based on this model, solvation occurs only when the enthalpic gain from the solute-solvent multipoint interaction outweighs the combined effects of entropy gain by solvent extrusion during nucleation and enthalpic gain from forming robust supramolecular synthons among solute molecules. In other words, solvation could be imagined as a result of interruption of 'normal' crystallization⁶ by the formation of directional hydrogen bonds. This implicitly makes compounds with less than the optimum number of hydrogen bonds more probable to form solvates.

Unlike host molecules, guest molecules seldom receive any special attention and most of the time solvates are obtained by trial and error methods, rather than chosen for any strategic significance. A recent CSD study reveals that only 20 common solvents are

incorporated more than 50 times, out of a quarter of a million crystal structures, wherein the overwhelming majority of O-containing solvents further shows the significance of the multipoint recognition model⁵. However it is surprising enough to note, that not a single amine solvate secures a place in the list, albeit amines, next to hydroxyl groups are the most extensively studied functional group in the field of crystal engineering. This is perhaps due to the hostile environment associated with the amines and the subsequently unstable nature of the solvates.

The absence of a direct correlation between the molecular functionality and the crystal structure, is a major challenge in crystal engineering. It becomes even more challenging for solvates, wherein the all-important location and position of functionalities belonging to the incorporating guest molecule (solvent), are not precise but random. In this work we attempt to draw a correspondence between molecular functionality and crystal structures among the sixteen different pseudopolymorphs of 1,5-dichloro- *trans*-9,10-diethynyl-9,10-dihydroanthracene-9,10-diol (DDDA). This work aims to gain some insight into the interaction hierarchy of four molecular functionalities, namely, hydroxy (benzylic), ethynyl, aromatic chlorine and amine group. In an unconventional way, we investigate systematically the structural interference, with the solvent being the provider of one functional group and also of steric variance of the incorporating solvents.

6.2. Crystallization.

All crystallization experiments were carried out under almost identical environment, by dissolving the crude material in the respective solvent systems, followed by the slow evaporation at room temperature. However most of the amines used in these studies are either volatile or have low boiling points, and the corresponding solvates are mostly unstable. Due to hostile nature of the amines most of the crystallisation experiments were carried out in controlled manner. When removed from the mother liquor, some of

the crystals suffer from the loss of solvent molecule from the lattice, resulting in polycrystalline or opaque material. As expected, amines with larger rings and bulky secondary amines are stable up to hours, sometimes days, hence create less problems, while special care had been taken for the others. In order to overcome this problem, once the crystals were taken out of the sample vial, they were soaked immediately into oil with a high surface tension and mounted on a goniometer with oil at 120K.

6.3. Result and Discussion

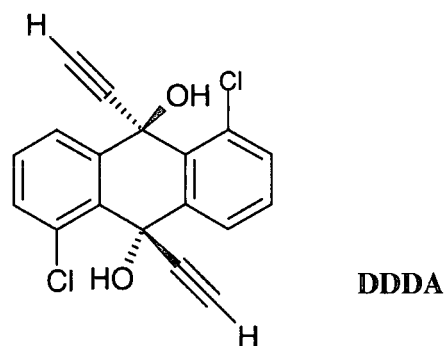
The crystal structure of DDDA is quite unusual, being part of only 1% of molecules that contain *i* as the *only* molecular symmetry element, but that do not lie on an inversion centre in the crystal⁷. The less than optimal formation of hydrogen bonds in the packing was compensated with a tetrachloro supramolecular synthon lying on the inversion centre. That enables the largest number of atoms to aggregate with the shortest possible separations. The reason for this apparently incomprehensible crystal structure was attributed to the steric hindrance resulting from the close juxtaposition of the two chlorine atoms to the gem-alkynol groups and subsequently formation of intramolecular O-H...Cl-C hydrogen bridges.^{7b} In effect, the DDDA having failed to satisfy the hydrogen bond potential, emerged as a potential host molecule.

Five solvates of DDDA have already been reported elsewhere,⁷ wherein the DDDA molecules occupy an *i* site and form strong and linear O-H...O hydrogen bonds with solvent molecules. Previous results of DDDA structures show a relaxation of awkward hydrogen bond patterns via solvation, and led us to believe that these compounds are worthy of further structural studies.

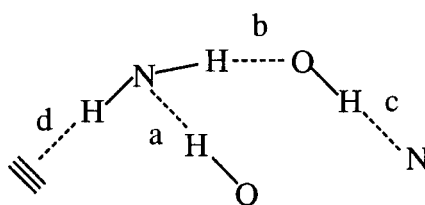
For this work instead of any common solvents we specifically chose amines for two reasons, firstly, even though 15% of organic crystals of the CSD are pseudopolymorphs, only a handful of them contain amine as solvent. Organic bases are well known to

promote solvation effectively; hence amines should do the same. However even a cursory inspection in the CSD shows the occurrences of amine solvates are random and either disordered or unstable, and most importantly, only few of them involve free amine, i.e., most of them are in ionic/protonated form. To the best of our knowledge we are the first to report a complete series of solvates with amines. Secondly, as a part of our ongoing project on crystal engineering, we, the Durham and Hyderabad groups, have dealt previously with hydrogen bond properties of three different functional groups, viz, hydroxyl, amine and alkyne in two different sets of crystals and molecular complexes, each containing two different functional groups; amine-hydroxyl (supraminol)⁸ and ethynyl-hydroxyl (gem-alkynol)⁹. Notwithstanding, vis-à-vis structural interplay among these three functional groups in a single crystal structural hitherto has not been studied.

Initially we tried to crystallize DDDA from/with aromatic amines like aniline or with amino phenols that had been studied separately, so far we failed to achieve them. Attention shifted therefore to the non-aromatic amines, both cyclic and acyclic. It has been observed earlier during different supraminol studies, that saturation of hydrogen bond potential and resultant characteristic β -As sheet packing, seldom occurs for amine group, especially when the C-N and C-O vectors are not parallel. Instead of that, we often experience crystal structures with different supramolecular synthons like the square synthon or an infinite chain. Wherein one of the two donor amine hydrogen atoms either remain 'inactive' or form relatively weak N-H... π interactions. Based on this background, we used amines with variable donor protons, primary (two), secondary (one) and tertiary amine (none). This should help us to understand the importance of the number of donor amine hydrogen atom(s) toward synthon selection and hence overall packing. In this work we further subdivided the solvates into three groups containing (A) primary amines, (B) secondary amines or (C) tertiary amines.

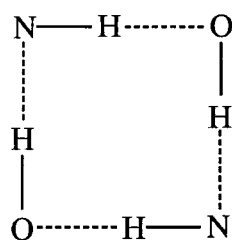


Synthons



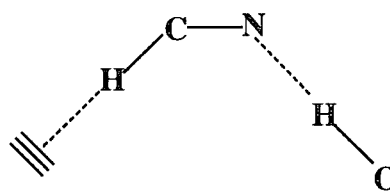
I

Infinite array of O-H...N-H...O-H...N

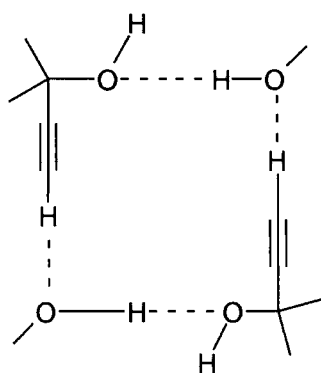


II

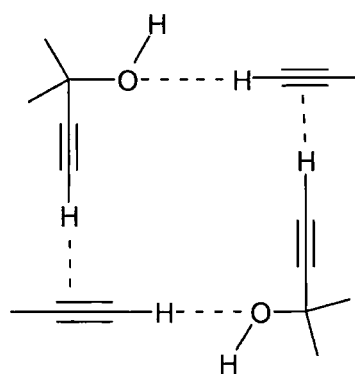
Centrosymmetric Square Synthon



III



V



VI

Scheme 6.I. Showing the DDDA molecules and synthons of interest for this study.

6.4. CSD Search: As mentioned earlier solvates containing amine solvates are rare, a brief search in the Cambridge Structural Database (CSD)¹⁰ was carried out for the amine molecules used in this study. The result as shown in the following table clearly reveals that only a very few of them exist as free amine molecules.

Sl. No	Amine Molecule	No of Hits
1.	Cyclopentyl amine	0
2.	Cyclohexyl amine	2
3.	Cycloheptyl amine	0
4.	Cyclooctyl amine	0
5.	Octyl amine	1
6.	1,2-cyclohexyl diamine	1
7.	Diethyl amine	8
8.	Dipropyl amine	4
9.	Dibutyl amine	1
10.	Di-isopropyl amine	0
11.	Dicyclohexyl amine	3
12.	N,N,N-Ethyl dimethyl amine	0
13.	Triethylamine	12
14.	N,N-dimethylcyclohexylamine	0

6.5. Primary amine solvates:

Three different types primary amines are used, cyclic (monoamines), acyclic and cyclic diamine. The steric bulk of the cyclic amines was gradually increased by using cyclopentyl amine (1), cyclohexyl amine (2), cycloheptyl amine (3) and cyclooctyl amine (4,5). Octyl amine (6) was used as an acyclic amine and 1,2-cyclohexyl diamine (7) was used to study the effect of interaction interferences on crystal packing.

6.5.1. (Cyclopentyl amine)₂. DDDA [1]: The crystal structure of **1** contains a half molecule of DDDA and one full molecule of cyclopentyl amine in the monoclinic space group $P2_1/c$. Crystal packing shows some equally interesting features. As in its other solvates with dipolar aprotic solvents, DDDA molecules form good, directional hydrogen bonds and lie on an inversion centre to give a more or less 'normal' crystal structure. More interestingly, characteristics of both the supraminol and gem-alkynol moiety are prominent in a 1:2 solute-solvent module. An infinite cooperative array of O-H...N (1.87 Å, 177.9°), N-H...O (2.379 Å, 146.3°) and O-H...N hydrogen bonds dictate the interaction pattern. The other amine hydrogen atom is directed towards the ethynyl groups, forming an N-H... π (2.835 Å, 168.9°) bond, creating the supramolecular synthon **I**, (Figure 6.1.) while the ethynyl hydrogen atom forms a C-H...Cl-C (3.115 Å, 169.5°) interaction. Such an infinite cooperative array accompanied by a N-H... π

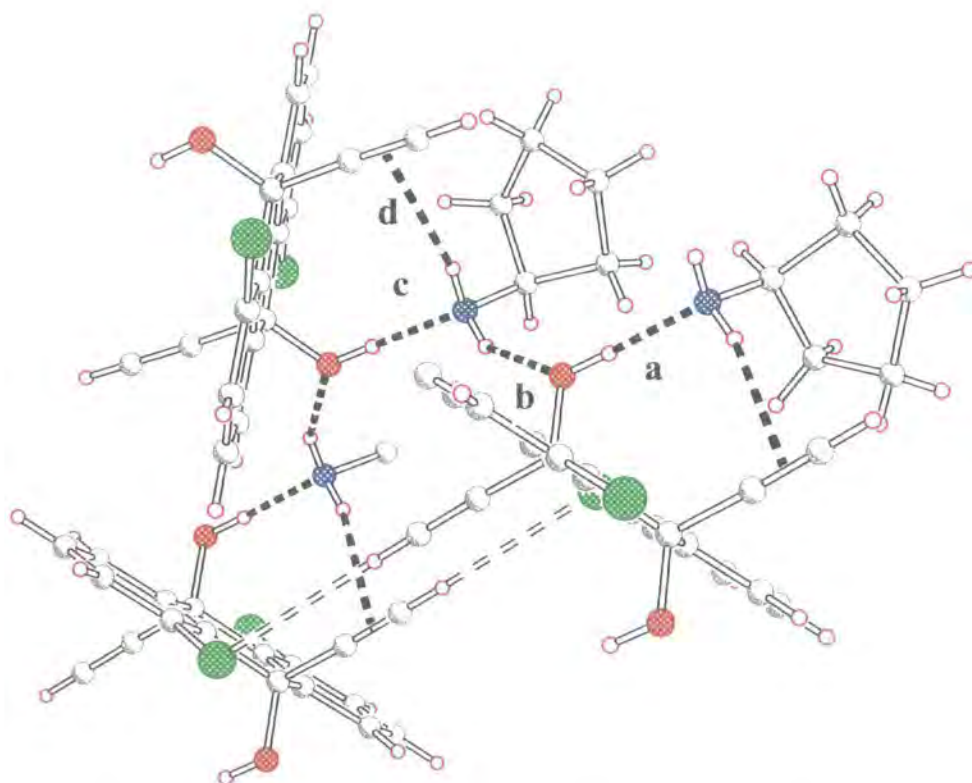


Figure 6.1. Crystal packing of **1**, showing synthon **I** composed with cooperative (a) N...H-O (b) O...H-N (c) N...H-O and (d) N-H... π interaction

interaction is one of three of the most frequently observed structural motifs, alongside the β -As sheet and centrosymmetric square motif, for supraminols, or aminophenols and molecular complexes containing amine and hydroxyl groups⁸, such as for 2-aminophenol (2AP) and 3-aminophenol (3AP) (Figure 6.2)

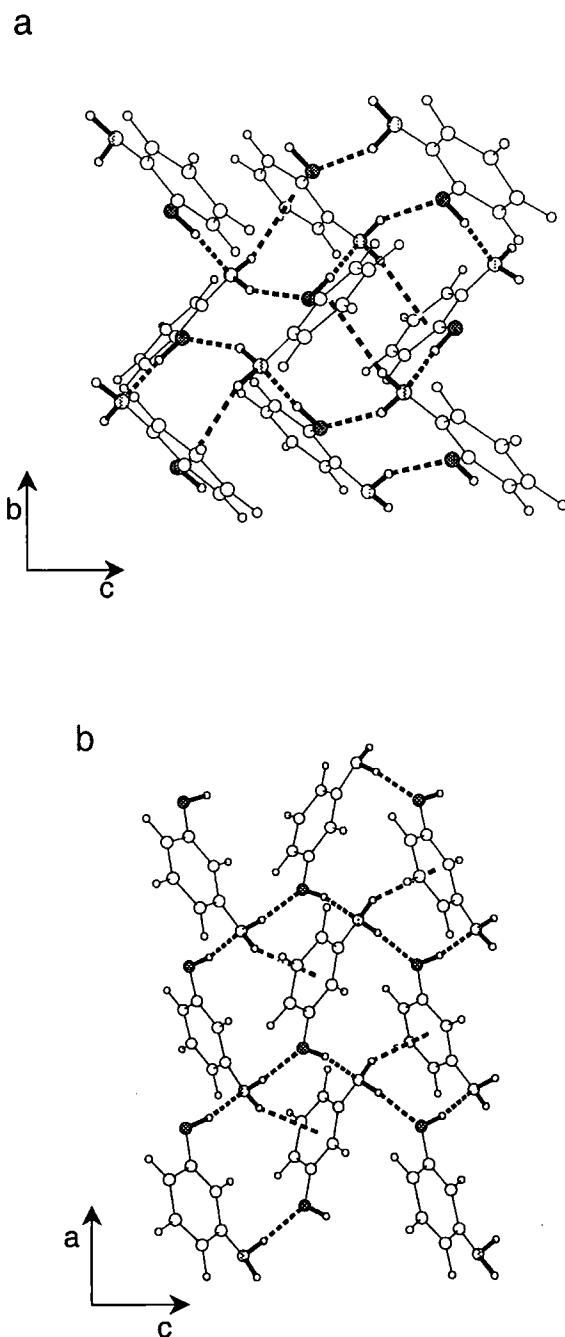


Figure 6.2. Hydrogen bridges in (a) 2-aminophenol (2AP); (b) 3-aminophenol (3AP). The infinite chain N(H)O synthon is highlighted in both cases

The packing is reminiscent of other gem-alkynol molecules too, except the amine group is replacing the hydroxyl group and the unavailability of one more ethynyl group in a solvent rich system leads to formation of a C-H...Cl bond¹¹ rather than C-H... π or C-H...O bonds and diminishes the probability of forming supramolecular synthon V and VI, usually observed for gem-alkynol family⁹.

6.5.2. (Cyclohexyl amine)₂.DDDA [2] : The crystal packing of **2** is almost analogous to that of **1** or **2AP** and **3AP** with a monoclinic space group P2₁/n. Again a 1:2 solute-solvent module is obtained with similar kind of infinite cooperative arrangement with synthon I. Although the topology is the same, the larger steric requirement of the six

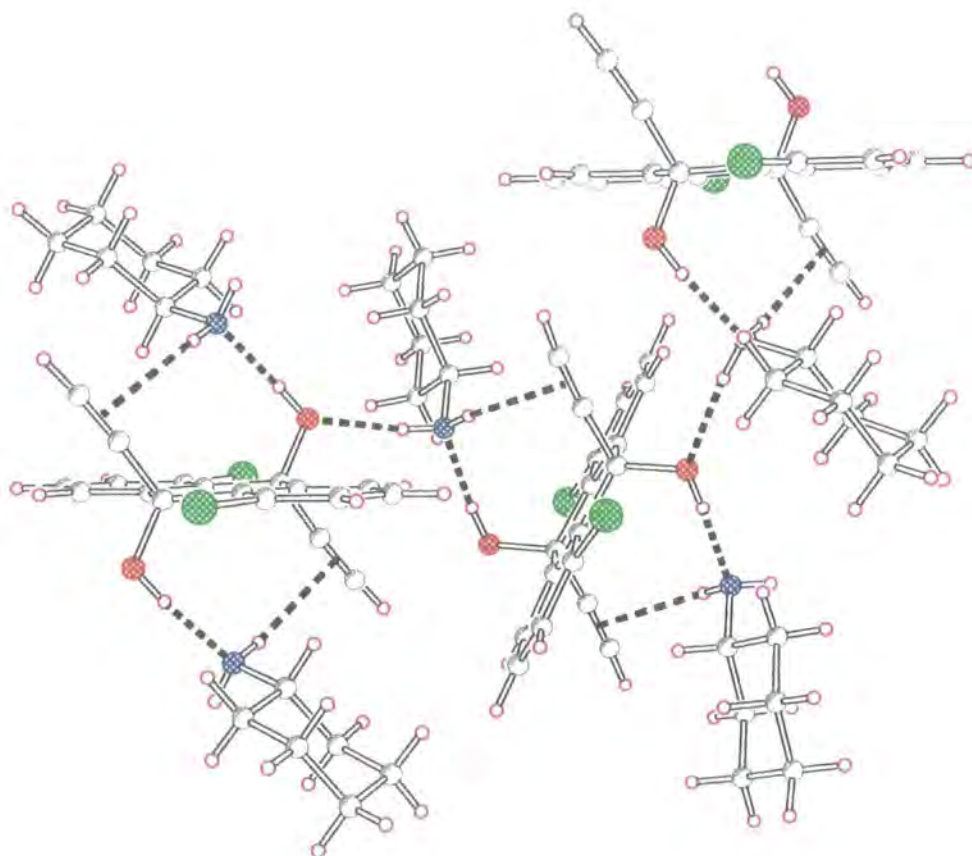


Figure 6.3. Crystal packing of **2** showing synthon I. Notice how the orientation of cyclohexyl ring restricting the ethynyl hydrogen to take part in hydrogen bond.

membered ring does make its presence felt on the matrices. The almost perpendicular alignment of the cyclohexyl ring with respect to DDDA makes the ethynyl hydrogen atom too far away to form any bond, and it remains almost 'free'. As if to compensate for this, both O-H...N (1.81 Å, 177°) and N-H...O (2.21 Å, 163.5°) interactions are shorter than that of **1**, while N-H... π is comparable (Figure 6.3).

6.5.3. (Cycloheptyl amine)₂. DDDA [3]: Even with larger ring like cycloheptyl, the crystal packing of **3** closely resembles that of **1** and **2**, with DDDA molecule sitting on a distinct inversion centre in a monoclinic space group $P2_1/c$. An infinite cooperative arrangement with synthon **I** reappears with the 1:2 solute-solvent module. There is hardly any noticeable difference in crystal packing for **3** than from **2**. Again the almost perpendicular orientation of the cycloheptyl ring, ruled out any possibility of hydrogen bonding with the ethynyl hydrogen atom (Figure 6.4).

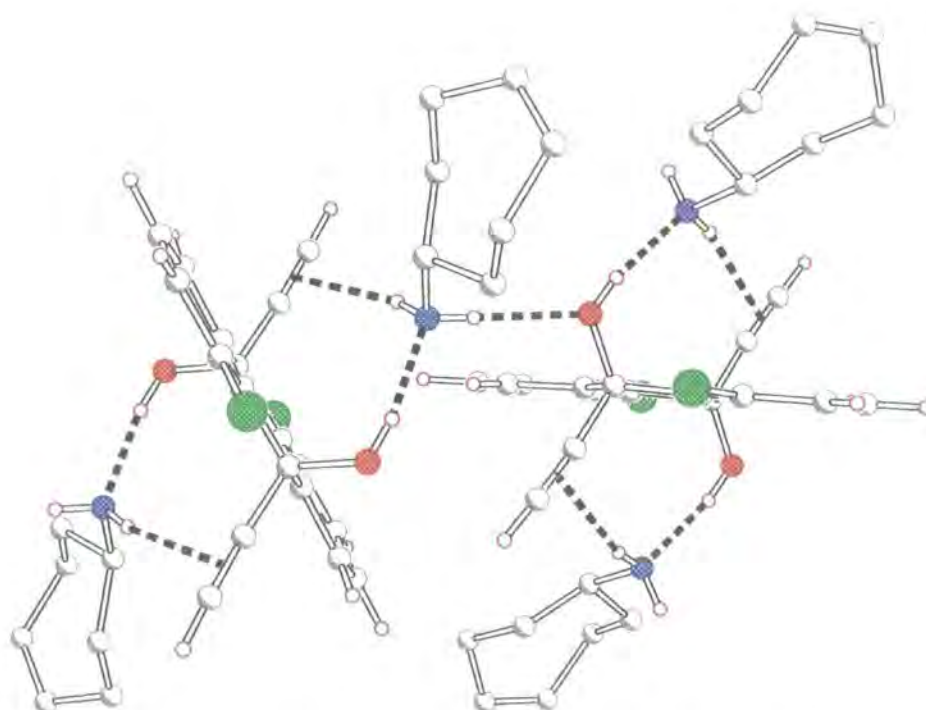


Figure 6.4. Crystal packing of **3** showing synthon **I**, note that ring hydrogen atoms of cycloheptyl amines are not shown for clarity.

6.5.4. (Cyclooctyl amine)₂. DDDA [4], (Cyclooctyl amine). DDDA [5] : The Crystal structures of **4** and **5** represent an unusual occurrence of conformational pseudopolymorphism¹². In an unprecedented occurrence two different conformations of cyclooctyl amine, the crown and tub conformations form two distinct 1:2 (**4**) and 1:1 (**5**) solvates respectively (Figure 6.5a,b). The crystal structure of **4** is directly analogous to those of the other cyclic amines with a monoclinic P2₁/c space group with one half molecule of DDDA and one cyclooctylamine molecule in the asymmetric unit. As expected, the synthon **I** appears to be the major interaction pattern (Figure 6.5c). It is imperative to note here, that the occurrence of two energetically different conformations of a conformationally flexible solvent molecule being trapped in the crystal lattice of the same solute molecule, is extremely rare. Recently we were successful in trapping both the gauche and staggered rotamers of diethylamine with cis isomer of DDDA¹².

On the other hand, the crystal structure of **5** shows some unusual behaviour from the rest of the solvates. The asymmetric unit of **5** (Triclinic, P1) comprises two half molecules of DDDA sitting on distinct inversion centres and one cyclooctyl amine molecule. Interaction hierarchies of the two DDDA molecules are distinctly different. Interestingly, while one of the gem-alkynol functionalities forms a supramolecular synthon **V** that is the hallmark of gem-alkynol family⁹, the hydroxy group of the other one, forms a strong O-H...N bond with the amine and restricts the other two ethynyl groups from forming supramolecular synthon **VI**. However, the orientation of the ethynyl group is closely reminiscent to the cooperative synthon **V** and **VI**. This is so far the closest example of interrupted crystallisation, where a strong O-H...N bond with the solvent outweighs the weakest C-H... π bond of the supramolecular synthon **VI**. Sudden appearance of the supramolecular synthon **V** once again proves the difficulty of doing a systematic study on this groups with interaction interference. The steric demand of the cyclic octyl rings in two different conformations, act as a buffer to these packing

differences. For **4**, less steric hindrance makes it possible for the two hydrogen atoms to take part in hydrogen bonding resulting in synthon **I**, while in **5**, due to greater steric demand of the tub conformation, amine hydrogen atoms could only form a very weak N-H... π bond, and the structure is further rather stabilised by forming the robust supramolecular synthon **V** (Figure 6.6). Again, two relatively weak ‘diminishing’

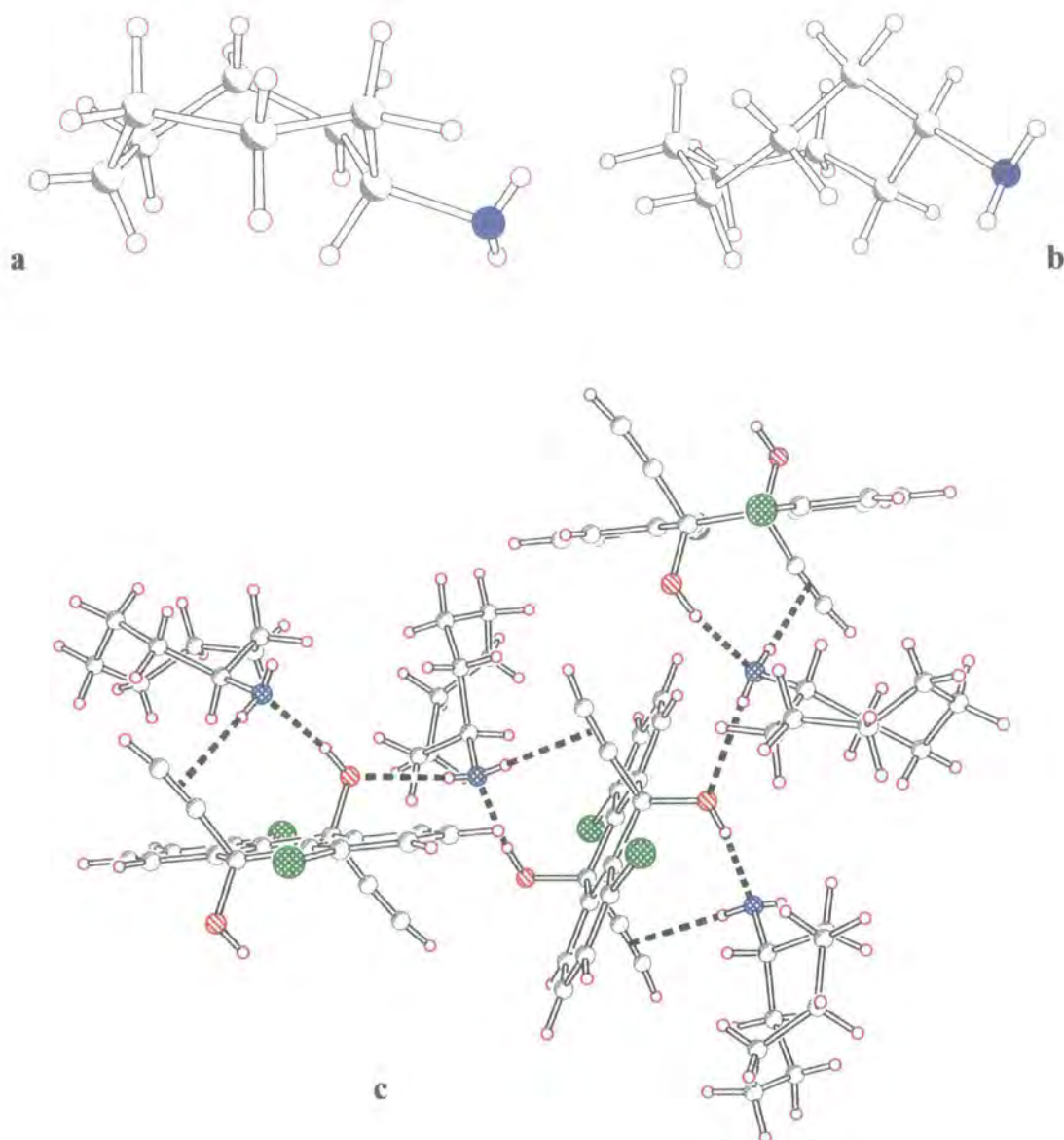


Figure 6.5. Two different conformations of cyclooctyl amines in (a) **4** and (b) in **5**. (c) Crystal packing of **4** showing synthon **I**.

N-H... π (2.96Å, 3.15Å) interactions could be rationalised as one step closer to the crystallisation point of unsolvated DDDA, with solvent extrusion from the bulk which is further corroborated from the solute rich structure.

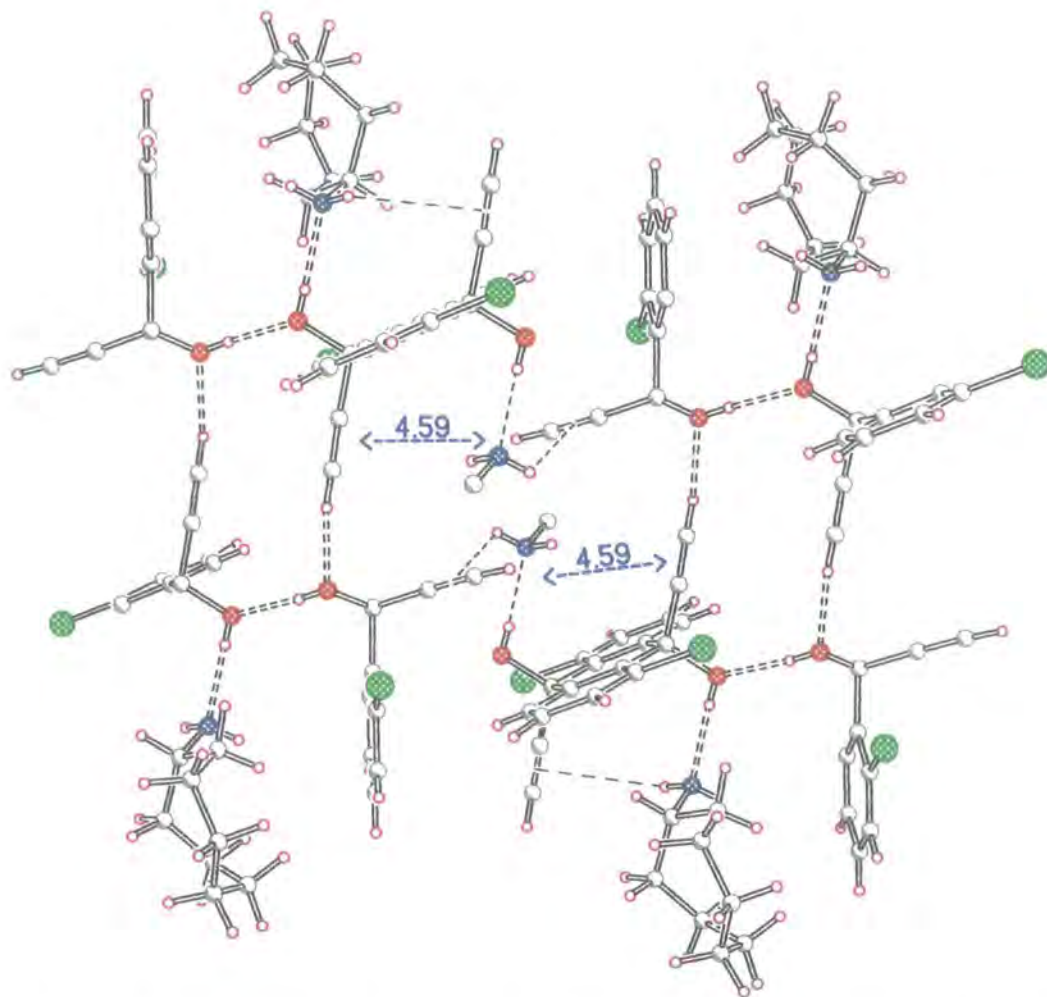


Figure 6.6. Crystal packing of **5** showing synthon **V**, notice the orientation of two other ethyl groups (separated by 4.59Å) shows close similarity to synthon **VI**.

6.5.5. (tert-Octylamine)₂. DDDA [6]: Having noticed that steric hindrance could force the DDDA molecule to adopt a ‘normal’ gem-alkynol like crystal packing, the question then arose whether the crystal packing with synthon **V** or **VI** could be reproduced with increasing steric bulk of the amine. For **6**, DDDA crystallised in monoclinic space group $P2_1/c$, with one half molecule of DDDA and one octyl amine molecule.

Crystal packing of **6** is different from other primary (cyclic) amines we have seen so far, though a similar 1:2 solute-solvent model persists. Steric bulk likewise in **5**, restricts the amine hydrogen atoms from taking part in any strong bonds, as the non-polar part of the molecule swings away from the aromatic ring to form a channel-layer pattern. Although there is a strong O-H...N bond between DDDA and the amine, no infinite cooperative arrangement was observed due to 'inactive' amine hydrogens. Instead a C-H... π bond makes a structural motif close to supramolecular synthon **III** with a donor hydrogen atom from β -C atom rather than from α -C atom, while the ethynyl group is aligned towards the aromatic ring to form a C-H... π bond rather than C-H...Cl bond (Figure 6.7). Interestingly, the major difference between synthon **I** and **III** is the absence of N-H...O or N-H... π , topologically there is hardly any difference between the corresponding structures.

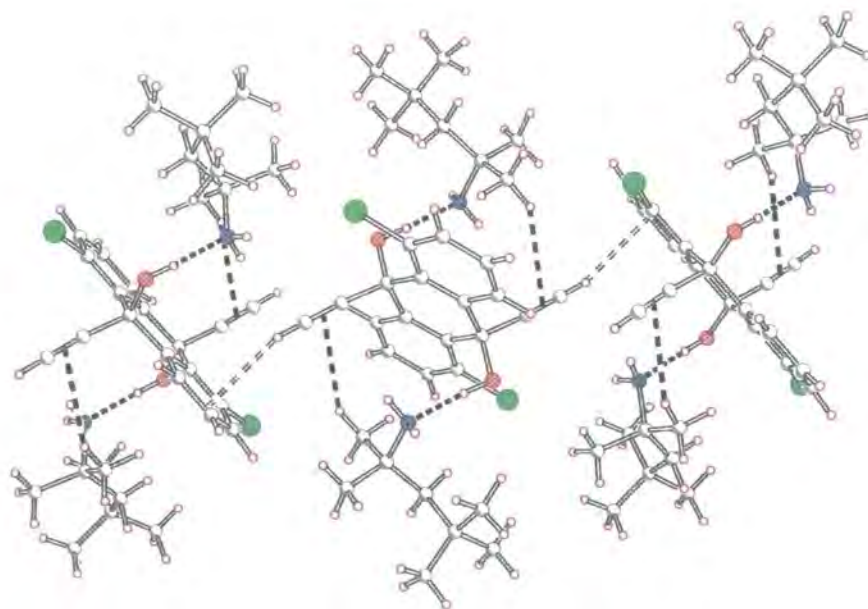


Figure 6.7. Crystal packing of **6** showing synthon **III** like interaction pattern with a weak C-H... π (arene) interaction shown in light dashed line.

6.5.6. (1,2-cyclohexyl diamine)₂. DDDA [7] : In all the amine solvents used so far, the non-polar parts are flexible. To identify the effect of strain, we then shifted our experiment to a more rigid primary amine system. The crystal structures of 5 and 6 indicate that not only the flexibility of the non-polar part of the solvent, but also the number of amine hydrogen atoms involved in the hydrogen bond is also an important factor for synthon selection. In order to study the structural as well as interaction interference we crystallised DDDA with 1,2-cyclohexyl diamine. The crystal structure is unique with an asymmetric unit comprised of three symmetry independent half molecule of DDDA and one full amine molecule (1:1.5) in triclinic $P\bar{1}$ space group. Interaction hierarchies of the two-amine groups are distinctly different. To our surprise, a supramolecular square synthon **II** (O-H...N, 1.92Å, 172°; N-H...O, 2.67 Å, 154°) dominates the packing. The second amine group, on the other hand, involves itself with an finite interaction pattern O-H...O-H...N-H... π that is closely related to synthon **I**, except that an O-H...O (1.90Å, 176°) and a second rather weak N-H... π (2.83 Å, 157.5°)

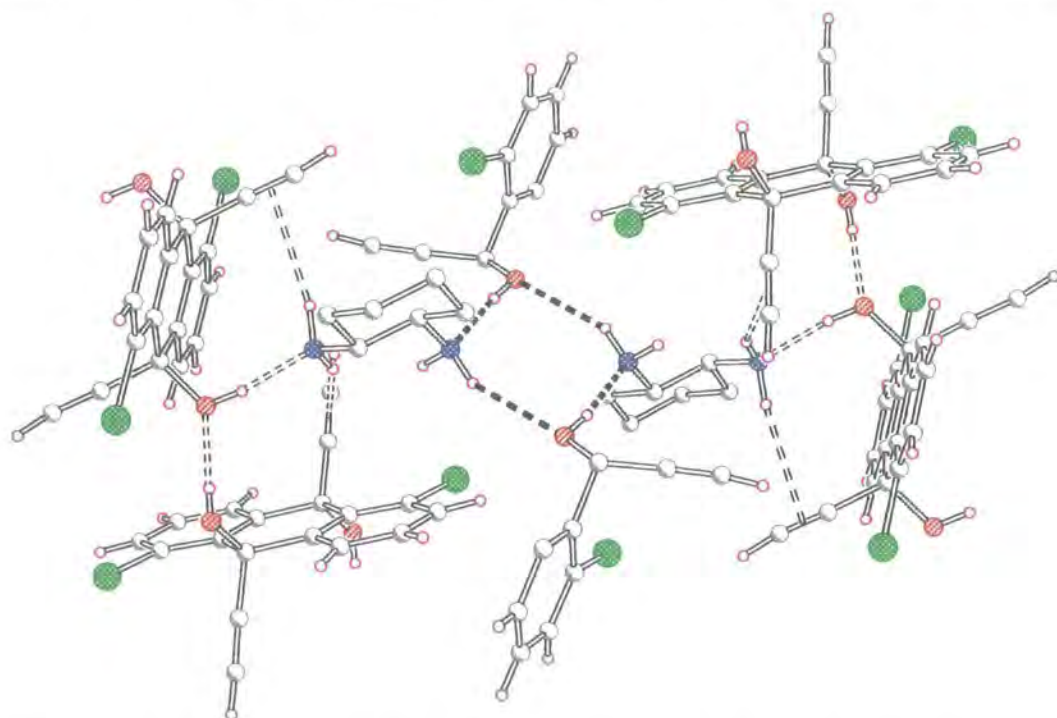


Figure 6.8. Crystal packing of 7 showing square synthon **II** sandwiched between two interaction patterns similar to synthon **I**.

interaction replaces the infinite chain (Figure 6.8). The crystal structure of **7** is closely related to those of supraminols, as a cyclohexyl group could be envisaged as the spacer group between two supramolecular synthons. It is quite unusual to see two amine groups in the same molecule showing such kind of anomalous behaviour. While the amine group that forms synthon **I** behaves more like primary amine, the second amine group with one 'inactive' hydrogen atom behaves more like secondary amine. Nonetheless, two different supramolecular synthons in a single crystal structure of a supraminol hitherto have not been observed.

6.6. General Discussion of primary amine solvates:

Crystal structures **1-7** show an interesting, and at the same time, unusual trend, with a composite crystal packing of gem-alkynol and supraminols. Such composite packing highlights the importance of all the functional groups and the structural repetition and hence changes in crystal packing can be understood and explained from both the supraminol and gem-alkynol perspectives.

From a supraminol point of view, amine and hydroxyl groups are perfectly complimentary to each other. For 1:1 supraminols, complete saturation of the hydrogen bond potential should lead to β -As sheet type packing. Recently we studied a series of supraminols with an aim to draw some correspondence of molecular structure and packing type. It has been noted that complete saturation of hydrogen bond potential of amine and hydroxyl groups and the resultant β -As sheet type packing, occurred only when the C-O and C-N vectors are nearly parallel in molecular structures (as in the archetypal 4-aminophenol). On the contrary when the C-O and C-N vectors are not parallel, we observed crystal structures with supramolecular synthons like the infinite chain and square motifs. A closer inspection of the space group could help us to understand the absence of the β -As network. Detailed analysis reveals that structures containing the β -As network always lack the 2_1 screw axis, whereas for structures

containing an infinite chain the 2_1 screw axis is quite important. Amine solvates containing infinite chains all crystallise here in a space group which contains 2_1 screw axis. The reason behind this is that a 2_1 screw axis permits greater flexibility which matches the flexibility of an infinite chain. In agreement with this assumption all those structures that adopt an infinite chain crystallise in $P2_1/c$ and those adopting other kinds of packing adopt a $P\bar{1}$ space group. The absence of the β -As network can be rationalised as, in the $P2_1/c$ space group, the DDDA molecule lies on an inversion centre, whereas the corresponding amine molecule sits in a general position. This makes C-O and C-N vectors almost perpendicular to each other, with least probability of forming β -As network. Instead an infinite chain with N-H... π interactions dominates the crystal packing. Interestingly, these infinite chain patterns closely resemble those of supraminols, where instead of an ethynyl group benzene ring takes part in the N-H... π interaction. A higher amount of strain in the two amine groups in **7** create an interaction interference and the infinite chain was terminated by a shorter O-H...O bond on either side of a square synthon. A square motif could be considered as a short section of the infinite chain as being wrapped back itself to form a loop rather than chain.

From the gem-alkynol point of view, the whole series could be better understood from the theory of pseudopolymorphism and a multipoint recognition model. Solvation is considered as an interruption of normal crystallisation, where a strong bond between solute and solvent intervene in the formation of the robust supramolecular synthon. A good acceptor like primary amine nucleates by means of a infinite N(H)O chain which stops formation of other supramolecular synthon. In this successive process the compound crystallises with the solvent molecule trapped with its framework. In other words, crystallisation of DDDA was interrupted up to the formation of synthon **I**, for **5**, this 'interruption' was further delayed until synthon **V** was formed, but does interrupt the formation of synthon **VI**.

Table 6.1. Crystallographic data and structure refinement parameters of 1° amine solvates.

	1	2	3	4	5	6	7
Empirical formula	C ₁₄ H ₁₆ ClNO	C ₃₀ H ₃₆ Cl ₂ N ₂ O ₂	C ₁₆ H ₂₀ ClNO	C ₁₇ H ₂₂ ClNO	C ₂₆ H ₂₇ Cl ₂ NO ₂	C ₁₇ H ₂₄ ClNO	C ₃₃ H ₂₉ Cl ₃ N ₂ O ₃
Formula wt.	249.73	527.51	277.78	291.81	456.39	293.82	607.93
Temp (°K)	120	120	120	120	120	120	120
Crystal System	Monoclinic	Monoclinic	Monoclinic	Monoclinic	Triclinic	Monoclinic	Triclinic
Space group	P2 ₁ /c	P2 ₁ /n	P2 ₁ /c	P2 ₁ /c	P-1	P2 ₁ /c	P-1
<i>a</i> [Å]	10.8061(3)	9.6765(19)	13.8867(3)	14.1447(9)	10.2504(3)	14.877(3)	9.787(2)
<i>b</i> [Å]	11.4830(3)	11.311(2)	11.3975(3)	11.4170(9)	10.3633(3)	8.7544(18)	11.727(2)
<i>c</i> [Å]	10.0223(2)	26.025(5)	9.4693(2)	9.5945(7)	12.7980(4)	13.476(3)	13.902(3)
α [°]	90	90	90	90	67.256(1)	90	79.01(3)
β [°]	93.518(1)	92.57(3)	101.280(1)	91.844(3)	71.800(1)	113.52(3)	82.36(3)
γ [°]	90	90	90	90	68.257(1)	90	67.48(3)
<i>Z</i> '	0.5	1.0	0.5	0.5	1.0	0.5	1.5
Volume [Å ³]	1241.29(5)	2845.6(10)	1469.79(6)	1548.6(2)	1141.67(6)	1609.2(6)	1443.6(5)
<i>D</i> _{calc} [g/cm ³]	1.336	1.231	1.255	1.252	1.328	1.213	1.399
μ [mm ⁻¹]	0.290	0.257	0.252	0.243	0.308	0.234	0.356
2θ [°]	5.18 to 55	3.92 to 55	3.0 to 55	2.88 to 52	3.52 to 55	5.52 to 55	3.8 to 55
Range <i>h</i>	-14 to 14	-12 to 12	-18 to 18	-17 to 17	-13 to 13	-19 to 19	-12 to 12
Range <i>k</i>	-14 to 14	-14 to 14	-14 to 14	-13 to 14	-13 to 13	-11 to 11	-15 to 15
Range <i>l</i>	-13 to 13	-32 to 33	-12 to 12	-11 to 11	-16 to 16	-17 to 17	-18 to 18
Reflns. collected	12440	22256	20502	9708	12815	24128	17147
Unique reflns.	2843	6545	3385	3041	5224	3692	6632
Obs. reflns.	2436	5000	2767	1379	3991	2798	5677
<i>R</i> ₁ [<i>I</i> > 2 σ (<i>I</i>)]	0.0316	0.0386	0.0444	0.0600	0.0530	0.0596	0.0375
<i>wR</i> ₂ [all]	0.0839	0.0988	0.1224	0.1212	0.1127	0.1506	0.1015
Goodness-of-fit	1.042	1.025	1.037	0.824	1.040	1.121	1.047
Crystal size mm ³	0.42 x 0.16 x 0.08	0.42 x 0.32 x 0.28	0.4 x 0.04 x 0.02	0.22 x 0.16 x 0.08	0.26 x 0.20 x 0.16	0.22 x 0.18 x 0.02	0.26 x 0.20 x 0.12
Largest diff. peak and hole (e.Å ⁻³)	0.423 and -0.251	0.362 and -0.251	0.408 and -0.426	0.557 and -0.331	0.714 and -0.239	0.512 and -0.438	0.538 and -0.278

6.7. Secondary Amines

Having noticed recurrent crystal packing reminiscent to the supraminol family with the primary amines, more precisely the second amine hydrogen forming N-H... π bonding most of the time, and the appearance of the square synthon in **7** involving only one 'active' hydrogen atom, we were prompted to study the packing pattern with secondary amines. Secondary amines with only one donor amine hydrogen should be prone to form strong N-H...O rather than weak N-H... π bond. This in effect, should change the crystal packing from synthon **I**. It is noteworthy that an infinite chain of only N(H)O bonds but without N-H... π interaction is seldom observed for supraminols. Formation of the infinite chain, which we have seen in most of the primary amine solvates, needs much more flexibility; strained systems like secondary amines should change the track into a different type of network. Accordingly, five different, both cyclic and acyclic secondary amines, were investigated with increasing steric bulk.

6.7.1. (DDDA). (Et₂NH)₂ [**8**] :

As we observed earlier, emergence of synthon **I** appears to be directly related to the space group, with **5** and **7** showing different packing in P $\bar{1}$. The structure of **8** with one half molecule of DDDA and one Et₂NH in P $\bar{1}$, further reinforced the findings. With the DDDA molecule being able to sit on an inversion centre, instead of any infinite array, a closed loop of hydrogen bonds forming a square synthon (**II**) dominates the packing. Interestingly, the perpendicular orientation of the ethyl moiety from the synthon plane, makes it sterically less crowded to propagate, with DDDA molecules interlinking themselves through C-H...Cl bonding (Figure 6.9). The topology of the packing with square synthon in **8** is almost analogous to those of supraminols, such as 4-(4aminobenzyl)phenol^{8b} (Figure 6.10). However, this is in sharp contrast with **7**, where synthon **II** is sandwiched between two synthons **I**, primarily due to steric hindrance caused by the 'in-plane' orientation of 1,2-cyclohexyl diamine.

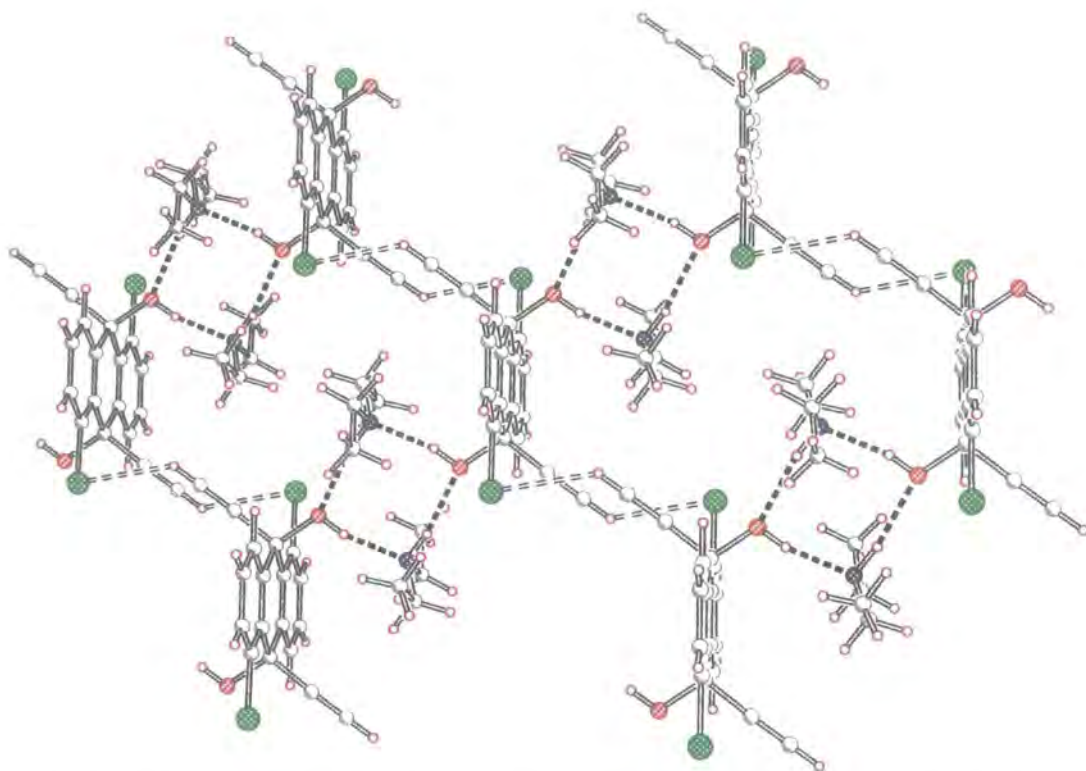


Figure 6.9. Crystal packing of **8** showing square motifs in bold bond, while the DDDA molecules interlink with C-H...Cl bonds shown as light bonds.

Crystal packing of two conformational pseudopolymorphs of *cis* isomer of DDDA with diethylamine is worth mentioning here¹². For both crystal structures, an infinite cooperative arrangement of O...H-N...H-O...H-O...H-N linkages dictate the packing with supporting C-H... π and C-H...Cl interactions.

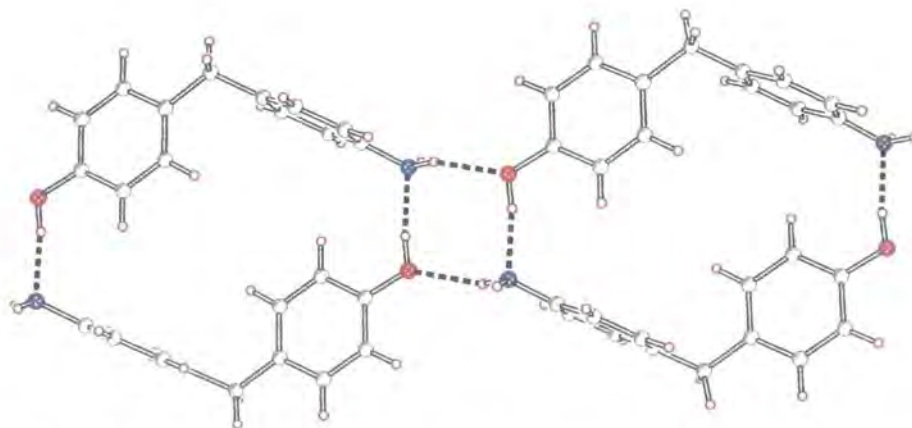


Figure 6.10. Crystal packing of 4-(4aminobenzyl)phenol showing square motifs.

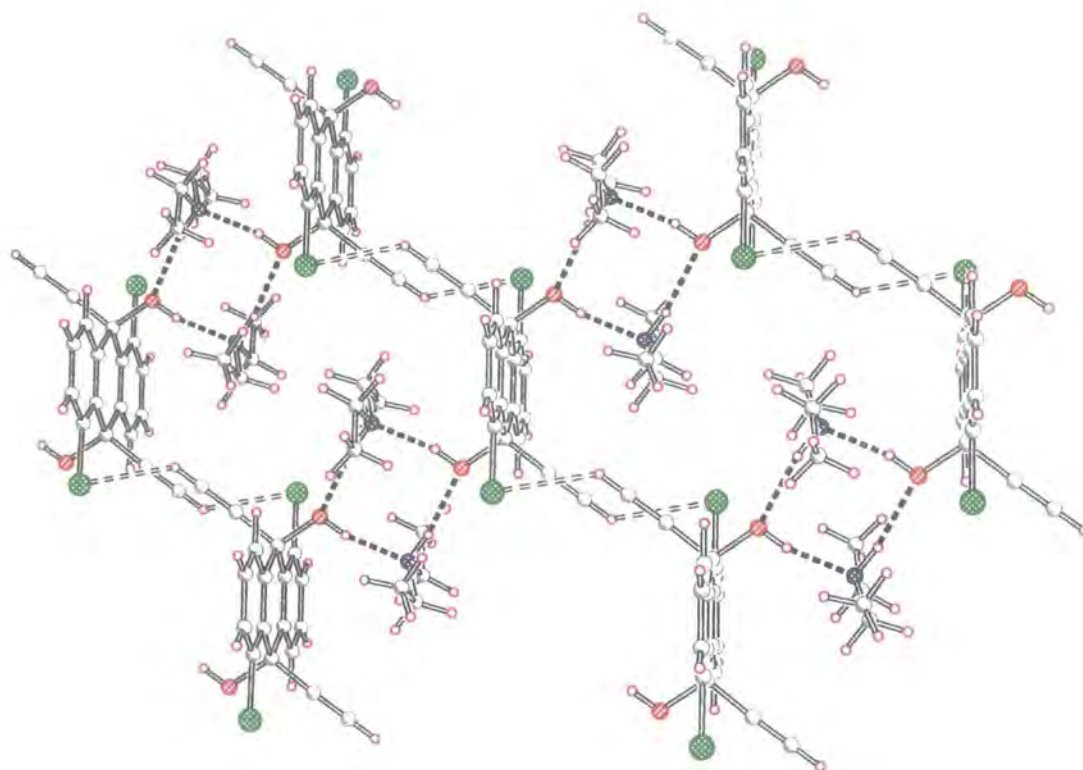


Figure 6.9. Crystal packing of **8** showing square motifs in bold bond, while the DDDA molecules interlink with C-H...Cl bonds shown as light bonds.

Crystal packing of two conformational pseudopolymorphs of *cis* isomer of DDDA with diethylamine is worth mentioning here¹². For both crystal structures, an infinite cooperative arrangement of O...H-N...H-O...H-O...H-N linkages dictate the packing with supporting C-H... π and C-H...Cl interactions.

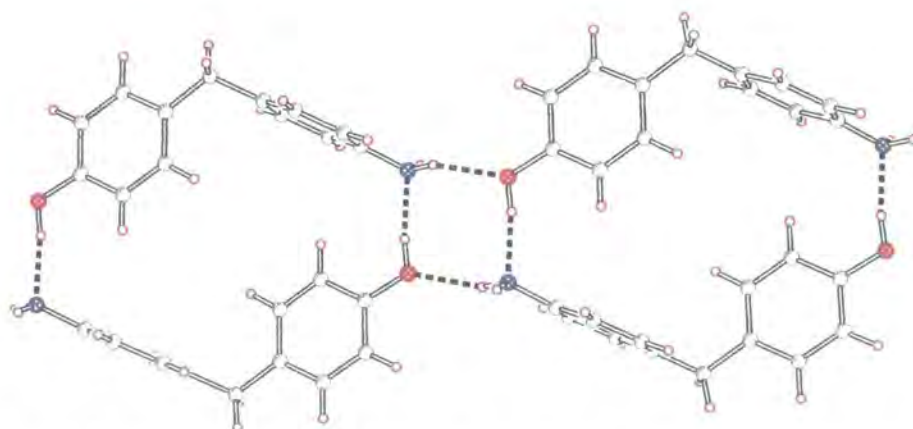


Figure 6.10. Crystal packing of 4-(4aminobenzyl)phenol showing square motifs.

Understandably, the cis orientation of the gem-alkynol groups made it feasible to form this unusual infinite chain without any N-H... π interactions (Figure 6.11).

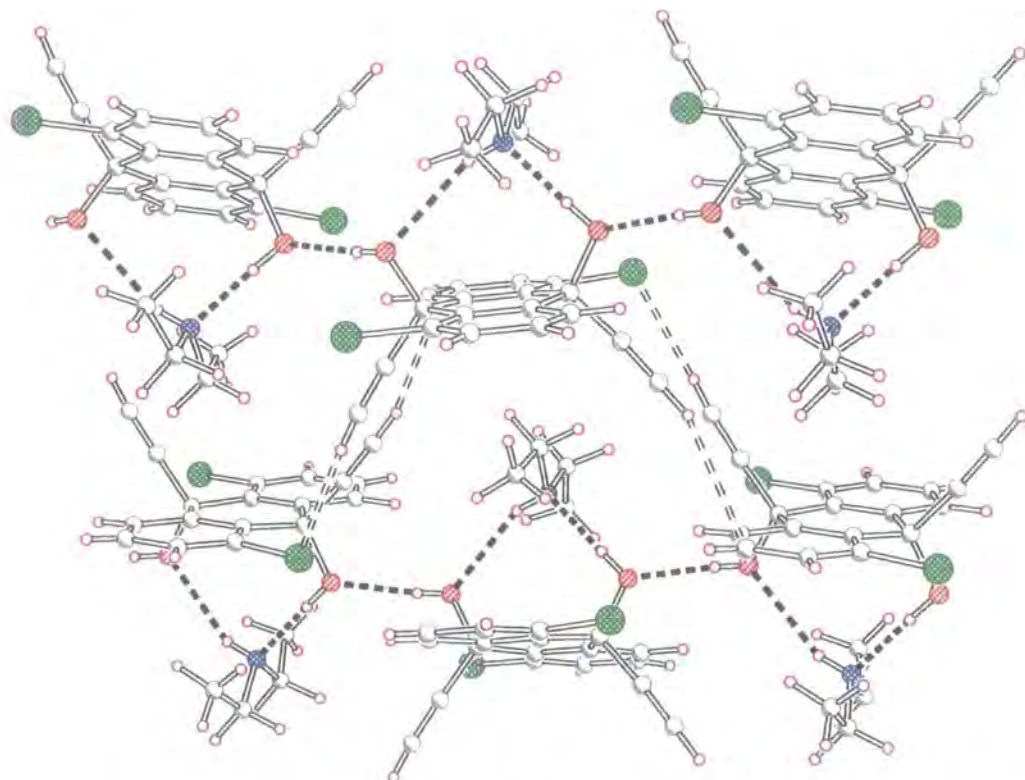


Figure 6.11. Crystal packing of cis-DDDA with diethyl amine showing infinite cooperative arrangement of O...H-O....H-N...O.

6.7.2. (Pr₂NH)₂, DDDA [9]: Crystal packing of **9** is almost identical with that of **8** with supramolecular square synthon **II** as major interaction pattern and C-H...Cl interaction interlinking to DDDA molecules (Figure 6.12). Even though the crystal structures of **8** and **9** are similar with a square motif as the major synthon, there is a subtle difference in the structural layout. In order to accommodate the relatively larger propyl groups the molecules are tilted in **9** compared to **8**. As a result of that, the synthons are arranged in a parallel fashion with the interlacing molecules stacked in two different layers of similar kind of molecules.

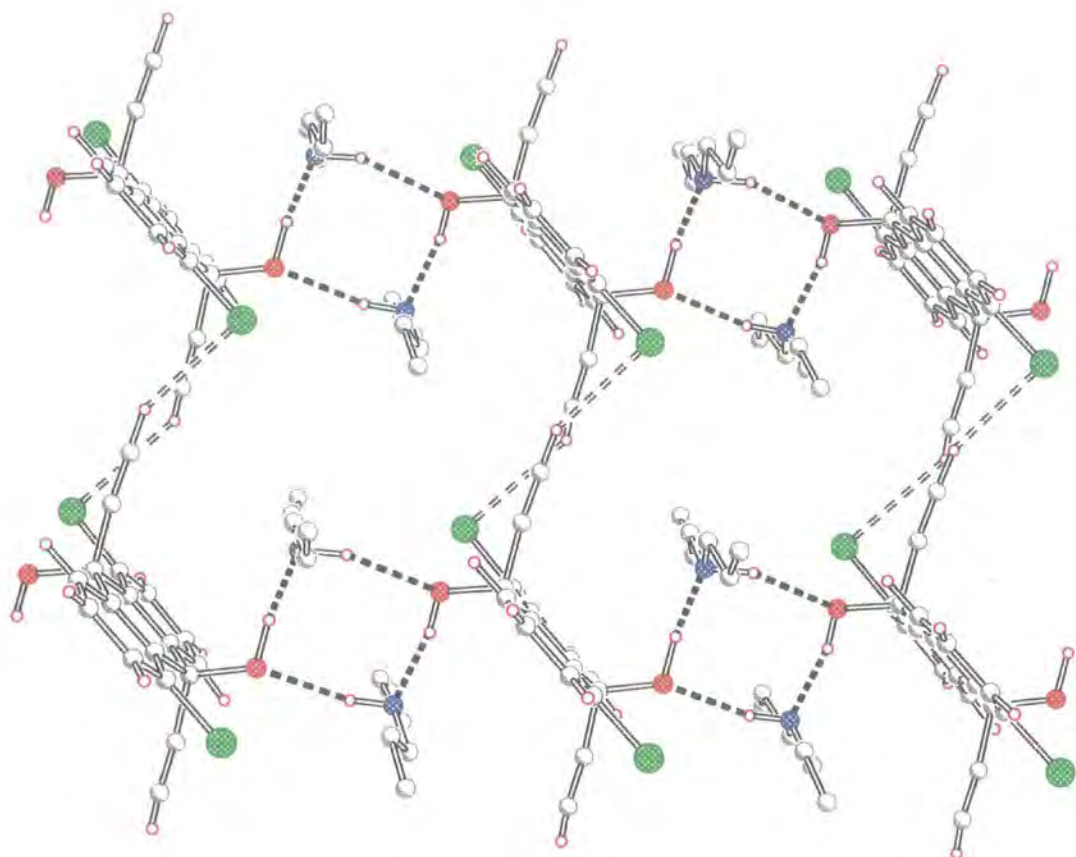


Figure 6.12. Crystal structure of **9** showing synthon **II** in bold bonds and C-H...Cl interaction in light bonds. Notice the tilted orientation of DDDA molecules compared to those of **8**.

6.7.3. (Bu₂NH)₂. DDDA [10]: Crystal packing of **10** is almost a replica of **9** in a triclinic $P\bar{1}$ space group with one half molecule of DDDA and one full molecule of amine. As expected, for **10**, again acentrosymmetric supramolecular square synthon **II** (O-H...N, 1.89 Å, 165°; N-H...O, 2.49 Å, 158°) playing the central role with C-H...Cl bond interlinking the DDDA molecules. Likewise in **9**, in order to accommodate the even larger butyl groups the DDDA as well as butyl molecules are tilted (Figure 6.13), resulting a slight lengthening of the bonds of synthon **II**, especially the N-H...O bonds, which force the square synthons to be arranged in parallel fashion.

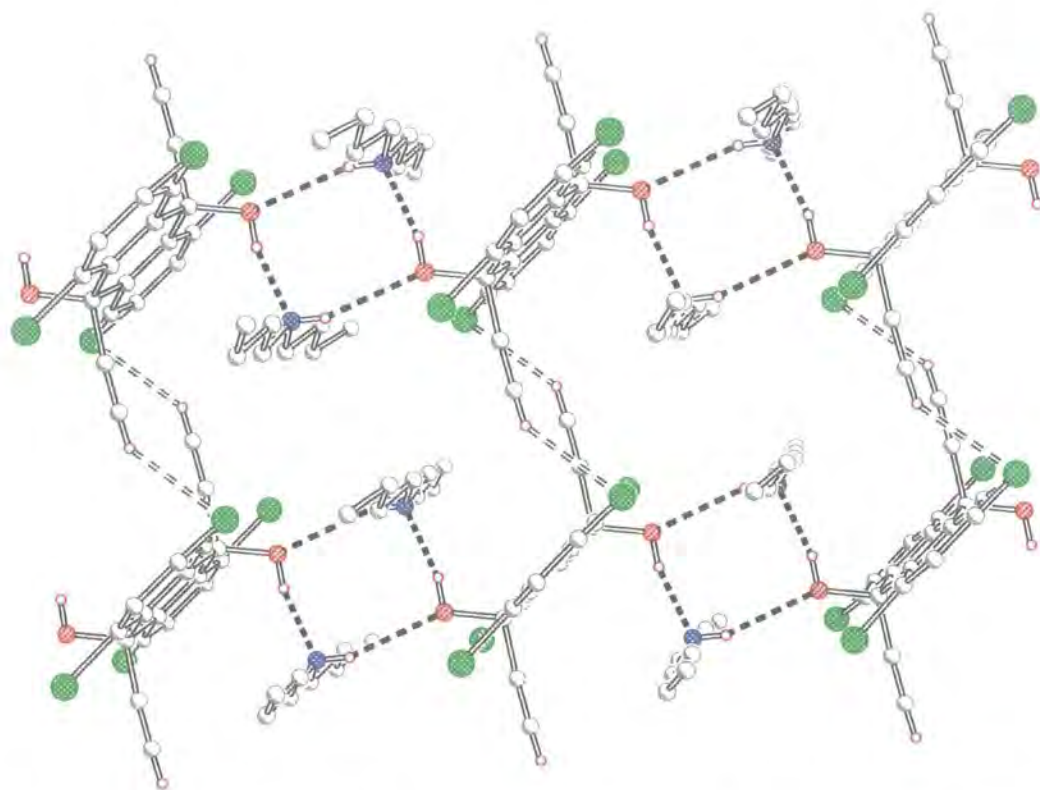


Figure 6.13. Crystal packing of **10** showing square synthon **II** with interlinking C-H...Cl bond. Notice not only the DDDA molecules but the butyl chain is also tilted.

6.7.4. (Dicyclohexyl amine)₂. DDDA [11] :

The DDDA was recrystallised from acetone and dicyclohexyl amine mixture in order to compare with acyclic secondary amines. The amine molecule adopts a chair-chair conformation, which orients the ring carbon atoms somewhat more like two parallel propyl chains away from the hydroxyl groups. In other words, the dicyclohexyl ring does not increase any effective steric interference from that observed for the propyl amines. Therefore the crystal packing does not experience any extra influence from the presence of the rigid rings, as one might expect. This is manifested as synthon **II** to become the recurrent theme, however the cyclohexyl rings orient themselves in such a way that nonpolar parts come closer, which restrict the ethynyl hydrogen from forming C-H...Cl bond (Figure 6.14).

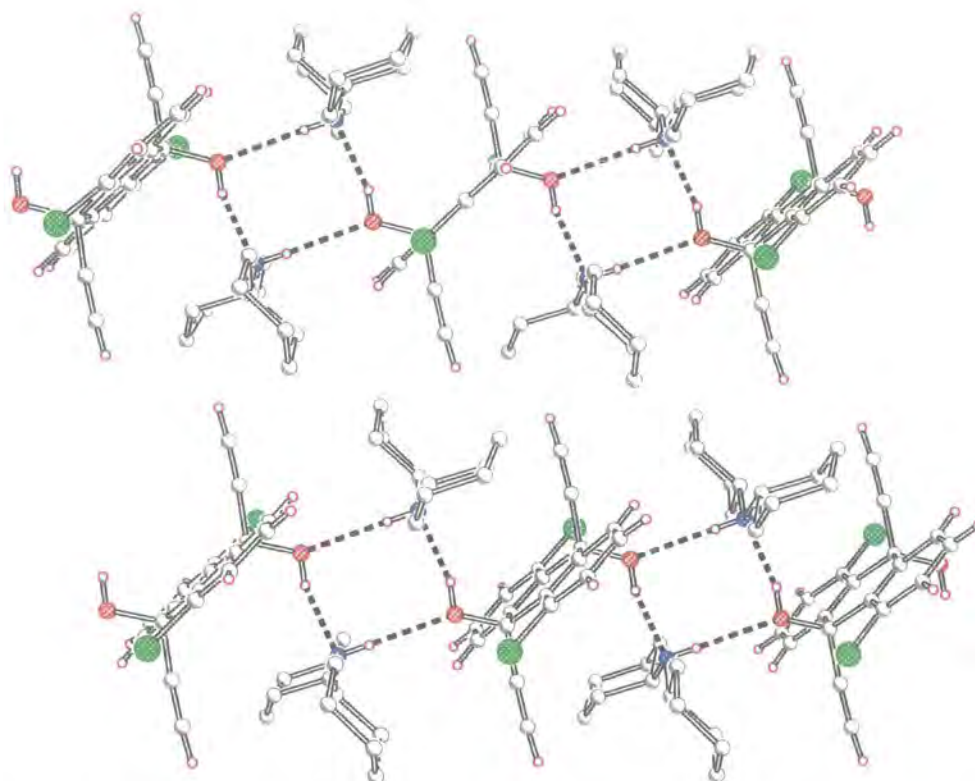


Figure 6.14. Crystal packing of **11** showing square motifs (synthon **II**). Note that the orientations of cyclohexyl rings restrict the formation of C-H...Cl bond.

6.7.5. (Pr₂NH)₂.DDDA [12] : The crystal structure of **12** is implicitly unique and compelling, although it adopts a similar 1:2 module in the triclinic Pī space group with one half molecule of DDDA and one amine molecule in the asymmetric unit. To our surprise, diisopropyl amine adopts a packing not like secondary amines but similar to those of primary amines with synthon **III**. The only donor hydrogen atom of the amine forms a relatively weak N-H...π bond rather than an N-H...O bond, while the ethynyl hydrogen atom forms the usual C-H...Cl bond (Figure 6.15). Structural similarity and adopting a similar supramolecular synthon such as that observed in **6**, put the impetus on steric hindrance. For both these structures (**6** and **12**), the bulky non-polar chain extensions are enough to restrict the other polar functional groups from coming closer and forming the square synthon (**II**).

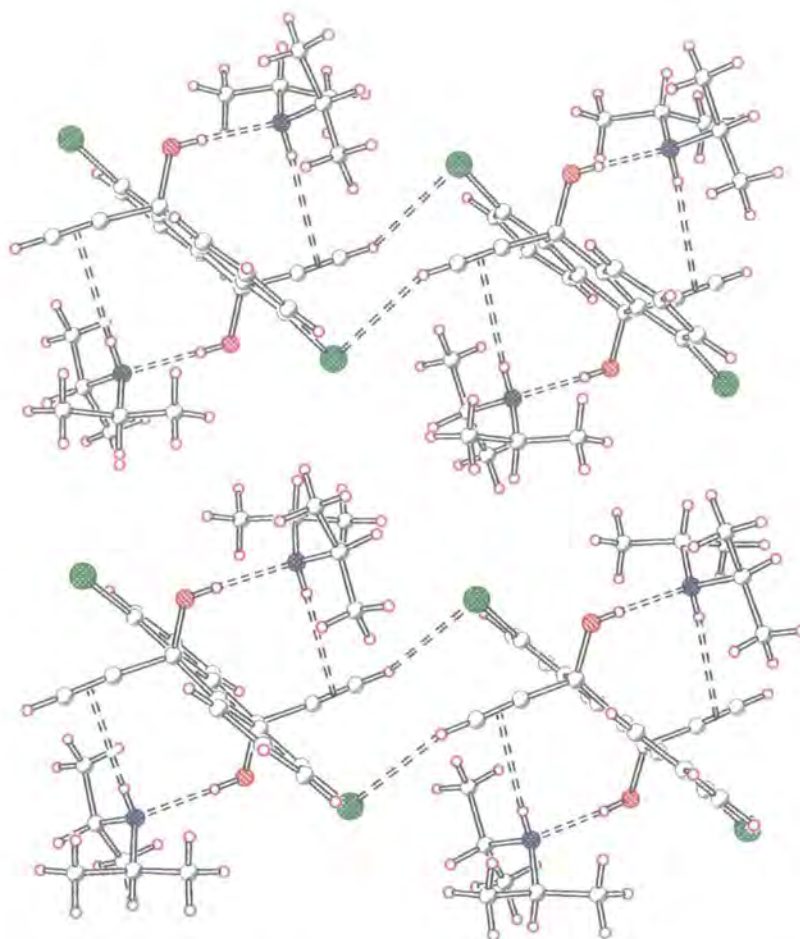


Figure 6.15. Crystal packing of **12** showing synthon I like interaction pattern. Note the the absence of the N-H...O bond.

6.8. General Discussion of secondary amine solvates:

Crystal structures from **8-12** are apparently simple but intriguing and deserve some more attention. Structural similarity and adoption of the same supramolecular synthon in the packing as seen in **5**, put the impetus on steric hindrance, but a closer inspection of all the structures could make it easy to rationalise these structures. We found for secondary amines, that most of them are in the staggered conformation and symmetrically extended on either side of the nitrogen in a (planar) zigzag fashion. The extension of the aliphatic portion of all those secondary amines seem to pack in a manner perpendicular with respect to the synthon plane and parallel with respect to the

Table 6.2. Crystallographic data and structure refinement parameters of 2° amine solvates.

	8	9	10	11	12
Empirical formula	C ₁₃ H ₁₆ ClNO	C ₃₀ H ₃₈ Cl ₂ N ₂ O ₂	C ₁₇ H ₂₄ ClNO	C ₂₁ H ₂₈ ClNO	C ₁₅ H ₂₀ ClNO
Formula wt.	237.72	529.52	293.82	345.89	265.77
Crystal System	Triclinic	Monoclinic	Triclinic	Triclinic	Triclinic
Space group	P-1	P2 ₁ /c	P-1	P-1	P-1
Temp (°K)	120	120	120	120	120
<i>a</i> [Å]	8.8625(4)	9.1953(2)	8.4193(4)	8.8402(2)	7.8515(2)
<i>b</i> [Å]	8.8881(5)	8.8721(2)	8.9984(4)	10.3480(2)	9.1728(3)
<i>c</i> [Å]	9.5190(5)	36.8624(9)	11.6634(5)	11.3207(2)	10.4275(3)
α [°]	109.609(2)	90	99.546(2)	90.198(1)	84.469(1)
β [°]	116.003(2)	91.6250(10)	109.882(2)	112.793(1)	73.486(1)
γ [°]	90.739(2)	90	90.202(2)	103.555(1)	79.571(1)
Z'	0.5	1.0	0.5	0.5	0.5
Volume [Å ³]	623.39(6)	3006.08(12)	817.73(6)	922.99(3)	707.31(4)
D _{calc} [g/cm ³]	1.266	1.170	1.193	1.245	1.248
μ [mm ⁻¹]	0.285	0.243	0.230	0.214	0.259
2 θ [°]	4.96 to 55	4.43 to 55	3.78 to 55	3.92 to 55	4.08 to 55
Range <i>h</i>	-11 to 11	-11 to 11	-10 to 9	-11 to 11	-10 to 10
Range <i>k</i>	-10 to 11	-11 to 11	-11 to 11	-13 to 13	-11 to 11
Range <i>l</i>	-12 to 12	-47 to 47	-15 to 15	-14 to 14	-13 to 13
Reflns. collected	7477	34671	9681	10985	8431
Unique reflns.	2862	6904	3749	4241	3247
Obs. reflns.	2634	3694	2451	3503	2920
<i>R</i> ₁ [<i>I</i> > 2 σ (<i>I</i>)]	0.0370	0.0666	0.0513	0.0361	0.0323
wR_2 [all]	0.0997	0.1793	0.1175	0.0936	0.0897
Goodness-of-fit	1.051	1.093	0.947	1.031	1.065
Crystal size mm ³	0.28 x 0.08 x 0.04	0.32 x 0.10 x 0.08	0.2 x 0.12 x 0.04	0.42 x 0.15 x 0.14	0.38 x 0.20 x 0.17
Largest diff. peak and hole (e.Å ⁻³)	0.341 and -0.259	0.824 and -0.604	0.378 and -0.229	0.341 and -0.241	0.309 and -0.268

aromatic portion of the gem-alkynols, resulting in the reduced effective steric requirement. On the other hand, a bulky diisopropyl amine, in a similar manner to the octylamine, shows puckered geometry rather than planar, resulting in a different synthon from **I** and **II**. This indicates a correlation between steric interference and a preference for certain synthons, with primary amines being more flexible than secondary amines. This flexibility leads to the preference for infinite chains, rather than the square synthon in most of the primary amines. All of these amine solvates again support the observation that the infinite chain is the key synthon in the supraminol system. Furthermore, the formation of the square motif took place when the steric hindrance around the supraminol system is quite high, but not so drastic so that it changes into synthon **III**. Nonetheless, we have to admit that we would be rather surprised if the β -As sheet type packing would have appeared in any of the cases described above. A fixed network like β -As sheet always demands a fixed geometry which will be too much of a demand for this series of flexible solvent molecules. It has been observed earlier that up to a certain limit, changes in the molecular structure may be carried out over a range of substituent groups without perturbing the crystal structure. But at the limit of a range, just a slight change in the molecular structure may change the whole crystal packing. In the present context, the change in steric hindrance in diisopropyl amine was enough to change the whole crystal packing and make it more gem-alkynol-like than supraminol-like.

6.9. Tertiary amine solvates:

Structural analyses from crystal structures with primary amines in **1-7**, and secondary amines in **7-12**, shows a clear correspondence between the crystal structure adopted and the number of amine hydrogen atoms. This inevitably shifts our attention towards the tertiary amines, which being devoid of any donor amine hydrogen atom, should neither

form any infinite chains nor any square motifs, and in effect will help us to validate the importance of amine hydrogen atom(s) towards crystal packing. Following the trend, tertiary amines with increasing steric bulk were used as solvents for the completeness of this study.

6.9.1. (EtMe₂N)₂. DDDA [13]

N,N,N-Ethyl dimethyl amine forms crystals with DDDA (**13**) with a structure that is directly analogous to that of **6**. Despite the fact that there is no donor amine hydrogen atom, in many respects, the crystal packing closely follow those of the primary amines

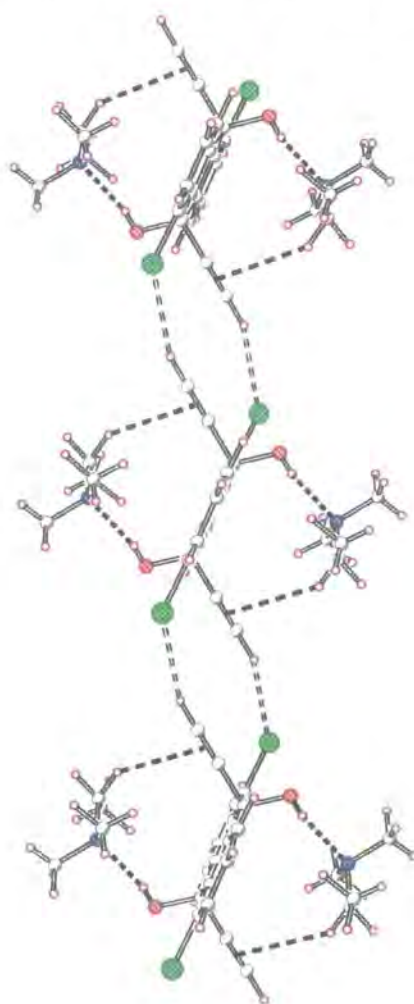


Figure 6.16. Crystal packing of **13** (N,N –dimethyl ethylamine), showing synthon **III** with interlinking C-H...Cl interaction

rather than secondary amines, with a 1:2 solute-solvent motif reappearing with strong O-H...N interactions. The orientations of the amine with respect to DDDA, closely resemble those of a primary amine, although the lack of any donor amine hydrogen atom rules out any infinite cooperative arrangement. Notwithstanding, one methylene hydrogen atom directed towards the ethylene group to form a C-H... π bond, results in synthon **III**. Interestingly this discrete hydrogen bonded unit propagates with familiar C-H...Cl bonds (Figure 6.16).

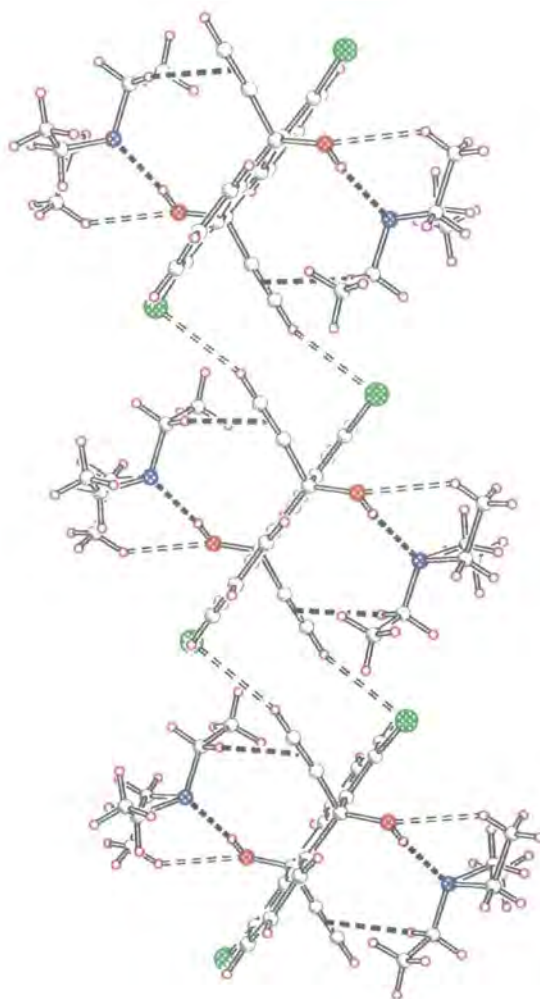


Figure 6.17. Crystal packing of **14** showing synthon **III** in bold lines while the C-H...Cl interaction are shown in light lines. Note the C-H...O interaction from the methyl group.

6.9.2. (Et₃N)₂. DDDA [14]:

The crystal structure of **14** is similar to that of **13** with one half molecule of DDDA and a half molecule of amine in the triclinic $P\bar{1}$ space group. Synthone **III** again plays a dominant role in the packing and as seen in the structure of **13**, discrete hydrogen bonded units propagate with familiar C-H...Cl bonds (Figure 6.17). It is interesting to note that in all synthons **III**, the donor hydrogen atom is a methylene hydrogen (from α -carbon atom) and not a methyl hydrogen. The only difference in packing is a strong C-H...O bond with one of the methyl hydrogen atoms.

6.9.3. (Me₂ Cycl)₂. DDDA [15]: There is one common trend in **14** and **15** that is, the donor hydrogen atom forming C-H... π bond attached to the α -C atom. By examining these two structures, the question arose as to whether this particular structural type

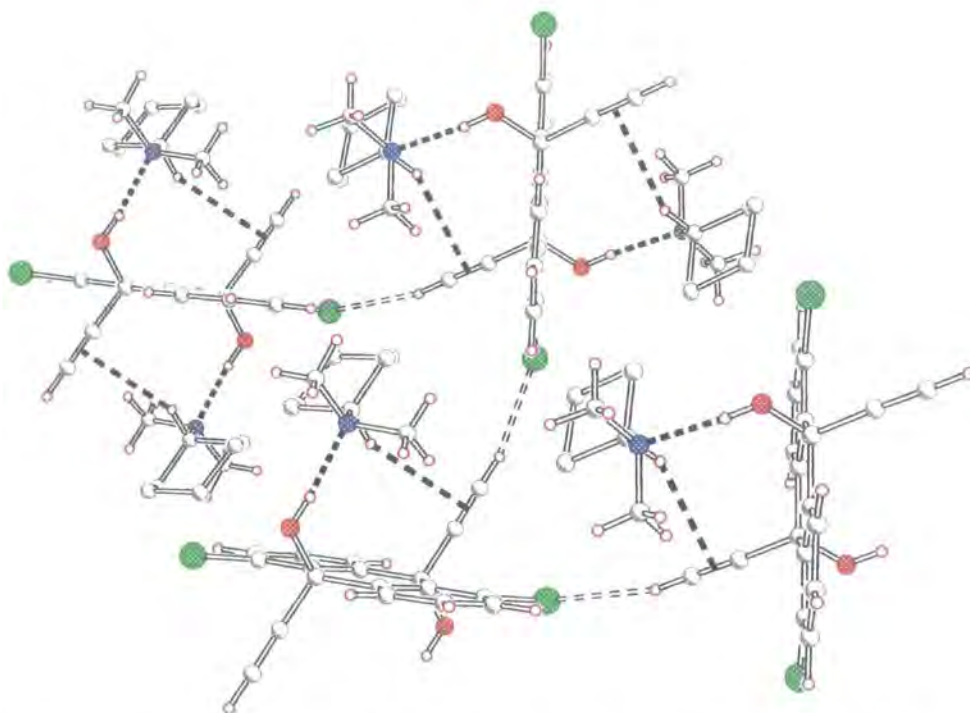


Figure 6.18. Crystal packing of **15** showing synthon **III** with C-H...Cl bond showing in light bonds.

could be reproduced with more complex tertiary amines. To study this question we crystallised DDDA with N,N-dimethylcyclohexylamine, which having two free methyl groups would be more probable to form C-H... π interactions than a rigid cyclohexyl ring. It was astonishing to see that, synthon **III** becomes the major interaction pattern, with a C-H... π interaction (Figure 6.18) formed by methylene hydrogen atom of cyclohexyl ring and not from methyl group.

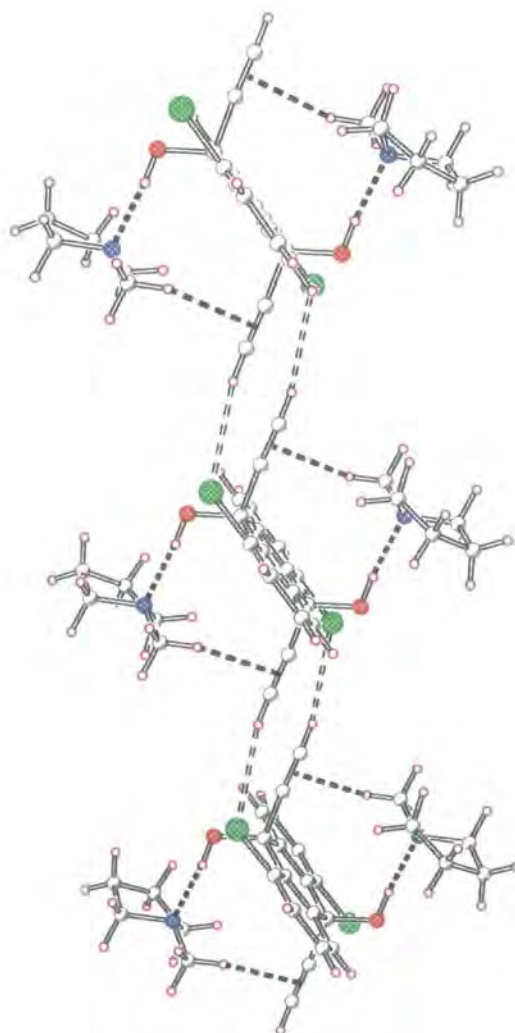


Figure 6.19. Crystal packing of **16** showing synthon **III** with C-H...Cl interaction.

6.9.4. (4-methyl-pyrrolidine)₂. DDDA [16] : In order to study the robustness of the synthon **III** DDDA was crystallized from 4-methyl pyrrolidine. Although 4-methyl-

pyrrolidine is not a tertiary amine, the molecule offers enough strain with the N atom being a part of the rigid ring. The interaction pattern of **16** is almost similar to those of the tertiary amine solvates, with synthon **III** playing the crucial role and the discrete units propagating with C-H...Cl interactions (Figure 6.19). However there is a strong influence of the rigid ring on the crystal structure. There are two competing hydrogen atoms for a C-H... π interaction, from both methyl hydrogen atom (2.83Å) and a methylene hydrogen atom (2.90Å).

6.10. General Discussion of tertiary amine solvates :

Crystal structures of **13-16** represent an interesting series, in which all the molecules crystallise with synthon **III** with supporting C-H...Cl interactions. All these solvates show that even a single strong solute-solvent O-H...N interaction is enough to stabilise a solvate. More steric demand for tertiary amines than secondary amines and topological similarities with primary amines suggests a correlation between number of 'active' amine hydrogen atoms participation and the corresponding synthon involved. Crystal packing of **6**, **7** and **14** is important in this respect. For the crystal structure of **14**, steric hindrance was the driving force for a secondary amine to adopt a crystal structure more like a primary amines. On the other hand, for the crystal structure of **7** rigidity of the cyclohexyl ring restrict the second amine hydrogen from bond formation, effectively turning a primary amine to a secondary amine with a square synthon. While in **6**, steric hindrance of octyl group was enough to restrict both the amine hydrogen atom from bond formation, and in effect turn it to a equivalent of tertiary amine, which could be further corroborated by the appearance of synthon **III** for **6**.

In a way, steric hindrance does control synthon formation somewhat indirectly by controlling the number of amine hydrogen atoms participating in strong bond formation with DDDA.

Table 6.3. Crystallographic data and structure refinement parameters of 3' amine solvates.

	13	14	15	16
Empirical formula	C ₂₆ H ₃₂ Cl ₂ N ₂ O ₂	C ₁₅ H ₂₀ ClON	C ₁₇ H ₂₂ ClNO	C ₁₄ H ₁₆ ClON
Formula wt.	475.44	265.77	291.81	249.73
Crystal System	Triclinic	Triclinic	Monoclinic	Orthorhombic
Space group	P-1	P-1	P2 ₁ /n	Pbca
a [Å]	9.9854(3)	7.8896(3)	7.9119(2)	9.9617(5)
b [Å]	10.2540(3)	9.0728(3)	17.7382(5)	13.7380(7)
c [Å]	12.7257(4)	11.4777(4)	11.1360(3)	18.884(1)
α [°]	88.2500(10)	79.135(1)	90	90
β [°]	72.4310(10)	70.273(1)	102.270(1)	90
γ [°]	87.2610(10)	71.331(1)	90	90
Z'	1.0	0.5	0.5	0.5
Volume [Å³]	1240.61(7)	729.69(4)	1527.16(7)	2584.3(2)
D_{calc} [g/cm³]	1.273	1.210	1.269	1.284
μ [mm⁻¹]	0.287	0.251	0.246	0.279
2θ [°]	4.57 to 55	3.78 to 55	4.39 to 55	5.5 to 55
Range h	-12 to 12	-10 to 10	-10 to 10	-12 to 12
Range k	-13 to 13	-11 to 11	-23 to 23	-17 to 17
Range l	-16 to 16	-14 to 14	-14 to 14	-24 to 24
Reflns. collected	16897	8469	20485	28924
Unique reflns.	4873	3326	3520	2960
Obs. reflns.	4949	2793	3145	2749
R₁ [I > 2σ(I)]	0.488	0.0661	0.0303	0.0391
wR₂ [all]	0.1265	0.1692	0.0825	0.1033
Goodness-of-fit	1.119	1.038	1.042	1.045
Crystal size mm³	0.30 x 0.18 x 0.08	0.36 x 0.16 x 0.12	0.28 x 0.22 x 0.16	0.36 x 0.34 x 0.22
Largest diff. peak and hole (e.Å⁻³)	0.847 and -0.348	0.495 and -0.469	0.392 and -0.215	0.504 and -0.341

6.11. Conclusion:

The background of this work laid for the quest for better hydrogen bonding by solvation using good hydrogen bond accepting solvents^{7,12}. However, this particular series vindicate our strategy of using amine not as a solvent but as an essential 'component' molecule for the competitive study among amine, hydroxyl and ethynyl groups; as if they are forming molecular complexes. Principally there is not much difference of usage of amines here than those are used for molecular complexes in supraminols⁸, wherein, as a part of a strategy, we vary one component while keeping the other fixed.

In the present case, introduction of any new functional group to the already crowded gem-alkynol moiety would create enough interaction interference for a molecule to crystallize in a predictable manner. In this background, DDDA with less than optimum hydrogen bond, provides us with a unique opportunity to overcome this problem, by pumping amines in form of solvent into crystal structures just like phenols are cocrystallizes with amines in solid state for molecular complexes. We feel a good level of understanding has now been obtained for these solvates, although molecular complexes might be a better term for these multicomponent systems. We have been able to identify three major synthons that would be helpful for prediction of structural motifs of these kinds of systems. We were successful to quantify the importance of amine hydrogen atoms. There was a clear correlation between the number of amine hydrogen atoms present (or type of amine used) and the supramolecular synthon involved, accordingly we can always term synthon I, II and III as primary, secondary and tertiary synthons. Interestingly, the exceptions of these trends do show the importance of steric hindrance and structural interferences on crystal packing. For instance, ring strain and consequently structural interferences in 4 and 5 did change the crystal packing from typical supraminol packing to that of the characteristic gem-alkynol family. These

results further help us to understand that what structure would then be obtained when the β -As sheet is disrupted by a sterically bulky group.

It has been noted earlier that the terms like solvates, pseudopolymorph, donor-acceptor complex, molecular complex is a subjective matter¹³. As remarked earlier, "*problems with nomenclature are necessary evils in the development of a new subject*"; in early days of a subject, enthusiasm and inability of old terms to describe new concepts make it easier to coin new names. However, *What is easy is sometimes not what is best*¹⁴. The definition of pseudopolymorph falls far short of being unambiguous¹⁵. In the present case, molecular complex might be more aptly chosen term though all the amines used were in liquid state.

6.12. References:

- (1) Some of the recent references on host-guest materials: (a) F. Toda, H. Miyamoto, M. Inoue, S. Yasaka, I. Matijasic, *J. Org. Chem.*, 2000, **65**, 2728-2732. (b) E. Weber, T. Hens, T. Brehmer, I. Csöreg, *J. Chem. Soc., Perkin Trans. 2*, 2000, 235-241. (c) R. K. R. Jetti, F. Xue, T. C. W. Mak, A. Nangia, *J. Chem. Soc., Perkin Trans. 2*, 2000, 1223-1232. (d) K. Kobayashi, T. Shirasaka, A. Sato, E. Horn, N. Furukawa, *Angew. Chem., Int. Ed.*, 1999, **38**, 3483-3486. (e) L. R. MacGillivray, J. L. Atwood, *Angew. Chem., Int. Ed.*, 1999, **38**, 1018-1033. (f) S. S.-Y. Chui, S. M.-F. Lo, J. P. H. Charmant, A. G. Orpen, I. D. Williams, *Science*, 1999, **283**, 1148-1150. (g) M. R. Caira, L. R. Nassimbeni, F. Toda, D. Vujovic, *J. Chem. Soc., Perkin Trans. 2*, 1999, 2681-2684. (h) O. M. Yaghi, H. Li, C. Davis, D. Richardson, T. L. Groy, *Acc. Chem. Res.*, 1998, **31**, 474-484. (i) J. A. Swift, A. M. Pivovar, A. M. Reynolds, M. D. Ward, *J. Am. Chem. Soc.*, 1998, **120**, 5887-5894. (j) K. Endo, T. Ezuhara, M. Koyanagi, H. Masuda, Y. Aoyama, *J. Am. Chem. Soc.*, 1997, **119**, 499-505.
- (2) (a) S. R. Byrn, *Solid-State Chemistry of Drugs*; Academic: New York, 1982. (b) J. Bernstein, *Polymorphism in Molecular Crystals*; Clarendon: Oxford, 2002. (c) V. S. S. Kumar, S. S. Kuduva, G. R. Desiraju, *J. Chem. Soc., Perkin Trans. 2*, 1999, 1069-1074. (d) W. C. McCrone, *Physics and Chemistry of the Organic Solid State*, Vol. 2, Eds. D. Fox, M. M. Labes, A. Weissberger, Wiley Interscience, New York, 1965. (e) L.R. Nassimbeni, *Acc. Chem. Res.*, 2003, **36**, 631-637. (f) J. A. R. P. Sarma, G. R. Desiraju, *Polymorphism and Pseudopolymorphism in Organic Crystals: A Cambridge Structural Database Study*; In *Crystal Engineering*; Eds. Seddon, K. R., Zaworotko, M., Kluwer: Norwell, MA, 1999; pp 325-356. (g) J. Bernstein, *Polymorphism in Molecular Crystals*; Clarendon; Oxford, 2002.
- (3) E. Weber, *In inclusion compounds*; J.L. Atwood, J.E.D. Davis, D.D. Macnicol, Eds; Oxford University Press, Oxford, 1991, Vol. 4, pp. 188-263.

- (4) (a) R. Bishop, *Synlett*, 1999,1351-1358. (b) R. Thaimattam, F. Xue, J. A. R. P. Sarma, T. C. W. Mak, G. R. Desiraju, *J. Am. Chem. Soc.*, 2001, **123**, 4432-4445.
- (5) A. Nangia, G.R. Desiraju, *Chem. Comm.*, 1999, 605-606, (b) H. Gorrbitz, P. Hersleth, *Acta. Cryst.*, 2000, **B56**, 526-534.
- (6)(a) G. R. Desiraju, in '*Simulating Concepts in Chemistry*', Eds. S. Shibaski, S. Stoddart, F. Vögtle, Wiley, Chichester, 2000, pp.293. (b) A. Anthony, G. R. Desiraju, *Supramol. Chem.*, 2001, **13**, 11-23.
- (7) (a) R. Banerjee, G. R. Desiraju, R. Mondal, A.S. Batsanov, C. K. Broder, J. A. K. Howard, *Helv. Chim. Acta.*, 2003, **86**, 1339-1351. (b) R. Banerjee, G. R. Desiraju, R. Mondal, J. A. K. Howard, *Chem. Eur. J.*, 2004, **10**, 3373-3383.
- (8) Selected references on supraminol: (a) F. H. Allen, V. J. Hoy, J. A. K. Howard, V. R. Thalladi, G. R. Desiraju, C.C. Wilson, G. J. McIntyre, *J. Am. Chem. Soc.*, 1997, **119**, 3477-3480. (b) V. R. Vangala, B. R. Bhogala, A. Dey, G. R. , Desiraju, C. K. Broder, P. S. Smith, R. Mondal, J. A. K. Howard, C.C. Wilson, *J. Am. Chem. Soc.*, 2003, **125**, 14495-14509. (c) O. Ermer, A. Eling, *J. Chem. Soc., Perkin Trans.*, 2, 1994, 925-944. (d) S. Hanessian, A. Gomtsyan, M. Simard, S. Roelens, *J. Am. Chem. Soc.*, 1994, **116**, 4495-4496, (e) S. Hanessian, M. Simard, S. Roelens, *J. Am. Chem. Soc.*, 1995, **117**, 7630-7645. (f) S. Hanessian, R. Saladino, R. Margarita, M. Simard, *Chem. Eur. J.*, 199, **5**, 2169. (g) S. Hanessian, R. Saladino, in *Crystal Design, Structure and Function, Perspective in Supramolecular Chemistry*, Ed. G. R. Desiraju, Wiley, New York, 2003, 7, 77.
- (9) Work on Gem-Alkynol (a) N. N. L. Madhavi, C. Bilton, J. A. K. Howard, F.H. Allen, A. Nangia, G. R. Desiraju, *New J. Chem.*; 2000, **24**, 1-4. (b) N. N. L. Madhavi, G. R. Desiraju, C. Bilton, J. A. K. Howard, F. H. Allen, *Acta. Cryst.*, 2000, **B56**, 1063-1070. (c) C. Bilton, J. A. K. Howard, N. N. L. Madhavi, F. H. Allen, C. C. Wilson,

- Chem. Comm.* 1999, 1675-1676. (d) C. Bilton, J. A. K. Howard, N. N. L. Madhavi, A. Nangia, G.R. Desiraju, F. H. Allen, C. C. Wilson, *Acta. Cryst.*, 2000, **B56**, 1071-1079
- (10) (a) F. H. Allen, O. Kennard, *Chem.Des.Autom.News.*, 1993, **8**, 30-37, (b) F. H. Allen, *Acta. Cryst.*, 2002, **B58**, 380-388.
- (11) C-H...halogen interactions have been the topic of recent papers: (a) P. K. Thallapally, A. Nangia, *CrystEngComm.*, 2001, **27**, 1-6; (b) L. Brammer, E. A. Bruton, P. Sherwood, *Cryst. Growth Des.*, 2001, **1**, 277-290; c) F. Neve, A. Crispini, *Cryst. Growth Des.*, 2001, **1**, 387-393; d) S. L. James, G. Verspui, A. L. Spek, G. van Koten, *Chem. Comm.*, 1996, 1309-1310; e) C. B. Aakeröy, T. A. Evans, K. R. Seddon, I. Pálinkó; *New J. Chem.*, 1999, **23**, 145-152; f) G. Aullón, D. Bellamy, L. Brammer, E. A. Bruton, G. A. Orpen, *Chem. Comm.*, 1998, 653-654.
- (12) R. Mondal, J. A. K. Howard, R. Banerjee, G. R. Desiraju, *Chem. Comm.*, 2004, 644-645
- (13) Jetti, R.K.R.; Boese, R.; Thallapally, P.; Desiraju, G.R.; *Cryst. Growth and Des.*, 2003, **3**(6), 1033-1040.
- (14) Desiraju, G.R.; *CrystEngComm.*, 2003, **5** (28) 466-467.
- (15) (a) Threlfall, T. L. *Analyst*, 1995, **120**, 2435-2460. (b) McCrone, W.C., in *Physics and Chemistry of the Organic Solid State*, Vol. 2, Ed. Fox, D.; Labes, M.M.; Weissberger, A.; Wiley Interscience, New York, 1965. (c) *Comprehensive Supramolecular Chemistry*, Eds. MacNicol, D. D.; Toda, F.; Bishop, R.; Pergamon, Oxford, 1996, vol. 6.

Chapter 7

**A Systematic Study of the Coordination Geometry of Three-
Coordinate Metal Complexes**

7.1 Introduction

In this chapter, a detailed systematic study was carried out using the Cambridge Structural Database (CSD)¹ on (a) the coordination sphere geometry of three-coordinated metal complexes and (b) the reaction pathway for their generation from two-coordinate species respectively. The major objective of this study includes a symmetry-modified principal component analysis (PCA) in order to visualise the geometrical distortion of three-coordinate metal centres and to interpret the transition from T-shaped geometries to the trigonal planar form in terms of a reaction pathway for a ligand addition to linear two coordinate species.

With the invention of CCD detector and direct method for structure determination, single crystal X-ray diffraction analysis became the quickest and most reliable method for structure determination. However, one of the most paradoxical shortcomings of the X-ray diffraction techniques is that the information obtained is by and large a static view of the molecules rather than a dynamic one. Even with all the advancements in software technology and sophisticated instruments, it is not fully possible to observe directly the changes at the molecular level during the course of a chemical reaction². Usually the geometric characteristics of a reaction are inferred from the dynamic NMR or kinetic studies or from the volume of activation measurements; sometimes theoretical studies and computational methods are used, yet, they often failed to provide a quantum chemical solution for real systems³.

Several scientists addressed this difficulty and tried to develop new methodologies for the 'direct visualisation' of molecules at dynamic stage, studies with *ab initio* methods are noteworthy here. The structure correlation method is among the most successful methods and is used in the present work. The principle of structure correlation has been stated by Bürgi as: "*Although direct observation of a chemical molecule along a given reaction coordinate does not seem feasible, its visualisation at least does*". The

structure correlation hypothesis assumes that, if we have a molecular fragment existing in a large variety of crystalline environments, then its geometrical change along a reaction coordinate is manifested in gradual distortion or static deformation by the crystalline environments. The various crystals or molecular structures are considered to constitute a series of 'frozen in' points or 'snap shots', taken along the reaction pathway, which, when viewed in the correct order, yield a cinematic film of the reaction⁴.

Crystalline structures represent a stable atomic arrangement, so they appear close to energy minima in the Born-Oppenheimer potential energy surface. Therefore from the structure correlation hypothesis we can say that, if there is any correlation between two or more independent parameter describing the structure of a fragment in a variety of environments, then the correlation function maps a minimum energy path in the corresponding parameter space⁴.

The prime aim of structure correlation⁵ studies involves searching for correlation (similarities) between the suitable crystal or molecular datasets that are closely related to the fragment of interest.

Classical work on structural correlation studies include some of the earliest work of auf der Heyde and Bürgi in the field of systematic study of the molecular geometry of five coordinate complexes with d^8 configuration^{4e-g}. In this pioneering work they exhaustively studied the conformation, archetypal geometries, static deformations and for the first time mapping of reaction coordinates using methodologies like cluster analysis and structure correlation. The formations of five coordinate intermediates were postulated for many ligand exchange reactions of square-planar molecules. From the database study, Bürgi was able to draw the correlation between the axial distance increment and out of plane displacement for cadmium complexes, which could be interpreted in terms of an S_N2 distortion coordinate^{4,5,6}.

The number of crystal structures in the CSD since then has increased very significantly and the database now holds over 320,000 crystal structures. Interestingly, among these crystal structures ~50% are organometallic or metal complex structures. This certainly represents an enormous store of information of coordination, organometallic and main group element chemistry.

However, except for a few devotees, the primary research interest of the CSD has primarily been directed at the other half the structures, namely, for organic chemists and biologists. Until recently, for inorganic chemists the CSD has often represented a secondary indirect tool for locating the experimental data from prior examples, often using a known crystallographer or a CSD-user as an intermediary.

In a series of papers, Orpen investigated different applications of the CSD to molecular inorganic chemistry ranging from metal-ligand bonding, conformation analysis, to such diverse topics as the correlation of crystal packing with the standard deviation of different crystallographic parameters⁷. In an interesting study, Orpen and co-workers analysed the conformation of fused ring chelate complexes and their interconversion pathways using principle component analysis of the intra-ring torsion angles⁸. Alvarez and Avnir further extended the quest by seeking the interconversion pathway for tetra coordinate bis(chelate) metal complexes⁹.

Usage of principal component analysis becomes more and more frequent for the description of metal coordination sphere and Allen has been one of the major promoters of the CSD to the inorganic chemist¹⁰. A detailed systematic study of the metal coordination polyhedra ML_n by Allen and co workers is directly related to this work. In that paper they outlined the general methods for the description of archetypal geometries for ML_n systems, especially for ML_4 and ML_7 systems, wherein principal component analysis proved to be highly useful tool¹¹.

Four coordinate metal complexes, because of their two well-defined, square planar and tetrahedral archetypal geometries, are the natural choices for coordination chemists. This is coupled with the huge abundance of four-coordinate metal complexes and their unique relationship with d-electron configuration which makes it a highly interesting field of research. However there is hardly any attempt to correlate the observed stereochemistries using statistical or numerical methods. Recent studies of Allen and co-workers clearly demonstrate the influence of oxidation state on geometries of four-coordinated Cu complexes. Symmetry deformation coordinate (SDC) analysis shows the advantage of using numerical methods with a clear visualisation of Cu(I) complexes adopting a tetrahedral coordination geometry whereas Cu(II) forms square planar complexes. It was relatively much easier to understand/identify the geometrical as well as electronic factors that cause the deviation from the idealised geometries, e.g., while chelating ligands bolster the formation of square-planar geometry, presence of these kind of ligands is the main reason for deviations from tetrahedral geometry¹².

In comparison, the systematic study of three coordinated species is less common¹³. The current work concentrates on the description of the molecular coordination geometry of the three coordinate molecules, and processes involved in changing this geometry, using principal component analysis. Detailed study of four coordinate metal complexes and their transformation from three coordinate species is beyond the scope of this chapter and will be reported at some point later.

7.2. Geometry of three-coordinate species

Three coordinate transition metal complexes with non d^{10} configurations are rare. So much so that in a comprehensive review on coordination numbers and stereochemistry of coordination compounds, three coordination complexes were not considered^{14a}. Three coordinated transition metal complexes occur mainly for elements Cu, Ag, Au, Zn and

Hg. The 16-electron rule for trigonal planar structures is believed to accounts for the stability for the d^{10} electron configurations, especially for Hg (II), Cu (I) and Ag (I), and is well documented¹⁴.

The archetypal three-coordinate geometries are predominantly trigonal planar (D_{3h}) and trigonal pyramidal (C_{3v}) with the former dominant. However these are rather idealised geometries and there exists an angular distortion from the ideal D_{3h} symmetry to two different geometries, namely, 'Y-shaped' and 'T-shaped'¹⁵. The D_{3h} point group is the highest possible symmetry for ML_3 structures, and for symmetry deformation coordinate (SDC) methodologies it is considered as the reference geometry and any observed deformations are calculated from this geometry. In theory, deviation away

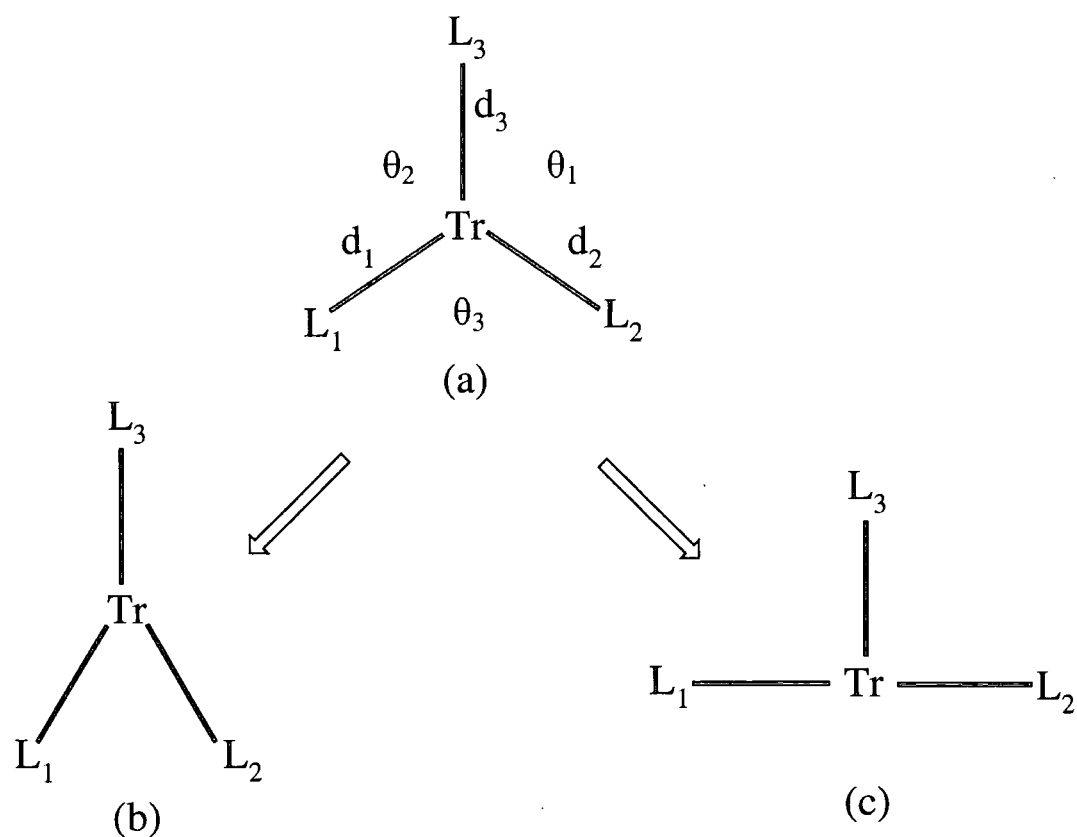


Figure 7.1 (a). Trigonal planar D_{3h} coordination geometry, and the bond lengths (d_n and θ_n) angles parameters used in this analysis. (b) Y-shaped deformation from D_{3h} symmetry. (c) T-shaped deformation from D_{3h} symmetry.

from this idealised geometry can be analysed in terms of either valance angles or bond distances. However, in reality, bond distances can only be used when the two bonded atoms are known and their respective covalent radii are accounted for in the analysis.

This is certainly not easy and an impractical task for the analysis of metal coordinate centres from a couple of hundreds of crystal structures. Therefore, the distortions away from the reference structures of three coordinate fragments for this work will be reported in terms of the deformation of angles from the reference structure.

Deformation of the D_{3h} structure can take place in two distinct paths: (i) the concerted increase of two of the basal angles from 120° ($\theta_2, \theta_3 \rightarrow ca. 150^\circ$) and consequent reduction of the third angle ($\theta_1 \rightarrow ca. 60^\circ$) to form a Y-shaped structure, and (ii) the concerted decrease of the two angles ($\theta_2, \theta_3 \rightarrow 90^\circ$) and subsequent increase in the third ($\theta_1 \rightarrow 180^\circ$) which leads to a T-shaped form (**Figure 7.1**). The ideal set of three basal angles for D_{3h} symmetry would be $120^\circ, 120^\circ, 120^\circ$ and with the metal atom perfectly coplanar with the three ligand atoms, for the Y-shaped molecule the set of angles would be $150^\circ, 150^\circ, 60^\circ$ whereas for the T-shaped the ideal situation would be $180^\circ, 90^\circ$ and 90° . However, in reality, it is difficult to pin-point the exact values and more convenient to adopt a range of angles.

7.3. PRINCIPAL COMPONENT ANALYSIS (PCA)

Symmetry modified principle component analysis¹⁶ has been used in this work for the visualisation of the geometrical distortion of N_f examples of three coordinated metal centres. This section will highlight the qualitative derivation and importance of PCA. The major objective of PCA is to derive a set of uncorrelated variables, or principal components, from a set of N_p correlated variables. The principal components are derived by taking the linear combination of the original variables in N_p dimensional space in decreasing importance. That is, the first component attempts to account for the majority

of the variance found in the original data and the successive components are derived until all of the variance in the original set of data is accounted for.

Detail quantitative derivation and analysis of the principal components from the original variables using eigenanalysis is described fully by Chatfield and Collins¹⁷. We will, herein, emphasize the simple working formula and interpretation of the methodology. The first component is derived in N_p dimensional space as a vector in such a way that the sum of the squares of the displacement of the $(N_p \times N_f)$ points of the vector is minimised in N_p dimensional space. This will satisfy the condition that the first component accounts for the maximum amount of the variance in the datasets as a whole. Since principal components are uncorrelated, they are mutually orthogonal.

Therefore the second component must be orthogonal to the first one, and derived similar to the first PC, with minimised sum of square of displacement from it to each of the $(N_p \times N_f)$ points. Subsequently the other PCs are derived until the original variance (N_p parameter space) is accounted for.

The principal component analysis technique performs an eigen-analysis on either the covariance or correlation matrix, with the generated components being the eigenvectors of these matrices. For original variables in the form $[x_i (i=1, 2, \dots, N_p)]$ the principal components are found to be linear combinations that satisfy:

$$(PC)_j = a_{1j}x_1 + a_{2j}x_2 + a_{3j}x_3 + \dots + a_{N_pj}x_{N_p}$$

The coefficients a_{ij} determine the relative contribution from each of the original variables to the derived $(PC)_j$ and are known as PC loadings. While the eigenvalues of the matrix $1_j (j=1, 2, \dots, N_p)$ represent the proportion of the total variance in the original dataset accounted for by each PC, and the PC “scores” that are generated are the coordinates of the original fragment that are relocated in the N_c -dimensional PC-space.

It is these scores that are plotted against one another to generate some of the scatterplots that will be seen to be significant visual aids in the interpretation of each dataset.

There are three major advantages of using PCA:

7.3.1. Dimension Reduction. From the linear combination N_p number of original variables may give rise to N_p number of PCs. However, if the analysis of an N_p dimensional problem can generate N_n principle component (where $N_n < N_p$) which account for *ca* >95% of the variance in the original data, then it is much more convenient to address the problem with this fewer number of new variables. In this way PCA reduces the dimensionality of the problem. A simple example will put this into perspective, e.g., for a tetra-coordinated metal complex, a set of six angles or six correlated variables are required for a complete description of the geometry at the metal centre. However, if two PCs can account for the vast majority (>95%) of the variance, then it would be much more convenient and logical to use this two new (uncorrelated) components to describe the geometry instead of the six original variables (angles).

7.3.2. Better Visualisation of Results: PCA not only help to reduce the dimensionality it can also assist significantly the visualisation of result, which might have been quite difficult to discern from the original dataset. It is important to remember here that the PCs are derived by a mathematical technique and that they are uncorrelated, so often the PCs do not carry any direct interpretable chemical meaning or they do not represent any chemical parameters. However subsequent analysis of PCs often turned out to be highly informative in terms of pattern recognition. When two components are plotted against one another the resulting scattergram may show definite signs of data agglomeration, or clustering, in that 2-dimensional representation, that would not have been visible by taking any two of the original parameters and plotting them. For example, for tetra-coordinate metal complexes two distinct types of clustering make it much easier to recognise and differentiate the square planar geometry from the tetrahedral examples,

which would have been much more difficult to achieved from a set of original valence angles for a series of structures.

7.3.3. Correlation With Chemical Parameters: Principal components are mutually orthogonal so the correlation between any two is always zero, and as such PCs may not have any chemical meaning. However it is a normal practice to correlate PCs with other parameters generated in other ways (e.g. the symmetry deformation coordinates). These results are potentially very useful in assessing the chemical meaning of the PC's, as we will see for the present work in the result and discussion part.

7.4. Symmetry Deformation Coordinates (SDCs)

In this analysis, each molecular fragment is treated as a distorted version of the reference D_{3h} configuration. Murray-Rust, Burgi and Dunitz¹⁸ put forward this approach to analysing the systematic geometrical data and further developed the idea in 1978-1979.

In this methodology, the structure with the highest possible symmetry is considered as the reference structure. Any observed structure is then described in terms of symmetry deformation coordinates as being a distorted version of this reference structure. SDCs are calculated and described in terms of several components each of which retain some of the symmetry elements of the reference structure. Any displacement along a given SDC, which can be transformed as a particular irreducible representation (IR) preserves at least a certain part of the symmetry, known as Kernel symmetry of the IR in question. These kernel symmetries can be derived from group tables.

For the three coordinated metal complexes the highest possible symmetry is D_{3h} , that is a trigonal planar structure. And corresponding SDCs can be derived from the D_{3h} reference structure with the help of 12 different Cartesian displacement vectors as

shown in Figure 7.2. Derivation of SDCs from the reference structure can be followed in books on group theory¹⁹, and the detailed derivation from the D_{3h} reference structure is shown in the appendix A. The SDCs for D_{3h} symmetry are

$$\text{SDC1 } S_{4a}(E') : 1/\sqrt{6}\{2\theta_1 - \theta_2 - \theta_3\} \quad \text{PC1} : 0.816 \theta_1 - 0.408 \theta_2 - 0.408 \theta_3$$

$$\text{SDC2 } S_{4b}(E') : 1/\sqrt{2}\{\theta_2 - \theta_3\} \quad \text{PC2} : 0.707 \theta_2 - 0.707 \theta_3$$

$$\text{SDC3 } S_5(A_2'') : 1/\sqrt{3}\{\theta_1 + \theta_2 + \theta_3\} \quad \text{PC3} : 0.577 \theta_1 + 0.577 \theta_2 + 0.577 \theta_3$$

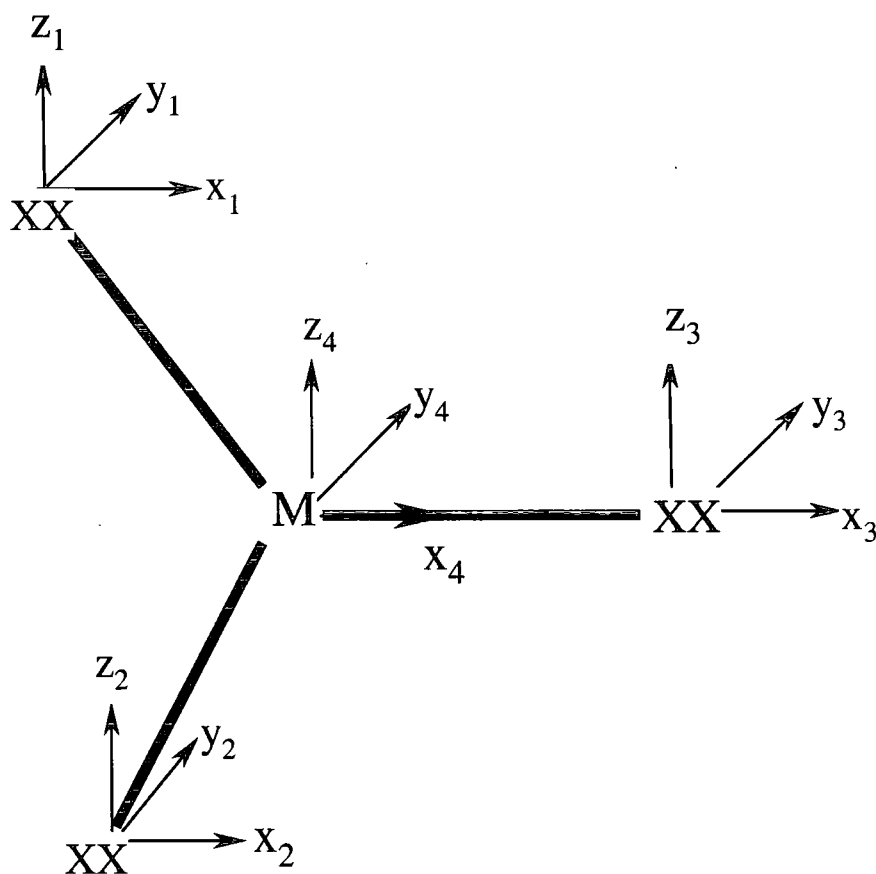


Figure.7.2. The $3N=12$ Cartesian displacement vectors for the D_{3h} trigonal planar reference structure.

7.5. Symmetry Considerations

Symmetry of the PCA plots is ensured by a permutation process to expand the set of points over the hyperdimensional parameter space. A crude knowledge of the algorithm for the normal search in CSD would be helpful for simplification of the symmetry problem. The normal search in CSD, atom-by-atom, bond-by-bond, attempts to find mappings of the query fragment to atoms present in each 'target' CSD molecule. For example if the target molecule is $\text{Hg}(\text{N})(\text{O})(\text{F})$, the search might find the first hit as $L_1 \rightarrow \text{N}$, $L_2 \rightarrow \text{O}$, $L_3 \rightarrow \text{F}$, and finally $M \rightarrow \text{Hg}$. The algorithm for substructure search in QUEST3D developed in such a way that it will also find five other additional (equivalent) matches, which are basically other permutational isomers ($L_1 \rightarrow \text{O}$, $L_2 \rightarrow \text{F}$, $L_3 \rightarrow \text{N}$; $L_1 \rightarrow \text{F}$, $L_2 \rightarrow \text{N}$, $L_3 \rightarrow \text{O}$; etc). For a three-coordinated metal complex there would

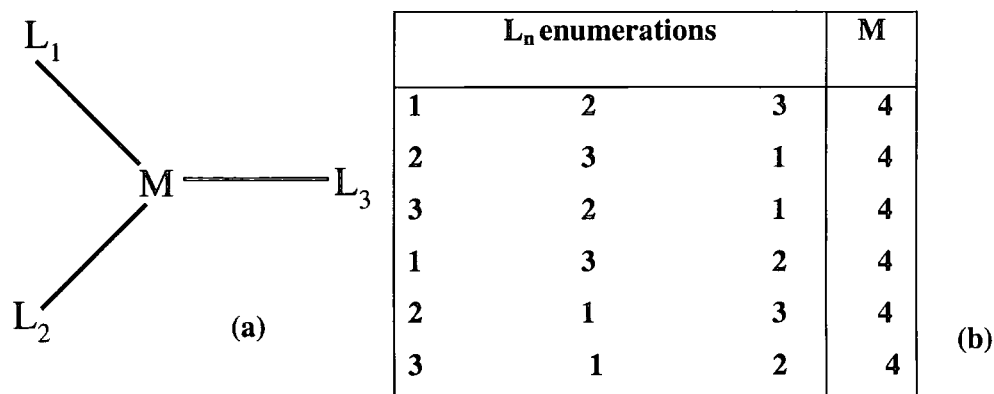


Figure 7.3. (a) One possible labelling scheme, together with the necessary permutations of these labels (b) that are required to describe fully the configurational space.

be six possible hits involving same four atoms. Because the substructure of Figure 7.3 (a) (or 1(a)) is topologically symmetric, it is not possible for the CSD search software to superimpose these six sub structural query on to successive CSD structures by a unique atomic enumeration. It is not possible, for example, to ensure that the search result always have atom 1 opposite to the largest θ angle, atom 2 opposite to the next largest,

and atom 3 opposite to the smallest angle. If it were possible, such an action would cause the software to generate θ_1 , θ_2 , θ_3 such that they fall within a single asymmetric unit of valence angle space. To avoid this difficulty we have used the 'permute' function in Quest3D, this will include geometric data for all permutational isomers of each substructure in the resulting data matrix. As result, valence angle space will be filled completely.

The present work²⁰ will be presented via two different sets of results. In the first part of the analysis we investigate the coordination geometry of all three-coordinate species TrL_3 , where Tr is any transition element and L is a ligand connecting to Tr via bonds to the elements C, N, O, F, Cl, Br, I, Si, As, Te, S, P and Se. In the second part, we examine the geometrical distortions of some individual three coordinated species, with $\text{Tr} = \text{Cu, Ag, Au, Hg and Zn}$.

7.6. Database search and retrieval mechanism

We have used Cambridge Structural Database¹ (Version 5.24, November, 2002 release containing 272,066 entries) for this study. Quest3D²¹ has been used for searches and geometrical data retrieval while Vista²² Version 1.2 and Mercury²³ Version 1.1 were used for data analysis and structure visualisation, respectively. The substructure fragment considered for this search consisted of a metal atom (Cu, Ag, Au, Zn and Hg) connected by single bonds to exactly three ligand atoms. Symmetry expansion was used to include all topological variants in the output datasets, and total coordination number of the metal is specified to be three. For the analysis of geometric distortion, intraligand valence angles θ_1 , θ_2 , θ_3 are calculated for each substructure along with bond distances d_1 , d_2 , d_3 as indicted in Figure 7.1(a). For each substructure we also calculated the out-of-plane displacement of the metal atom from the plane of the three ligating atoms. For each substructure the covalent radii (standard covalent radii stored in the CSD) of the

metal as well as each of the ligating atoms were also included in the table of retrieved data.

The search was further constrained by secondary search, which required, (1) atomic coordinates available, (2) no residual errors following CSD check procedures, (3) no reported disorder in the structure, (4) not polymeric (catena) structures (5) only 'organometallic' compounds according to CSD definitions. Various R-factor criteria were introduced based on different conditions and will be discussed later.

7.7. Results and Discussion:

Statistics of Three-Coordination: We start our initial search of the CSD by locating all TrL_3 species, without any restriction of R-factor. Results are shown in Table 7.1, in terms of N_{ent} , the number of CSD entries located, and N_{frag} , the number of unique TrL_3 substructure located within those entries. A total of 1076 three coordinate metal complexes were found in the CSD; about half of the entries (48%) are copper complexes, while 90% of three coordinate species are accounted for by five elements Cu, Ag, Hg, Zn and Au. The remaining 10% comprise complexes of a further 17 elements. (Table 7.1) The overwhelming majority of the complexes of the five most frequent transition metals arise most probably because of their d^{10} electronic configuration¹⁴. The 16-electron rule for trigonal planar systems is believed to be the prime reason for extra stabilisation of a d^{10} electronic configuration, especially for Hg(II), Cu(I) and Ag(I). It is important to note here that the classification according to oxidation state is only possible in Quest3D if the author specified the oxidation state of the metal in the corresponding published paper²⁴.

Table 7.1. Statistics of TrL₃ substructures in crystal structures recorded in the CSD, N_{ent} is the number of CSD entries, N_{frag} is the number of discrete substructures in those entries.

Tr -Element	N_{ent}	N_{frag}	% Total N_{frag}
Cu	453	793	48.0
Ag	216	297	18.0
Hg	148	204	12.3
Zn	80	109	6.6
Au	60	80	4.8
Fe	29	48	2.9
Mn	20	31	1.9
Pt	13	15	0.9
Cd	12	20	1.2
Ni	12	15	0.9
Others	33	40	2.4
Totals	1076	1652	100.0

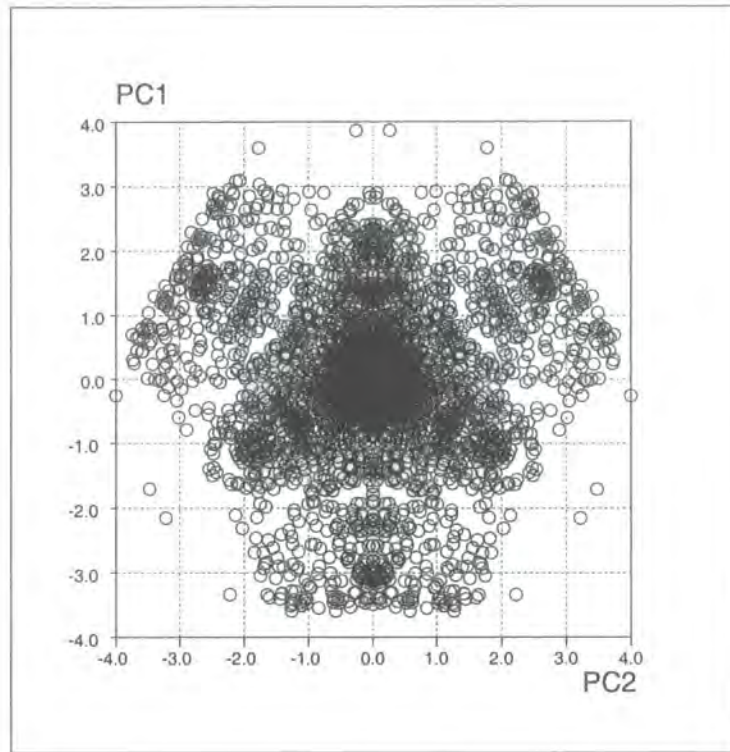
7.7.1. PCA results-All TrL₃ species: A new search was carried out using the same criteria as for the previous search except adding a new constraint, accepting hits only when the R-factor was less than 0.07. This yielded 1032 TrL₃ substructures from 611 CSD entries, which subsequently produce 6192 parameters sets in the final data matrix after symmetry expansion. The principal components were generated based on valence angles using the Vista (Version 1.2) programme. This yielded a degenerate pair of PCs (PC1 and PC2) each accounting for 49.1% of variance, while the third PC (PC3) accounts for the remaining 1.8% of variance in the dataset (Table 2). The result clearly demonstrates the first advantage of using PCA, i.e., reduction in dimensionality. In the present case two parameters (PC1 and PC2) accounts for 98.2% of the original variance and should be enough to describe

Table 7.2. Results of PC analysis for various datasets in terms of the percentage variance (var %) accounted for by each PC, together with the numbers of CSD entries (N_{ent}) and symmetry-expanded substructures (SEN_{frag}) located by each search within the R-factor limit shown.

Dataset	R-factor limit	N_{ent}	SEN_{frag}	Var% (PC1)	Var% (PC2)	Var% (PC3)
TrL ₃	0.07	611	6192	49.10	49.10	1.80
CuL ₃	0.10	445	5970	49.40	49.40	1.20
AgL ₃	0.10	214	2472	48.10	48.10	3.80
HgL ₃	0.10	139	1308	49.97	49.97	0.05
ZnL ₃	0.10	77	864	49.95	49.95	0.10
AuL ₃	0.10	60	588	49.96	49.96	0.09

the system completely rather than the three original valence angles. The scatterplots of PC1 vs PC2 and PC1 vs PC3 are shown in Figure 7.4(a) and (b) respectively. Scatterplot of PC1 vs PC2 maps the deformation away from the trigonal planar (D_{3h}) geometry towards T or Y-shaped geometry, largely due to angular distortion. For PC1 vs PC2 plots, we are effectively viewing from a point above the plane of the ligands, looking down. The large central cluster in the plot corresponding to PC1, PC2 = 0.0,0.0 represents the geometry with highest symmetry (D_{3h} trigonal planar geometry) and no distortion. Also observed are two distinct types of three-fold extension from this central core corresponding to two distinct types of deformation as shown in **Figure 7.5** (these directions also apply consistently to other PC1 vs PC2 plots as will be discussed in later sections). While one distortion maps the T-shaped configuration, the other corresponds to the Y-shaped configuration. The greatest degree of distortion is attributed to the T-shaped geometry and the smaller one to Y-shaped geometry. Effectively, the angular distortion for T-shaped required more distortion, from 120° , 120° and 120° for D_{3h} to 90° , 90° and 180° than that of Y-shaped (to around 60° , 60° and 150°). PC1 vs PC3 on

(a)



(b)

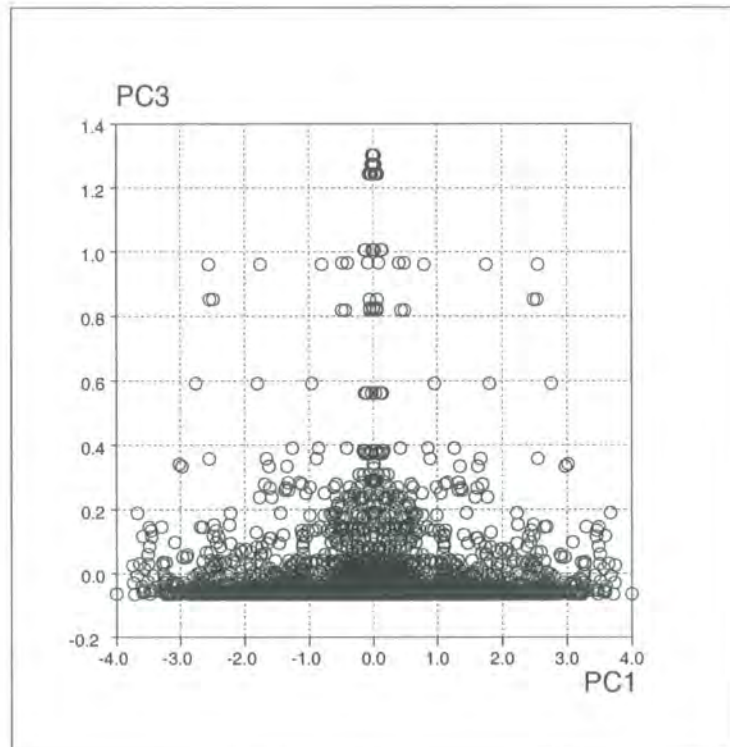


Figure 7.4. (a) Scatterplot of PC1 vs PC2 for all TrL₃ species. (b) Scatterplot of PC1 vs PC3 for all TrL₃ species

the other hand, maps the out-of-plane displacement of the metal atom from the plane of the ligands towards pyramidal geometries. Out-of-plane displacement of the metal atom can be determined directly from the dataset, and a subsequent analysis showed that out of 1032 retrieved substructures the deviation of metal atom by $d > 0.2 \text{ \AA}$ from the ligand plane was observed for 153 cases (14.8%) while 58 (5.6%) cases are observed having $d > 0.4 \text{ \AA}$.

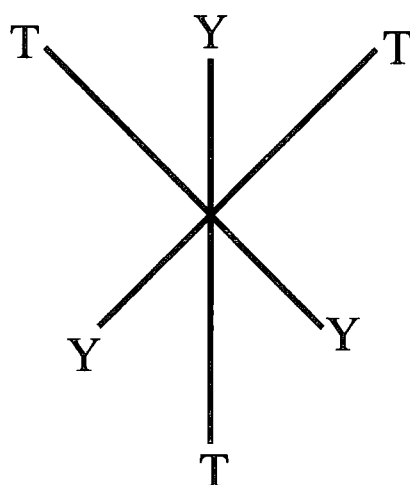
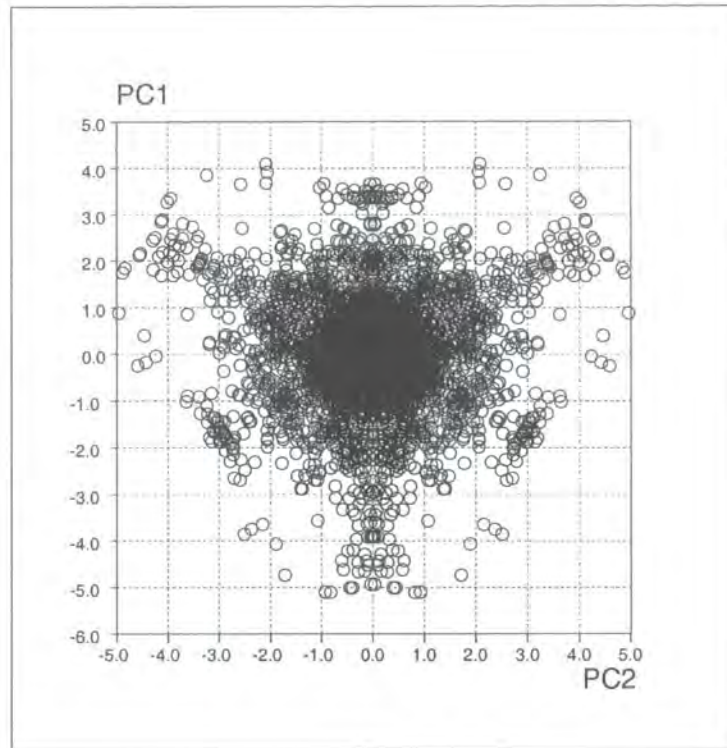


Figure 7.5. Schematic diagram indicating the deformation directions revealed in the PC1 vs PC2 scatterplots.

7.7.2. PCA results for individual TrL3 species: PCA analysis was carried out for five most common elements in table 1, viz, Cu, Ag, Hg, Zn and Au with similar criteria as earlier but with the restriction of R-factor < 0.10 . The subsequent results are tabulated in table 2, while we will concentrate on individual results in the following section.

For Cu, principal component analyses produce two degenerate PCs (PC1 and PC2) each accounting for 49.4% while the third, PC3, accounts for 1.20%. The scatterplot of PC1 vs. PC2 shows a large central cluster of trigonal planar structures (perfect and distorted) with some light scattering for T-shaped (BAHMON, BUXNIR) and Y-shaped

(a)



(b)

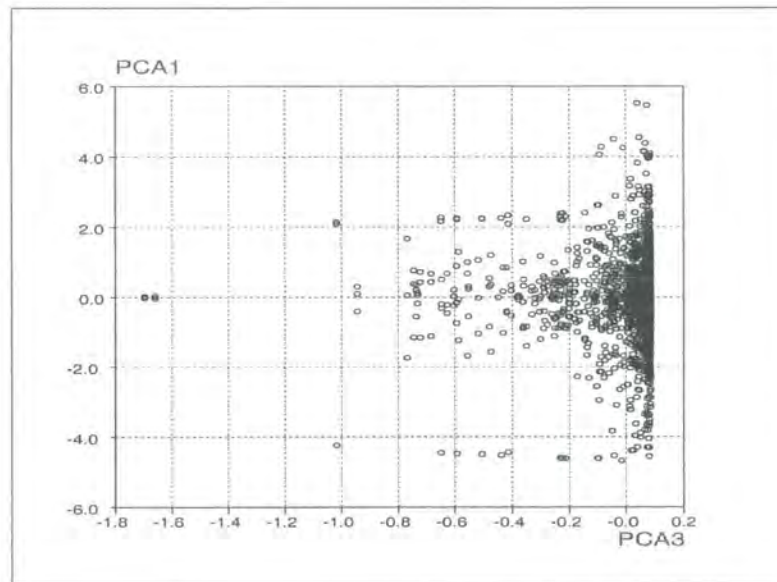
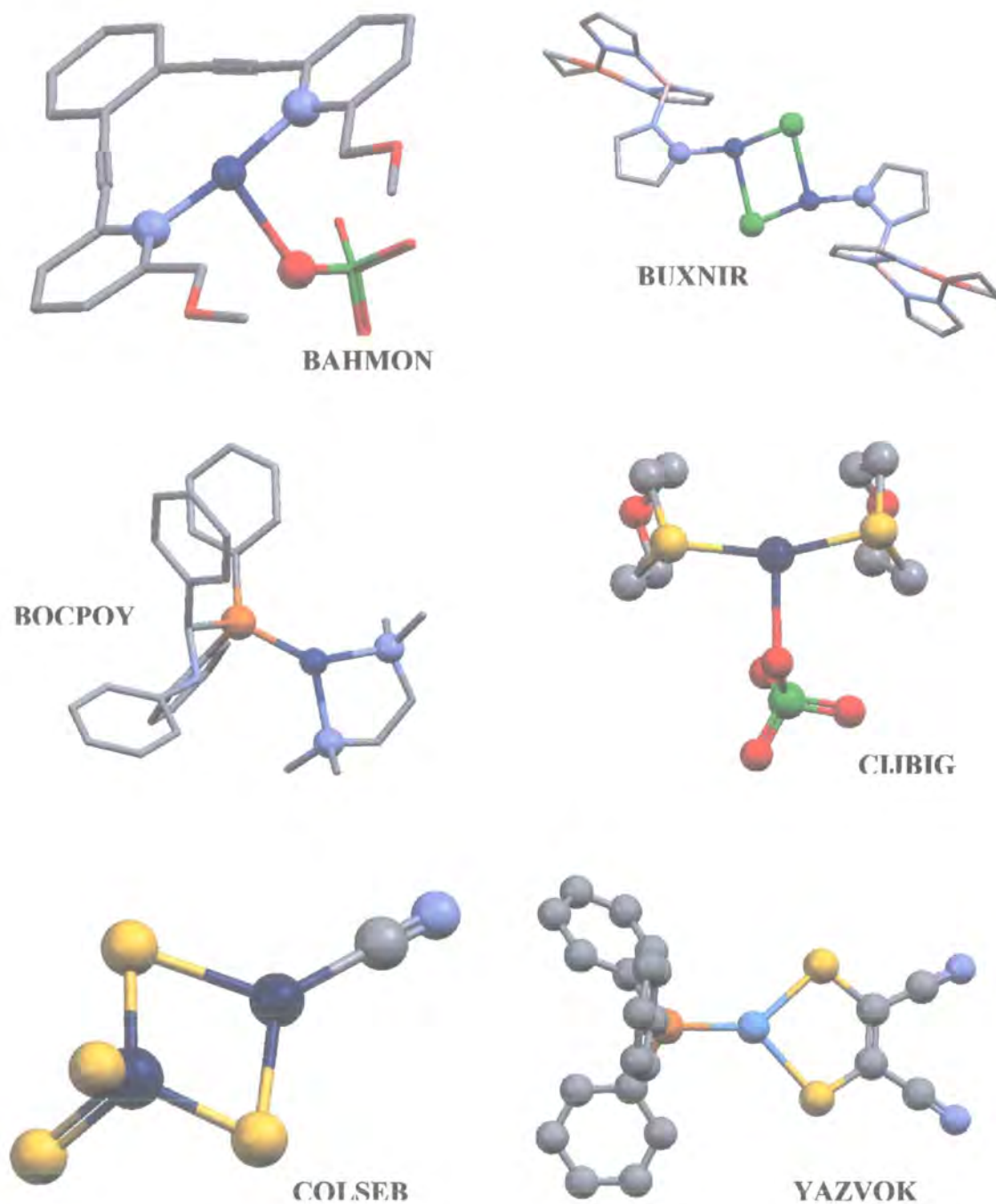


Figure 7.6. (a) Scatterplot of PC1 vs PC2 and (b) PC1 vs PC3 for Cu

molecules (BOCPOY, MAVQUV). On the other hand, the scatterplot of PC1 vs. PC3 (Figure 7.6b) shows that for most of the cases Cu atom is coplanar with the ligand plane, however there is considerable amount of out-of-plane movement with some significant amount of movement for few substructures.



Scheme 7.I. Representative molecules from Cu, Ag and Au datasets highlighting the Y- and T-shaped geometry.

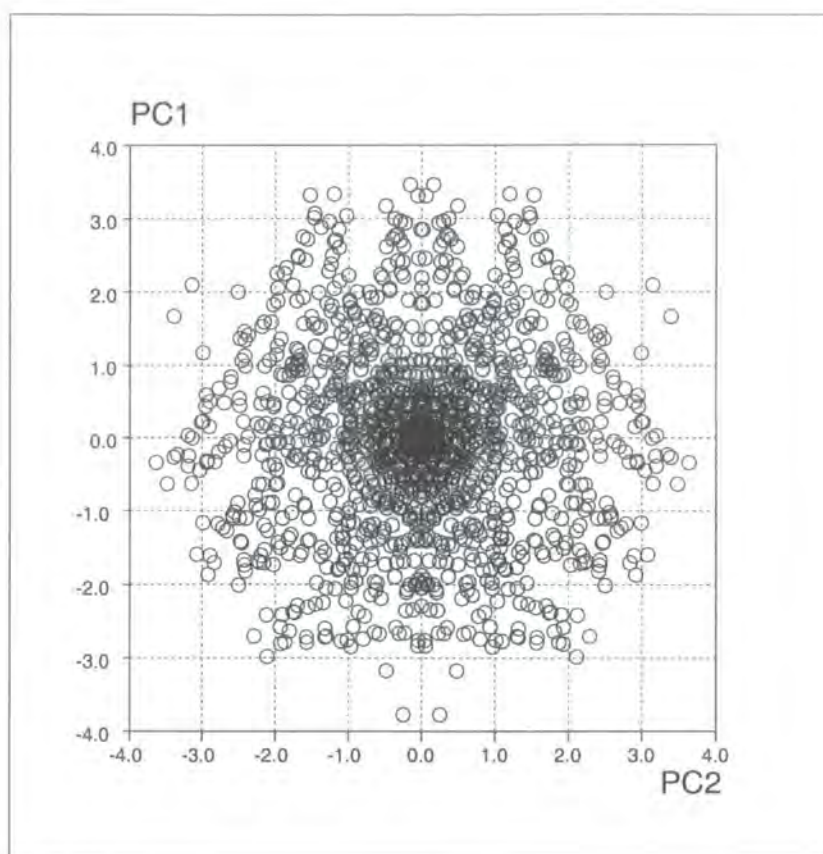


Figure 7.7. Scatterplot of PC1 vs PC2 for Ag, Notice considerable amount of scattering with centralised cluster for trigonal planar geometry

For Silver, PC1 and PC2 accounts for 96.20%, and PC3 the remaining 3.8%. Interestingly, except for Cu and Ag the value of PC3 is very small and one can always argue about the importance of PC3 for other elements. However, the relatively considerable amount of PC3 variance for Cu and Ag suggests that most of the out-of-plane displacements towards pyramidal geometries (eg, in molecules like CADXOU, CAMREN) observed for the complete TrL_3 datasets arise from these two elements.

The PC1 vs PC2 plot (Figure 7.7) shows significant scatter, though a preference for D_{3h} structure and to some extent for Y-shaped structures can be noticed easily. A closer inspection of Y-shaped structures shows that they have similar chelate ring formation or multidentate binding by ligands that have small bite angles.

An almost similar kind of plot is observed for Au complexes (Figure 7.8.), where structures predominantly approximate trigonal planar geometry with small number of substructures showing deformations towards T- and Y-shaped geometries (YAZVOK). For Au, the out-of-plane displacement and hence pyramidalization is not a prominent feature as PC3 accounts for a negligible 0.09% of the variance.

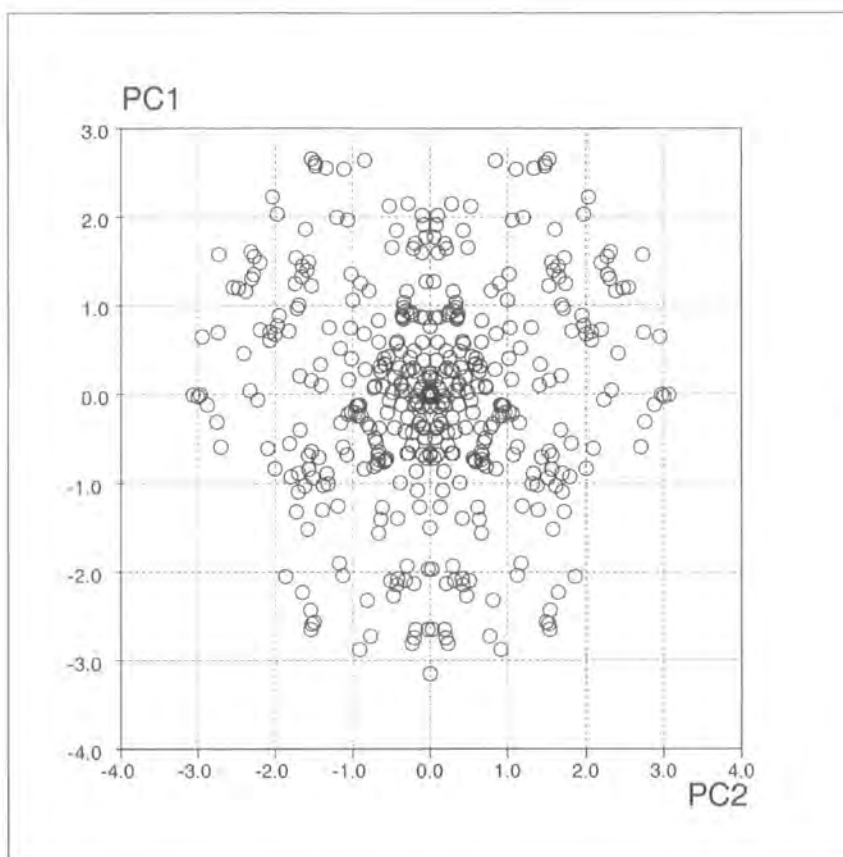


Figure 7.8. Scatterplot of PC1 vs PC2 for Au, Notice considerable amount of scattering with predominant centralised cluster for trigonal planar geometry.

For mercury, the PC1 vs. PC2 plot (Figure 7.9) shows that there is a definite preference for T-shaped geometry, together with entries in the central core that represent the D_{3h} structure, but with almost no Y-shaped examples. Most noticeable and exciting part of the plot is that there is a well-defined density linking the D_{3h} and T-shaped density that indicate a smooth distortion pathway leading from the T-cluster to the relatively small

central trigonal core cluster at the origin of PC1, PC2 space. This is certainly highly encouraging for mapping the reaction coordinate and structure correlation studies, as will be discussed in detail in a later section. Out of plane displacement of the mercury atom is not so important mainly because PC3 accounts for only 0.05% of the total variance.

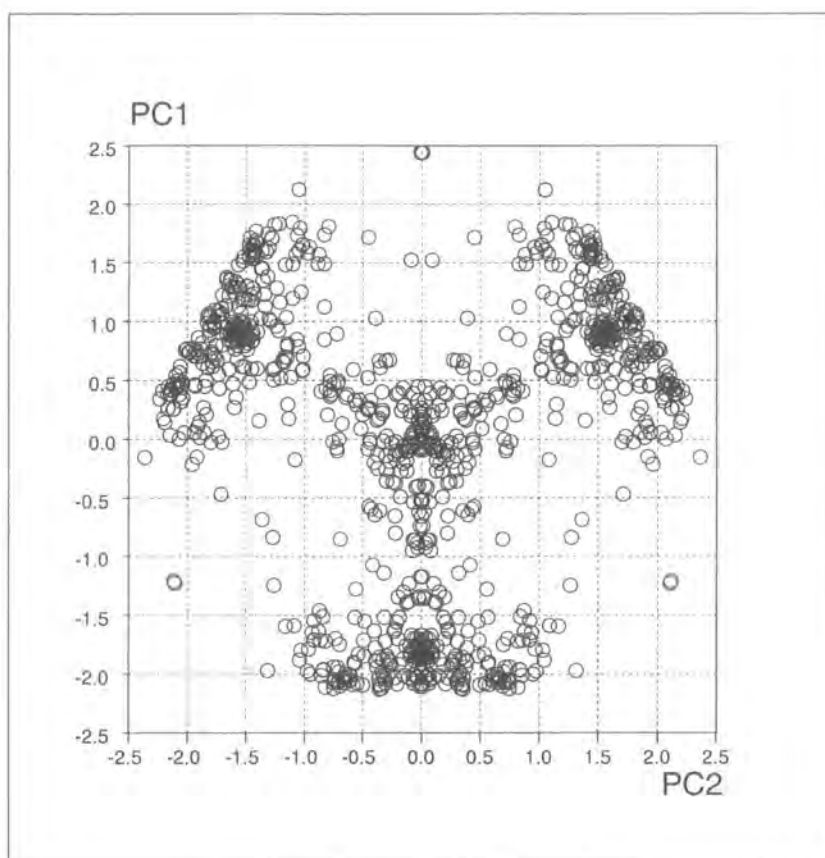


Figure 7.9. Scatterplot of PC1 vs PC2 for Hg. Notice the predominant T-shaped geometries and with a well-defined pathway leading from the T-cluster to the relatively small central cluster at origin.

The scatterplot of PC1 vs PC2 for Zn is however quite different from the rest (Figure 7.10). Two major features can be noticed immediately, a core cluster for trigonal planar and a discrete cluster of Y-shaped geometries with almost no T-shaped examples. However, unlike Hg, the lack of density linking the D_{3h} and Y-shaped density indicate that not enough structures in the dataset lie on a smooth distortion path, in comparison.

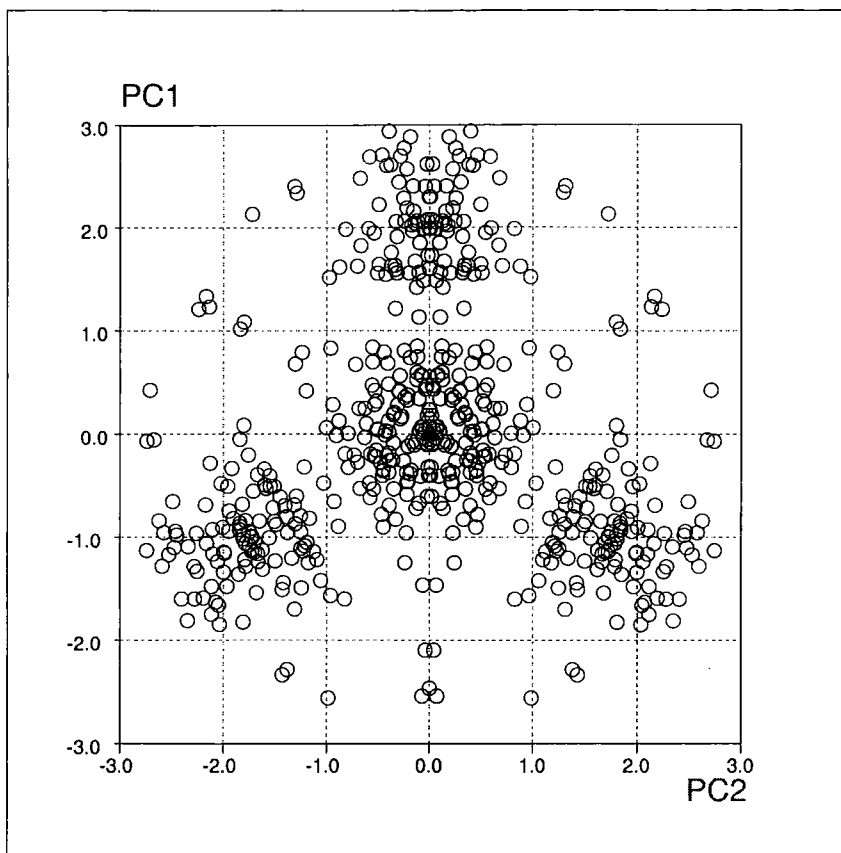


Figure 7.10. Scatterplot of PC1 vs PC2 for Zn. Notice The central cluster for D_{3h} and a discrete cluster of Y-shaped geometries with almost no T-shaped examples

A closer inspection of the Y-cluster reveals that virtually all of the contributors arise from substructure with Zn having an oxidation number +2. Interestingly, all of these Y-shaped geometries arise from the formation of four-membered rings as shown in Figure 7.11, where of necessity, one of the angles at Zn is forced towards 90° by the four

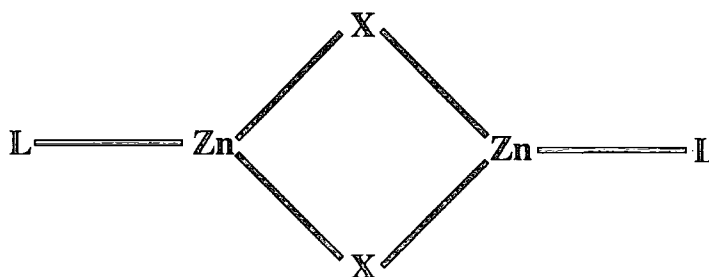
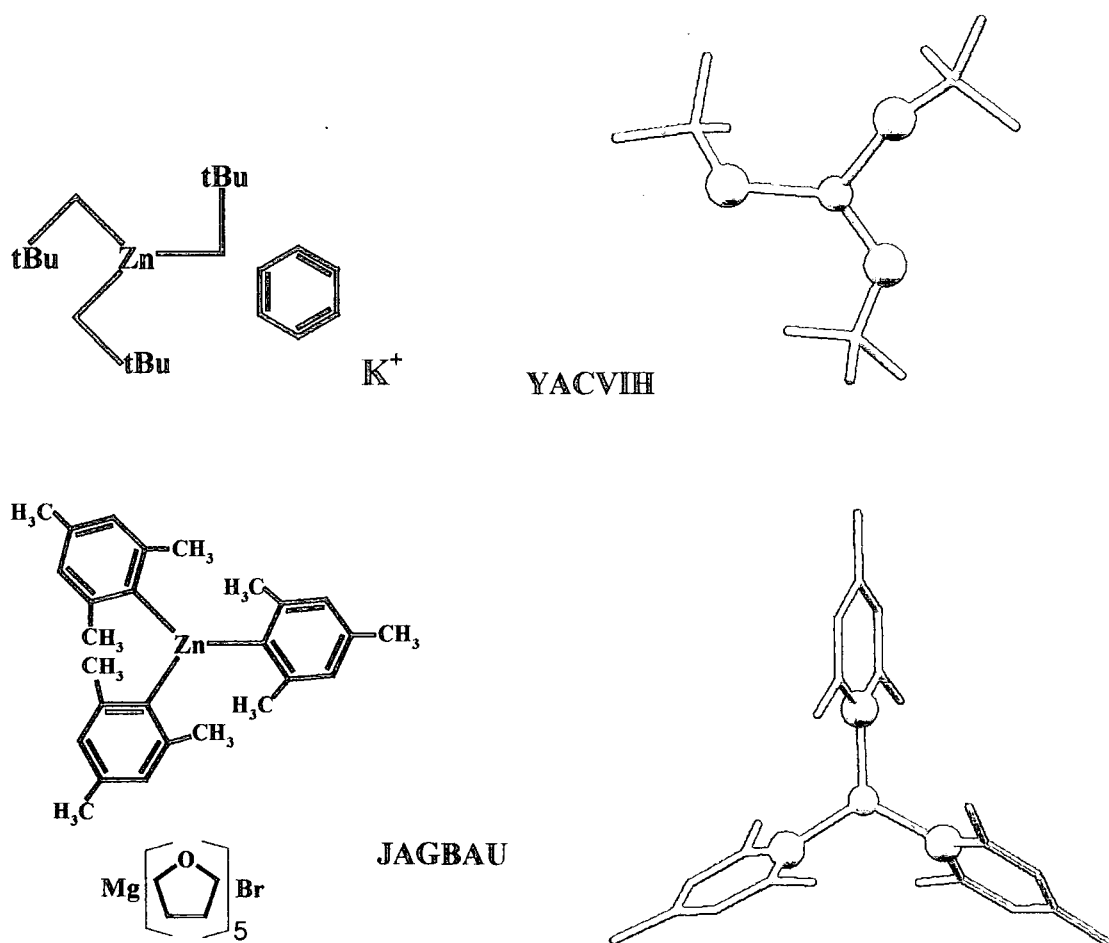
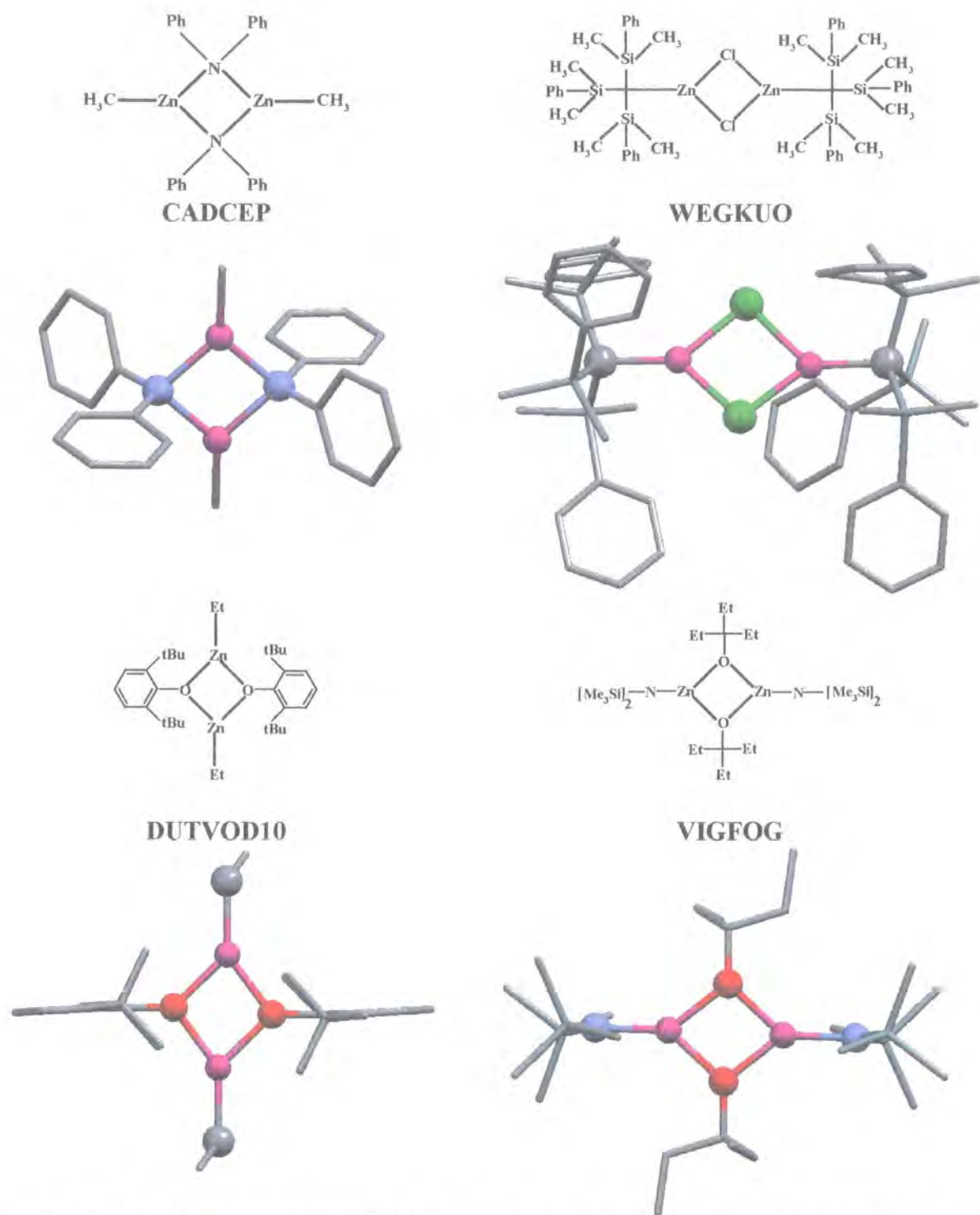


Figure 7.11. A schematic impression of the substructure causing Y-shaped deformations of three coordinate Zn species, the most common elements X are O, N, and Cl.

membered ring formation via X= O, N, Cl. For example, molecules like CADCEP, DUTVOD10, VIGFOG, WEGKUO, the four-member ring formation force one of the angles at Zn^{II} towards 90° and hence adopting the Y-shaped geometry as shown in Figure 7.11. Taking a more general perspective, for most of the structures in the TrL₃ data sets formation of four-membered rings involving Tr is by far the most common cause of Y-shaped geometries. On the contrary most of the trigonal planar substructures arise when the Zn atom is symmetrically linked to some hydrocarbon groups in a cartwheel manner (YACVIH, JAGBAU).



Scheme 7.III. Characteristic molecules from Zn dataset showing trigonal planar geometry.



Scheme 7. III. Some characteristic molecules from Zn dataset showing the Y-shaped structures with four membered ring formation via N, Cl and O.

7.8. Symmetry Deformation Coordinate (SDC) results for individual TrL_3 :

As we have seen earlier, the principal components are derived by taking linear combinations of original variables. This in effect derives some uncorrelated parameters from some correlated variables. PCA is a purely numerical method for which there is no

statistical model. In a way, the PCs as such do not carry any significant chemical meaning. However, it is common to find correlations of PCs to parameter axes with chemical meaning generated in other ways. In the present case the PCs are directly correlated to the group theoretic symmetry deformation coordinates (SDC) which map deviation from the reference D_{3h} symmetry (Figure 7.2).

SDC plots show identical features to those of the PCA plots, i.e., they are giving the same information as the PC plots reported earlier, but with the PC1 and PC2 rotated by 60° and 30° respectively from SDC1 and SDC2 (Figure 7.12). It is obvious that the two descriptors, PC and SDC's are not directly correlated. Rather the correlation coefficients for SDC/PC relationship for three coordinated metals are related to the degree of rotation of the PC axes.

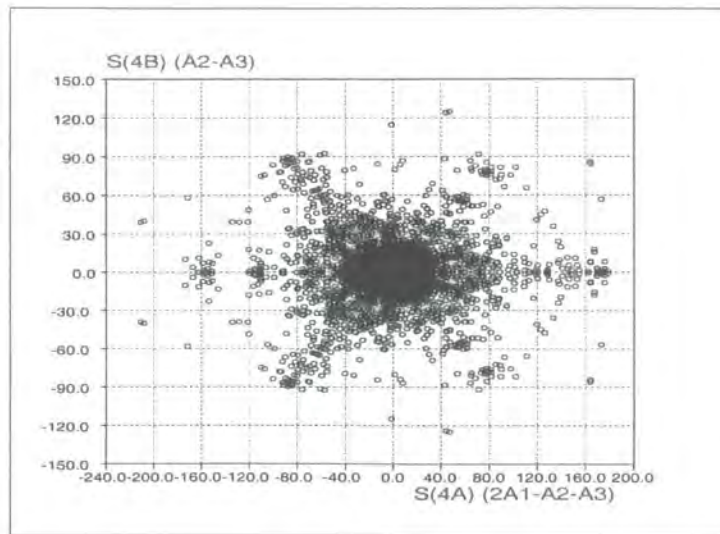
Interestingly, for PCA3: SDC1, the correlation coefficient is perfectly 1.0 (Figure 7.12).

These results are potentially very useful in assessing the chemical meaning of the PC's.

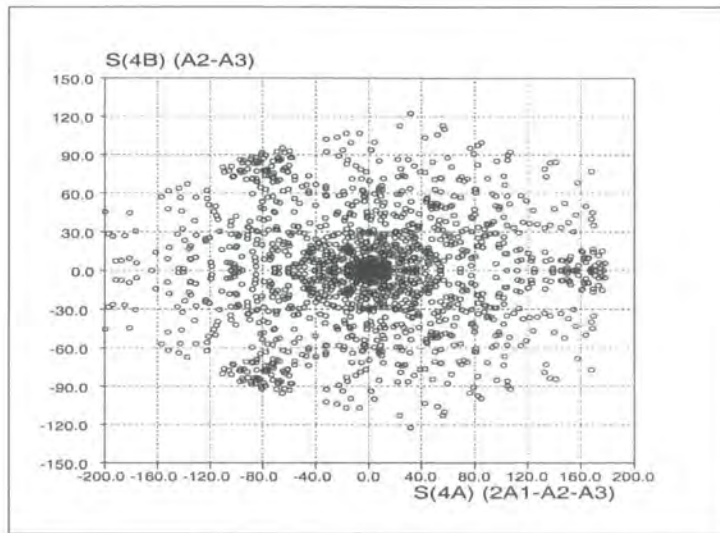
Since SDC1 is the function of summation of three valance angle, and for three coordinated complexes, a value other than 360° maps the out-of-plane displacement of the metal atom. From this we can immediately infer that the PC3 axis is exactly aligned with a molecular axis, SDC1 ($\theta_1 + \theta_2 + \theta_3$), that maps the out of plane movement of the metal atom and subsequently geometrical changes from the D_{3h} trigonal planar to C_{2v} pyramidal shape. This result is quite significant from structure correlation point of view. The rationale of correlating PCA3:SDC1 can be found from the hypothesis of structure correlation. The relationship of structure correlation with features of energy surface has been stated by Bürgi and co-workers as⁴:

“If a correlation can be found between two or more independent parameters describing the structure of a given structural fragment in a variety of environments, then the correlation function maps a minimum energy path in the corresponding parameter space”

(I)

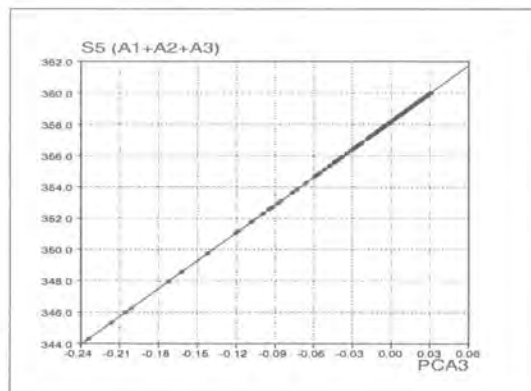


(II)



III

(A)



(B)

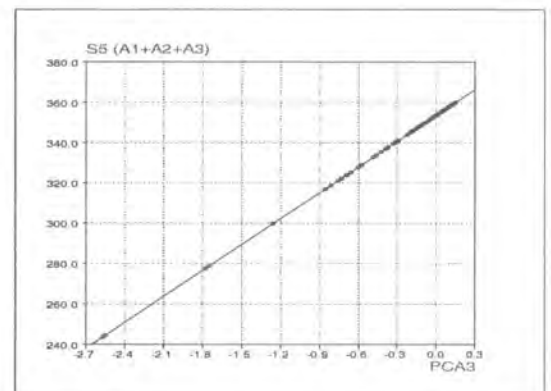
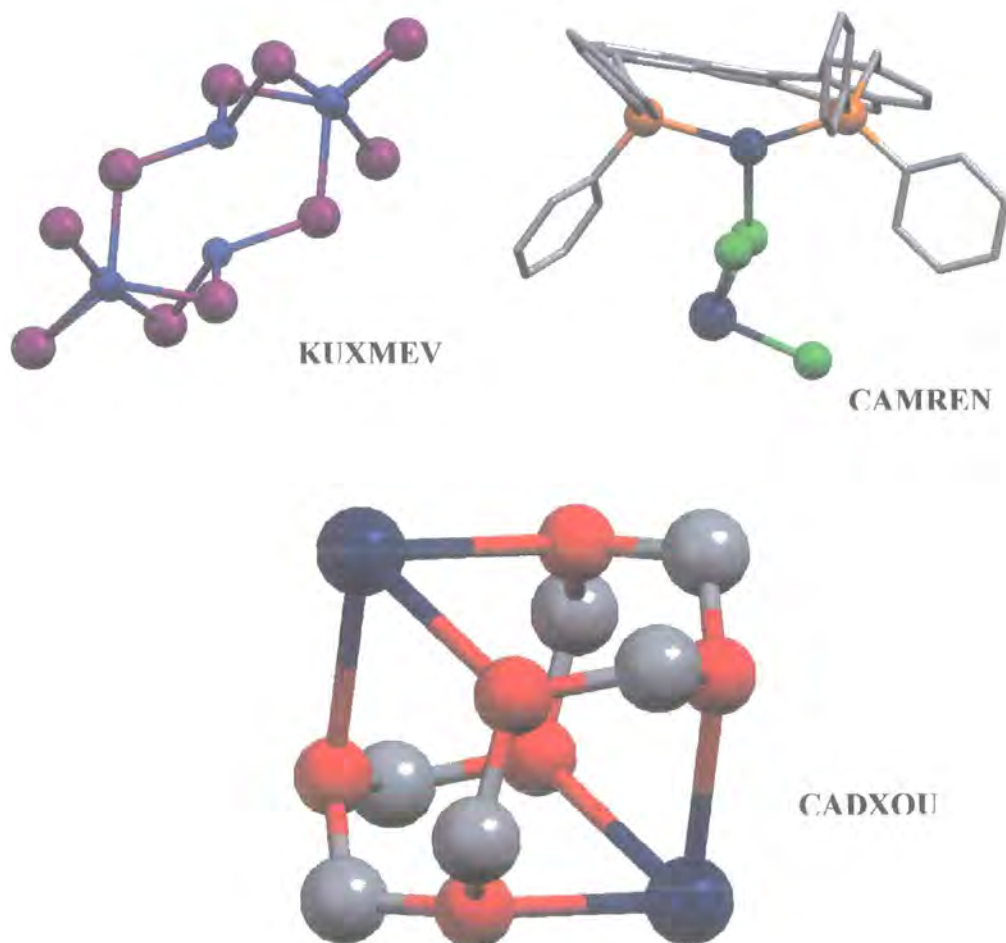


Figure 7.12. SDC1 vs. SDC2 plots of (I) for Copper, (II) Silver, note that here A1, A2 and A3 are three valence angles. (III) SDC vs. PCA plots with correlation coefficient of 1.0, (A) for Hg, (B) for Ag. Plots for Au and Cu are not shown here which are identical to these plots.

7.9. Out-of-Plane Displacement of the Metal Atom

Out-of-plane displacement of the metal atom can be easily quantified from the original out-of-plane displacement data. The histograms in Figure 7.13 show that although the vast majority of these out-of-plane displacements occur in the region of $d < 0.2 \text{ \AA}$, Cu and Ag atoms do show significant amounts of out-of-plane displacement. This is exactly what we observed from principal component analysis, wherein a relatively high value of PC3 is observed for Cu and Ag than for the rest of the elements. In a way, being a chemical parameter (and similar to SDC1), out-of-plane displacement of the metal atom further confirms the results of PCA.



Scheme 7.IV, Representative molecules showing large out-of-plane displacement of the metal atom from ligand plane with pyramidalisation.

Interestingly, these structures tend to retain their three-fold symmetry, i.e., a pyramidalization of D_{3h} structures (KUXMEV, SARBOC). The crystal structure of CAMREN is highly interesting in this regard; wherein out of two Ag atoms one forms a T-shaped geometry while the other adopts a pyramidal C_{2v} shape. Pyramidalisation of D_{3h} can be explained in two ways, firstly, due to highly constrained environments around the metal atom, e.g., cage structures or fused ring assemblies as observed for CADXOU (Scheme 7.IV). Secondly, pyramidalisation can be caused by an approach of a 'fourth ligand', in other words, when a non-bonded ligand comes into very close proximity to a metal atom, the metal atom starts shifting out of the plane of the ligand atoms causing pyramidalisation.

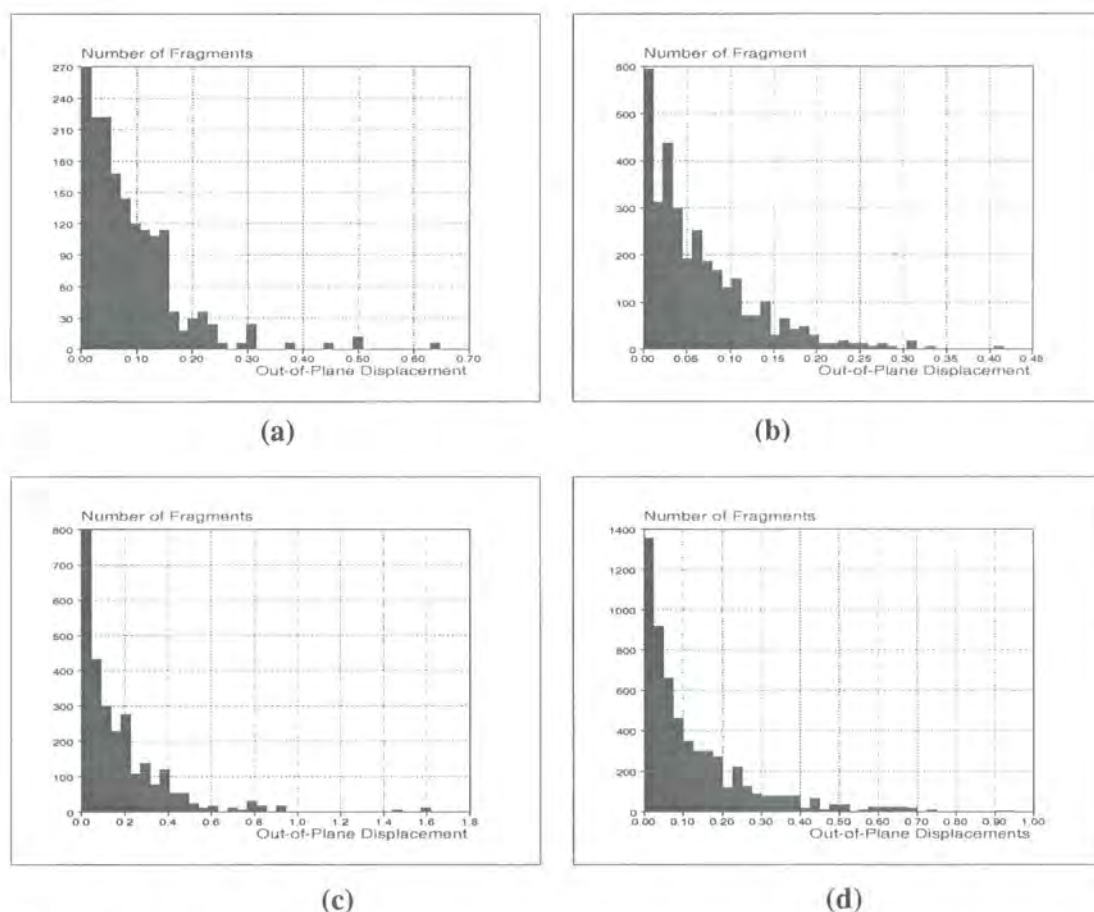


Figure 7.13. Histograms of out-of-plane displacements (\AA) of (a) mercury, (b) gold, (c) silver and (d) copper from the plane of three ligand atoms.

In that case, out-of-plane displacement can act as a reaction coordinate and map the reaction pathway for conversion of three to four coordination, a possibility, which is a the second and subsequent part of this ongoing project and beyond the scope of this Chapter.

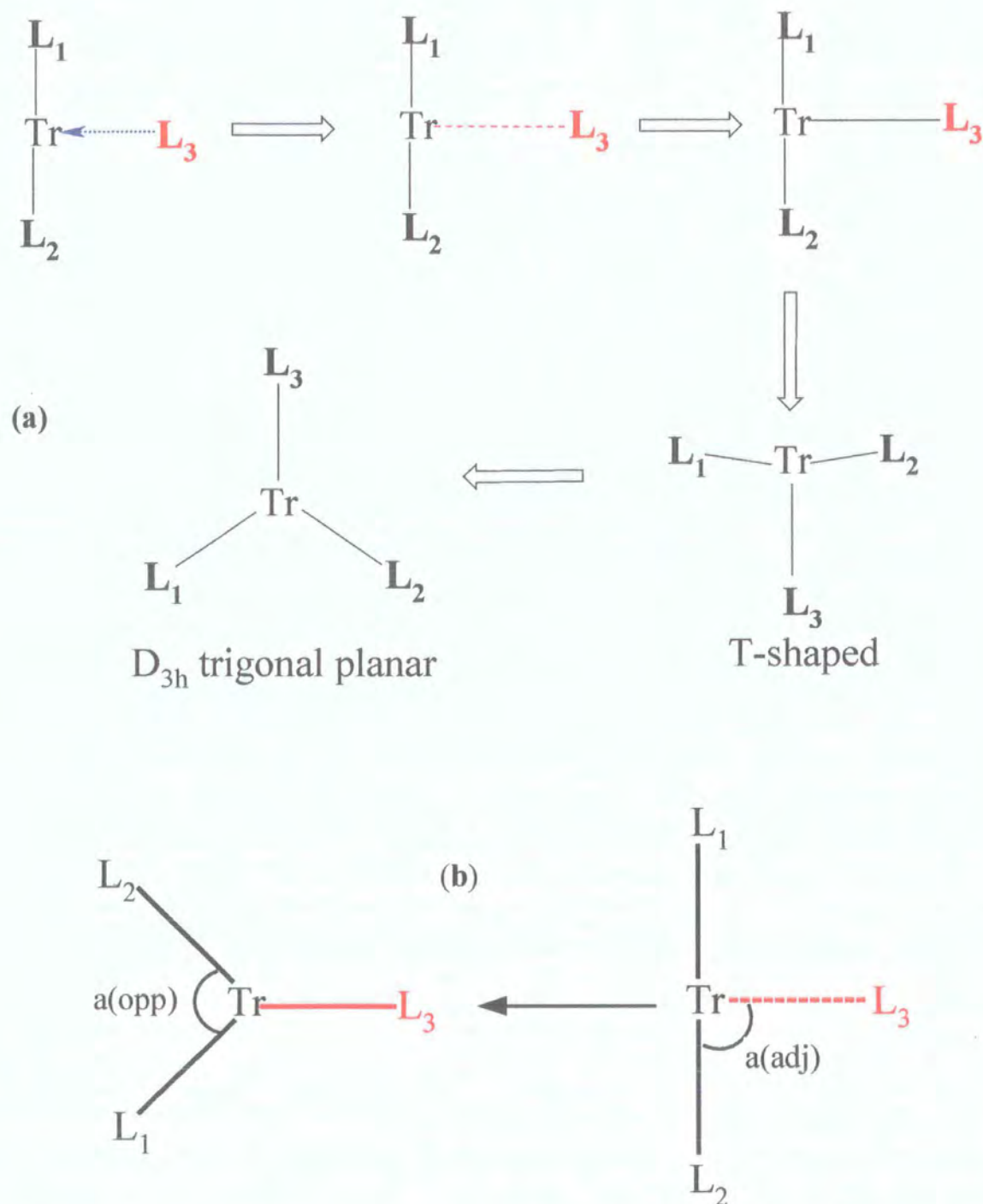


Figure 7.14. (a) Schematic representation of the reaction mechanism for the conversion of two coordinated species to three coordinated D_{3h} geometry. (b) One step representation of the reaction with the parameters used.

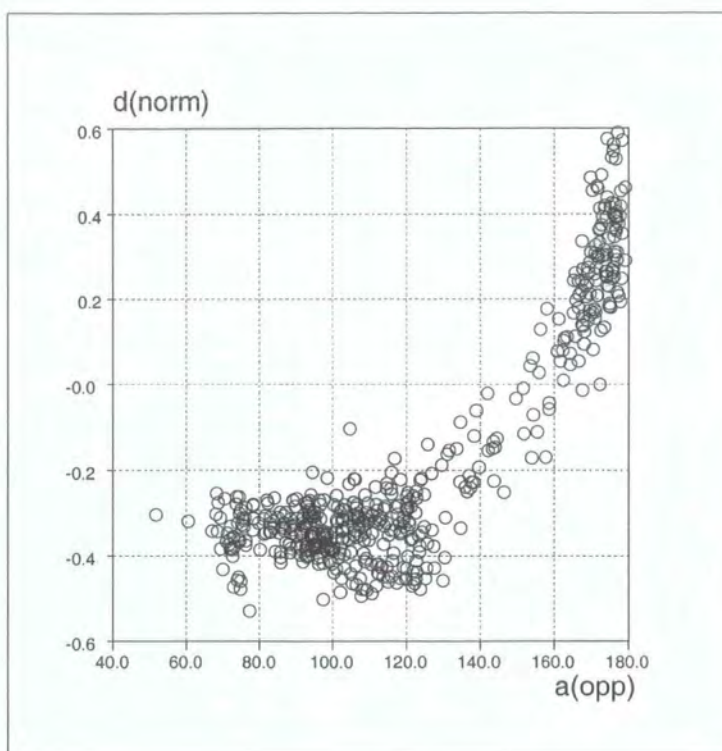
7.10. Reaction pathway for ligand addition to two-coordinate species:

For some metals, the three-coordinated structure can be viewed as the addition of a third ligand to a linear two coordinate species. The addition reaction of the third ligand can be perceived as a stepwise reaction as shown in Figure 7.14. In the initial stages of the bonding, the third ligand would approach the metal perpendicular to the linear ligand-metal- ligand unit, and consequently form a very weak bond with two 90° and one 180° valence angles.

The progress of the reaction can be monitored with the formation of the third ligand-metal bond in terms of the changes in the valence angles at the metal centre. As the reaction progresses, i.e., the bonding becomes stronger, there would be two concerted changes in the valence angles, a decrease in the linear angle opposite to the incoming ligand, while a concerted increase of the two adjacent angles from 90° . Such an interpretation is in accord with the structure-correlation principle, i.e., that the static distortion exhibited by a specific molecular substructure (fragment) in a wide range variety of crystalline environment can be assumed to map the distortion that the fragment would undergo along a reaction pathway. The relationship between geometrical distortion and potential energy¹⁸ can be termed as: *“If a correlation can be found between two or more independent parameters describing the structure of a given structural fragment in a variety of environments, then the correlation function maps a minimum energy path in the corresponding parameter space”*

As we have seen earlier for the scatterplot of the PC1 vs. PC2 for Hg (Figure 7.9), there is a well-defined pathway leading from the cluster of T-shaped geometries to the relatively small central cluster at the origin. given the fact that Hg^{II} is well known to form linear two-coordinate complexes, it is reasonable to assume that this transition from T-shaped to trigonal planar Hg^{II} complexes maps the low-energy pathway for addition of L_3 to the linear $\text{L}_1 - \text{Hg}^{\text{II}} - \text{L}_2$ system.

(a)



(b)

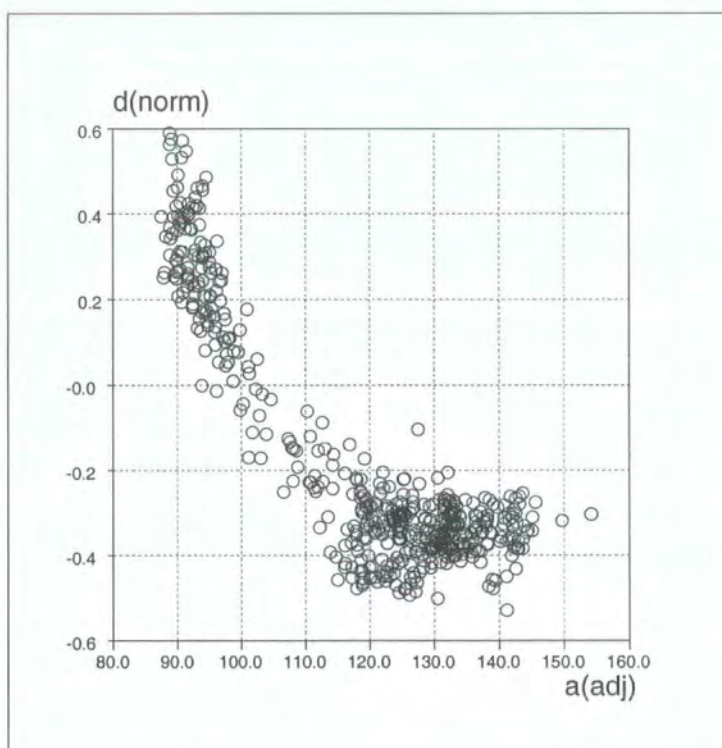


Figure 7.15. Plots of (a) $d(\text{norm})$ vs $a(\text{opp})$ and (b) $d(\text{norm})$ vs $a(\text{adj})$ for Hg^{II} .

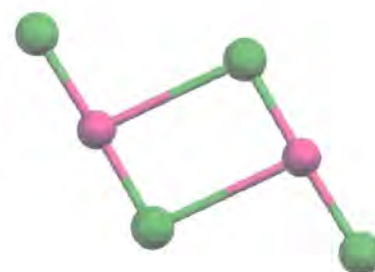
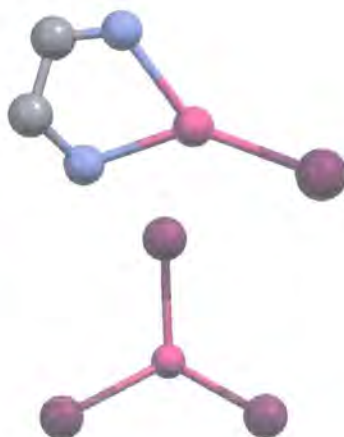
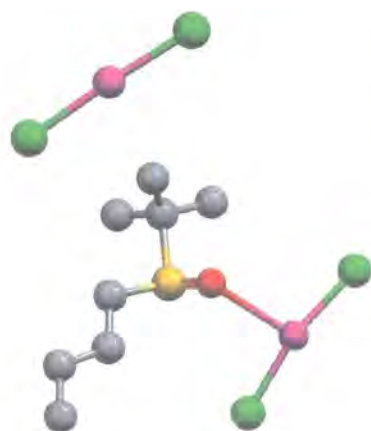
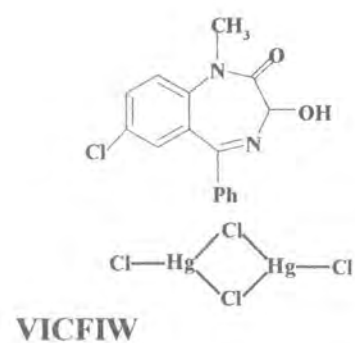
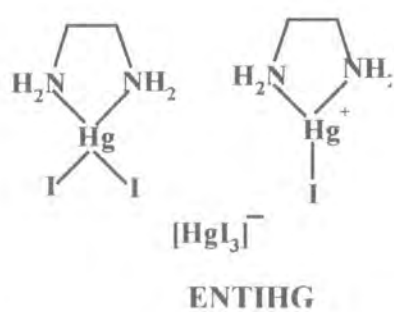
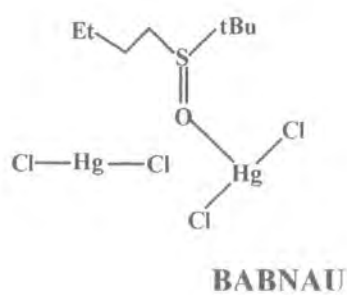
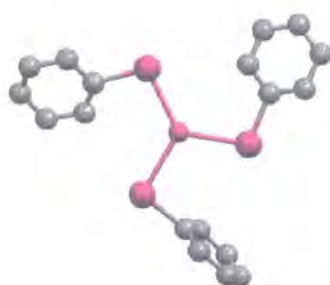
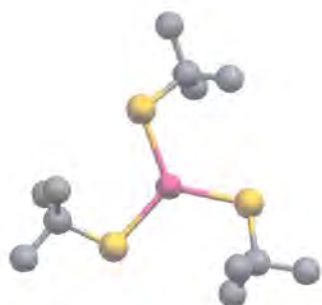
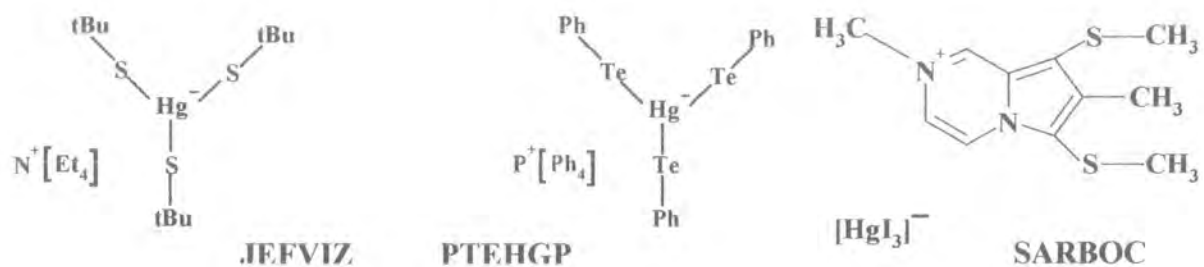
The hypothesis was tested for ligand addition to the two-coordinated species. We have examined the coordination in terms of the normalized bond distance, which is defined as the subtraction of sum of covalent radii of metal and ligand atom from the bond length, i.e.,

$$d(\text{norm}) = d(\text{Hg-L}) - r_{\text{cov}}(\text{Hg}) - r_{\text{cov}}(\text{L})$$

where, $r_{\text{cov}}(\text{Hg})$ and $r_{\text{cov}}(\text{L})$ are the standard covalent radii of the metal atom and the incoming ligand, respectively. The standard covalent radii values are used as stored in the CSD. The quantity $d(\text{norm})$ is calculated from each hit substructure during permutational expansion, so that $d(\text{norm})$ is calculated for each of the bond lengths d_1 , d_2 and d_3 in Figure 7.1.

The hypothesis was tested by plotting $d(\text{norm})$ vs. $a(\text{opp})$ where $a(\text{opp})$ is the valence angle 'opposite' to the 'incoming ligand', ie, it is θ_n for normalized d_n ($n=1-3$) in the nomenclature of Figure 7.1(a). Due to the formulation of $d(\text{norm})$, positive values of $d(\text{norm})$ indicate bond lengths that are longer than the sum of covalent radii, i.e., weaker than might be expected. On the other hand a negative value is a manifestation of stronger bond. This mechanism provides a geometrical formalism to map the reaction pathway by plotting $d(\text{norm})$ against $a(\text{opp})$ and $a(\text{adj})$, where $d(\text{norm})$ is a measure of bond strength of the 'third' bond and decrease in $a(\text{opp})$ (from 180° to 120°) or an increase in $a(\text{adj})$ (from 90° to 120°) value is the measure of progress of the ligand addition reaction.

Exact reproduction of this behaviour in Figure 7.15(a) and (b) further vindicates our hypothesis for the mechanism of the addition reaction. This provides direct evidence of the mechanism and geometry of ligand addition to linear two-coordinated mercury compounds, which manages to preserve the linearity of the parent system before the



Scheme 7.V: Characteristic molecules from Hg^{II} datasets showing different structural variations like trigonal planar, T-shaped, Y-shaped and pyramidal.

strength of the third additive bond increases and transforms the system into a 3-coordinated D_{3h} system

A detailed investigation was carried out for all the Hg^{II} in order to gain some more insight. As observed most of the molecules in the list form a T-shaped geometry with one angle [a(opp)] close to 180° and the corresponding opposite bond distance is considerably longer than the other two. One interesting example is BABNAU, wherein of the two types of $HgCl_2$ moiety present in the asymmetric unit, one forms a 'third' bond with sulfoxide group while the second one remain as a discrete linear $HgCl_2$ species. Angles and bond distances strongly support our observation. On the other hand most of the trigonal planar structures show two common trends: most of the alkyl or aromatic groups linked with S or Te form a windmill type of structure (DELFJ, GEZPEG, JEFVIZ, KINZAI PTEHGP etc.) with a core trigonal planar geometry at the metal centre. Again almost all the HgX_3^- (X= Br I) species form D_{3h} geometry, sometimes exhibiting pyramidalisation (SARBOC) with the sum of valence angles (115.77, 111.98 and 116.55) well below 360° , a pre-requisite for D_{3h} geometry. However for $HgCl_3^-$ species (e.g. DOTLIH, FOCLOY) structures are more T-shaped with one longer bond and a(opp) around 145° . Structure like VICFIW represents some unique geometry: although it forms a four-membered ring like some Zn complexes (Figure 7.10), it adopts a rectangular (2.28, 3.26Å) shape rather than the square ring geometry in Zn. This simple modification (with one characteristic longer bond) helps it to adopt a T-shaped geometry rather than Y-shaped. A rare Y-shaped structure does indeed appear for a unique complex of Hg^{II} (ENTIHG) wherein three different Hg complexes formed depending on the number of Γ , tetrahedral, trigonal planar, and Y-shaped wherein chelete formation forced one angle to be very small to form Y-shaped geometry.

7.11. Conclusion

In this work we have seen the importance of the stereochemistry of three coordination of transition metal complexes, which has hitherto been ignored. This work also highlights the importance of symmetry modified principal component analysis in visualising the deformation in metal-coordination geometry exhibited in crystal structure determination. Although for some limited number of structures these deformations are well known, but structural classification and visualisation for all the available structures as a whole are little-studied. CSD analysis coupled with principal component analysis immediately provided a mapping of all available structures, which enable us to visualize them with characteristic and more easily identifiable clustering than any mapping based on individual valence angles. At the same time PCA mappings help to identify any interconversion pathways that connect these clusters. For the present study, with the help of PCA techniques, we are able to characterise the major deformations for the three coordinate complexes, namely, to Y-shaped and T-shaped geometries, together with mapping of interconversions from trigonal planar to pyramidal geometries. We were able to correlate these PCA mapping with symmetry deformation coordinates, which can be derived from group theory. In the case of Hg^{II} , the mapping indicated a well-defined smooth interconversion from T-shaped to trigonal species, which has been interpreted here in terms of reaction pathway for a ligand addition reaction to linear $\text{L}_1\text{-Hg}^{\text{II}}\text{-L}_2$ systems.

7.12. References:

1. (a) F. H. Allen, O. Kennard, *Chem. Des. Autom. News.*, 1993, **8**, 30-37, (b) F. H. Allen, *Acta. Cryst.* 2002, **B58**, 380-388.
2. (a) S. J. Weininger, *J. Chem. Educ.*, 1984, **61**, 939-944, (b) R. G. Wooley, *J. Chem. Educ.*, 1985, **62**, 1083-1084. (c) A. Amann, W. Gans, *Angew. Chem. Int Ed. Engl.*, 1989, **28**, 268-276.
3. (a) D. G. Truhlar, R. Steckler, M. S. Gordon, *Chem. Rev.*, 1987, **87**, 217-236. (b) W. F. van Gunsteren, H. J. C. Berendsen, *Angew. Chem. Int Ed. Engl.*, 1990, **29**, 992-1023.
4. (a) H.-B. Bürgi, *Inorg. Chem.* 1973, **12**, 2321-2326. (b) H.-B. Bürgi, *Angew. Chem. Int. Ed. Engl.* 1975, **14**, 460-473. (c) H.-B. Bürgi, J. D. Dunitz, *Acc. Chem. Res.*, 1983, **16**, 153-161. (d) H.-B. Bürgi, J. D. Dunitz, *J. Am. Chem. Soc.* 1975, **97**, 921-922. (e) T. P. E. Auf der Heyde, H.-B. Bürgi, *Inorg. Chem.* 1989, **28**, 3960-3969. (f) T. P. E. Auf der Heyde, H.-B. Bürgi, *Inorg. Chem.* 1989, **28**, 3970-3981 (g) T. P. E. Auf der Heyde, H.-B. Bürgi, *Inorg. Chem.* 1989, **28**, 3982-3989.
5. H.-B. Bürgi, J. D. Dunitz, *Structure Correlation*, VCH, Weinheim, 1994.
6. T. P. E. Auf der Heyde, *Angew. Chem. Int. Ed. Engl.* 1994, **33**, 823-839.
7. (a) G. Aullón, D. Bellamy, L. Brammer, E. A. Bruton, A. G. Orpen, *Chem. Comm.* 1998, 653-654. (b) A. G. Orpen, *Acta. Cryst.* 2002, **B58**, 398-406. (c) A. Martin, A. G. Orpen, *J. Am. Chem. Soc.* 1996, **118**, 1464-1470. (d) A. G. Orpen, L. Brammer, F. H. Allen, O. Kennard, D.G. Watson, R. Taylor, *J. Chem. Soc. Dalton Trans*, 1989, S1-S83.
8. S. E. Harris, I. Pascal, A. G. Orpen, *J. Chem. Soc. Dalton Trans.*, 2001, 2996-3009.
9. S. Alvarez, D. Avnir, *J. Chem. Soc. Dalton Trans.*, 2003, 562-569.

10. (a) F. H. Allen, M. J. Doyle, R. Taylor, *Acta. Cryst.*, 1991, **B47**, 29-40. (b) F. H. Allen, M. J. Doyle, R. Taylor, *Acta. Cryst.*, 1991, **B47**, 41-49, (c) F. H. Allen, M. J. Doyle, R. Taylor, *Acta. Cryst.*, 1991, **B47**, 50-61
11. (a) J. A. K. Howard, R. C. B. Copley, J. -W. Yao, F. H. Allen, *Chem. Comm.*, 1998, 2175-2176. (b) J.-W. Yao, R. C. B. Copley, J. A. K. Howard, F. H. Allen, W. D. S. Motherwell, *Acta Cryst.*, 2001, **B57**, 1080-1084.
12. P. R. Raithby, G. P. Shields, F. H. Allen, W. D. S. Motherwell, *Acta Cryst.* 2000, **B56**, 444-454.
13. D. Venkataraman, Y. Du, S. R. Wilson, K. A. Hirsch, P. Zhang, J. S. Moore, *J. Chem. Educ.*, 1997, **74**, 916.
14. (a) D. L. Keppert, in *Comprehensive Coordination Chemistry*, Eds.: G. Wilkinson, R. D. Gillard, J. A. McCleverty, Vol. 1, Pergamon Press, Oxford, 1987, (b) J. H. Huheey, E. A. Keiter, R. L. Keiter, *Inorganic Chemistry, Principles Structure and Reactivity*, 4th, Harper Collins, New York, 1993. (c) N. Greenwood, A. Earnshaw, *Chemistry of the Elements*, Pergamon Press, Oxford, 1993. (d) S. Alvarez, *Coord. Chem. Rev.*, 1999, **193-195**, 13-41.
15. T. A. Albright, J. K. Burdett, W. -H, Whangbo, *Orbital Interactions in Chemistry*, Wiley, New York, 1985.
16. F. H. Allen, M. J. Doyle, T. P. E. Auf der Heyde, *Acta Cryst.*, 1991, **B47**, 412-424.
17. C. Chatfield, A. J. Collins, *Introduction to Multivariate Analysis*, Chapman and Hall, London, 1980.
18. (a) P. Murray-Rust, H. B. Bürgi, J. D. Dunitz, *Acta. Cryst.*, 1978, **B34**, 1787-1793 (b) P. Murray-Rust, H. B. Bürgi, J. D. Dunitz, *Acta. Cryst.*, 1978, **B34**, 1793-1803. (c) P. Murray-Rust, H. B. Bürgi, J. D. Dunitz, *Acta. Cryst.*, 1978,

- A35, 703-713. (d) P. Murray-Rust, H. B. Bürgi, J. D. Dunitz, *J. Am. Chem. Soc.*, 1975, **97**, 921-922.
19. (a) F. A. Cotton, *Chemical Applications of Group Theory*, 1990, Cornell University Press, Ithaca, New York. (b) S. F. A. Kettle, *Symmetry and Structure*, John Wiley, London, 1987.
20. F. H. Allen, R. Mondal, N. A. Pitchford, J. A. K. Howard, *Helv. Chim. Acta*, 2003, **86**, 1129-1139.
21. F. H. Allen, J. E. Davies, J. J. Galloy, O. Jonshon, O. Kennard, C. F. Macrae, E. M. Mitchell, G. F. Mitchell, J. M. Smith, D. G. Watson, *J. Chem. Inf. Comput. Sci.*, 1991, **31**, 187.
22. Vista – A program for the analysis and display of data retrieved from the CSD, Version 1.2, Cambridge Crystallographic Data Centre, 12 Union Road, Cambridge, CB2 1EZ, UK.
23. I. J. Bruno, J. C. Cole, P. R. Edgington, M. Kessler, C. F. Macrae, P. McCabe, J. Pearson, R. Taylor, *Acta. Cryst.* 2002, **B58**, 389-397.
24. G. P. Shields, P. R. Raithby, F. H. Allen, W. D. S. Motherwell, *Acta. Cryst.* 2000, **B56**, 455-465.

Appendix A

Derivation of SDC's for a D_{3h} reference structure

The vibrationally active normal modes of the reference molecule, can be compared directly to the processes involved in the distortion of the reference molecule towards the observed configuration, and so the derivation of these modes is the crucial first step in the overall derivation of the SDC's. There are of course $3N-6$ active modes to be found, and for the four atom fragment shown in the diagram below this amounts to six normal modes of vibration.

By applying the D_{3h} point group operations to the $3N=12$ Cartesian displacement vectors as represented below the following reducible representation can be found. A C_3 operation on this set of vectors will only affect those vectors at the central atom, transforming x, y into $-1/2x$, and $-1/2y$ while leaving z unchanged.

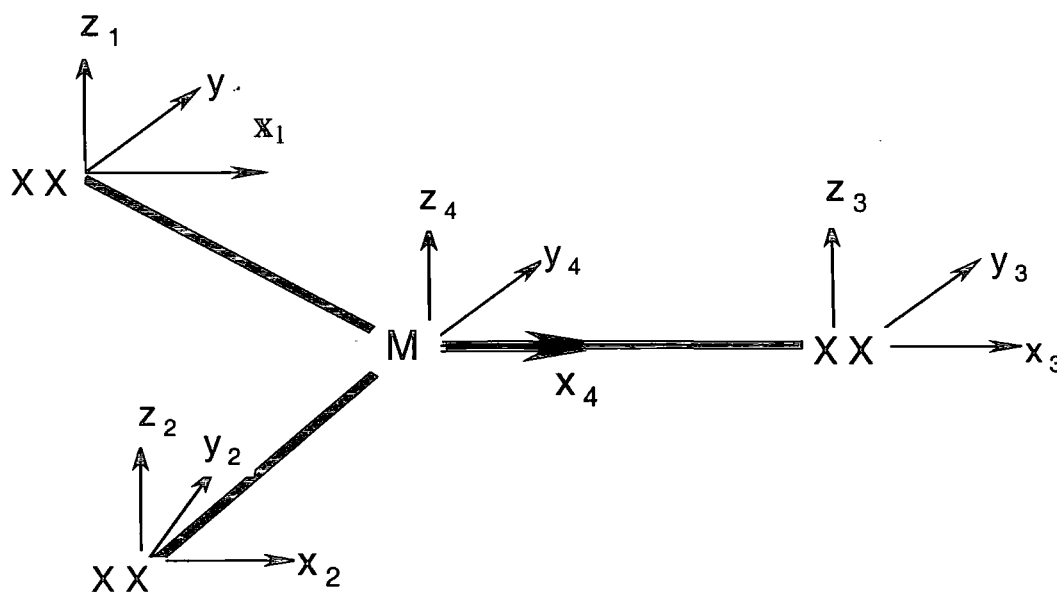


Figure.2. The $3N=12$ Cartesian displacement vectors for the D_{3h} trigonal planar reference structure.

D_{3h}	E	$2C_3$	$3C_2$	σ_h	$2S_3$	$3\sigma_v$
τ_1	12	0	-2	4	-2	2

τ_1 can be re-expressed as the reducible representation:

$$\begin{aligned}
 \tau_1 &= A_1' + A_2' + 3E' + 2A_2'' + E' \\
 \text{rotation} &= A_2' + E' \\
 \text{translation} &= E' + A_2'' \\
 \text{vibration} &= A_1' + 2E' + A_2'' \quad [1]
 \end{aligned}$$

We now have irreducible representations for the $3N-6$ normal modes of vibration for a molecule exhibiting D_{3h} symmetry. To use these to find suitable symmetry coordinates, we have first to change the perspective from which we are describing the molecular fragment, and recognise (see figure 2) that it is the combination of the six physically accessible quantities of bond angles and bond lengths, that will ultimately form the basis set for description of the total deformation.

D_{3h}	E	C_3	C_3^2	$C_2(a)$	$C_2(b)$	$C_2(c)$
P $A_1'(r_1)$	r_1	r_2	r_3	r_1	r_3	r_2
P $A_2''(r_1)$	$+1(r_1)$	$+1(r_2)$	$+1(r_3)$	$-1(r_1)$	$-1(r_3)$	$-1(r_2)$
P $E'(r_1)$	$+2(r_1)$	$-1(r_2)$	$-1(r_3)$	0	0	0
D_{3h}	σ_h	S_3	S_3^2	$\sigma_v(a)$	$\sigma_v(b)$	$\sigma_v(c)$
P $A_1'(r_1)$	r_1	r_2	r_3	r_1	r_2	r_3
P $A_2''(r_1)$	$-1(r_1)$	$-1(r_2)$	$-1(r_3)$	$+1(r_1)$	$+1(r_2)$	$+1(r_3)$
P $E'(r_1)$	$+2(r_1)$	$-1(r_2)$	$-1(r_3)$	0	0	0

Using the bond angles and lengths as our descriptors, the appropriate linear combinations are found by applying the projection operators of the IR's above, to just one of the members of the basis set, e.g. r_1 . The results are shown above and can be summarised as:

$$P \quad A_1'(r_1) = 4(r_1 + r_2 + r_3) \quad \text{approximating to} \quad (r_1 + r_2 + r_3)$$

$$P \quad A_2''(r_1) = 0$$

$$P \quad E'(r_1) = 2(2r_1 - r_2 - r_3) \quad \text{approximating to} \quad (2r_1 - r_2 - r_3)$$

As the E' representation is two-dimensional we need to find a second expression which will be jointly responsible for the overall representation. To arrive at this second function, it is necessary to state that any member of a set of functions forming the basis for a representation, must be affected by the symmetry operations of the group in one of two ways:

1. It will go into ± 1 times itself.
2. It will go into another member of the set or a combination of members of the set.

If we chose an operation that does not convert the function into +1 times itself, for instance C_3 , we find that under the operation:

$$\hat{C}_3(2r_1 + r_2 + r_3) = (2r_2 - r_3 - r_1)$$

which clearly does not go into itself ± 1 times. However this function is also not orthogonal to the first, as the partner must be. It follows therefore, that this function must be a linear combination of the first function and its partner, and so we can deduce

the partner function by subtracting an appropriate number of the first function from the second, leaving the remainder as the partner.

$$(2r_2 - r_3 - r_1) - (-1/2)(2r_1 - r_2 - r_3) = 3/2 r_2 - 3/2 r_3 \quad \text{approximating to } (r_2 - r_3)$$

This function is orthogonal to the first function and so the two together form the basis for the E' representation. The same calculations can be performed for the bond angles, the projection operators being applied to just one of these angles, e.g. θ_1 . The resulting set of normalised orthogonal functions from the basis of our symmetry deformation coordinates:

$$\begin{array}{ll} 1/\sqrt{3} (r_1 + r_2 + r_3) & 1/\sqrt{3} (\theta_1 + \theta_2 + \theta_3) \\ 1/\sqrt{6} (2r_1 - r_2 - r_3) & 1/\sqrt{6} (2\theta_1 - \theta_2 - \theta_3) \\ 1/\sqrt{2}(r_2 - r_3) & 1/\sqrt{2}(\theta_2 - \theta_3) \end{array}$$

It should be noted at this stage that the use of only the bond lengths and the bond angles has resulted in the derivation of a set of six basis functions, which in theory is all that we need to describe the displacements of the observed distorted geometries from that of the reference structure. However six functions come from only the A_1' and the E' irreducible representations, since the projection of the bond length or bond angle in the A_2'' representation always come to zero. To find a function that describes this representation we have to recognise that the current set of functions describe only movement in the plane of a planar entity and take no direct account of the possible movement of the central atom out of the plane. If we describe this movement to the term Δ and take account of the sense of the displacement and then apply the projection operators as above we find that:

$$P A_1' (\Delta) = 0$$

$$P A_2'' (\Delta) = 12 \Delta \quad \text{approximating to } \Delta$$

$$P E' (\Delta) = 0$$

In presenting Δ as one of the six necessary functions for description of this system it is obvious that one of the functions already derived must become redundant.

The function is

$$S_5 = 1/\sqrt{3} (\theta_1 + \theta_2 + \theta_3)$$

which does describe the out of plane displacement of the central atom but gives no account of the direction of displacement. A displacement along S_5 can however be related to Δ by the approximation (where d is the mean bond length) :

$$S_2^2 = \Delta^2 \cong S_1^2 (2\pi \sqrt{3} - S_5)/9 \cong d^2 (2\pi \sqrt{3} - S_5)/3$$

The complete set of symmetry coordinates can now be given for the D_{3h} point group as:

$$S_1 (A_1') = 1/\sqrt{3} (r_1 + r_2 + r_3)$$

$$S_2 (A_2'') = \Delta \cong S_5$$

$$S_{3a} (E') = 1/\sqrt{6} (2r_1 - r_2 - r_3)$$

$$S_{3b} (E') = 1/\sqrt{2} (r_2 - r_3)$$

$$S_{4a} (E') = 1/\sqrt{6} (2\theta_1 - \theta_2 - \theta_3)$$

$$S_{4b} (E') = 1/\sqrt{2} (\theta_2 - \theta_3)$$

The derivation of the relevant kernel and co-kernel symmetries can be found from the character tables for the point group. Here the only representations that need to be looked at, are the A_1' , A_2'' and E' [1]. The character for these are shown below

D_{3h}	E	$2C_3$	$3C_2$	σ_h	$2S_3$	$3\sigma_v$
A_1'	1	1	1	1	1	1
A_2''	1	1	-1	-1	-1	1
E'	2	-1	0	2	-1	0

The symmetry elements preserved in the kernel group are those whose characters equal the character of the identity element for each irreducible representation. It follows therefore that the S_2 coordinate, from the A_2'' irreducible representation, preserves the symmetry elements (E, $2C_3$ and $3\sigma_v$), i.e. those forming the C_{3v} point group, while the kernel symmetry of the S_3 and S_4 coordinates is that of the C_s point group. The kernel of the A_1' representation is similarly the D_{3h} group.

The S_{3a} and S_{4a} coordinates are chosen so that both of them are transformed into themselves by a mirror plane passing through r_1 and bisecting θ_3 in the reference structure. Displacements along either of these coordinates will therefore show co-kernel symmetry, $\text{CoK}(E', \sigma_v) = C_{2v}$.

When using the SDC's calculated above in the actual analysis of the datasets, it is important to recognise that the terms in the functions are displacements away from the ideal reference geometry. This means that instead of using actual bond angles, e.g. ϕ , it is necessary to replace these in the derived functions by $(\theta = \phi - 120^\circ)$, since 120° is the bond angle appropriate to the reference frame of D_{3h} symmetry.

Appendix B

Departmental Seminars:

Date	Title	Speaker
31/10/2001	Supramolecular Chemistry: Synthesis and Self-organisation	Dr. Collin Raston
5/12/2001	Drugs and Future	Dr. Mike Eaton Celltech
16/01/2002	Electronically Unsaturated Sterically Crowded Tetrahedral Catalysis for Asymmetric Ring Closing Metathesis and the Living Polymerisation of Ordinary Olefins.	Prof. P. R. Schrock MIT, USA
20/01/2002	Effects of Magnetic Fields on Chemical Reactions	Dr. Peter Hore University of Oxford
31/01/2002	Some Supramolecular Chemistry of Magnets and Superconductors	Prof. Peter Day
13/02/2002	Defining Effective Chiral Binding sites at Lanthanides – Enantioselective Reagents and Catalysis	Dr. Helen Aspinall
20/02/2002	The Heart of the Matter: Designing Ligands for Sensors of Risk Assessment	Dr. Lisa Hall Univ. of Cambridge
27/02/2002	Dynamic Experiments in Environmental SEM	Dr. Bradley Theil Univ. of Cambridge
6/03/2002	Laser Probing the Gas Phase Chemistry Involved in Diamond Chemical Vapour Deposition	Prof. Mike Ashfold University of Bristol

20/03/2002	Simple and Complex Fluids Under Extreme Confinement	Prof. Jacob Klein University of Oxford
7/05/2002	Understanding the Properties of Molecular Solids: Structure, Dynamics and Applied Aspects	Dr. K. D. M. Harris University of Birmingham
13/06/2002	Single Crystal Neutron Diffraction at the ILL: Science and Facilities	Dr. Gary J. McIntyre
22/07/2002	New Types of on-classical Interligand H-Si Interactions in Transition Metal Hydrides	Dr. Georgii Nikonov Russian Academy of Science, Russia
19/08/2002	Communication Between Spin Crossover Centre: Thermal, Pressure and Light Induced Spin Changes in Fe(II) Complexes	Prof. Jose A. Real University of Valencia, Spain
09/10/2002	New Design Approaches for NLO Chromophores and for Molecular Conductive Magnets	Dr. Jinqi Qin Wuhan University, China
10/10/2002	Are Crystal Structures Predictable?	Prof. Jack Dunitz ETH Zurich, Switzerland.
12/02/2003	Adventures in Organometallic Polymer Chemistry	Prof. Paul Raithby University of Bath
25/02/2004	Raman Microscopy: A Powerful Technique in Inorganic Chemistry and Surface, Nanoparticulate and Pigment studies.	Prof. Robin Clark
02/07/2004	2010: A Nanospace Odyssey	Prof. Sir Harry Kroto Nobel Laureate in Chemistry (1996)

12/11/2003	BCA Autumn Meeting Accelrys, Cambridge
8/12/2003-	BCA Winter Meeting
9/12/2003	ISIS, Abingdon
8/01/2004-	37 th National Seminar on Crystallography
10/01/2004	National Chemical Laboratory, Pune, India.
12/05/2004-	CCDC Students Day
13/05/2004	Presented Talk: Organic Chlorine as a Hydrogen Bond Acceptor: Evidence for the Existence of Intramolecular O-H...Cl interactions in some Gem-Alkynols
9/06/2004-	35 th International School of Crystallography
20/06/2004	Erice, Italy

Departmental Courses

Course Number	Course Title	Lecturer/Instructor
408Q	Experimental Design	Dr. A. Beeby
PG10	Electroanalytical Techniques	Dr. R. Katakya
PG4	Diffraction and Scattering Methods	Dr. A. E. Goeta
408K	Practical Spectroscopy Assessment	Dr. Alan M. Kenwright

Appendix C

Publications:

- [1] 4,4-Diphenyl -2,5-Cyclohexadienone: Four Polymorphs and Nineteen Crystallographically Independent Molecular Conformations,
V. S. Senthil Kumar, Anthony Addlagatta, Ashwini Nangia, Ward T. Robinson, Charlotte K. Broder, Raju Mondal, Ivana R. Evans, Judith A. K. Howard, Frank H. Allen., *Angew. Chem. Int. Ed.*, 2002, **41**, No. 20, 3448-3851.
- [2] Correspondence Between Molecular Functionality and Crystal Structures: Crystal Chemistry of a Family of Extended Amino-Phenols,
Venugopal V. Rao, Charlotte K. Broder, Raju Mondal, Judith A. K. Howard, Gautam R. Desiraju, Frank H. Allen, *J. Am. Chem. Soc.*, 2003, **125**, 14495-14509
- [3] Mapping the Geometry of Metal Three-Coordination Using Crystal Structure Data: Reaction Pathway for Liagnd Addition to Linear Hg^{II} Species,
Frank H. Allen, Raju Mondal, Nigel A. Pitchford and Judith A. K. Howard, *Helv. Chim. Acta.*, 2003, **86**, 1129-1139.
- [4] Dilemmas in crystallisation. The 'unusual' behaviour of 1,5-dichloro-trans-9, 10-diethynyl-9, 10-dihydroanthracene-9, 10-diol and the more 'normal' behaviour of its pseudopolymorphs with dipolar aprotic solvents.
Rahul Banarjee, Gautam R. Desiraju, Raju Mondal, Andrei S. Batsnanov, Charlotte K. Broder, Judith A. K. Howard, *Helv. Chim. Acta.*, 2003, **86**, 1339-1351

[5] Kinetic and equilibrium studies of sigma-adduct formation and nucleophilic substitution in the reactions of 2-phenoxy-3,5-dinitropyridine and 2-ethoxy-3,5-dinitropyridine with aliphatic amines in dipolar aprotic solvents.

Miahael R. Crampton, Thomas. A .Emokpae, Judith A. K. Howard, Chukwuemeka Isanbor, Raju Mondal, *Organic and Biomolecular Chemistry*, 2003, **1**, 1004-1011#

[6] Leaving group effects on the mechanism of aromatic nucleophilic substitution (S_NAr) reactions of some phenyl 2,4,6 trinitrophenyl ethers with aniline in acetonitrile.

Miahael R. Crampton, T. A .Emokpae, Judith A. K. Howard, Chukwuemeka Isanbor, Raju Mondal, *J. Phys. Org. Chem.*, 2003, **17**, 65-70

[7] Gauche and staggered forms of diethylamine in solvates of 1,5-dichloro-*cis*-9,10-diethynyl-9,10-dihydroanthracene-9,10-diol. A case of conformational pseudopolymorphism?

Raju Mondal, Judith A. K. Howard, Rahul Banerjee, Gautam R. Desiraju, *Chem. Comm.*, 2004, 644-645.

[8] A 1:1 molecular complex of 4-aminocyclohexanol and (4-hydroxycyclohexyl) canbamic acid.

Archan Dey, Gautam R. Desiraju, Raju Mondal, Judith A. K. Howard, *Acta. Cryst.* 2004, **E60**, 857-859.

[9] Organic Chlorine as a Hydrogen-Bridge Acceptor: Evidence for the Existence of Intramolecular O-H...Cl-C interactions in Some Gem-Alkynols.

Rahul Banerjee, Gautam R. Desiraju, Raju Mondal and Judith A. K. Howard, *Chem. Eur. J.*, 2004, **10**, 3373-3383.

[10] Molecular Recognition Among Alcohols and Amines. Novel Carborundum Network in a Supramolecular Homologous Series.

Archan Dey, Gautam R. Desiraju, Raju Mondal, Judith A. K. Howard, *Chem. Comm.*, 2004, in press.

[11] Variable Temperature Neutron Diffraction Analysis of a Very Short O-H...O Hydrogen Bond in 2,3,5,6-Pyrazinetetracarboxylic Acid Dihydrate: Synthron-Assisted Short $O_{\text{acid}}\text{-H}\dots O_{\text{water}}$ Hydrogen Bonds in a Multicenter Array.

Peddy Vishweshwar, N. Jagadeesh Babu, Ashwini Nangia, Sax A. Mason, Horst Puschmann, Raju Mondal, Judith A. K. Howard, *J. Phys. Chem. A.*, 2004, in press.

[12] Dianiline-Diphenol Molecular Complexes Based on Supramolecular Recognition.

Venugopal R. Vangala, Raju Mondal, Judith A. K. Howard, Gautam R. Desiraju, *Cryst. Growth Des.*, 2004, Advanced Article.

